Journal of the Mississippi

Academy of Sciences

Volume 65, Number 3 **July 2020**

SPECIAL EDITION

Agricultural Sciences

Guest Editor: Professor K. Raja Reddy

Mississippi State University

Journal of the Mississippi Academy of Sciences
ISSN 0076-9436

Editorial policy:
General. The Editorial Board publishes articles on all aspects of science that are of general interest to the Mississippi scientific community. General articles include short reviews of general interest, reports of recent advances in a particular area of science, current events of interest to researchers and science educators, etc. Research papers of sufficiently broad scope to be of interest to many Academy members are also considered. Articles of particular interest in Mississippi are especially encouraged. Research papers are reports of original research. Descriptions of laboratory or field exercises suitable for high school or college teaching laboratories are accepted. Brief communications not exceeding two pages are accepted. Submission of any manuscript implies that the paper has not been published and is not being considered for publication elsewhere.
Copyright. Copyright protection is secured automatically for contributing authors through publication of this journal. The Board of the Mississippi Academy of Sciences recognizes ownership of this published material belongs solely to the author(s) of individual articles.
Review. All papers submitted for publication will be peer-reviewed. You are encouraged to have one or more of your colleagues review the manuscript before submitting it for formal review.
Proofs and reprints. When a manuscript is accepted for publication the author of correspondence will receive a PDF file in lieu of reprints.
Page charges. Authors or their institutions must pay page charges of $150.00 for special edition. The remainder of the printing cost comes from Academy membership dues.
Letters policy. We welcome reader's opinions and comments about the journal and about science in general. Send you letters to the editor. Include full name, address, and daytime telephone number. Letters may be edited.

All correspondence concerning publication should be directed to:

Dr. Michelle Tucci
Mississippi Academy of Sciences
Post Office Box 55907
Jackson, MS 39296-5907

msacademyofscience@comcast.net
601-366-2995

Administrative policy:
Membership. Membership is open to anyone interested in science in Mississippi. The basic annual membership fee is $30; students may join for $10. Information about other membership categories is available through the MAS office.
Advertising. The Journal of the Mississippi Academy of Sciences accepts paid advertising. Contact the editor or the MAS Office for current rates.

Direct correspondence concerning administration of the Mississippi Academy of Sciences and its journal to:

Dr. Michelle Tucci
Mississippi Academy of Sciences
Post Office Box 55907
Jackson, MS 39296-5907

msacademyofscience@comcast.net
601-366-2995
The Mississippi Academy of Sciences operates a web site: http://www.msacad.org/

On the cover: The Soil-Plant-Atmosphere-Research (SPAR) Facility (https://www.spar.msstate.edu/) is a controlled environment research facility located on the Mississippi State University's campus. SPAR has a set of ten outdoor naturally-lit chambers, with computer control of the environmental factors. This facility was established in 1977 and has since been used for determining plant responses to a variety of environmental factors, including future climatic conditions. See the associated article, "Temperature Effects on Soybean Seedling Shoot and Root Growth and Developmental Dynamics", on pages 247- 257. Photo credit: David Ammon.

PREFACE

This special issue of the Journal of Mississippi Academy Sciences (JMAS) focusing on Agriculture and Plant Sciences is the first attempt in 84 years of continuous publication of JMAS.

All the papers in this special issue have been peer-reviewed to the standard of the journal. We express our deep and sincere gratitude to all the authors for their timely response and careful revisions. They have made tremendous contributions and offered generous support to this issue. The topics cover various aspects of agriculture covering soils to crops fundamental and production and applied problems in the Magnolia State. We also thank several reviewers for their voluntary work and expert reviews.

It is hoped that this JMA Special Issue on Agriculture will make a good source of scientific material, but also an inspiration for other divisions of the Mississippi Academy Sciences to initiate such special issues in the coming years.

We thank all the sponsors both in and outside the state for their generous support. We express special appreciation to Drs. Saha, Benghuzzi, and the MAS Board and Council Members for their support during the special issue initiation and further development.

K. Raja Reddy
Guest Editor

Michelle A. Tucci
Editor

Journal of the Mississippi Academy of Sciences

Volume 65 July 2020 Number 3

The Journal of the Mississippi Academy of Sciences (ISSN 0076-9436) is published in January (annual meeting abstracts), April, July, and October, by the Mississippi Academy of Sciences. Members of the Academy receive the journal as part of their regular (nonstudent) membership. Inquiries regarding subscriptions, availability of back issues, and address changes should be addressed to The Mississippi Academy of Sciences, Post Office Box 55709, Jackson, MS 39296-5709, telephone 601-977-0627, or email msacademyofscience@comcast.net.

Special Issue-Agricultural Sciences

(Guest Editor: Dr. K. Raja Reddy, Mississippi State University)

Research Articles

218 **Herbicide Resistance in Weed Populations of Mississippi: A Review**
Vijay K. Nandula

228 **Spatiotemporal Analyses of Changing Cropping Patterns and Crop Rotations in the Mississippi Delta**
Shrinidhi Ambinakudige and Adjoa Intsiful

237 **Harvest Management Effects on Bermudagrass Yield and Nutrient Utilization in a Swine-Effluent Spray Field**
John J. Read, Ardeshir Adeli, and Timothy E. Fairbrother

247 **Temperature Effects on Soybean Seedling Shoot and Root Growth and Developmental Dynamics**
Firas Ahmed Alsajri, Chathurika Wijewardana, Ryan Rosselot, Bhupinder Singh, L. Jason Krutz, Wei Gao, and K. Raja Reddy

258 **Estimates of Turf-Type Hybrid Bermudagrass Base and Optimal Growth Temperatures**
James D. McCurdy, Ethan T. Flournoy, Barry R. Stewart, H. Wayne Philley, K. Raja Reddy, William C. Kreuser, Eric H. Reasor, and Christian M. Baldwin

267 **Factors Affecting *Listeria monocytogenes* Biofilm Formation in Food Processing Environments and Its Control**
Mohit Bansal, Nitin Dhowlaghar, Ramakrishna Nannapaneni, Divya Kode, Sam Chang, Wen-Hsing Cheng, Tomi Obe and Aaron Kiess

283 **Effect of Herbicide Additions on pH for Approved Dicamba Tank-Mixtures in Cotton**
J. Connor Ferguson, Justin S. Calhoun, Kayla L. Broster, Luke H. Merritt, Michael T. Wesley, and Zachary R. Treadway

292 **Antifeedant effect of sicklepod extract on soybean looper *Chrysodeixis includens* (Lepidoptera: Noctuidae)**
Ziming Yue, Natraj Krishnan, and Te-Ming Tseng

300 **Soil Waterlogging and Nitrogen Fertilizer Source Effects on Soil Inorganic Nitrogen**
Gurpreet Kaur, Peter P. Motavalli, Kelly A. Nelson, Gurbir Singh, and Taghi Bararpour

Journal of the Mississippi Academy of Sciences

Volume 65 July 2020 Number 3

CONTENTS continued

319 **Evaluation of Rice Genotypes for Early- and Mid-season Vigor Using Morphological and Physiological Traits**
Salah H. Jumaa, Akanksha Sehgal, Naqeebullah Kakar, Edilberto D. Redoña, Daryl Chastain, Marilyn L. Warburton and K. Raja Reddy

346 **Cover Crops and Landscape Positions Impacts Infiltration and Anion Leaching in Corn-Soybean Rotation**
Gurbir Singh, Gurpreet Kaur, Karl Williard, Jon Schoonover, and Taghi Bararpour

358 **Molecular and Physiological Response to Dicamba in Dicamba-Tolerant Wild Tomato**
Rouzbeh Zangoueinejad, Mohammad Taghi Alebrahim, and Te Ming Tseng

374 ***In Vitro* Seed Germination Response of Corn, Cotton, and Soybean to Temperature**
Charles Hunt Walne, Firas A. Alsajri, Bandara Gajanayake, Suresh Lokhande, Ramdeo Seepaul, Chathurika Wijewardana, and K. Raja Reddy

Departments

385 Call for Abstracts

386 MAS 2020 Meeting Information

387 Instructions for Abstracts and Poster Presentations

388 Author Guidelines

392 Advertisements

Herbicide Resistance in Weed Populations of Mississippi: A Review

Vijay K. Nandula

Crop Production Systems Research Unit, Agricultural Research Service,
USDA, Stoneville, MS 38776, USA

Corresponding Author: Vijay K. Nandula, E-mail: vijay.nandula@usda.gov

ABSTRACT

Since the mid-twentieth century, herbicides rapidly replaced all other means of weed management. Overreliance on 'herbicide-only' weed control strategies hastened the evolution of herbicide-resistant (HR) weed species. Glyphosate-resistant (GR) crop technology revolutionized weed management in agronomic crops. Still, GR weeds, led by Palmer amaranth, severely reduced returns from various cropping systems and affected the bottom line of growers across the world. An additional problem was the lack of commercialization of a new herbicide mode of action since the 1990s. Auxinic herbicide-resistant crops (HRCs) offer a short-term alternative for the management of GR Palmer amaranth and other weed species. New HRCs stacked with multiple herbicide resistance traits and at least two new herbicide modes of action expected to be available in the mid-2020s provide new chemical options for weed management in row crops in the next decade. This article reviews the chronological confirmation and reporting of HR weeds in Mississippi and outlines current and future weed management tools available to growers of Mississippi.

Keywords: Glyphosate resistance, herbicide resistance, metabolism, Mississippi, multiple resistance, point mutation, resistance mechanism, target site, weed species

Abbreviations: 2,4-D, 2,4-dichorophenoxyacetic acid; ACCase, Acetyl CoA carboxylase; ALS, Acetolactate synthase; DSMA, Disodium methyl arsonate; EPSPS, 5-enolpyruvylshikimate-3-phosphate synthase; GR, Glyphosate-resistant; HPPD, 4-hydroxyphenylpyruvate dioxygenase; HR, Herbicide resistant; HRC, Herbicide-resistant crop; MSMA, Monosodium methyl arsonate; PPO, Protoporphyrinogen oxidase; PS I, Photosystem I; PS II, Photosystem II

INTRODUCTION

Weeds cause extensive losses amounting to billions of US$ (WSSA, 2019), primarily through increased production costs and decreased quality and quantity of produce. Other negative effects from weeds include reduced aesthetic value of landscapes that they thrive in, health consequences for humans and pets, and fuel for forest fires. Over the past several centuries, weeds have been controlled with mechanical, biological, and cultural tools. Chemical weed control with inorganic compounds was extensively practiced in the late-nineteenth to mid-twentieth century. The 'Chemical Era' of weed control started in the 1940s with the discovery of 2,4-dichorophenoxyacetic acid (2,4-D) during World War II chemical warfare research (Timmons, 2005). Since then, several herbicides belonging to different chemical classes and possessing diverse modes of action have been synthesized and commercialized around the world.

Herbicides rapidly replaced all other means of weed management due to their superior efficacy, relatively low cost, selectivity, and targeted weed control. There has been at least one herbicide labeled for every cropping system imagined. Herbicides provided

advantages such as increased productivity, improved quality of produce, reduced drudgery from hand weeding, and reduced soil erosion and topsoil loss due to reduced cultivation and tillage (enhanced by less fossil fuel use). Overreliance on herbicides alone pushed weed species toward evolving resistance to herbicides. This paper reviews the herbicide-resistant (HR) weed populations in Mississippi with regards to the timeline of the evolution of resistance, the current scenario in the state, and expected weed management tools available to growers in the next decade.

HISTORY OF CHEMICAL WEED CONTROL

The timeline of events described in this section has been mostly derived from Timmons (2005) and Appleby (2005), up until 1970 and beyond, respectively. The domestication of crops started nearly 10,000 years ago. Traditionally, hand weeding by women and children using simple cultivation tools had been the most common weed control method. Jethro Tull (1674-1741), an English agricultural pioneer, invented a horse-drawn hoe for mechanically controlling weeds (Timmons, 2005). Weed control with chemicals, predominantly inorganic compounds, and dates back to the Romans. The French used copper sulfate to manage charlock (wild mustard, *Sinapis arvensis* L.) in wheat (*Triticum aestivum* L.) in 1896. Sulphuric acid, arsenicals, and sodium chlorate were used in Europe and the U.S from 1900 to 1940. After the discovery of 2,4-D and related herbicides in the early 1940s, the latter part of the decade saw the development of aliphatic acids and carbanilate derivatives with 'public use' herbicides increasing from 15 in 1940 to 25 in 1950. Later, phenoxyethylsulfate and phenoxy propionic/phenoxybutyric acids were discovered in the early 1950s. In 1950s/60s, organic soil sterilizer herbicides belonging to substituted ureas and uracils, chlorobenzoic acid and phenylacetic acid derivatives, s-triazines, triazoles, and other heterocyclic derivatives were commercialized in addition to paraquat. There was an emphasis on selective herbicides from carbamate, carbanilate, amine, acetamide, anilide, toludine, nitrile, s-triazine, and substituted urea families. More than 75 herbicides were developed since 1950. The US Bureau of Census estimated that 91 million kg of herbicides were applied on 36 million ha at the cost of $200 million in 1962; in 1964, 48 million ha were treated with herbicides, and in 1967, 158 million kg of active ingredients were applied. In the Canadian prairie provinces of Alberta, Manitoba, and Saskatchewan, phenoxy herbicides increased ~3-fold from 1954 to 1968; other herbicides increased >11-fold from 1963 to 1968.

During the thirty-five years between 1970 and 2005, 184 new herbicides had been discovered, but all were not commercialized. In 1970, glyphosate was discovered and went on to be classified as the 'herbicide of the 20th century (Duke and Powles, 2008). It has been extensively used as a nonselective herbicide across various agricultural and urban landscapes for controlling nearly 300 annual and perennial weed species. The rapid and widespread adoption of glyphosate-resistant (GR) crop technologies (discussed later) beginning in the mid-1990s vastly contributed to the popularity of glyphosate among growers.

Diclofop-methyl, the first graminicide, was discovered in 1975. Also, in 1975, triclopyr replaced 2, 4, 5-T, with the latter banned in 1979 due to dioxin contamination. Chlorsulfuron was introduced in 1980 as the first acetolactate synthase (ALS)-inhibiting herbicide. This and other ALS-inhibiting herbicides, characterized by favorable properties such as low dosage use, a specific mode of action, and a broad spectrum of selectivity, were responsible for the exponential increase of no-till production systems. However, the rapid evolution of herbicide resistance to ALS inhibitors among weed species made these herbicides rapidly lose their luster. Glufosinate was discovered in 1981, adding to growers' herbicide portfolio. The 1980s witnessed the commercialization of several ALS inhibitors and graminicides. In 1995, isoxaflutole belonging to the 4-hydroxy phenylpyruvate dioxygenase (HPPD)-inhibiting herbicide family was developed. The HPPD inhibitors were the last unique mode of herbicide action commercialized. The next new herbicide mode of action is expected to be available in the mid-2020s (Nandula 2019).

Until 1970, the commercial use of herbicides was regulated by the Federal Insecticide, Fungicide, and Rodenticide Act (FIFRA) passed in 1947. In 1970, the US Environmental Protection Agency was established, and d had been responsible for the regulation of pesticides, including herbicides. Herbicide use in the environment was further subject to the regulatory provisions of the Federal Seed Act (1939), Endangered Species Act (1973), Federal Noxious Weed Act (1974), Food Quality Protection Act (1996), and Plant Protection Act (2000).

The astronomical cost of commercializing a new herbicide active ingredient [(cost of discovery, development, and regulatory approval of a new synthetic pesticide was estimated to be $280 million in 2016 (Marrone, 2019)] coupled with the paucity of new herbicide modes of action (Marrone, 2019) steered the agrochemical industry toward engineering/development of crops resistant to 'currently' registered (subject to change) herbicides. Herbicide-resistant crops (HRCs) can be classified as nontransgenic (traditional genetic methods of selection of resistance traits) and transgenic (genetically engineered). Nontransgenic HRCs were developed using conventional breeding techniques (see Reddy and Nandula, 2012). Agronomic performance of nontransgenic HRCs met with modest acceptance in the marketplace and often did not reach the expectations of growers and commodity groups. Scientists began to look at alternative ways to develop HRCs as weed management tools, to manage a broad spectrum of weeds, with superior agronomic characteristics.

The most popular transgenic HRCs were the GR crops such as soybean (*Glycine max* Merr.), cotton (*Gossypium hirsutum* L.), and corn (*Zea mays* L.) launched in 1996, 1997, and 1998, respectively (Duke and Powles, 2008). Three other GR crops were also introduced: canola (*Brassica napus* L.) in 1996, sugarbeet (*Beta vulgaris* L.) in 1999 (withdrawn and re-introduced in 2007), and alfalfa (*Medicago sativa* L.) in 2005 (regulated since 2007) (Duke and Powles, 2008; Reddy and Nandula, 2012). Additional transgenic HR crop traits include glufosinate resistance and multiple resistance to glyphosate and one or more of glufosinate, auxin-type herbicides (2,4-D, dicamba), and HPPD-inhibiting herbicides. For the latest information on transgenic corn and soybean HR traits, readers are referred to Nandula (2019). Glyphosate and auxin-type herbicide resistance traits have been introduced in several generations, with each generation possessing improved agronomic and genetic performance compared to the previous one.

The popularity of GR crops was unprecedented due to ease of production and management, reduction in the price of glyphosate after patent expiry in 2000, as well as the added benefits of reduced or zero tillage. Growers grew accustomed to weed-free fields and the highest yields in corn, cotton, and soybean. Record use of glyphosate for weed control and lack of diversification in weed management techniques resulted in a rapid increase in the number of glyphosate-resistant weeds, in particular, Palmer amaranth [*Amaranthus palmeri* (S.) Wats.]. An unintended consequence of GR crops was a drastic decrease in the development of new herbicides. Auxin-type herbicide resistance was offered as a new 'silver bullet' to combat GR Palmer amaranth. While successful control of GR broadleaf weeds was achieved with dicamba in dicamba-resistant soybean and cotton, the off-target movement of the herbicide caused injury to non-dicamba-resistant crops and other plant species. Long term impact of auxin-type herbicide-resistant crop technologies is unclear.

HERBICIDE-RESISTANT WEED POPULATIONS IN MISSISSIPPI

The chronological confirmation and reporting of HR weed species from Mississippi are represented in Table 1 with respective herbicide sites of action, herbicides, and known mechanisms of resistance. Below is a summary of reported research on these weeds, separated by species, with all known herbicide resistance cases described therein.

Table 1. Herbicide-resistant weeds of Mississippi.

Weed species	Herbicide site of action	Herbicide	Year first documented	Resistance mechanism	Reference
Common cocklebur	ALS inhibitors	Imazaquin	1989	Unknown	Heap, 2019
		Imazethapyr	1989	Unknown	Heap, 2019 Ohmes and Kendig, 1999
Johnsongrass	ACCase inhibitors	Fenoxaprop	1991	Unknown	Heap, 2019
		Fluazifop	1991	Unknown	Smeda et al., 1997
		Quizalofop	1991	Unknown	Smeda et al., 1997
Johnsongrass	Microtubule inhibitors	Pendimethalin	1992	Unknown	Heap, 2019
Common cocklebur	Nucleic acid inhibitors	DSMA	1994	Unknown	Heap, 2019
		MSMA	1994	Unknown	Nimbal et al., 1995, 1996
Goosegrass	Microtubule inhibitors	Pendimethalin	1994	Unknown	Heap, 2019
		Trifluralin	1994	Unknown	Heap, 2019
Horseweed	PS I Electron Diverter	Paraquat	1994	Unknown	Heap, 2019
Italian ryegrass	ALS inhibitors	Sulfometuron	1995	Unknown	Taylor and Coats, 2006
Annual bluegrass	PS II inhibitors	Atrazine	1996	Unknown	Heap, 2019
		Simazine	1996	Unknown	Hutto et al., 2004
Horseweed	EPSP synthase inhibitors	Glyphosate	2003	Reduced translocation	Koger et al., 2004 Koger and Reddy, 2005
Italian ryegrass	EPSP synthase inhibitors	Glyphosate	2005	Reduced translocation	Nandula et al., 2007, 2008
Horseweed	EPSP synthase inhibitors	Glyphosate	2007	Unknown	Eubank et al., 2012
	PS I Electron Diverter	Paraquat	2007	Unknown	Eubank et al., 2012
Johnsongrass	EPSP synthase inhibitors	Glyphosate	2008	Unknown	Heap, 2019
Palmer amaranth	EPSP synthase inhibitors	Glyphosate	2008	Reduced translocation	Nandula et al., 2012 Ribeiro et al., 2014
	ALS inhibitors	Pyrithiobac	2008	Gene amplification Unknown	Nandula et al., 2012
Rice flatsedge	ALS inhibitors	Bispyribac	2009	Altered target site	Riar et al. 2015
		Halosulfuron	2009	Altered target site	Riar et al. 2015
		Imazamox	2009	Altered target site	Riar et al. 2015
		Penoxsulam	2009	Altered target site	Riar et al. 2015
Tall waterhemp	EPSP synthase inhibitors	Glyphosate	2010	Altered target site & Reduced translocation	Nandula et al., 2013
Goosegrass	EPSP synthase inhibitors	Glyphosate	2010	Altered target site	Molin et al., 2013
Giant ragweed	EPSP synthase	Glyphosate	2010	Reduced	Nandula et al., 2015

	inhibitors			translocation	
Redroot pigweed	ALS inhibitors	Imazaquin	2010	Altered target site	Unpublished
		Pyrithiobac	2010	Altered target site	Unpublished
		Trifloxysulfuron	2010	Altered target site	Unpublished
Tall waterhemp	ALS inhibitors	Imazaquin	2010	Altered target site	Unpublished
		Pyrithiobac	2010	Altered target site	Unpublished
		Trifloxysulfuron	2010	Altered target site	Unpublished
Junglerice	ACCase inhibitors	Fenoxaprop	2011	Unknown	Wright et al., 2016
	ALS inhibitors	Imazamox	2011	Metabolism	Riar et al., 2012 Wright et al., 2018
	Cellulose inhibitors	Quinclorac	2011	Unknown	Wright et al., 2018
	PS II inhibitors	Propanil	2011	Unknown	Wright et al., 2018
Spiny amaranth	EPSP synthase inhibitors	Glyphosate	2012	Gene amplification	Nandula et al., 2014
Spiny amaranth	ALS inhibitors	Imazethapyr	2013	Altered target site	Molin et al., 2016
		Nicosulfuron	2013	Altered target site	Molin et al., 2016
		Pyrithiobac	2013	Altered target site	Molin et al., 2016
		Trifloxysulfuron	2013	Altered target site	Molin et al., 2016
Common ragweed	EPSP synthase inhibitors	Glyphosate	2014	Unknown	Nandula et al., 2017
Annual bluegrass	ALS inhibitors	Foramsulfuron	2014	Altered target site	Tseng et al., 2019
Junglerice	EPSP synthase inhibitors	Glyphosate	2015	Altered target site	Nandula et al., 2018
Italian ryegrass	ACCase inhibitors	Clethodim	2016	Altered target site	Nandula et al. 2019
Italian ryegrass	ALS inhibitors	Mesosulfuron	2016	Altered target site	Unpublished
Palmer amaranth	PPO inhibitors	Fomesafen	2018	Altered target site	Unpublished
	EPSP synthase inhibitors	Glyphosate	2019	Gene amplification	Unpublished
	ALS inhibitors	Pyrithiobac	2019	Altered target site	Unpublished
		Imazaquin	2019	Altered target site	Unpublished
		Trifloxysulfuron	2019	Altered target site	Unpublished

Common Cocklebur

Common cocklebur (*Xanthium strumarium* L.) populations resistant and cross-resistant to ALS inhibitors were reported in 1989 (Heap, 2019) and the ALS cross-resistance trait was characterized as dominant to semi-dominant (Ohmes and Kendig, 1999). In 1994, common cocklebur biotypes resistant to the nucleic acid inhibiting arsenical herbicides MSMA and DSMA were documented (Heap, 2019; Nimbal et al., 1995, 1996).

Johnsongrass

Two Johnsongrass [*Sorghum halepense* (L.) Pers.] populations were identified in 1991 with resistance to the ACCase inhibitors, fenoxaprop (Heap, 2019), fluazifop, quizalofop, and sethoxydim (Smeda et al., 1997). Resistance levels to fluazifop, quizalofop, and sethoxydim in plants raised from seedling and rhizome were >388, >15, 2.3 to 3.4, and >388, >16, 2.8 to 8.5, respectively (Smeda et al. 1997). No cross-resistance to clethodim was reported. Resistance to pendimethalin, a microtubule inhibitor, and glyphosate (from Coahoma County) in Johnsongrass was confirmed in 1992 and 2008, respectively (Heap, 2019).

Goosegrass

A trifluralin- (also a microtubule inhibitor) and pendimethalin-resistant goosegrass (*Eleucine indica* L.) was confirmed in 1994 (Heap, 2019). Glyphosate resistance, 4-fold, was confirmed in a goosegrass population from Washington County in 2010 (Molin et al., 2013). DNA sequencing studies indicated a point mutation leading to a proline to serine substitution at the 106 loci of the *epsps* gene, whose product enzyme, 5-enolpyruvylshikimate-3-phosphate synthase (EPSPS), is the target of glyphosate. Herbicides such as pendimethalin, *s*-metolachlor, clethodim, paraquat, and fluazifop controlled the GR goosegrass 93% to 100%.

Annual Bluegrass

In a statewide survey of resistance to triazine herbicides in annual bluegrass (*Poa annua* L.), a common turfgrass weed, collections, 43% of samples demonstrated resistance to simazine (Hutto et al., 2004). Recently, Tseng et al. (2019) reported a 45-fold resistance to foramsulfuron, an ALS inhibitor, in an annual bluegrass biotype. DNA sequencing results identified a mutation leading to tryptophan to leucine replacement at the 574 loci in the *als* gene of the resistant biotype.

Horseweed

Horseweed [*Conyza canadensis* (L.) Cronq.] populations resistant to paraquat, a photosystem I (PS I) inhibitor belonging to the bipyridilium chemical family, were documented in 1994 (Heap, 2019). In 2003, the first case of a GR weed in Mississippi, GR horseweed populations with an 8- to 12-fold resistance to glyphosate, were confirmed (Koger et al., 2004) and characterized to have a reduced translocation type of resistance mechanism (Koger and Reddy, 2005). A horseweed population with multiple resistance to glyphosate (12-fold) and paraquat (9-fold) was first reported in 2007 (Eubank et al., 2012). Infield studies, the addition of metribuzin to paraquat improved horseweed control.

Italian Ryegrass

The first cases of HR Italian ryegrass [*Lolium perenne* L. ssp. *multiflorum* (Lam.) Husnot] in Mississippi were two sulfometuron (ALS inhibitor belonging to the sulfonylurea family)-resistant biotypes from rights-of-way of U.S. Highway 49E in Holmes County and State Highway 14 in Humphreys County (Taylor and Coats, 2006). In 2005, two Italian ryegrass populations from Washington County were determined to be 3-fold resistant to glyphosate (Nandula et al., 2007) with reduced translocation of glyphosate (Nandula et al., 2008) as the mode of resistance. The role of an altered target site as a resistance mechanism was not investigated. This report was the first in the world to document GR Italian ryegrass in a row crop situation. Recent research confirmed 4- to 10-fold resistance to clethodim in Italian ryegrass with the resistance mechanism being an altered ACCase due to one or more point mutations at loci I2041N, C2088R, and G2096A (Nandula et al., 2019); these mutations result in substitution of isoleucine with asparagine, cysteine with arginine, and glycine with alanine, respectively.

Just concluded research on Italian ryegrass populations from across Mississippi found several to be resistant to mesosulfuron, an ALS inhibitor belonging to the sulfonylurea family (unpublished data).

Amaranthus *spp.*

Two GR Palmer amaranth biotypes were 17- and 14-fold, and 7- and 8-fold resistant to glyphosate and pyrithiobac (a ALS inhibitor), respectively (Nandula et al., 2012) with mechanism of resistance being *epsps* gene amplification in one biotype (Ribeiro et al., 2014) and reduced translocation in the other (Nandula et al., 2012). Recently, a Palmer amaranth accession was confirmed to possess multiple resistances to glyphosate, fomesafen (a protoporphyrinogen oxidase, PPO inhibitor), and several ALS inhibitors (unpublished data).

A close 'cousin' of Palmer amaranth, tall waterhemp [*Amaranthus tuberculatus* (Moq.) Sauer] from Washington County had a 5-fold resistance to glyphosate with an altered target site, point mutation leading to a proline to serine substitution at the 106 loci of *epsps*, as the resistance causing mechanism (Nandula et al., 2013). The above point mutation is the first report in the world of a point mutation-based resistance to glyphosate in a dicot weed species. Additionally, reduced translocation of glyphosate was also determined to be a resistance mechanism. Lately, a tall waterhemp population from Monroe County has been confirmed to be resistant to several ALS inhibitors, including imazaquin, pyrithiobac, and trifloxysulfuron with a point mutation at the 574 loci of the *als* gene leading to a tryptophan substitution with leucine (unpublished data).

Populations of two other weed species belonging to the *Amaranthus* genus, redroot pigweed (*Amaranthus retroflexus* L.) and spiny amaranth (*Amaranths spinosus* L.), have evolved resistance to various herbicides. For example, a redroot population from Jasper County was confirmed to be resistant to several ALS inhibitors such as imazaquin, pyrithiobac, and trifloxysulfuron with a tryptophan to leucine substitution-causing point mutation at the 574 loci of its *als* gene (unpublished data). Spiny amaranth biotypes exhibited a 5-fold increase in resistance compared with a glyphosate-susceptible biotype and *epsps* was amplified 33-37 times and expressed 37 times more in the glyphosate-resistant spiny amaranth biotypes than in a susceptible biotype (Nandula et al., 2014). The *epsps* sequence in resistant plants was identical to the *epsps* in GR Palmer amaranth, but differed at 29 nucleotides from the *epsps* in susceptible spiny amaranth plants. PCR analysis revealed similarities between the GR Palmer amaranth and GR spiny amaranth. Glyphosate resistance in spiny amaranth is caused by the amplification of the *epsps* gene. Evidence suggests that part of the *epsps* amplicon from GR Palmer amaranth is present in GR spiny amaranth. This is likely due to a hybridization event between spiny amaranth and GR Palmer amaranth somewhere in the lineage of the GR spiny amaranth plants. Similarly, it has been shown that ALS resistance traits, endowing resistance to imazethapyr, nicosulfuron, pyrithiobac, and trifloxysulfuron, were transferred to spiny amaranth from resistant Palmer amaranth in a natural field setting (Molin et al., 2016).

Weeds of Rice

A rice flatsedge (*Cyperus iria* L.) accession was >21-fold resistant to several ALS inhibitors including bispyribac, halosulfuron, imazamox, and penoxsulam with a point mutation at the 574 loci of the *als* gene leading to a tryptophan substitution with leucine (Riar et al., 2015). A junglerice [*Echinochloa colona* (L.) Link] population from Sunflower County was resistant to multiple herbicide modes of action including ALS inhibitors (Riar et al., 2012), ACCase inhibitors (Wright et al. 2016), photosystem II (PS II) inhibitors (Wright et al., 2018), and cellulose inhibitors (Wright et al., 2018). The mechanism of resistance to ALS inhibitors has been indirectly determined to be due to herbicide metabolism (Riar et al., 2012), wherein treatment with ALS inhibitors such as imazamox plus malathion, a known inhibitor of cytochrome P450 enzymes that metabolize xenobiotics in most living organisms (Nandula et al., 2019), increased susceptibility of resistant plants. Of late, several incidents of glyphosate failure on junglerice have been reported in Mississippi. A

resistant biotype was 4-fold more resistant to glyphosate than a susceptible biotype and possessed a single-nucleotide substitution of T for C at codon 106 positions of *epsps*, resulting in a proline-to-serine substitution (CCA to TCA) (Nandula et al., 2018).

Ragweeds

Giant ragweed (*Ambrosia trifida* L.) population was 1.5-fold more resistant to glyphosate than a susceptible population (Nandula et al., 2015). The amount of translocated glyphosate was more the susceptible than resistant biotypes at 48 and 96 hours after treatment and no target-site mutation was identified in the *epsps* sequence of the resistant biotype. In similar research, GR common ragweed (*Ambrosia artemisiifolia* L.) biotypes that were 4- to 5-fold more resistant than a corresponding sensitive biotype did not demonstrate either a target site mutation or reduced absorption and translocation of glyphosate (Nandula et al., 2017).

IMPACT OF HERBICIDE-RESISTANT WEED POPULATIONS

Herbicide resistance in weed populations of Mississippi and elsewhere can have a significant impact on crop production costs via increased weed management costs. For example, increased costs associated with control of GR weeds in Mississippi per ha were estimated in 2010 to be $21 to 38.75 (horseweed), $27.13 to 51.13 (Italian ryegrass), and $15 to 27.5 (Palmer amaranth) in soybean, $4.55 to 40 (horseweed), $10.5 to 54.9 (Italian ryegrass), and $4.55 to 87.55 (Palmer amaranth) in corn, and $13.6 to 38.53 (horseweed), $36.3 to 53 (Italian ryegrass), and $15.5 to 51.1 (Palmer amaranth) in cotton (Carpenter and Gianessi, 2010). In addition to increased costs, HR weeds can significantly reduce yield. Corn yield was reduced by 50% by the presence of 4 GR Italian ryegrass plants per meter of row (Nandula, 2014). Weed populations can independently evolve resistance to two or more unique herbicide modes of action. A metabolic resistance mechanism can endow resistance to herbicides across different modes of action as well as to yet-to-be commercialized herbicides. Other consequences of HR weeds are wear and tear on cultivation and harvesting equipment, reduction in irrigation and harvest efficiency, reduced crop yield quality, alternate hosts for pests and diseases, and reduction in overall land productivity.

FUTURE OUTLOOK AND CONCLUSIONS

Chemical weed control will continue to remain the dominant method of weed management in the short term, despite the evolution of GR and other HR weeds. New corn, soybean, cotton, and other crop technologies, providing resistance to multiple herbicides and improved formulations, and new herbicide modes of action [expected in the next five to ten years (Nandula, 2019)] offer additional tools to growers toward effective and sustainable weed management. Public and private land managers must implement nonchemical control strategies such as cultural, biological, and mechanical means wherever and whenever possible to sustain the rapidly depleting herbicide portfolio as well as to prepare for new patterns of weed emergence, growth, and resistance evolution in response to prevailing weather conditions. Precision agriculture, remote sensing, unmanned aerial vehicle (UAV), and other emerging technologies will help meet current and future challenges of weed management.

CONFLICT OF INTEREST

There is no conflict of interest to declare.

LITERATURE CITED

Appleby AP. A history of weed control in the United States and Canada-a sequel. Weed Sci. 2005; 53: 762-768.

Carpenter JE, Gianessi LP. Economic impact of glyphosate-resistant weeds. In: V.K.Nandula, editor, Glyphosate resistance in crops and weeds: history, development, and management. John Wiley and Sons, Inc., Hoboken, NJ. 2010; p. 297-312.

Duke SO, Powles SB. Glyphosate: a once in a century herbicide. Pest Manag. Sci. 2008; 64: 319–325.

Eubank TW, Nandula VK, Poston DH, Shaw DR. Multiple resistance of horseweed to glyphosate and paraquat and its control with paraquat and metribuzin combinations. Agronomy 2012; 2: 358-370.

Heap I. *The International Survey of Herbicide Resistant Weeds.* http://www.weedscience.com. Accessed 15

Oct. 2019.

Hutto KC, Coats GE, Taylor JM. Annual bluegrass (*Poa annua*) resistance to simazine in Mississippi. Weed Technol. 2004; 18: 846–849.

Koger CH, Poston DH, Hayes RM, Montgomery RF. Glyphosate-resistant horseweed (*Conyza canadensis*) in Mississippi. Weed Technol. 2004, 18, 820–825.

Koger CH, Reddy KN. Role of absorption and translocation in the mechanism of glyphosate resistance in horseweed (*Conyza canadensis*). Weed Sci. 2005; 53: 84–89.

Marrone PG, Pesticidal natural products – status and future potential. Pest Manag. Sci. 2019; https://doi.org/10.1002/ps.5433.

Molin WT, Nandula VK, Wright AA, Bond JA. Transfer and expression of ALS inhibitor resistance from *Amaranthus palmeri* to an *A. spinosus* X *A. palmeri* hybrid. Weed Sci. 2016; 64: 240-247.

Molin WT, Wright AA, Nandula VK. Glyphosate resistant *Eleusine indica* from Mississippi. Agronomy 2013; 3: 474-487.

Nandula VK. Italian ryegrass (*Lolium multiflorum*) and corn (*Zea mays*) competition. Am. J. Plant Sci. 2014; 5: 3914-3924.

Nandula VK. Herbicide resistance traits in maize and soybean: current status and future outlook. Plants 2019; 8: 337. https://doi.org/10.3390/plants8090337.

Nandula VK, Giacomini DA, Lawrence BH, Molin WT, Bond JA. Resistance to clethodim in Italian ryegrass (*Lolium perenne* ssp. *multiflorum)* from Mississippi and North Carolina. Accepted for publication in Pest Manag. Sci. 2019.

Nandula VK, Montgomery GB, Vennapusa AR, Jugulam M, Giacomini DA, Ray JD, Bond JA, Steckel LE, Tranel PJ. Glyphosate-resistant junglerice (*Echinochloa colona*) from Mississippi and Tennessee: confirmation and resistance mechanisms. Weed Sci. 2018; 66: 603-610.

Nandula VK, Poston DH, Eubank TW, Koger CH, Reddy KN. Differential response to glyphosate in Italian ryegrass (*Lolium multiflorum*) populations from Mississippi. Weed Technol. 2007; 21: 477-482.

Nandula VK, Ray JD, Ribeiro DN, Pan Z, Reddy KN. Glyphosate resistance in tall waterhemp (*Amaranthus tuberculatus*) from Mississippi is due to both altered target site and non-target site mechanisms. Weed Sci. 2013; 61: 374-383.

Nandula VK, Reddy KN, Koger CH, Poston DH, Rimando AM, Duke SO, Bond JA, Ribeiro DN. Multiple resistance to glyphosate and pyrithiobac in Palmer amaranth (*Amaranthus palmeri*) from Mississippi and response to flumiclorac. Weed Sci. 2012; 60: 179-188.

Nandula VK, Reddy KN, Poston DH, Rimando AM, Duke SO. Glyphosate tolerance mechanism in Italian ryegrass (*Lolium multiflorum*) from Mississippi. Weed Sci. 2008; 56: 344-349.

Nandula VK, Riechers DE, Ferhatoglu Y, Barrett M, Duke SO, Dayan FE, Goldberg-Cavalleri A, Tétard-Jones C, Wortley DJ, Onkokesung N, Brazier-Hicks M, Edwards R, Gaines T, Iwakami S, Jugulam M, Ma R. Herbicide metabolism: Crop selectivity, bioactivation, weed resistance, and regulation. Weed Sci. 2019; 67: 149-175.

Nandula VK, Tehranchian P, Bond JA, Norsworthy JK, Eubank TW. Glyphosate resistance in common ragweed (*Ambrosia artemisiifolia* L.) from Mississippi, USA. Weed Biol. Manag. 2017; 17: 45-53.

Nandula VK, Wright AA, Bond JA, Ray JD, Eubank TW, Molin WT. EPSPS amplification in glyphosate-resistant spiny amaranth (*Amaranthus spinosus*): A case of gene transfer via interspecific hybridization from glyphosate-resistant Palmer amaranth (*Amaranthus palmeri*). Pest Manag. Sci. 2014; 70: 1902-1909.

Nandula VK, Wright AA, Van Horn CR, Molin WT, Westra P, Reddy KN. Glyphosate resistance in giant ragweed (*Ambrosia trifida* L.) from Mississippi is partly due to reduced translocation. Am. J. Plant Sci. 2015; 6: 2104-2113.

Nimbal CI, Shaw DR, Duke SO, Byrd JD. Response of MSMA-resistant and -susceptible common cocklebur (*Xanthium strumarium*) biotypes to cotton (*Gossypium hirsutum*) herbicides and cross-resistance to arsenicals and membrane disruptors. Weed Technol. 1995; 9: 440-445.

Nimbal CI, Shaw DR, Wills GD, Duke SO. Environmental effects on MSMA phytotoxicity to wild-type and arsenical herbicide-resistant common cocklebur (*Xanthium strumarium*). Weed Technol. 1996; 10: 809-814.

Ohmes, GA, Kendig JA. Inheritance of an ALS-cross-resistant common cocklebur (*Xanthium strumarium*) biotype. Weed Technol. 1999; 13: 100-103.

Reddy KN, Nandula VK. Herbicide resistant crops: History, development and current technologies. Ind. J. Agron. 2012; 57: 1-7.

Riar DS, Norsworthy JK, Srivastava V, Nandula VK, Bond JA, Scott RC. Physiological and molecular basis of acetolactate synthase-inhibiting herbicide resistance in barnyardgrass (*Echinochloa crus-galli*). J. Ag. Food Chem. 2012; 61: 278-289.

Riar DS, Tehranchian P, Norsworthy JK, Nandula V, McElroy S, Srivatsava V, Chen S, Bond JA, Scott RC. Acetolactate synthase-inhibiting herbicide-resistant rice flatsedge (*Cyperus iria*): cross resistance and molecular mechanism of resistance. Weed Sci. 2015; 63: 748-757.

Ribeiro DN, Pan Z, Duke SO, Nandula VK, Baldwin BS, Shaw DR, Dayan FE. Involvement of facultative apomixis in inheritance of EPSPS gene amplification in glyphosate-resistant *Amaranthus palmeri*. Planta 2014; 239: 199-212.

Smeda RJ, Snipes CE, Barrentine WL. Identification of graminicide-resistant johnsongrass (*Sorghum halepense*). Weed Sci. 1997; 45: 132-137.

Taylor JM, Coats GE. Identification of sulfometuron-resistant Italian ryegrass (*Lolium multiflorum*) selections. Weed Technol. 1996; 10: 943-946.

Timmons FL. A history of weed control in the United States and Canada. Weed Sci. 2005; 53: 748-761.

Tseng T-M, Shrestha S, McCurdy JD, Wilson E. Target-site mutation and fitness cost of acetolactate synthase inhibitor-resistant annual bluegrass. Hort. Sci. 2019; 54: 701-705.

Wright AA, Nandula VK, Grier L, Showmaker KC, Bond JA, Peterson DG, Ray JD, Shaw DR. Characterization of fenoxaprop-P-ethyl-resistant junglerice (*Echinochloa colona*) from Mississippi. Weed Sci. 2016; 64: 588-595.

Wright AA, Rodriguez-Carres M, Koski L, Sasidharan R, Peterson DG, Nandula VK, Ray JD, Bond JA, Shaw DR. Multiple herbicide resistant *Echinochloa colona*: identification of genes potentially involved in resistance through differential gene expression analysis. Weed Sci. 2018; 66: 347-354.

WSSA. *Crop Loss*. http://wssa.net/wssa/weed/croploss-2/. Accessed 15 Oct. 2019.

Spatiotemporal Analyses of Changing Cropping Patterns and Crop Rotations in the Mississippi Delta

Shrinidhi Ambinakudige and Adjoa Intsiful

Department of Geosciences, Mississippi State University, Mississippi State, MS 39762, USA

Corresponding Author: Shrinidhi Ambinakudige, E-mail: *sa60@msstate.edu*

ABSTRACT

Crop rotation plays an important role in both traditional and modern agriculture. Effective crop rotation helps to improve soil health and nutrient management. This study analyzed the spatial and temporal dynamics of crop rotation in the 18 Mississippi Delta counties from 1999 through 2018, using the data collected from remote sensing techniques. The USDA's National Agricultural Statistics Service Cropland Data Layer data were used in the analysis. The results indicated that, over the last two decades, cropping preference had changed significantly in the Mississippi Delta. During the study period, the soybean area increased enormously, whereas the cotton area showed a significant decrease. Between 1999 and 2018, the corn area also increased tremendously. A time-series analysis of the cropping sequence between soybean and cotton and other crops showed that between 2000 and 2018, the percentage of the soybean area that has shifted to cotton cultivation the following year gradually decreased. The percentage of the soybean area that was planted with soybean again in the next year increased tremendously, from about 43 percent in 2000 to about 80 percent in 2018. The results also showed that, while the cotton yield per acre increased over the years, the crop rotation from soybean to cotton decreased, indicating that other improved farming practices also played a significant role in increasing the cotton yields in the Mississippi Delta.

Keywords: Crop rotation, the Mississippi Delta, soybean, cotton

INTRODUCTION

Crop rotation can break pest cycles and add extra nutrients to the soil. It helps to control weeds, diseases, and insects; and add to crop and market diversity (Baldwin, 2006; Stevens, 2018). Crops absorb and deposit nutrients in different ways that are helpful to other crops. A careful selection of crops in each season may reduce the nutrient requirement and, in turn, reduce the cost of production. A legume crop, such as soybean, can fix the nitrogen in the soil and make the soil fertile for whatever crop will be grown in the next season. One major impact of crop rotation is the significant increase in the crop yields of both crops involved in the crop rotation (Bruns et al., 2018; Bryson et al., 2003; Guidry et al., 2001; Hunt et al., 2017). For instance, studies have shown that the crop rotation sequence with soybean (*Glycine max*) and cotton (*Gossypium hirsutum*) increases the yields of both crops (Bruns et al., 2018; Guidry et al., 2001). Further, studies have shown that crop rotation can suppress weeds while providing an enhanced environmental performance (Blackshaw et al., 2017; Bryson et al., 2003; Hunt et al., 2017).

This study analyzed the spatial and temporal dynamics of crop rotation in the 18 Mississippi Delta counties from 1999 through 2018, using the data collected from remote sensing techniques. First, the spatial extents of the cropping pattern from 1999 to 2018 were analyzed, and then, the cropping sequence in each pixel to estimate the degree of crop rotation between two consecutive years was estimated. Further, an analysis to correlate the yields of cotton and the degree of crop rotation between cotton and soybean over the years was conducted.

STUDY AREA AND BACKGROUND

The Mississippi Delta counties included in this study were Bolivar, Carroll, Coahoma, Desoto, Holmes, Humphreys, Issaquena, Leflore, Panola, Quitman, Sharkey, Sunflower, Tallahatchie, Tate, Tunica, Warren, Washington, and Yazoo (Figure 1). The Mississippi Delta is part of the greater Mississippi Alluvial Valley, which extends from southern Illinois through southeastern Louisiana, where it exits into the Gulf of Mexico (Storell, 2005). The Delta in Mississippi is a floodplain, subject to periodic flooding from the Mississippi River. The region's alluvial soils provide ideal conditions to cultivate cotton.

Agriculture played and still plays a vital role in the economy of the Mississippi Delta (Cobb, 1994; Meikle, 2016). Specifically, cotton has played a significant role in changing the physical and cultural landscape of the Delta region of Mississippi. Cotton farms were small and manually operated in Mississippi before 1930; however, by 1970, most farms in the Mississippi Delta were large and mechanized commercial farms growing cotton, rice, and soybean (Hagge, 2018). In the United States, 17 states produce cotton. The Delta area of Mississippi, Arkansas, and Louisiana; the Texas High and Rolling Plains; central Arizona; and California's San Joaquin Valley are the major cotton-growing regions. About 98 percent of the cotton in the U.S. is Upland cotton. In the Mississippi Delta, Upland cotton is also the dominant cotton.

Historically, cotton plantations depended heavily on farm laborers. Slavery and the plantation economy were notoriously linked in the history of the Mississippi Delta. Farms in Mississippi today no longer operate as traditional family farms but are organized more like businesses. Due to mechanization and investments, farm labor is no longer a significant economic activity for the population in the Delta (Cobb, 1994; Meikle, 2016).

Changes in global cotton production, outmigration, technological innovations in agriculture, the civil movement, and the laws of the land all influenced farming in the Mississippi Delta. Over the decades, farming in Mississippi has seen tremendous changes in the types of crops that are grown and the methods by which they are grown. For example, soybean, which is currently, one of the main crops in the Mississippi Delta, was introduced to the United States during World War II as a substitute for protein foods and edible oil (Meikle, 2016; Hymowitz and Shurtleff, 2005); it has outstripped cotton as the main crop in the Delta. About 94 percent of soybean-cultivated land in the U.S. is continuously rotated. Primarily, soybean, a legume crop, is alternated with corn (*Zea mays* L.), wheat (*Triticum aestivum* L.), and sometimes, cotton in the southern U.S. (Kuipers, 2018).

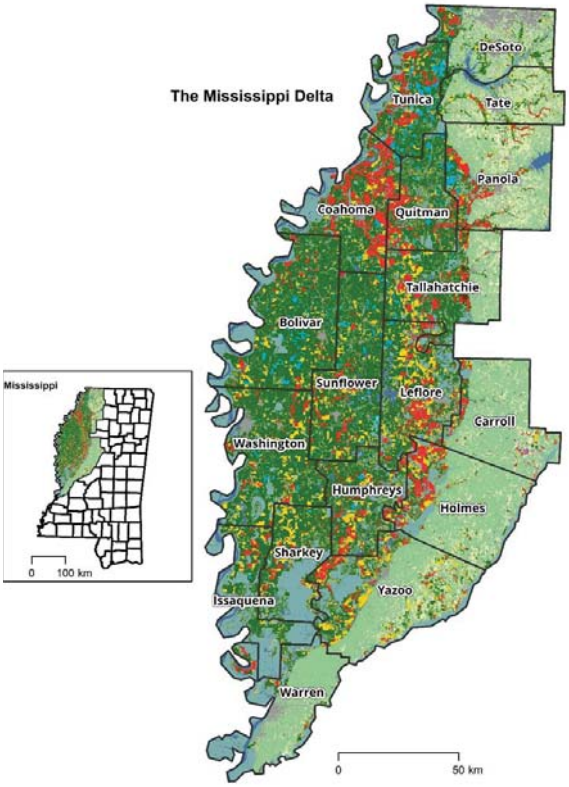

Figure 1. The study area: counties of the Mississippi Delta.

Agriculture in the Mississippi Delta counties is heavily dependent upon subsidies from the

federal government. According to data from the Environmental Working Group, compiled from the USDA (EWG, 2019), Mississippi ranks 14th in the list of states that receive farm subsidies. Farmers have received over $9.96 billion in subsidies between 1995 and 2019 in Mississippi. The top 4 counties in Mississippi that receive commodity payments are Bolivar, Washington, Sunflower, and Coahoma counties; these are all Delta counties. Cotton, rice, and soybean were the top three crops that received commodity subsidies in Mississippi (EWG, 2019).

Overall, the Mississippi Delta's economy depends on farming, and cropping patterns and crop rotations are the two important factors among others that help to sustain the Mississippi Delta's economy. Therefore, it is imperative to analyze the spatial- and temporal patterns of crop cultivation and crop rotation in the Mississippi Delta.

METHODS

This study used the USDA's National Agricultural Statistics Service (NASS) Cropland Data Layer (CDL) data. The CDL is a raster, geo-referenced, crop-specific land cover data layer (Han et al., 2012; Han et al. 2014). It has a ground resolution of 30 meters and is produced from various satellite imageries from Landsat TM, +ETM, Landsat 8 OLI/TIRS, the Disaster Monitoring Constellation (DMC), DEIMOS-1 and UK2, the ISRO ResourceSat-2 LISS-3, and the ESA SENTINEL-2 sensors collected during the growing season (NASS, 2019). Additional satellite imagery and ancillary inputs were also used to supplement and improve the classification. These include the United States Geological Survey (USGS), the National Elevation Dataset (NED), and the imperviousness and canopy data layers from the USGS National Land Cover Database. The USDA validated the data using data derived from the Farm Service Agency (FSA) Common Land Unit (CLU) Program and the current version of NLCD (NASS, 2019).

After the CDL data were downloaded from the NASS CropScape web portal, the data were uploaded to a geodatabase file in ArcGIS 10.6—a geographic information system software. A boundary layer of 18 Mississippi Delta counties were then overlaid on the CDL data for further spatial analysis. In ArcGIS, each crop and nonagricultural land use were tabulated for each county in the Delta.

To estimate the extent of crop rotation, an analysis was carried out at the pixel level. The CDL of 1999 was used as the base year layer. The CDL pixels were converted to points using a raster-to-vector conversion tool. Over 31 million points converted from pixels were then used to extract pixel values from 1999 through 2018. Crosstabs to show the crops grown in each pixel were created between the data of consecutive years. If the crop value in year 1 was the same as the crop value in year 2 in a pixel, then no crop rotation occurred in that pixel. If the crop values were different between two consecutive years in a pixel, then a crop rotation occurred.

This study used Circos - a visualization tool to study a cropping pattern. The Circos software was developed initially to facilitate the identification and analysis of similarities and differences arising from comparisons of genomes (Meyers, 2015). It has been used to visually represent the flow of refugees, whereby a relationship between two elements (i.e., countries) represents the extent of ingress and egress. This is the first time that this tool is being used to study a cropping pattern.

RESULTS

The results of the analysis of the USDA's NASS Cropland Data Layer CDL data (Figure 2) indicate that, over the last two decades, cropping preferences have changed significantly in the Mississippi Delta. A major change in cropping patterns has been witnessed from the early to the mid-2000s. During this period, the soybean crop area started to increase, while the cotton area showed an opposite trend, with a significant decrease in the cultivated area. Besides, the corn area increased, while the rice area remained more

or less constant throughout the study period. A decrease in cotton production from 2005 to 2008 occurred not only in the Mississippi Delta but in the entire U.S, due to poor planting weather and competition from other field crops for acreage, particularly corn and soybean (Meyer, 2019). However, while U.S. cotton production has rebounded since 2015, the Mississippi Delta saw only a slight increase in cotton cultivation.

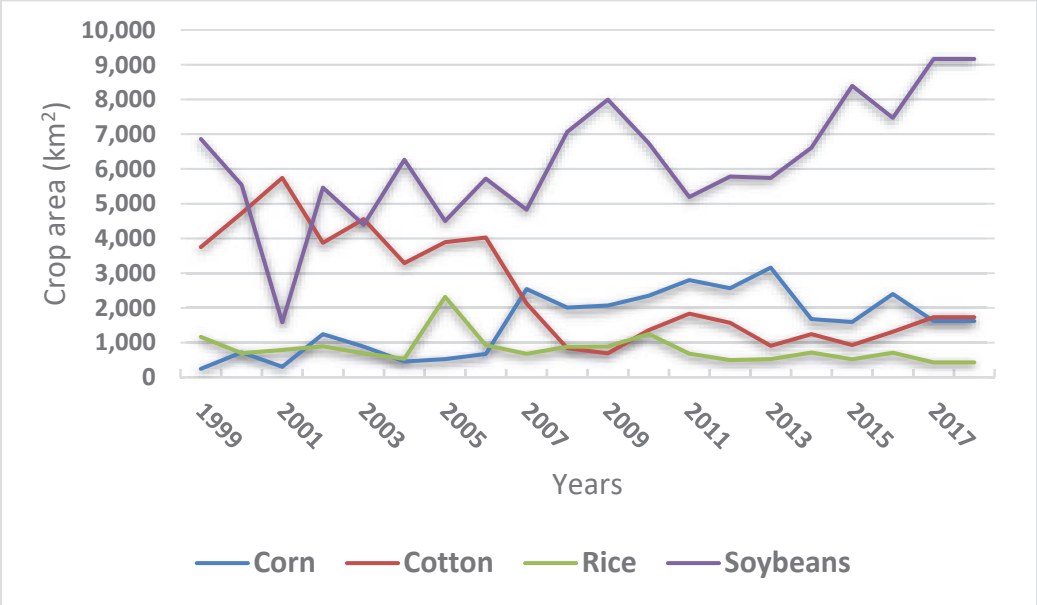

Figure 2. The overall change in cropping patterns in the Mississippi Delta from 1999 to 2018.

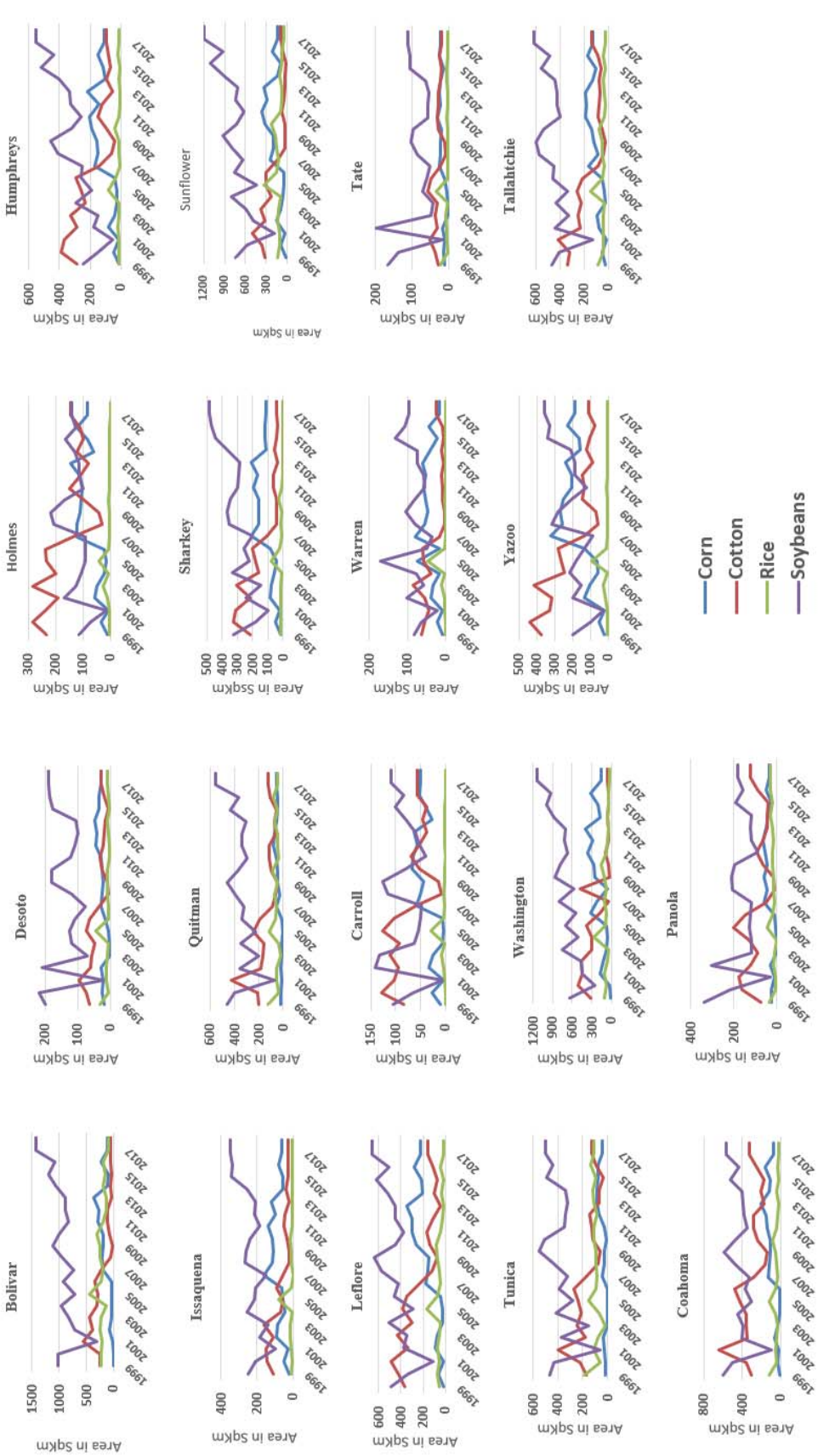

Figure 3. The cropping trends in each of the 18 Mississippi Delta counties are similar to overall trends in the Delta (Figure 3). A significant decline in the cotton area was shown in all the counties from 2005 to 2018. The soybean area either increased or remained stable in all of the counties from 1999 to 2018. The corn area fluctuated over the years, but many counties did show an increasing trend in the area under corn cultivation.

To illustrate the changes in crop rotation preferences over the years, the Circos visualization tool was used. Cotton, corn, soybean, and rice were included in the analyze; the rest of the crops are grouped as *others*. For the visualization, cropping rotation only data between 1999 and 2000, and between 2017 and 2018 were used. The Circos visualization tool enables researchers to analyze many kinds of matrix-based and relational data using circular axes. Originally designed to visualize genome maps (Krzywinski et al., 2009), the Circos tool has been used to analyze many kinds of data in which the user wishes to relate A to B as measured by Value C (Myers, 2015).

The circular plots (Figure 4) depict the cropping sequence between 1999 and 2000 and between 2017 and 2018. Each crop is assigned a color and is represented by the circle's segments. The direction of the crop rotation (e.g., from cotton to soybean) is encoded by both the previous year's crop color and a gap between the flow and the destination crop's segment. The volume of crop rotation is indicated by the width of the flow. Because the flow width is nonlinearly adapted to the curvature, it corresponds to the flow size only at the beginning and endpoints. Tick marks on the circle segments show the percentage area of a particular crop that was replaced by a different crop the next year (Abel and Sander, 2014).

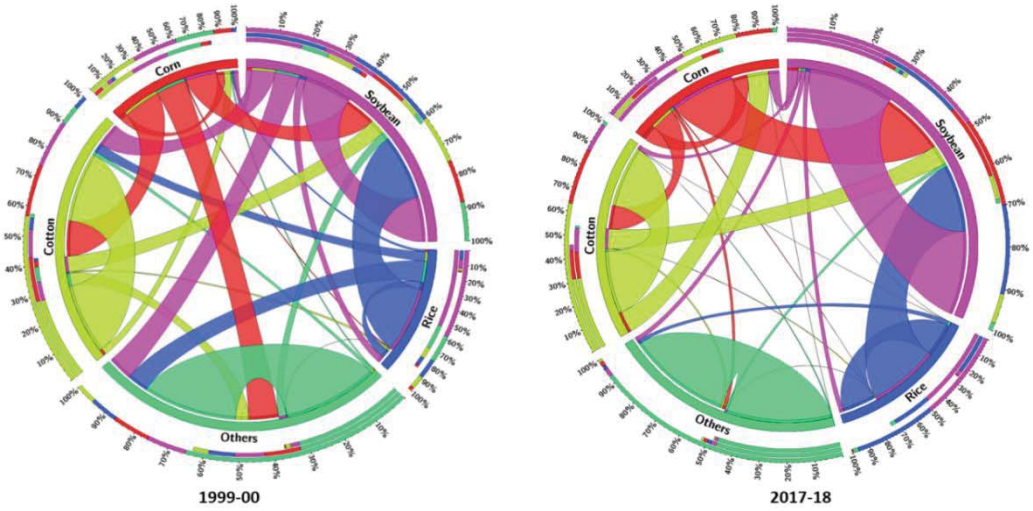

Figure 4. Crop rotation patterns between1999 & 2000, and between 2017 and 2018, shown in percent areas.

Between the two decades, there has been a significant change in the cropping pattern in the Delta. Between 1999 and 2017, while the corn- and soybean-cultivated areas have increased by 560 percent and 33%, respectively, the cotton-, rice-, and sorghum-cultivated areas have decreased by 54%, 63% and 83%, respectively. Among the five major crops (corn, cotton, rice, sorghum, and soybean) grown in the Delta, in 1999, soybean and cotton were the top two crops grown, but in 2017, soybean was the top crop, and cotton and corn were second in the cultivated area.

Accordingly, cropping sequences also have changed significantly. Between 1999 and 2000, soybean was the main crop in the cropping sequence, followed by cotton and other crops. About 29 percent of the corn area, 15 percent of the cotton area, 62 percent of the rice area, and 44 percent of the soybean area in 1999 shifted to soybean cultivation in 2000 (Figure 4). Between 2017 and 2018, cotton and corn came in a distant second to soybean in the cropping sequence. Soybean became the dominant crop in the cropping sequence, with 60 percent of the corn area, 19 percent of the cotton area, 65 percent of the rice area, and 79 percent of the soybean area

in 2017 shifting to soybean cultivation in 2018 (Figure 4).

A time-series analysis of the cropping sequence between soybean and cotton and other crops (Figure 5) shows that the percentage of the soybean area between 2000 and 2018, the percentage of the soybean area that has shifted to cotton cultivation the following year gradually decreased. The percentage of the soybean area that was planted with soybean again in the next year increased tremendously, from about 43 percent in 2000 to about 80 percent in 2018. The cropping sequence from soybean to other crops also has reduced significantly.

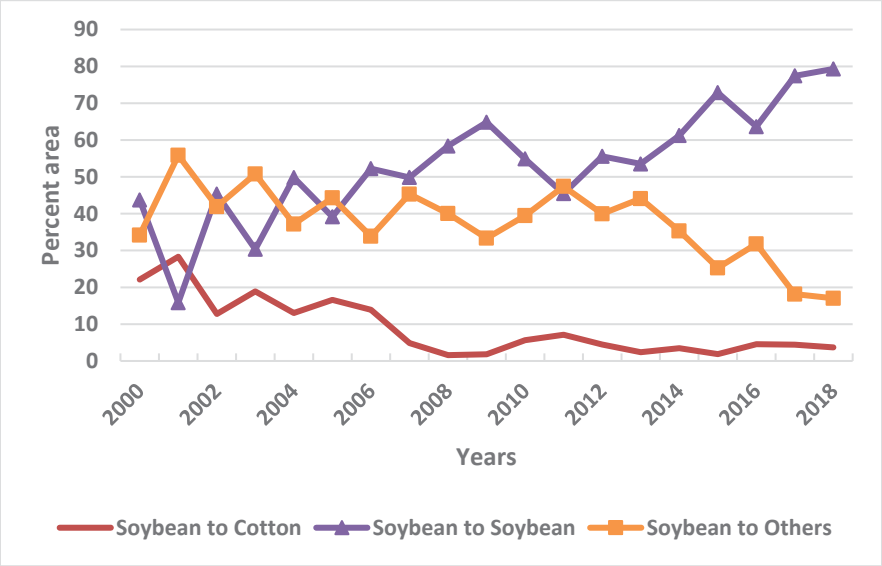

Figure 5. Soybean cropping sequence with cotton and other crops, from 2000 to 2018.

Crop rotation between a legume and another crop will help to improve the soil and thus help to increase the yield. Soybean is a legume crop, so a crop rotation with soybean should help other crops to increase the yield. In Figure 6, we show the relation between a cotton yield (pound per acre of upland cotton (NASS, 2019) and the percentage of the soybean area in the previous year that shifted to cotton cultivation. The result shows that, although the cotton yield increased over the years, the crop rotation from soybean to cotton decreased over the years. It is important to understand that cotton yields in the U.S. have increased significantly over the years due to the cultivation of better varieties, improved pest management practices, and overall farming practices. Therefore, crop rotation might have benefitted cotton cultivation, but the role of the other factors previously mentioned contributed more to the increased cotton yields.

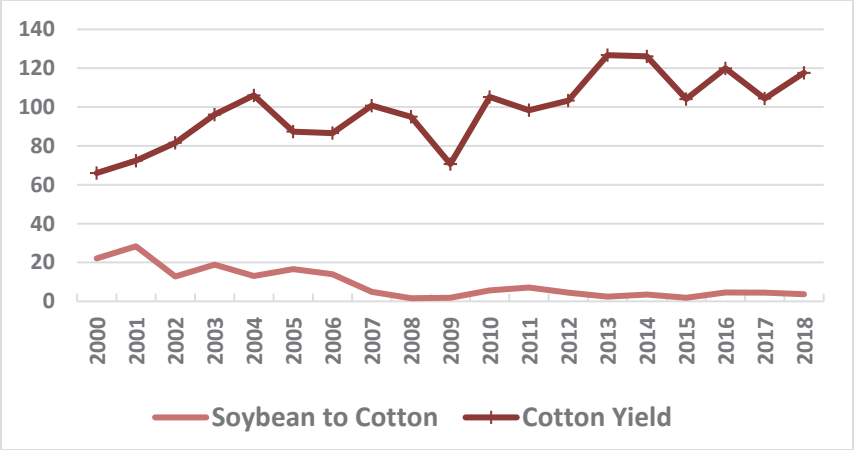

Figure 6. The relationship between soybean and cotton crop rotation and the cotton yields.

DISCUSSION AND CONCLUSIONS

In this study, we analyzed the cropping pattern and crop rotation patterns in the Mississippi Delta region. The Mississippi Delta's economy continues to depend on agriculture. However, the farming structure and practices have changed significantly over time. Once dominated by the cotton crop and family farming, today, it embraces the farm business approach and cultivates multiple crops, mostly dominated by soybean. We considered the cotton-based system due to the historical significance of cotton to this region of the U.S. The years 2005–2018 showed a major shift from cotton to soybean as the major crop. Global cotton market price fluctuations and a significant increase in cotton production by other countries, such as India and China, also affected U.S. cotton cultivation. Cotton production in the U.S. and the Mississippi Delta has increased in recent years, but soybean and corn have made significant inroads in the cotton-growing regions. The area under rice cultivation in the Mississippi Delta has somewhat stagnated. Crop rotation patterns have changed over the years, with a dominance of soybean. Despite soybean's dominance, the percentage area of soybean rotating with cotton has decreased in the Mississippi Delta. However, the cotton yields have increased significantly in the Delta.

Hake et al. (1991) noticed that, compared to other crops, cotton's yield response to crop rotation is relatively small. Referring to a crop rotation study in Alabama, Hake et al. (1991) noticed an 11 percent increase in the cotton yield with legume–cotton rotations compared to continuous cotton. According to them, this yield increase seems rather small when compared to 95 years of continuous cotton. They also discussed another study that compared continuous cotton with 1-year rotations of corn, soybean, or double-crop wheat-soybean, which has shown only small yield benefits. Therefore, crop rotation with soybean is not the only factor that helped to increase the cotton yields; other improved cultivation practices have played a significant role in increasing the cotton yields.

CONFLICT OF INTEREST

There is no conflict of interest to declare.

LITERATURE CITED

Abel GJ, and Sander N. Quantifying global international migration flows. Science 2014; 343: 678.

Baldwin KR. Crop rotations in organic farms. The center for environmental farming systems. North Carolina A&T State University. 2006.

Blackshaw R, Pearson D, Larney F, Regitnig P, Nitschelm J, Lupwayi N. Conservation management and crop rotation effects on weed populations in a 12-year irrigated study. Weed

Tech. 2015; 29: 835-843. doi:10.1614/WT-D-15-00071.1.

Bruns A, Reddy KN, Pettigrew WT. A lack of response of irrigated soybean (*Glycine max L. Merr*.) in rotation with cotton (*Gossypium hirsutum L*.) in the Mississippi Delta, USA. Arch. Agric. Environ. Sci. 2018; 3: 261-263.

Blackshaw RE, Pearson D, Larney F, Regitnig P. Conservation management and crop rotation effects on weed populations in a 12-year irrigated study. Weed Tech. 2015; 29: 835-843.

Bryson CT, Reddy KN, Molin WT. Purple nutsedge (*Cyperus rotundus)* population dynamics in narrow row transgenic cotton (*Gossypium hirsutum*) and soybean (*Glycine max*) rotations. Weed Techn. 2003;17: 805-810. https:// doi.org/10.1614/WT02-177.

Cobb J. The most southern place on earth: the Mississippi Delta and the roots of regional identity. New York: Oxford University Press. 1994.

EWG. EWG's Farm subsidy database. 2019. https://farm.ewg.org/index.php. Accessed on 10/14/2019.

Guidry K, Boquet DJ, Hutchinson RL. Profitability of cotton crop rotation systems in northeast Louisiana. LSU AgCenter. 2001. http://www.lsuagcenter. com/portals/ communications/ publications/ agmag/ archive/2001/ summer/ profitability-of-cotton-croprotation-systems-in-northeast-louisiana.Accessed on 9/30/2019.

Hagge DP. From mule to John Deere. Elements of rural landscape change in the Mississippi Delta, 1930-1970. Arkansas review. J. Delta Stu. 2018; 49: 25–39.

Hake K, Blsingame D, Goodell, PB, Stichler C. Crop rotation. Physiol. Today. 1991. 3;1. The National Cotton Council.

Han W, Yang Z, Di L, Mueller R. CropScape: A Web service based application for exploring and disseminating U.S. conterminous geospatial cropland data products for decision support. Comp. Electron. Agric. 2012; 84: 111–123.

Han W, Yang Z, Di L, Yue P. A geospatial Web service approach for creating on-demand Cropland Data Layer thematic maps. Trans. ASABE. 2014; 57: 239-247.

Hunt ND, Hill JD, Liebman, M. Reducing freshwater toxicity while maintaining weed control, profits, and productivity: effects of increased crop rotation diversity and reduced herbicide usage. Environ. Sci. Technol. 2017; 51:1707-1717. DOI: 10.1021/acs.est.6b04086

Hymowitz T, Shurtleff WR. Debunking soybean myths and legends in the historical and popular literature. Crop Sci. 2005; 45: 473-476.

Krzywinski et al. Circos: An information aesthetic for comparative genomics. Gen. Res. 2009. 19:1639-1645. doi:10.1101/gr.092759.109.

Kuipers P. Sustainable U.S. farming practices by the numbers. US Soy.org. 2018. https://ussoy.org/sustainable-u-s-farming-practices-by-the-numbers/

Meikle P. 2016. Globalization and its effects on agriculture and agribusiness in the Mississippi Delta: a historical overview and prospects for the future. J. Rural Soc. Sci. 2016; 31: 130–154.

Meyer L. Cotton Sector at a Glance. https://www.ers.usda.gov/topics/crops/cotton-wool/cotton-sector-at-a-glance/ United States Department of Agriculture, Economic Research Service. 2019. Accessed on 9/30/2019.

Myers R. Using circos data visualizer to analyze trade data: a review and how to guide. Soc. Sci. Comp. Rev. 2015; 33: 779-784.

NASS. CropScape – Cropland Data Layer. United States Department of Agriculture. 2019. https://nassgeodata.gmu.edu/CropScape/.

Stevens AW. Review: The economics of soil health. Food Pol. 2018; 80: 1–9.

Storell J. The use of geospatial technologies to examine spatial and temporal changes of aquaculture complexes in the delta region of Mississippi, 1984 TO 2001, 2005. M.S. thesis. Department of Geosciences, Mississippi State University, Mississippi State, MS.

Harvest Management Effects on Bermudagrass Yield and Nutrient Utilization in a Swine-Effluent Spray Field

John J. Read, Ardeshir Adeli, and Timothy E. Fairbrother

USDA-Agricultural Research Service, Genetics and Sustainable Agriculture Research Unit, 810 Hwy 12E, Mississippi State, MS 39762, USA.

Corresponding Author: John Read, E-mail: john.read@usda.gov, (http://orcid.org/0000-0001-6027-4917)

ABSTRACT

Swine (*Sus scrofa domestica*) waste management plans often include the use of lagoon effluent for the production of bermudagrass [C*ynodon dactylon* (L.) Pers.], the predominant forage in the southeastern USA. A 3-year (2001-2003) study was conducted at a commercial farm in northeast Mississippi on a Prentiss sandy loam to determine cutting height and frequency effects on common bermudagrass forage yield and uptake of N and P. Field plots (2 x 4 m) were irrigated with 7.5 cm ha^{-1} swine effluent from April–October, which provided approximately 520 kg ha^{-1} N and 110 kg ha^{-1} P during the growing season. After an initial harvest in early May, regrowth forage was harvested at 4-, 6-, 8-, 10-, and 12-week intervals and 3- and 9-cm cutting heights using a sickle-bar mower. A significant ($P<0.001$) year x harvest interval interaction for P uptake is attributed to obtaining maximum values with a 10-wk interval in 2001 and with a 6-wk interval in 2002 and 2003. Bermudagrass P uptake was affected by year x cutting height interaction ($P<0.05$); however, cutting at 3-cm height consistently increased P uptake by 18% in 2001, 28% in 2002, and 29% in 2003, as compared to 9-cm. If the goal is maximum utilization of manure nutrients in the effluent, bermudagrass should be cut at 6-10 week intervals as close to the ground as possible to maximize annual forage yield. Cutting more frequently (< 5-week interval) at 9-cm height reduced total yield, but can result in high-quality forage.

Keywords: Agriculture, bermudagrass, ecology, irrigation, nitrogen, phosphorus, wastewater
Abbreviations: DM, Dry matter

INTRODUCTION

The manure produced on commercial swine farms in Mississippi is typically washed into lagoons to facilitate anaerobic digestion. In Mississippi, this waste-water effluent is often used to irrigate summer hay crops in nearby fields. Nitrogen, P, and K are the most agronomically important nutrients of the multiple nutrients in swine effluent, while excess N and P also pose an environmental hazard. Adeli and Varco (2001) reported that summer forage grasses responded very similarly when fertilized with conventional fertilizer and when fertilized with swine effluent. These results suggest nutrient management plans do not have to be modified for swine waste, which improves the potential for expanded use of swine lagoon waste as a fertilizer. Nevertheless, because land application rates are dependent on rates of nutrient removal in the biomass (kg ha^{-1}), particularly P, maximizing P uptake by forages means less land is potentially affected by excessive nutrients.

Bermudagrass, the predominant warm-season forage in the region, is a recommended grass species for manure disposal due to a high annual N requirement (200 kg ha^{-1} or greater) and the potential to remove large amounts of nutrients through intensive (or multiple) hay harvests and off-site removal of the products (Burton and Hanna, 1995; Robinson, 1996). Nevertheless, a concern regarding repeated and/or heavy

applications of swine effluent to bermudagrass is the difference in nutrients applied vs. crop nutrient requirements may result in a build-up of not only soil P, but also total N (King et al., 1985). Water quality problems can occur if P enters the surface water in runoff and processes of nitrate (NO_3-N) leaching loss is of concern for both economic reasons and impact on groundwater quality (Pant et al., 2004; Read et al., 2008).

The annual P uptake for improved bermudagrass hybrids, such as 'Coastal', is approximately 40 kg ha^{-1} at a production level of 14.2 Mg ha^{-1} forage dry matter (DM), which is equivalent to 2.83 kg P Mg^{-1} DM (Osmond and Kang, 2008). Because forage P concentration tends to fluctuate little relative to other nutrients, annual P uptake is associated closely with forage DM yield, which may vary greatly depending on management, soil type, weather, quantity of nutrient applied, and cultivar (Robinson, 1996; Brink et al., 2003; Read et al., 2018). In a Mississippi study on a commercial swine farm, Brink et al. (2005) reported N, P, and K uptake of common and Coastal bermudagrass had a quadratic response to increasing maturity during the spring (May-July) and summer (July-September) harvest periods. In that study, bermudagrass P uptake after 56 days of maturity, when P uptake was maximal, was 24% greater in the spring than in the summer harvest period (31 vs. 25 kg P ha^{-1}). The distribution of forage yield during the growing season can be affected by the harvest interval. Harvesting every 28 days beginning June 1 resulted in a typical single peak yield curve or "hump." Shortening the harvest interval to 21 days tended to flatten out the curve, but reduced total yield. As with any forage, the stage of growth also affects bermudagrass nutrient content and digestibility; the more mature the forage, the lower the nutritive value (Trlica, 2006). With bermudagrass, crude protein concentration and in vitro DM digestibility decline rapidly with increasing harvest (or regrowth) interval, reducing its value as a component in ruminant diets (Burton and Hanna; 1995; Read et al., 2018). Additionally, frequent close cutting promotes shallow rooting, a trait that may increase the uptake of P, because unlike N, P is immobile in soil and tends to concentrate in the surface soil (Pant et al., 2004).

Studies have shown that unimproved, common bermudagrass has higher leaf N concentration and its leaves constitute a more significant fraction of the forage, as compared to either Coastal or 'Tifton 85' hybrid bermudagrass (Pederson et al., 2002; Brink et al., 2003; Brink et al., 2004]. These studies also found that forage N:P ratio was relatively low in common bermudagrass, ranging from 6.2 to 7.3 across harvest dates, and common bermudagrass had a higher P concentration than the two bermudagrass hybrids in both the stem (2.2 vs. 1.8 g kg^{-1}) and leaf (2.1 vs 1.8 g kg^{-1}) fractions. Given these results, we hypothesized that increasing the leaf-to-stem ratio in forage should increase P uptake by common bermudagrass fertilized with swine effluent. The present study determined if harvesting high-quality (i.e., leafier) bermudagrass hay removes more nutrients than low-quality hay, and thereby provide both forages for ruminant animals and a means to increase the uptake of P and other nutrients from the field.

MATERIALS AND METHODS

The site was a common bermudagrass hay meadow at a commercial swine facility located near Pheba, MS (lat 33.59 N, long 88.95 W) on a soil mapped as a Prentiss sandy loam (coarse-loamy, siliceous, semiactive, thermic Glossic Fragiudults, Ultisols) with 2 – 5% slope (USDA-NRCS, 1976). In the previous 7 yr, the producer fertilized common bermudagrass sod using center-pivot irrigation that pumped swine effluent from single-stage anaerobic lagoons. The field was irrigated from April through October of each year with approximately 7.5 cm each season; about 0.5 cm of swine effluent was provided at each irrigation. The effluent had nominal nutrient concentrations of 300 to 420 mg N L^{-1} and approximately 60 mg P L^{-1}. In the effluent, the N was about 84% NH_4/NH_3 and the P was 80% water-soluble ortho-P (Read et al., 2008). The mean annual fertilization rates were

approximately 520 kg N ha^{-1} and 110 kg P ha^{-1}. Timing and amounts of effluent applications were determined by the farm manager, considering forage needs, requisite draw-down of the lagoon effluent, and regulations preventing puddles (which are influenced by weather, plant growth stage, and soil hydraulic properties, among other factors).

The experimental plots (2 x 4 4m each) were located under one section of the center-pivot system and evaluated in 2001, 2002, and 2003. The experimental design was a randomized complete block with four replicates and the different treatments were re-randomized each year. Adjacent plots were separated by a 1-m alley and adjacent blocks were separated by a 2-m alley. The different harvest management treatments were two cutting heights of 3 and 9 cm (from the soil surface), and four harvest intervals of 4, 6, 8, 10, and 12 weeks (Table 1). All plots were initially harvested in early May, before spring green-up. At each subsequent harvest date, forage yields were determined by clipping a 1 by 5 m swath through the center of each plot using the sickle bar mower (Garden Way, Inc., Troy, NY; no longer manufactured). A subsample of 600 to 800 g fresh weight was taken from each yield sample and dried at 60°C for 72 h to determine forage DM. The dried forage was ground to pass a 1-mm screen using a Wiley mill (Model 4, Thomas Scientific, Swedesboro, NJ) and samples were stored in plastic bottles for nutrient analysis. Briefly, forage N was assessed using an automated dry combustion analyzer (Model NA 1500 NC, Carlo Erba, Milan, Italy) and forage P was evaluated using an inductively coupled argon plasma optical emission spectrometer (ICP-OES, Thermo Jarrell Ash Model 1000 ICAP, Franklin, MA) according to methods described by Read et al. (2018). Apparent N and P uptake (kg ha^{-1}) were calculated as the product of DM yield and forage nutrient concentration at each harvest date, and total nutrient uptake was determined by summing average values across harvest dates.

Data were subjected to analysis of variance using the general linear models and repeated measure procedures in SAS (SAS Institute, 2010). In these models, block and year were random effects, and harvest interval and cutting height were fixed effects. A probability level of $P \leq 0.05$ was significant and treatment means were compared using Fisher's protected least significant difference (LSD) test. To estimate the optimum harvest interval for total P uptake, regression parameters were estimated using mixed model analysis with covariates (i.e., fitting a polynomial regression over harvest interval) for the 3 and 9 cm cutting heights in each year (n=5). The optimum interval (independent variable) was determined by solving for the local maximum (or 1st derivative) of each polynomial function, which gives the point on a relationship where the rate of change in the response variable is zero.

RESULTS

A significant ($P<0.01$) harvest interval x year interaction effect was detected for DM yield, P uptake, and N uptake (Table 2). Maximum forage DM yield in 2001, 2002, and 2003 occurred at 10, 8, and 12-week harvest intervals, respectively (Table 3; Figs. 1-3). This result was probably influenced by the difference in rainfall, as well as the difference in timing of an effluent application relative to the harvest date. With regard to P uptake, maximum values occurred with a 10-week harvest interval in 2001 and with a 6-week interval in 2002 and 2003 (Table 4; Figs. 1-3). This result may be explained by seasonal changes in plant maturity, effluent N and P concentrations, or irrigation rate.

Table 1. Harvest schedule and harvest interval treatments used in the analysis of variance.

Date	Week	Harvest interval treatment			
		---------- weeks ----------			
29 May	4	4			
12 Jun	6	6			
26 Jun	8	4	8		
10 Jul	10	10			
24 Jul	12	4	6	12	
21 Aug	16	4	8		
6 Sep	18	6			
18 Sep	20	4	10		
19 Oct	24	4	6	8	12

Table 2. Significance of harvest interval, cutting height, year, and selected two-way interactions on annual dry matter (DM) yield, phosphorus uptake, and nitrogen uptake in common bermudagrass in 2001, 2002, and 2003.

Effect	df	DM yield	P uptake	N uptake
Harvest interval	4	**	**	**
Cutting height	1	**	**	**
Year	2	**	**	**
Interval x Year	8	**	**	**
Height x Year	2	NS	*	*
Interval x Height				
2001	4	NS	NS	NS
2002	4	**	NS	**
2003	4	**	**	*

*, ** Significant at P<0.05 and P<0.01, respectively; otherwise not significant (NS)

A significant (P<0.05) cutting height x year interaction effect was detected for P uptake, but not DM yield (Table 2). A cutting height of 3 cm consistently increased DM yield and nutrient uptake, as compared to 9-cm height (Figs. 1-3). The percentage increase differed across the three years, with the largest increases observed in 2003 of 38% for DM yield and 39% for P uptake (Table 5). Because the forage N:P concentration ratio in 2003 did not differ between cutting heights, the observed increase in P uptake resulted mostly from increased DM yield of the cuttings with 3-cm stubble height rather than increased P concentration (Table 6).

Table 3. Effect of harvest interval on annual dry matter yield in common bermudagrass averaged across two cutting heights of 3 and 9 cm.

Harvest interval	Number of harvests	2001	2002	2003
weeks		---------- Mg ha^{-1} ----------		
4	6	13.9	13.4	11.3
6	4	14.9	17.1	14.5
8	3	18.5	17.7	13.2
10	2	20.0	16.6	12.7
12	2	16.1	17.4	16.1
5% LSD		1.0	0.8	1.1

Table 4. Effect of harvest interval on annual P uptake in common bermudagrass averaged across two cutting heights of 3 and 9 cm.

Harvest interval	Number of harvests	2001	2002	2003
weeks		---------- kg ha^{-1} ----------		
4	6	30	41	32
6	4	30	47	39
8	3	37	45	27
10	2	51	44	30
12	2	30	42	28
5% LSD		5	3	3

Table 5. Effect of cutting height on annual dry matter (DM) yield and phosphorus uptake in common bermudagrass averaged across five harvest intervals of 4, 6, 8, 10, and 12 weeks.

Variable and cutting height	2001	2002	2003
DM yield, Mg ha^{-1}			
3 cm	18.4	18.0	15.7
9 cm	14.9	14.9	11.4
Increase with 3 cm, %	23	21	38
P uptake, kg ha^{-1}			
3 cm	40	49	36
9 cm	34	38	26
Increase with 3 cm, %	18	29	38

Table 6. Effect of cutting height on forage N:P concentration ratio in common bermudagrass averaged across five harvest intervals of 8, 10,, and 12 weeks.

Cutting height	2001	2002	2003	2003 week 4-20†
3 cm	7.5	7.3	8.4	7.5
9 cm	7.8	7.6	8.4	7.8

† Excluding data from the final sampling date in 2003 (that is, for week 24 of the harvest schedule, see Table 1) resulted in a relatively low N:P ratio, due to apparent poor regrowth that concentrated nutrients in the forage.

The trends in total P uptake across harvest intervals were similar for the two cutting heights (Figs, 1, 2, and 3). Therefore, regression analysis was performed on data for 3-cm cutting height, which is considered a standard for economical forage production. Results indicated strong correlation for a third-order (or cubic) polynomial trend in 2001 (r^2 = 0.99) and 2002 (r^2 = 0.96); this trend had a weaker correlation in 2003 (r^2 = 0.76). Calculation of the local maximum for each polynomial function gave optimum harvest intervals of 10.7, 6.5, and 6.9 weeks in 2001, 2002, and 2003, respectively. This variation between years is typical of the volatile and often stressful climate in the Mississippi. While harvest timing to optimize bermudagrass P uptake has its challenges, the practice can be of value for remediation or control of soil nutrient concentrations.

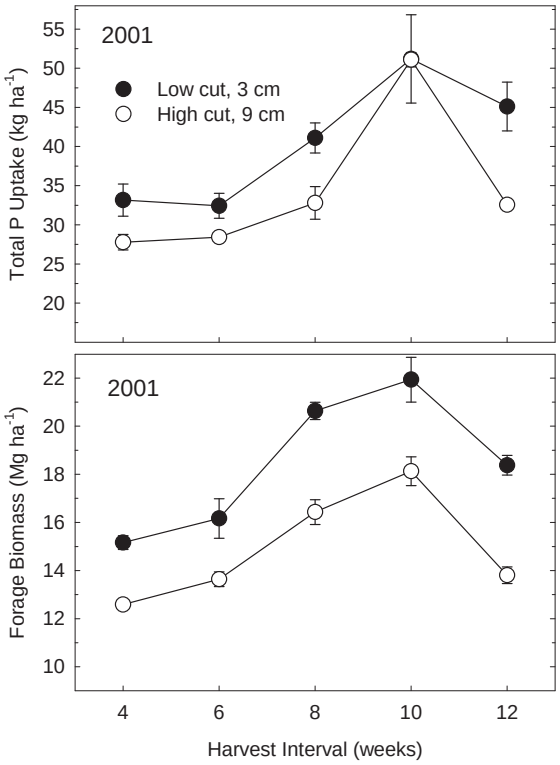

Figure 1. Harvest interval (or maturity) and cutting height effects on yields of phosphorus and forage dry matter in common bermudagrass receiving swine effluent application of 7.5 cm-ha from April to October 2001. Values are mean ± standard error of the mean.

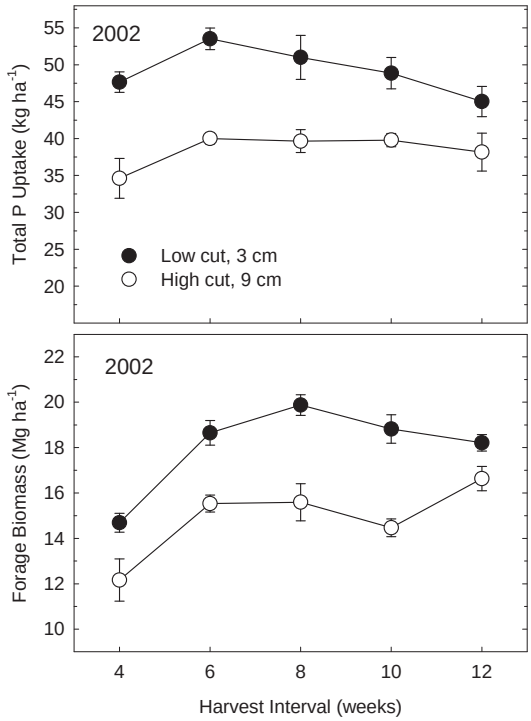

Figure 2. Harvest interval (or maturity) and cutting height effects on yields of phosphorus and forage dry matter in common bermudagrass receiving swine effluent application of 7.5 cm-ha from April to October 2002. Values are mean ± standard error of the mean.

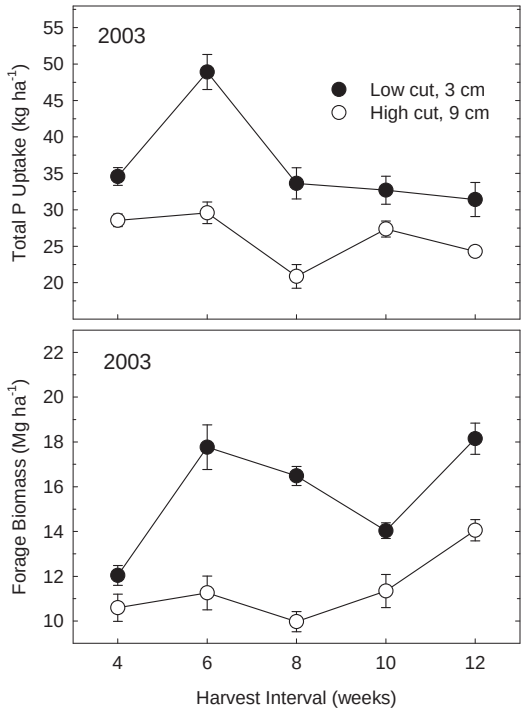

Figure 3. Harvest interval (or maturity) and cutting height effects on yields of phosphorus and forage dry matter in common bermudagrass receiving swine effluent application of 7.5 cm-ha from April to October 2003. Values are mean ± standard error of the mean.

DISCUSSION

In a study on the application of swine lagoon effluent to 'Alicia' bermudagrass harvested when the regrowth was at least 3-week old, Adeli and Varco (2001) reported annual P uptake of approximately 29 kg ha^{-1}, which is close to that shown in the present study for common bermudagrass at most of the harvest interval treatments in 2001 and 2003 (28 to 37 kg ha^{-1} P; Table 4; Figs. 1 and 3). Their results were from plots irrigated individually rather than part of a larger spray field, as in the present study. Experiments conducted within a common spray field would presumably have less variability in soil moisture conditions between experimental plots and may explain somewhat higher P removal rates for common bermudagrass, particularly in 2002 when values averaged 44 kg ha^{-1} (Fig. 2).

Total annual P uptake by bermudagrass can range from approximately 30 to 50 kg ha^{-1}. Brink et al. (2004) fertilized common bermudagrass and six bermudagrass cultivars with 15.75 Mg ha^{-1} broiler litter (540 kg ha^{-1} total N yr^{-1}) on soil with 30+ year history of broiler litter. They reported P uptake was greater in 'Tifton 44' than common bermudagrass, suggesting a greater potential to reduce high soil test P through haying improved hybrid bermudagrass due to superior biomass and high nutrient uptake capacity. Among all the hybrids in that study, only 'Russell' exhibited consistent superior P uptake relative to Coastal, considered the standard among hybrids. It is likely that many of the nutrient utilization differences observed among hybrid bermudagrasses will likely be obscured when evaluations are made under swine effluent irrigation because of abundant nutrients and moisture. Therefore, the cost of replacing common bermudagrass with a hybrid would not be justified.

Other producer options to minimize the potential risks of high soil test P on the environment include overseeding bermudagrass with a cool-season annual forage, though the amount of excess N and P removed over winter varies with forage species and number of hay harvests in spring (McLaughlin et al., 2005). Annual ryegrass (*Lolium multiflorum* L.) overseeded in fall into dormant bermudagrass is a common forage system in Mississippi. In a study of this forage system on a manure-impacted Savannah loam (fine-loamy, siliceous, semiactive, thermic Typic Fragiudult) and the response of annual ryegrass N fertilization level and timing, Read (2012) reported ryegrass increased total annual P uptake by an additional 22 to 47 kg ha^{-1}, depending on the N fertilization scheme. The use of a year-round cropping system for phytoremediation of P-enriched soil has potential only if the forage is managed correctly for hay production and removed permanently from the land as such (Pant et al., 2004).

As with most forages, there is a tradeoff between bermudagrass DM yield, which is related closely to nutrient removal (Robinson, 1996; Pant et al., 2004), and forage nutritive value; the more mature the forage, the lower the nutritive value (Trlica, 2006; Read et al., 2018). In bermudagrass, a 4- to 5-week harvest (or regrowth) interval provides a reasonable compromise between attaining DM yield and enhancing the amounts of crude protein and digestible DM, which are vital components that determine forage nutritive value (Burton and Hanna, 1995). In a Georgia study that fertilized Coastal bermudagrass with 672 kg ha^{-1} N (as NH_4NO_3), prolonging the harvest interval from 4 to 8 weeks decreased crude protein from approximately 172 to 117 g kg^{-1} (a 32% decrease) and digestible DM from around 592 to 523 g kg^{-1} (a 12% decrease) (Monson and Burton, 1982). Results of the present study indicate harvesting every 6, 8 or 10 weeks, when plants are at a more advanced stage of maturity, is a best management practice in situations where manure nutrient management is of a more significant concern than forage nutritive value. The present study comprised two harvest periods, the first was from 1 May to 10 July and the second was from 10 July to 18 September. In a 3-yr study on common bermudagrass fertilized with approximately 10 cm ha^{-1} yr^{-1} swine effluent, Brink et al. (2005)

harvested forage at weekly intervals during two, 9-week harvest periods in either spring, from April to June, or summer, from June to August. They reported the spring harvest period was the best time to maximize nutrient uptake through delaying bermudagrass harvest to more mature growth stages.

When data were averaged across years, an increase in cutting height from 3 to 9 cm decreased DM yield by approximately 19, 17, and 27% in 2001, 2002, and 2003, respectively. The significant harvest interval x cutting height interaction in 2002 and 2003 is attributed chiefly to the smaller decrease in DM yield with 3-cm stubble height at the 4-week harvest interval, as compared to harvesting less frequently (Figs. 1-3). Results for cutting height agree with Aiken et al. (1995) who harvested mixtures of Coastal bermudagrass and crabgrass [*Digitaria sanguinalis* (L.) Scop.] at 2.5-, 10-, and 18-cm stubble heights at harvest intervals of 1, 2, 3, 4, and 8 weeks and reported a linear decrease in DM yield as cutting height increased. Although the highest cutting height in that study enhanced bermudagrass-crabgrass nutritive value, meaning more of the forage could be consumed by ruminant livestock, this practice substantially compromised annual DM production and was not recommended. While leaving a tall stubble reduces DM yield per cutting, Morgan and Brown (1983) found that it preserves more leaf area, which may enable an extra cutting through improved light interception by the stand during the growing season.

At present, swine producers in Mississippi may apply effluent between 1 April and 31 October. This interval extends beyond the most active period of growth of bermudagrass (Brink et al., 2005). Read et al. (2008) determined that the N and P in swine effluent applied too late in the growing season, particularly at the high rate of 20 cm yr^{-1}, is less likely to be utilized by the bermudagrass forage. They reported low values for nitrogen-use efficiency (the amount of N recovered per unit of N applied) in the order of 30-38% for effluent applications in August-September increase the risk to surface and groundwater quality from excess N remaining in the soil. In that study, phosphorus-use efficiency was least in the August-September effluent timing and averaged 14% at the 10 cm yr^{-1} rate and 10% at the 20 cm yr^{-1} rate, suggesting late-season applications could increase the rate of soil P accumulation, particularly at the highest effluent rate and under low rainfall conditions that decrease optimal plant growth and N availability. Results inform producers who consider lowering the volume of effluent in a lagoon to avoid overflow during the winter (McFarland et al., 2000) through increasing irrigation rates during a dry, late-fall period.

CONCLUSIONS

This study determined the combined effects of harvest interval and cutting height on yields of biomass and nutrients in common bermudagrass irrigated in summer with swine-lagoon effluent. In general, the rate of P uptake closely followed trends in DM yield. Cutting height of 3 cm consistently increased DM yield and nutrient uptake, as compared to 9 cm. If the goal is to maximize nutrient uptake, harvest at 6 to 10-week intervals and as close to the ground as possible to maximize biomass yield. If the goal is to produce high-quality forage, bermudagrass should be cut frequently (< 5-wk interval) and as tall as practical to harvest more leaf tissue. These results provide information to land managers on methods to enhance bermudagrass uptake of N and P and thereby reduce the loss of these nutrients from hay fields.

DISCLAIMER AND EEO STATEMENT

Mention of trade names or commercial products in this publication is solely for the purpose of providing specific information and does not imply recommendation or endorsement by the U.S. Department of Agriculture.

USDA is an equal opportunity provider and employer.

LITERATURE CITED

Adeli A, Varco JJ. Swine lagoon effluent as a source of nitrogen and phosphorus for summer forage grasses. Agron. J. 2001; 93: 1174-1181.

Aiken GE, Sladden SE, Bransby DI. Cutting height and frequency effects on composition, yield, and quality of a bermudagrass-crabgrass mixture. J. Prod. Agric. 1995; 8: 79-83.

Brink GE, Rowe DE, Sistani KR, Adeli A. Bermudagrass cultivar response to swine effluent application. Agron. J. 2003; 95: 597-601.

Brink GB, Sistani KR, Rowe DE. Nutrient uptake of hybrid and common bermudagrass fertilized with broiler litter. Agron. J. 2004; 96: 1509-1515.

Brink GE, Pederson GA, Sistani KR. Nutrient uptake of swine effluent-fertilized bermudagrass during primary spring and summer growth. J. Plant Nutr. 2005; 8: 1337-1346.

Burton GW, Hanna WW. Bermudagrass. In: R.F. Barnes, D.A. Miller, and C.J. Nelson, editors, Forages: An introduction to grassland agriculture. 1995, Vol. 1, 421-430. Iowa State Univ. Press, Ames, IA, USA.

King LD, Westerman PW, Cummings GA, Overcash MR, Burns JC. Swine lagoon effluent applied to 'Coastal' bermudagrass: II. Effects on soil. J. Environ. Qual. 1985; 14: 14-21.

McFarland AMS, McFarland MJ, Sweeten JM. Dairy lagoon design and management under chronic rainfall. App. Eng. Agric. ASAE Publ. 2000, 16: 285-292.

Monson WG, Burton GW. Harvest frequency and fertilizer effects on yield, quality, and persistence of eight bermudagrasses. Agron. J. 1982, 74: 371-374.

Morgan JA, Brown RH. Photosynthesis and growth of bermudagrass swards. I. Carbon dioxide exchange characteristics of swards mowed at weekly and monthly intervals. Crop Sci. 1983; 23: 347-352.

Osmond DL, Kang J. 2008. Nutrient Removal by Crops in North Carolina. AG-493-16W. North Carolina Cooperative Extension Service, Raleigh, NC, USA. Available online at http://content.ces.ncsu.edu/20688.pdf (accessed 30 September 2019).

Pant HK, Adjei MB, Scholberg JMS, Chambliss CG, Rechcigl JE. Forage production and phosphorus phytoremediation in manure-impacted soils. Agron. J. 2004; 96: 1780-1786.

Pederson GA, Brink GE, Fairbrother TE. Nutrient uptake in plant parts of sixteen forages fertilized with poultry litter: Nitrogen, phosphorus, potassium, copper, and zinc. Agron. J. 2002; 94: 895-904.

Read JJ, Lang DJ, Adeli A, Jenkins JN. Harvest management effects on 'Tifton 44' bermudagrass phosphorus removal and nutritive value. Agron. J. 2018; 110: 879-889.

Read JJ. Spring nitrogen fertilization of ryegrass-bermudagrass for phytoremediation of phosphorus-enriched soils. Agron. J. 2012; 104: 908-916.

Read JJ, Brink GE, Adeli A, McGowen SL. Swine effluent application timing and rate affect nitrogen use efficiency in common bermudagrass. J. Environ. Qual. 2008; 37: 180-189.

Robinson DL. Fertilization and nutrient utilization in harvested forage systems: Southern forage crops. In: RE. Joost and CA. Roberts, editors, Nutrient cycling in forage systems. Potash and Phosphate Inst., Norcross, GA, USA. 1996, p. 65-92.

SAS Institute. SAS/STAT User's Guide. 2010. Version 9.3 edition, SAS Inst., Inc., Cary, NC.

Trlica MJ. 2006. Grass Growth and Response to Grazing. Colorado State University Extension Publication no. 6.108. Fort Collins, CO, USA. Available online at https://extension.colostate.edu/docs/pubs/natres/06108.pdf (accessed 30 September 2019).

USDA-NRCS. Soil Survey of Clay County, Mississippi. Soil Survey Staff, Natural Resources Conservation Service, United States Department of Agriculture. Web Soil Survey. 1976, Available online at http://websoilsurvey.nrcs.usda.gov (accessed 30 September 2019).

Temperature Effects on Soybean Seedling Shoot and Root Growth and Developmental Dynamics

Firas Ahmed Alsajri[a,b], Chathurika Wijewardana[a], Ryan Rosselot[a], Bhupinder Singh[c], L. Jason Krutz[d], Wei Gao[e], and K. Raja Reddy[a]*

[a]Department of Plant and Soil Sciences, 117 Dorman Hall, Mississippi State University, Mississippi State, MS 39762, USA, [b]Field Crops Dept., Tikrit University, Tikrit, Iraq, [c]Delta Research and Extension Center, Box 197, Stoneville, MS 38776,, USA, [d]Mississippi Water Resources Research Institute, Mississippi State University, Mississippi State, MS 39762, USA, [e]Wei Gao, USDA-UV-B Monitoring Network, Natural Resource Ecology Lab., Colorado State University, Fort Collins, CO 80521, USA

Corresponding Author: K. Raja Reddy, E-mail: krreddy@pss.msstate.edu

ABSTRACT

Temperature affects plant growth at all stages, and it is important to quantify soybean early-season responses to a wide range of temperatures. This research was conducted to determine whether seedlings of two soybean cultivars with different growth habits respond differently to increasing temperature. The effect of five day/night temperature regimes of 20/12, 25/17, 30/22, 35/27, and 40/32 °C on the below- and aboveground growth and development of Asgrow AG5332 (AG) and Progeny P5333 RY (PR) soybean cultivars with an indeterminate and determinate growth habit, respectively, were evaluated under controlled conditions from seedling emergence to 21 days after sowing. Temperature and cultivar interacted to affect plant height, root surface area, and root tips, while the main cultivar effect influenced the number of mainstem nodes and root volume. For all other root and shoot parameters, the main temperature effect was significant. Our analysis indicated that from emergence until 21 days after sowing, the evaluated root and shoot parameters for the cultivars responded similarly to increasing day/night temperature regime, and plant responses to temperature were best described by quadratic functions. The functional algorithms developed during this research should be incorporated into crop simulation models to help predict the effect of increasing temperature on the growth and development of soybean across the US.

Keywords Early-season growth, root traits, temperature stress, WinRHIZO, soybean

Abbreviations: AG, Asgrow AG5332; PR, Progeny P5333 RY; PVC, Polyvinyl chloride; DAS, Days after sowing; SPAR, Soil–plant–atmosphere–research; VPD, Vapor pressure deficit; ET, Evapotranspiration

INTRODUCTION

Soybean (*Glycine max* L. Merr.) is one of the important oilseed crops, with the considerable demand for processed soybean meals for the animal feed industry, soybean oil for human consumption, and biofuels. World soybean production has increased by 4.6% annually from 1961 to 2007 (Masudaa and Goldsmith, 2009) and reached 337.5 million metric tons (MMT) in 2017/18 (USDA, 2018). The United States was the world's largest producer of soybean grains with an estimated production of 120.04 MMT, followed closely by Brazil (119.80 MMT) and less so by Argentina (37.80 MMT) (USDA, 2018).

Climate models are projecting that temperatures across the globe will increase drastically over this century and will likely hurt global food security (Rosenzweig and Parry, 1994). Temperature is a major abiotic factor that can influence soil condition and variety in ways that can affect crop growth and development (Cober et al., 2014; George et al., 1990; Kurosaki and Yumoto, 2003; Setiyono et al., 2007; Thuzar et al., 2010). Accordingly, temperature effects on the growth and development of agriculturally essential plants must be elucidated for us to navigate climate change and ensure enough food, fiber, and fuel for an increasing global population (Hatfield and Prueger, 2015; Rosenzweig and Parry, 1994; Schlenker and Roberts, 2009).

Temperature varies spatially and temporally across the Soybean Belt, which affects the planting date

(Heatherly and Hodges, 1999). The planting window for soybean in the Midsouth ranges from April to June (Hoeft et al., 2000). However, in the last two decades, producers started to adopt the early soybean production system along with narrow row culture by planting soybean cultivars of Maturity Group V and IV from late March to early April (Heatherly and Hodges, 1999). Past changes in climate and improved cold tolerance of soybean and other crops (Koti et al., 2007; Salem et al., 2007; Wijewardana et al., 2015) might have helped adopt the early-season planting changes in soybean and other crops in the US Midsouth (Alsajri et al., 2019; Heatherly and Hodges, 1999; Singh et al., 2018). Early-planting of soybeans could potentially minimize yield losses avoiding high temperatures during flowering pod developing stage and low precipitation days during crop production system (Hoeft et al., 2000). Board and Settimi (1986) have accessed the differential response of soybean cultivars differing in maturity groups to cultural practices, including plant population density, row spacing, latitudes, and planting date. These studies concluded late maturing (MG V- VIII) determinate cultivars grown with wide row spacing (> 0.8 m row width) are well suited for the southern US States; whereas, indeterminate early maturing cultivars (MG 1- III) grown with narrow row spacing are suited for northern US states (> 35 ºN). Further, late maturity soybean cultivars differing in growth habits have also been evaluated for cultural practices based on late-season vegetative and reproductive growth (Parvez et al., 1986). The above studies have exploited plant morphological and developmental characteristics, including plant height, mainstem nodes, shoot biomass, stand counts, and soybean yields for accessing differential responses to cultural practices resulting from maturity and growth habit. Recent studies have also recognized the effects of low and high temperatures at different stages of soybean-based on plant morphological and physiological characteristics (Alsajri et al., 2020; Edwards, 1934; Lin et al., 1984; Sinclair et al., 1991; Tacarindua et al., 2013). However, the literature on responses of early maturing soybean cultivars differing in growth habit to varying temperatures is limited. Moreover, the influence of temperature on early-season soybean growth and development, particularly root growth dynamics and quantitative functional relationships between temperature and crop growth processes, are not well understood.

Temperature plays a dominant role in defining seedling growth and development of soybean cultivars in a given location with minimum interaction of photoperiod (Setiyono et al., 2007). The optimum temperature range for reproductive growth of soybeans is 23 to 39 °C, depending upon the type of maturity groups (Egli, 1980; Salem et al., 2007); however, limited information is available comparing cardinal temperatures for the early seedling stage of soybean with determinate and indeterminate growth habits.

Because vegetative growth at the stem apex ends before reproductive growth initiates in determinate soybean, high temperature may lead to an imbalance between reproductive and vegetative growth (Setiyono et al., 2007; Hampton et al., 2013). In contrast, indeterminate growth can slow reproductive growth through a modification of plant habit. The inflorescence on the auxiliary meristem coexist with the nodes bearing trifoliate leaves at the stem apex in indeterminate growth, and is, therefore, an advantageous trait under high temperatures (Setiyono et al., 2007). The determinate soybean cultivar with enhanced photosynthetic fixation and its translocation to reproductive structures could provide tolerance to high temperatures during reproductive growth. On the other hand, soybean seedlings exposed to low temperatures during early-season planting may lengthen the vegetative growth rate and increase the number of axillary branches; however, responses are cultivar specific. Such subsequent reactions could avoid exposure of soybean to low temperatures at the reproductive growth stage. Thus, plant growth and development characteristics in soybean are useful tools to ascribe specific growth habit responses to changes in temperature. The objectives of this study were to investigate seedling growth and development responses to a wide range of temperatures in soybeans differing in growth habit and to provide functional algorithms between temperature and crop growth processes, including root traits. This study hypothesized that differential tolerance to temperature in soybean seedlings is due to the

inherent difference in growth habit between determinate and indeterminate cultivars.

MATERIALS AND METHODS

This research was conducted in the Soil–Plant–Atmosphere–Research (SPAR) units located at the Rodney Foil Plant Science Research Center (Reddy et al., 2001), Mississippi State University, MS, USA during 2014 growing season. The experimental design was a two × five factorial with six replicates. The first factor was cultivar and included two Maturity Group V cultivars with different growth habits, Asgrow AG 5332 (AG), an indeterminate cultivar, and Progeny P5333 RY (PR) a determinate cultivar. The second factor was temperature and included five different day/night regimes of 20/12, 25/17, 30/22, 35/27, and 40/32 °C that were achieved through thermostatic settings for the five SPAR units. The daytime temperature was initiated at sunrise and returned to the nighttime temperature one after sunset.

Seeds were planted 1.5 to 2 cm deep in 15.2-cm diameter by 30.5-cm high PVC (polyvinyl chloride) pots. The pots contained 0.5 kg gravel at the bottom and were backfilled with a 3:1 mixture (v/v) of topsoil and sand. Plants were fertilized with full-strength Hoagland nutrient solution (Hoagland and Arnon, 1950) by an automated drip irrigation system that delivered nutrients each day at 0700, 1200, and 1700 h. Daily solar radiation was recorded with a pyranometer (Model 4-8; The Eppley Laboratory Inc., Newport, RI). Temperature treatments were imposed at emergence, 8 days after sowing (DAS), through harvest, 21 DAS. The environmental conditions, day/night average temperatures, vapor pressure deficit (VPD), evapotranspiration (ET), and carbon dioxide concentration [CO_2] were controlled during the experiment (Table 1).

Table 1. The chamber temperature setting and the measured average day/night temperature, vapor pressure deficit (VPD), evapotranspiration (ET), and [CO_2] for five SPAR units during the experimental period.

Day/night temperature settings, °C	Sunlit growth chambers environmental conditions			
	Mean Day/night temperature, °C	Mean daily VPD, kPa	Mean daily ET, L m^{-2} d^{-1}	CO_2, µmol mol^{-1}
20/12	17.1e	1.17d	6.5c	414a
25/17	21.8d	0.93e	6.6c	414a
30/22	28.0c	2.32c	10.6a	411a
35/27	31.2b	3.02b	8.9b	410a
40/32	35.6a	3.61a	9.1b	411a

Different lower-case letters within the column are significantly different at $P<0.05$ and compared the temperature treatment effects on the given parameter.

At harvest, shoot and root traits were determined. Plant height and number of mainstem nodes were measured/counted on all plants at the harvest (21 DAS). Stem lengths were estimated as the distance between the cotyledonary node and to the base of the most recently unfolded mainstem leaf. Leaf area was measured using a LI-3100 leaf area meter (Li-COR Inc., Lincoln, Nebraska, USA). Roots were prepared

for scanning with a WinRhizo optical scanner (Regent Instruments, Inc., Quebec, Canada) as previously described (Brand et al., 2016; Reddy et al., 2017; Wijewardana et al., 2015). The root images were then analyzed for total root length, root surface area, root volume, and a number of all the tips, forks, and crossings using the winRHIZO optical scanner and Pro software.

Shoot and root were separated, and the component parts dried in an oven set to 80 °C for three days and then weighed for leaf, stem, and root weights. Aboveground dry weight was calculated as the summation of leaf and stem weights. Total dry weight was calculated as the summation of the aboveground and root dry weight. Root to shoot dry weight ratio also was calculated.

Data Analysis

The data collected were subjected to analysis of variance using the PROC GLM procedure in SAS to determine the effects of temperature, cultivar, and temperature × cultivar interaction (SAS Institute, Inc., Cary, NC). Treatment means were separated using Fisher's protected least significant difference (LSD, $P < 0.05$). The growth and development responses to temperature were derived using best-fit regression functions using Sigma Plot 13.0 (Systat Software Inc., San Jose, CA) based on regression coefficients, $R^{2,}$ and root mean square error.

RESULTS AND DISCUSSION

A central hypothesis was differential tolerance to varying temperatures in soybean seedlings is due to the inherent difference between determinate and indeterminate growth habits. A temperature by cultivar interaction was observed for plant height, such that PR, with determinate growth habit, exhibited greater plant height than AG under high temperatures (Table 2 and Figure 1A). The number of mainstem nodes also was higher in PR than AG (Table 2 and Figure 1B). Past studies have recognized both increase and decrease in plant height and node numbers in response to planting time, growth habit, and maturity group. For instance, Gricher and Biles (2014) observed an increase in plant height of soybean when planting was delayed from February until mid-March in Texas. Still, no difference was observed when planting was delayed from mid-March until April.

Table 2. Results from analysis of variance for soybean morphological parameters in two cultivars measured 21 days after sowing with five temperature regimes imposed eight days after planting.

Source of variation	Treatment		
	Temperature	Cultivar	Temperature x cultivar
Plant height	***	***	**
Mainstem nodes	***	**	ns
Leaf area	***	ns	ns
Root dry weight	***	ns	ns
Total dry weight	***	ns	ns
Root-shoot ratio	***	ns	ns
Root length	***	ns	ns
Root surface	***	ns	*
Root volume	***	**	ns
Root forks	***	ns	ns
Root crossing	***	ns	ns
Root tips	***	**	***

*, **, and ***, indicates significance at 0.05, 0.01, 0.001 probability level respectively, and ns indicates non-significance.

In contrast, Board and Settimi (1986) and Parvez et al. (1989) observed a reduction in plant height and node number when planting was delayed. Parvez et al. (1989) also found greater plant height and node number at the time of harvest in indeterminate cultivar (MG VII) than determinate cultivar (MG VIII) under field conditions. The contradiction in the results of the present study from above field studies could be explained from the confounding influence of photoperiod, maturity groups, and cultural practices on the growth and development of soybean. Overall, a greater number of mainstem nodes bearing a corresponding number of vegetative branches in determinate growth cultivar would enable greater photosynthate assimilation and translocation to develop reproductive structures upon flowering. Such traits may be an effective heat tolerance mechanism for cultivars with determinate growth habit. In contrast, a reduced number of mainstem nodes in indeterminate growth cultivars may reduce the ratio of photosynthetic source to the magnitude of the reproductive structure during the flowering stage, thus making the whole plant structure more sensitive to heat stress and producing less grain yield.

Conversely, only the temperature main effect was significant on leaf area, leaf dry weight, and shoot dry weight (Table 2 and Figure 1C), which indicates that the effect of temperature on these parameters was similar between cultivars. Regardless of cultivar, the impact of temperature on all shoot parameters was described by a quadratic function. Generally, shoot parameters increased with temperature up to 33 °C, at which point temperature began to slow plant growth and development. Plant height, mainstem nodes, and leaf area for both cultivars increased with increasing temperature up to their optimum and then slightly declined with further increase in temperature (Fiure 1A, B, and C).

Similar effects of temperature on shoot growth and development are reported for soybean cultivars with different growth habit when planted in different planting dates (Alsajri et al., 2019; Wilcox et al., 1987), in cotton (Reddy et al., 2017; Singh et al., 2018), and corn (Wijewardana et al., 2015). Low temperatures affect node addition rate and cell elongation and division leading to shorter plants (Stitt and Hurry, 2002), and consequently, lower overall canopy development. Conversely, high temperatures caused a range of physiological, morpho-anatomical, and biochemical changes in plants (Crafts-Brandner and Michael, 2002; Kotak et al., 2004; Larkindale and Knight, 2002). Leaves being the primary source of carbohydrates, the importance of canopy leaf area development during the vegetative growth period was correlated well with yield traits in the past. Therefore, understanding the effect of abiotic stresses such as low or high temperature on leaf area development at different growth stages has been considered useful for producers.

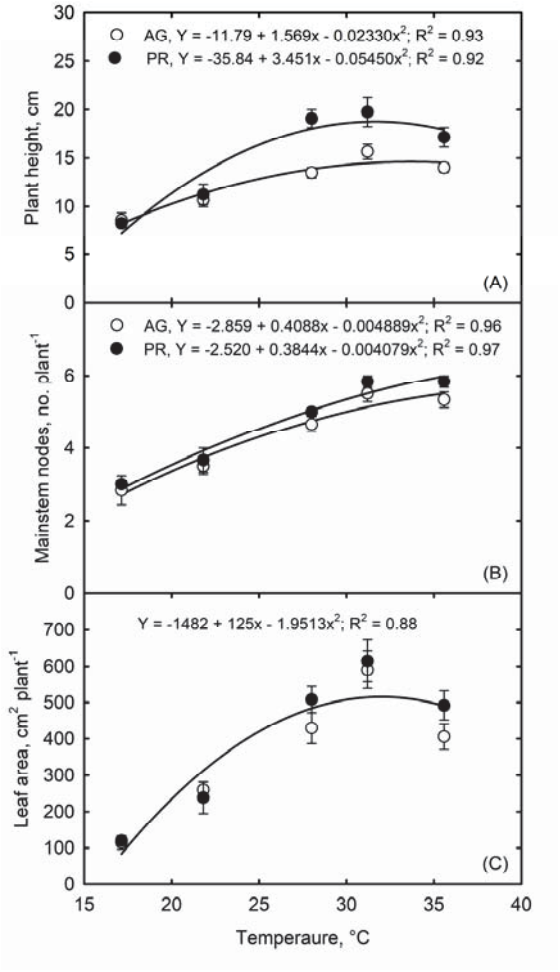

Figure 1. Temperature effects on two soybean cultivars, Asgrow AG5332 with indeterminate and Progeny P5333 RY with determinate growth habits, (A) plant height, (B) mainstem nodes, and (C) leaf area at 21 days after sowing.

Root Traits

As with soybean shoots, we postulated that the root response to heat stress would differ between determinate and indeterminate cultivars. Contrary to our hypothesis, the response of most root parameters to temperature was similar between the cultivars (Table 2). The two exceptions were root surface area and the number of root tips whereby a cultivar by temperature interaction and the main cultivar effect was significant. The root surface area and root tips maintained by PR under high temperatures may maintain its hydraulic conductance and simultaneous water uptake (Alsajri et al., 2019). For all cultivars, a quadratic model described the effect of temperature on all root parameters. Similar to the shoot response, all root parameters for both cultivars increased with temperature up to approximately 30 °C and then decreased as temperature increased. Like the shoot traits, root biomass increased with increasing temperature up to optimum levels and then slightly decreased (Figure 2). High correlation was observed between temperature and root growth and development traits including root tips (R^2 = 0.83 for AG; 0.70 for PR), root forks (R^2 = 0.84), root crossings (R^2 = 0.82) (Figure 3A, B, and C) root length (R^2 = 0.83), root surface area (R^2 = 0.84), and root volume (AG, R^2 = 0.93; PR, R^2 = 0.82) (Figure 4A, B, and C). Optimum temperatures for most root traits were around 29 °C, which is slightly lower than the optimum temperatures for shoot traits. In general, the lowest temperature regime, 20/12 °C, had a greater reduction in root length, 58%, root surface area, 56%, and root volume, 51%, compared with the maximum value at optimum temperature. Plants grown at the highest temperature regime, 40/33 °C, showed reductions in root length, root surface area, and root volume by 23, 25, and 24%, respectively. The root system for the two cultivars was impacted similarly; however, root volume was significantly greater in AG than PR cultivar (Figure 4C). Increasing temperatures rapidly increased the growth and development in soybean shoot and root system parameters. This increment reached its' peak level at the optimum temperature, which varied among the traits, and it decreased with elevated temperature

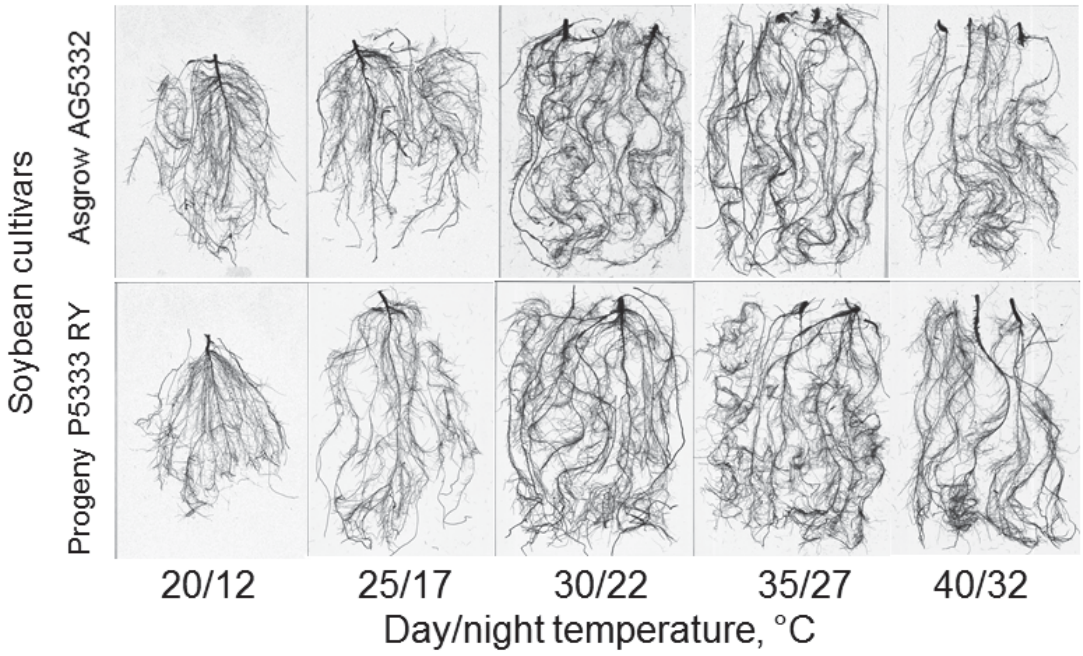

.

Figure 2. Pictorial representation of root images for two soybean cultivars, Asgrow AG5332 with indeterminate and Progeny P5333 RY with determinate growth habits, grown in five SPAR units set at different day/night temperature regimes and harvested 21 days after sowing.

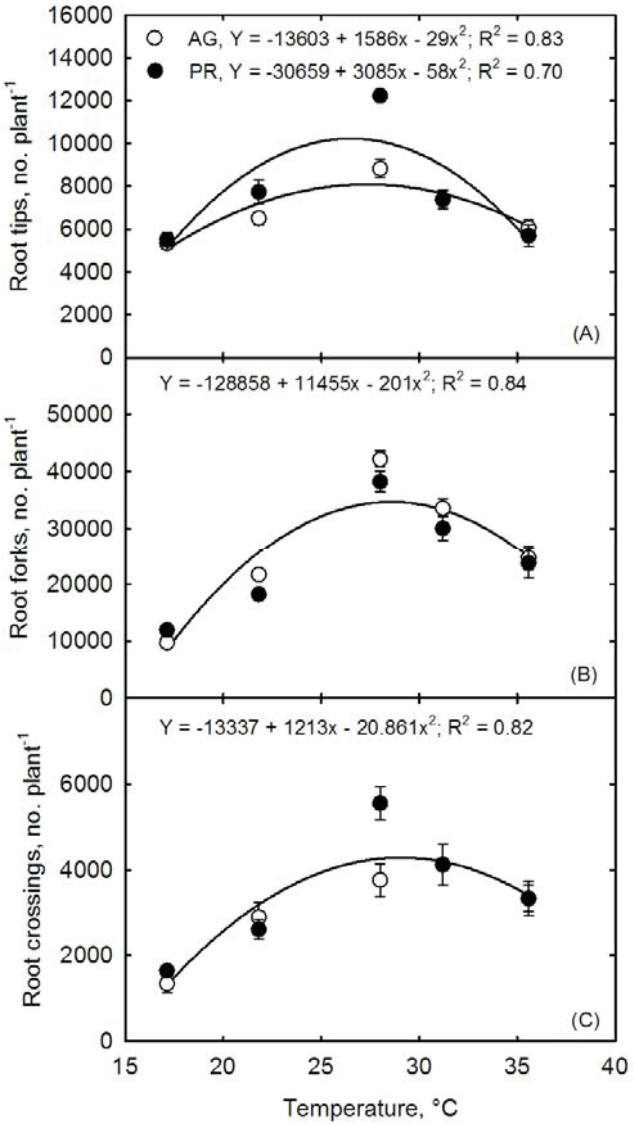

Figure 3. Temperature effects on two soybean cultivars, Asgrow AG5332 with indeterminate and Progeny P5333 RY with determinate growth habits, (A) root tips, (B) root forks, (C) root crossings 21 days after sowing. Temperature treatments were imposed eight days after planting. Each data point is the mean of six replications, and the standard error of the mean is shown if larger than the corresponding symbol.

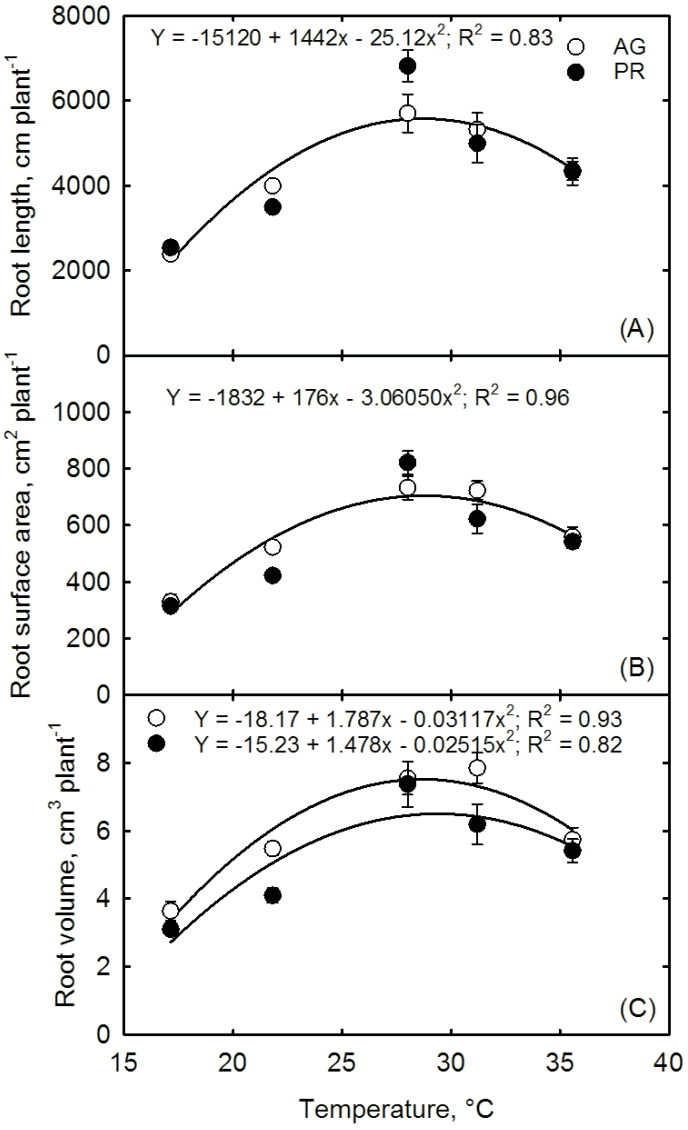

Figure 4. Temperature effects on two soybean cultivars, Asgrow AG5332 with indeterminate and Progeny P5333 RY with determinate growth habits, (A) root length, (B) root surface area, and (C) root volume at 21 days after sowing. Temperature treatments were imposed eight days after planting. Each data point is the mean of six replications, and the standard error of the mean is shown if larger than the corresponding symbol.

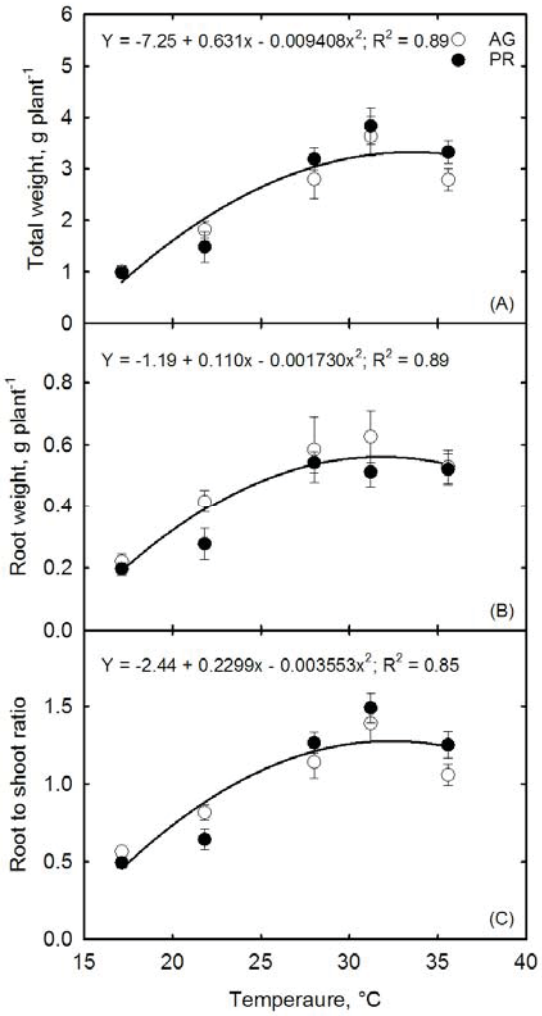

Figure 5. Temperature effects on two soybean cultivars, Asgrow AG5332 with indeterminate and Progeny P5333 RY with determinate growth habits, (A) total dry weight, (B) root weight, and (C) root-shoot ratio at 21 days after sowing. Temperature treatments were imposed eight days after planting. Each data point is the mean of six replications, and the standard error of the mean is shown if larger than the corresponding symbol.

Recent studies had made use of the root phenotype systems to study the effect of abiotic stresses like temperature and drought on seedling growth in various crops (Alsajri et al., 2019; Brand et al., 2016; Reddy et al., 2017; Singh et al., 2017, 2018; Wijewardana et al., 2015, 2018). Root length, root surface area, root diameter, and root volume are useful parameters describing the root performance under varied stress conditions and nutrient uptake efficiency (Alsajri et al., 2019; Rosolem and Assis, 1994; McMichael et al., 2010; Hammer et al., 2009). These traits are general indicators of the root functions and size (Costa et al., 2002).

Biomass

The cultivar x temperature interaction was not significant total weight, root weight, and root to shoot ratio (Table 2), suggesting a similar response to temperature for indeterminate and determinate growth habits. The observed increases in total weight, root weight, and root to shoot ratio as temperature increased were best described by the same quadratic trend in both cultivars (Figure 5A, 5B, and 5C). The same result for the maximum total weight for one of the soybean cultivars was observed at 25 °C soil temperature, which is considered as optimum temperature (Lindemann and Ham, 1979); however, the optimum temperature for maximum total weight in this study was 34 °C (Figure 5A). Root weight and root to shoot ratio were optimized at 32 °C (Figure 5B and 5C). Similar to the present study, Reddy et al. (2017) reported significant biomass partitioning towards roots in young cotton plants and Wijewardana et al. (2015) in corn. The increase in plant biomass with increasing temperature is mostly derived from rising rates of mitochondrial respiration (Setiyono et al., 2007). Similarly, the reduction in shoot and root biomass at low temperatures in soybean potentially corresponds to a decrease in respiration and, subsequently, less net dry matter accumulation when compared with growth at high temperatures (Hatfield et al., 2011). Besides mitochondrial respiration, past studies have recognized a reduced rate of imbibition and expansion of embryo tissue under low temperatures, which might contribute to a reduction in seedling biomass. Results of the present study support slowed vegetative growth of soybean planted in early-season (before May) compared to late-season planting in May or later (Heatherly and Hodges, 1999). For instance, Heatherly (1996) reported that blooming in

soybean occurred five days earlier for the crop planted in May than at a later planting date, and was primarily influenced by higher temperature and dry soil conditions. The reduced growth under low and high temperatures than optimum temperature may be advantageous to avoid respiration costs and to balance growth accumulation (Alsajri et al., 2019; Hatfield and Prueger, 2015). In contrast to the present study, Parvez et al. (1989) observed greater biomass in determinate than indeterminate soybean, which may have resulted from differences in planting patterns and photoperiod between the two studies. Also, the total seedling biomass at an optimum temperature in the present study had proportionally more root than shoot growth, which might be due to the 'priorities' of the seedling establishment stage.

CONCLUSIONS

The results of the study revealed a significant impact of increasing temperatures on soybean shoot and root traits at the seedling growth stage. Both cultivars showed a quadratic increase in measured growth and development traits to rising temperatures. Cultivar PR, with determinate growth habit, had greater plant height, root tips, and mainstem leaves across temperatures than AG, with indeterminate growth habit; however, PR had less root volume. The information from this study on temperature-dependent below- and aboveground growth and developmental functions will be beneficial to improve soybean simulation models for early vegetative growth response to elevated temperature in the current and projected warmer climate. The modeled data obtained for seedling growth in this study will guide producers in soybean management decisions for the present and future environment.

CONFLICT OF INTEREST

There is no conflict of interest to declare.

ACKNOWLEDGEMENT

We thank David Brand for technical assistance and graduate students of the Environmental Plant Physiology Lab at Mississippi State University for their support during data collection. We also thank the Mississippi Soybean Promotion Board and the National Institute of Food and Agriculture, NIFA 2016-34263-25763, and MIS 043040 for partial funding for this research.

LITERATURE CITED

Alsajri FA, Singh B, Wijewardana C, Irby JT, Wei G, Reddy KR. Evaluating soybean cultivars for low- and high-temperature tolerance during the seedling growth stage. Agronomy 2019; 9: 13.

Alsajri FA, Wijewardana C, Irby JT, Bellaloui N, Krutz LJ, Golden B, Gao G, Reddy KR. Developing functional relationships between temperature and soybean yield and seed quality. Agron. J. 2020; 112: 194-204.

Board JE, Settimi JR. Photoperiod simulation and branch development in soybean. Agron. J. 1986; 78: 995-1002.

Brand D, Wijewardana C, Gao G, Reddy KR. Interactive effects of carbon dioxide, low temperature, and ultraviolet-B radiation on cotton seedling root and shoot morphology and growth. Front. Earth. Sci. 2016; 10: 607–620.

Cober ER, Curtis DF, Stewart DW, Morrison MJ. Quantifying the effects of photoperiod, temperature and daily irradiance on flowering time of soybean isolines. Plants 2014; 3: 476-497.

Costa C, Dwyer LM, Zhou X, Dutilleul P, Hamel C, Reid LM, Smith DL. Root morphology of contrasting maize genotypes. Agron. J. 2002; 94: 96-101.

Crafts-Brandner SJ, Michael ME. Sensitivity of photosynthesis in a C4 plant, maize, to heat stress. Plant Physiol. 2002; 129:1773-1780.

Edwards TL. Relations of germinating soybeans to temperature and length of incubation time. Plant Physiol. 1934; 9: 1-30.

Egli, D.B., I.F. Wardlaw. Temperature response of seed growth characteristics of soybean. Agron. J. 72 (1980) 560–564

George T, Bartholomew DP, Singleton PW. Effect of temperature and maturity group on phenology of field grown nodulating and nonnodulating soybean isolines. Biotronics 1990; 19: 49-59.

Grichar WJ, Biles PS. Response of soybean to early-season planting dates along the upper Texas Gulf Coast. Int. J. Agron. 2014; ID 252563. https://doi.org/10.1155/2014/252563

Hammer GL, Dong Z, McLean G, Doherty A, Messina C, Schussler J, Zinselmeier C, Paszkiewic S, Cooper M. Can changes in canopy and/or root system architecture explain historical maize yield trends in the US Cornbelt? Crop Sci. 2009; 49: 299-312.

Hampton JG, Boelt B, Rolston MP, Chastain TG. Effects of elevated CO_2 and temperature on seed quality. J. Agric. Sci. 2013; 151: 154-162.

Hatfield JL, Prueger JH. Temperature extremes: Effect on plant growth and development. Weather Clim.

Extrem. 2015; 10: 4-10.

Hatfield JL, Prueger JH. Temperature extremes: Effect on plant growth and development. Wea. Cli. Ext. 2015; 10: 4-10.

Hatfield JL, Boote KJ, Kimball BA, Ziska LH, Izaurralde RC, Ort D, Thomson AM, Wolfe DW. Climate impacts on agriculture: implications for crop production. Agron. J. 2011; 103: 351-370.

Heatherly LG. Yield and germinability of seed from irrigated and non-irrigated early-and late-planted MG IV and V soybean. Crop Sci. 1996; 36: 1000-1006.

Heatherly LG, Hodges HF. Early soybean production system (ESPS). In: Soybean Production in the Midsouth; Heatherly, L.G., Hodges, H., Eds.; CRC Press: Boca Raton, FL, USA, 1999; 103-118 p.

Hoagland DR, Arnon DI. The water-culture method for growing plants without soil. The College of the Agriculture, 1950; University of California Berkeley, CA, USA.

Hoeft RG, Aldrich SR, Nafziger ED, Johnson RR. Modern corn and soybean production (1st ed.). MCSP Publications, Champaign, IL, USA, 2000.

Kotak S, Larkindale J, Lee U, Von Koskull-Doring P, Vierling E, Scharf KD. Complexity of the heat stress response in plants. Curr. Opin. Plant Biol. 2007; 10: 310-316.

Koti S, Reddy KR, Kakani VG, Zhao D, Gao W. Effects of carbon dioxide, temperature and ultraviolet-B radiation and their interactions on soybean (*Glycine max* L.) growth and development. Environ. Exp. Bot. 2007; 60: 1-10.

Kurosaki, H., S. Yumoto. Effects of low temperature and shading during flowering on the yield components in soybeans. Plant Prod. Sci. 2003; 6: 17-23.

Larkindale J, Knight MR. Protection against heat stress-induced oxidative damage in *Arabidopsis* involves calcium, abscisic acid, ethylene, and salicylic acid. Plant Physiol. 2002; 128: 682-695.

Lin CY, Roberts JK, Key JL. Acquisition of thermotolerance in soybean seedlings synthesis and accumulation of heat shock proteins and their cellular localization. Plant Physiol. 1984; 74: 152-160.

Lindemann WC, Ham GE. Soybean plant growth, modulation, and nitrogen fixation as affected by root temperature. Soil Sci. Soc. Am. J. 1979: 43: 1134-1137.

Masudaa T, Goldsmith PD. World soybean production: Area harvested yield, and long-term projections. Int. Food Agribus. Man. Rev. 2009; 12: 143-162.

McMichael, BL, Oosterhuis DM, Zak JC, Beyrouty CA. Growth and development of root systems. In: J. McD. Stewart et al. (Eds), Physiology of cotton. 2010; Springer, New York, 2010; 57-71p.

Parvez AQ, Gardner FP, Boote KJ. Determinate and indeterminate-type soybean cultivar responses to pattern, density, and planting date. Crop Sci. 1989; 29: 150-157.

Reddy KR, Brand D, Wijewardana W, Gao W. Temperature effects on cotton seedling emergence, growth, and development. Agron. J. 2017; 109: 1379-1387.

Reddy KR, Hodges HF, Read JJ, McKinion JM, Baker JT, Tarpley L, Reddy VR. Soil-plant–atmosphere-research (SPAR) facility: A tool for plant research and modeling. Biotronics 2001; 30: 27-50.

Rosenzweig C, Parry ML. Potential impact of climate change on world food supply. Nature 1994; 367: 133-138.

Rosolem, C.A., J.S. Assis, A.D. Santiago. Root growth and mineral nutrition of corn hybrids as affected by phosphorus and lime. Commun. Soil Sci. Plant Anal. 25 (1994) 2491–2499.

Salem MA, Kakani VG, Koti S, Reddy KR. Pollen-based screening of soybean genotypes for high temperature. Crop Sci. 2007; 47: 219-231.

Schlenker W, Roberts MJ. Nonlinear temperature effects indicate severe damages to US crop yields under climate change. Proc. Natl. Acad. Sci. 2009; 106: 5594-15598.

Setiyono TT, Weiss A, Specht J, Bastidas AM, Cassman KG, Dobermann A. Understanding and modeling the effect of temperature and day-length on soybean phenology under high-yield conditions. Field Crops Res. 2007; 100: 257-271.

Sinclair, T.R., S. Kitani, K. Hinson, J. Bruniard, T. Horie. Soybean flowering date: linear and logistic models based on temperature and photoperiod. Crop Sci. 1991; 31: 786-790.

Singh B, Norvell E, Wijewardana C, Wallace T, Chastain D, Reddy KR. Assessing morphological characteristics of elite cotton lines from different breeding programmes for low temperature and drought tolerance. J. Agron. Crop Sci. 2018: 204: 467-476.

Singh B, Reddy KR, Redona ED, Walker T. Screening of rice cultivars for morpho-physiological responses to early-season soil moisture stress. Rice Sci. 2017; 24: 322-335.

Stitt M, Hurry V. A plant for all seasons: alterations in photosynthetic carbon metabolism during cold acclimation in Arabidopsis. Curr. Opin. Plant Biol. 2002; 5: 99-206.

Tacarindua CRP, Shiraiwaa T, Hommaa K, Kumagaib E,

Sameshimab R. The effects of increased temperature on crop growth and yield of soybean grown in a temperature gradient chamber. Field Crops Res. 2013; 154: 74-81.

Thuzar M, Puteh AB, Abdullah NAP, Lassim MM, Jusoff K. The effects of temperature stress on the quality and yield of soya bean [(*Glycine max* L.) Merrill.]. J. Agric. Sci. 2010; 2:172-179.

USDA. World agricultural supply and demand estimates, economic research service and foreign agricultural service. https://www.fas.usda.gov/data/world-agricultural-production, Assessed Oct. (2018).

Wijewardana C, Reddy KR, Alsajr FA, Irby JT, Krutz J, Golden B. Quantifying soil moisture deficit effects on soybean yield and yield component distribution patterns. Irri. Sci. 2018; 36: 241-255.

Wijewardana C, Hock M, Henry B, Reddy KR. Screening corn hybrids for cold tolerance using morphological traits for early-season seeding. Crop Sci. 2015; 19: 851-867.

Wilcox JR, Frankenberger EM. Indeterminate and determinate soybean responses to planting date. Agron. J. 1987; 79: 1074-1078.

Estimates of Turf-Type Hybrid Bermudagrass Base and Optimal Growth Temperatures

James D. McCurdy[1], Ethan T. Flournoy[2], Barry R. Stewart[1], H. Wayne Philey[1], K. Raja Reddy[1], William C. Kreuser[3], Eric Reasor[1], and Christian M. Baldwin[1]

[1]Department of Plant and Soil Sciences, Mississippi State University, Mississippi State, MS 39762, USA, [2]Deerfield Golf Club, 264 Deerfield Club Dr, Canton, MS 39046, USA, and [3]Department of Agronomy and Horticulture, University of Nebraska, 161 Keim Hall, Lincoln, NE 68583, USA

Corresponding Author: James D. McCurdy, Email address: jmccurdy@pss.msstate.edu

ABSTRACT

Estimates of base and optimal growth temperatures of turf-type hybrid bermudagrass are limited and are prerequisites for model development. An experiment was conducted in sunlit plant growth chambers, known as Soil-Plant-Atmosphere-Research units, to estimate base- and optimal temperatures of 'Latitude 36', 'MSB-285', 'TifEagle,' and 'Tifway' hybrid bermudagrasses by varying day/night temperatures from 20/12 to 40/32°C. Shoot growth was measured by harvesting new growth at 3-day intervals for three weeks of temperature initiation. Root biomass was collected at the end of the experiment, 21 days after temperature treatment, clipping yield increased with an increase in temperature, and quadratic regression functions best described the relationship between temperature and clipping yield in all cultivars. Estimated bermudagrass base temperature was13.1°C. Optimal bermudagrass growth occurred at 32.7°C. Root dry mass, measured at the end of the experiment, declined linearly with temperature, 1.7 to 4.2 g m^{-2} $°C^{-1}$, depending upon cultivar. These base- and optimal-temperatures offer improved functionality for predicting turfgrass growth under field conditions.

Keywords: Bermudagrass, *Cynodon,* Growth model.

Abbreviations: DAT, Days after treatment; GDD, Growing degree day; PVC, Polyvinyl chloride; SPAR, Soil-Plant-Atmosphere-Research

INTRODUCTION

Temperature affects plant growth and development at all growth stages. In crop production systems, temperature varies spatially and temporally across the crop-growing areas and within a growing season for a given location. Therefore, heat accumulation models have been used to predict plant performance allowing practitioners to plan agronomic practices. Growing degree day (GDD) models are a commonly used method of calculating heat accumulation. McMaster and Wilhelm (1997) defined GDD models as a way to describe the amount of heat energy received by a crop over a given period. Growing degree days are used extensively in agriculture to predict when distinct plant growth stages will occur, such as days until flowering or days until maturity. In the turfgrass industry, GDD models have been used to optimize growth regulator and herbicide applications (Brosnan et al., 2010; Kreuser et al., 2011; Patton et al., 2018), and to predict seedhead development (Danneberger et al., 1987; McCullough et al., 2017), weed emergence (Fidanza et al., 1996), and disease outbreak (Ryan et al., 2012). The components of the commonly accepted GDD model (McMaster and Wilhelm, 1997) include average daily air temperature, as well as a base temperature (Eq. 1).

$$\left[\frac{Max\ Temp + Min\ Temp}{2}\right] - Base\ Temp \qquad Eq.1$$

McMaster and Wilhelm (1997) defined base temperature as the point that "plant processes of interest" do not progress; however, the base temperature can vary among species and growth stages (Wang, 1960). In previous turfgrass research and management, different base temperatures have been used. Brosnan et al. (2010) chose a base temperature of 10°C when scheduling post-emergent

herbicide applications in tall fescue [*Schedonorus arundinaceus* (Schreb.) Dumort.]. Similarly, McCullough (2014) also used 10°C for predicting seedhead formation in zoysiagrass [*Zoysia matrella* (L.) Merr.], seashore paspalum (*Paspalum vaginatum* Sw.), and hybrid bermudagrass [*Cynodon dactylon* (L.) Pers. x *Cynodon transvaalensis* Burtt Davy]. Kreuser and Soldat (2011), however, used 0°C for the base temperature when scheudling growth regulator application intervals on creeping bentgrass putting greens (*Agrostis stolonifera* L.).

Research to predict the physiological base temperature of warm-season turfgrasses has been limited (Unruh et al., 1996). The species and cultivars studied by Unruh et al. (1996) included: 'Midiron' hybrid bermudagrass and 'Arizona Common' bermudagrass [*Cynodon dactylon* (L.) Pers.], 'Kansas Common'and 'Texoka' buffalograss [Buchloe dactyloides (Nutt.) J.T. Columbus], 'Meyer' zoysiagrass,'Raleigh' and Floratam' St. Augustinegrass [Stenotaphrum secundatum (Walter) Kuntze], and 'Common' centipedegrass [Eremochloa ophiuroides (Munro) Hack.]. The authors reported that base temperatures ranged from -0.1 to 12.3°C across species, depending upon the regression model used (exponential or quadratic). The study was conducted in a growth chamber with a maximum photosynthetically active radiation (PAR) of 400 mol m^{-2} s^{-1} and a 14 h photoperiod (equiv. 20.2 mol m^{-2} d^{-1}) (Reddy et al., 1995). By contrast, total summertime PAR may reach 60 mol m^{-2} d^{-1} in the southeastern U.S. (an area where warm-season grasses predominate) when peak PAR may be greater than 2,500 mol m^{-2} s-1. The relatively low light quantity of Unruh et al. (1996) may have affected the growth potential of selected turf species by altering growth characteristics such as foliage length and clipping yield. To determine turfgrass growth response to temperature for field applications, an optimal growing environment, preferably under sunlit conditions, with precise temperature control is required. Therefore, research was conducted within controlled atmospheric research chambers under natural sunlight to determine the base and optimal growth temperatures of four hybrid bermudagrass cultivars and to investigate temperature effects on total root biomass.

MATERIALS AND METHODS

An experiment was conducted from 24 April to 15 May 2016 utilizing the Mississippi State University's Soil-Plant-Atmosphere-Research (SPAR) units located at the R.R. Foil Plant Science Research Center in Starkville, Mississippi (33.469°N, 88.780°W). The SPAR facility is composed of individual, naturally-lit units elevated on a 600 m^2 concrete pad. Each unit is composed of 2.5 m tall transparent Plexiglass® [Poly(methyl methacrylate); Evonik Performance Materials GmbH, Essen, Germany] chamber to accommodate aerial plant growth and a 1 m^2 steel soil bin for root growth. The Plexiglas chamber transmits approximately 95% of PAR (Reddy et al. 2001). Outside of the SPAR units, PAR was measured with a pyranometer (Model 4-8; The Eppley Laboratory Inc., Newport, RI) and ranged from 10.8 to 61.4 mol m^{-2} d^{-1} with an average of 39.5 mol m^{-2} d^{-1}. Within each unit, an air handler simulates natural airflow directly above the turfgrass canopy. The air handler includes an infrared model LI-6252 (LI-COR Biosciences, Lincoln, NE) gas analyzer to measure CO_2 concentration. The desired CO_2 concentration for the experiment was 400 µmol mol^{-1} and was maintained ± 10 µmol mol^{-1}. Chamber temperature within each SPAR unit is controlled ± 0.5°C of the desired temperature and recorded every 15 minutes. The relative humidity of each chamber is monitored with a humidity and temperature sensor (HMV 70Y, Vaisala, Inc., Helsinki, Finland) installed in the return path of airline ducts. Cooling coils located in the air-handler condense excess water vapor to regulate relative humidity. Chamber conditions are controlled by a dedicated computer system with algorithms described by Reddy et al. (2001).

Hybrid bermudagrass cultivars tested include: 'Latitude 36,' 'TifEagle,' 'Tifway,' and an experimental cultivar 'MSB-285.' Samples of each bermudagrass were harvested from established stands at the R.R. Foil Plant Science Research Center. Samples were washed free of native soil then transplanted into polyvinyl chloride lysimeters measuring 10 cm in diameter and 41 cm in height.

Lysimeters contained a 3:1 mixture of sand to native soil with 500 g of gravel at the bottom. The texture of the sand/soil mixture was classified as fine sand with 87% sand, 11% silt, and 2% clay.

The experiment utilized a completely randomized design with each bermudagrass replicated six times within each chamber. Before initiating temperature treatments, plants were maintained at a 30/22°C day/night temperature regime for a two-week acclimation period. Temperature treatments included 20/12, 25/17, 30/22, 35/27, and 40/32°C day/night temperatures (Table 1). The daytime temperature was initiated at sunrise and returned to the nighttime temperature one hour after sunset (Reddy et al., 2001). Each temperature treatment was conducted in a separate SPAR unit, and cultivars were arranged randomly in each unit.

TifEagle was maintained at 1.3 cm mowing height; where, Latitude 36, MSB -285, and Tifway were maintained at 1.9 cm mowing height. The difference in mowing height was due to the growth habit differences among bermudagrasses. Plants were fertilized and irrigated three times per day (0.7:00, 12:00, and 17:00 h) using a full strength Hoagland's nutrient solution (Hewitt, 1952). The solution was accurately applied with a computer-automated drip system according to treatment-based evapotranspiration rates measured in each SPAR unit as the rate at which the condensate was removed by the cooling coils at 900-s intervals (Reddy et al., 2001; Timlin et al., 2007). They were obtained by measuring the mass of water in collecting devices connected to a calibrated pressure transducer. No pesticides were applied during the experimental period.

Table 1. Specified day/night temperature treatments and the mean day, night, and average temperatures recorded in each Soil-Plant-Atmosphere-Research (SPAR) unit during the experimental period conducted at Mississippi State University, Mississippi State, MS.

Temperature Regime	Mean Temperature† (°C)		
(Day/Night °C)	Day	Night	Average
20/12	20.1	12.6	16.9
25/17	24.8	17.2	21.5
30/22	29.2	21.6	25.9
35/27	33.5	26.0	30.3
40/32	38.1	30.6	34.9

†Standard error of the mean was less than ± 0.1 throughout the experimental period between April 24 and May 15.

Data Collection: Bermudagrass foliar growth was harvested 0, 3, 6, 9, 12, 15, 18, and 21 days after temperature treatment (DAT) initiation. The clippings were dried for 72 h in a forced air oven at 75°C before weighing. Clipping weights are presented as g m^{-2} day^{-1} to describe bermudagrass shoot growth. After 21 DAT, roots of each lysimeter were separated using soil sieves, washed free of soil, oven-dried (as previously described), and then weighed. Root dry mass is presented as g m^{-2} accumulated over the duration of the study.

Statistical Analyses: Actual day/night time temperatures were averaged to facilitate regression analysis (Table 1). Clipping yield and total root dry mass were analyzed using least-squares regression in Prism 6.0 (GraphPad Software, San Diego, CA). Quadratic regression was conducted for each cultivar at each clipping harvest (0 through 21 DAT) to systematically eliminate harvests where plant material had not fully acclimated to chamber conditions. Quadratic models were chosen based upon goodness of fit and biological meaningfulness. Harvest dates 0, 3, and 6 DAT were omitted from further analysis due to lack of temperature acclimation, and cultivar data were assessed across remaining harvest dates.

The optimal growth temperature was calculated by solving the quadratic regression model for the y-coordinate of the vertex. Base temperatures were extrapolated from quadratic models but could not be compared using confidence estimates. Optimal temperature estimates were compared using 95% confidence intervals calculated from predicted parameter estimates. Root dry mass was measured 21 DAT upon study completion. The quadratic model was not representative of root dry mass reductions relative to increasing temperature; therefore, root mass data were analyzed by linear regression. Pair-wise model comparison with Extra Sums of Square F-test (P 0.05) was used to assess whether cultivar responses were similar and could be explained using combined or individual models.

RESULTS AND DISCUSSION

The quadratic models described the shoot growth response to temperature for all cultivars (Figure 1). This approach contrasts that used with linear models for predicting seed germination relative to temperature (Arnold, 1959; Jordan and Haferkamp, 1989) or that of an exponential model used to predict shoot growth (Unruh et al., 1996). Quadratic modeling enabled the prediction of optimal and base temperatures (Figure 1). Linear regression models were also used to estimate base temperatures.

For the presented results, harvests 0, 3, and 6 DAT were omitted from analysis due to a presumed lack of temperature acclimation. For instance, quadratic regression of shoot growth 6 DAT predicted optimal temperatures of 12.9, 46.1, 70.9, and 1,530°C for MS-285, TifEagle, Tifway, and Latitude 36, respectively. Predictions of 0 and 3 DAT were equally erratic and implausible.

Optimal Temperatures

Shoot growth (9, 12, 15, 18, and 21 DAT) was regressed with a quadratic equation to estimate an optimal growth temperature of 40.3°C for MSB-285, 31.1°C for Tifway, 32.2°C for Latitude 36, and 30.7°C for TifEagle (Table 2; Figure 1). Optimal temperatures were compared using estimated confidence intervals, and, in all instances, optimal temperatures were statistically similar. However, a single curve for all bermudagrass cultivars was not appropriate. Pairwise comparisons of quadratic models indicated that only Latitude 36 and Tifway shoot growth share a similar model. All other comparisons suggest the use of different curves for each data set. However, if a single model were used, optimal temperatures for shoot growth across bermudagrass cultivars would be 32.7°C.

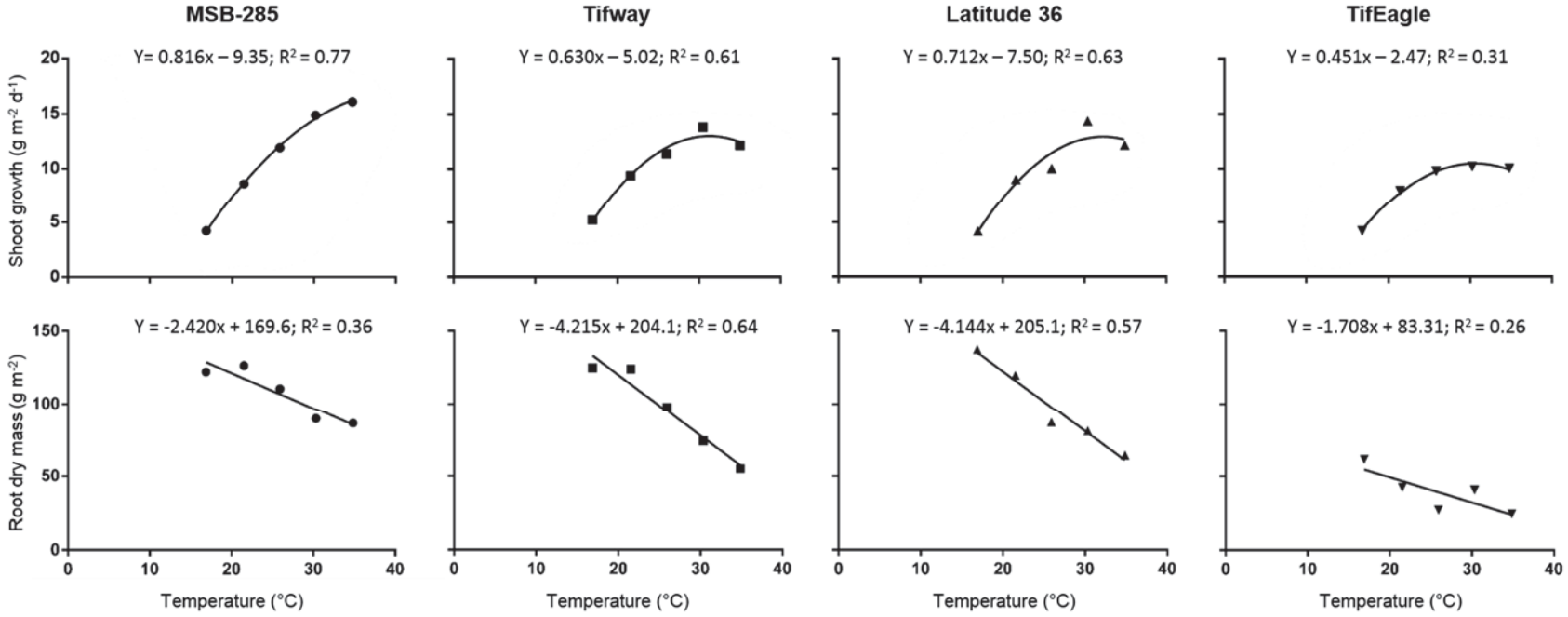

Figure 1. Temperature response of MSB-285, Tifway, Latitude 36, and TifEagle bermudagrasses. Shoot growth harvested 9, 12, 15, 18, and 21 days after study treatment (DAT). Root dry mass was measured 21 DAT upon study completion. Shoot growth was modeled using quadratic regression. The quadratic model was not representative of root dry mass reductions relative to increasing temperature; therefore, linear regression was conducted.

Table 2. Calculated base and optimal temperatures (°C) based upon bermudagrass shoot growth of MSB-285, Tifway, Latitude 36, and TifEagle bermudagrasses as determined by linear and quadratic models fit the data pooled across harvests 9, 12, 15, 18, and 21 days after treatment. Optimal temperatures were compared using estimated confidence intervals, and, in all instances, optimal temperatures were statistically similar.

	Base Temperature (°C)	Optimal Temperature (°C)
Cultivar	Quadratic	Quadratic
MSB-285	13.1 a	40.3 A
Tifway	13.0 a	31.1 A
Latitude 36	13.8 a	32.2 A
TifEagle	12.7 a	30.7 A
Combined‡	13.1	32.7

† Temperature estimates are comparable within column. The base and optimal temperatures did not differ among cultivars.

‡ A combined model can be assumed to reflect temperatures for all tested cultivars.

Latitude 36, Tifway, and TifEagle optimal growth temperatures were predicted to be within the range of other bermudagrasses (i.e., 30 to 40°C; Dudeck and Peacock, 1992). Notably, the hottest temperature regime did not cause a reduction in MSB-285 foliar growth. Thus estimates of optimal temperature for MSB-285 are above the normal reported range. Higher experimental temperatures could validate or invalidate this estimation. Temperature regimes were chosen based upon the ability of the SPAR units to maintain temperature (within the given threshold) during the time of the project (early May).

Base Temperature

Base temperatures for each bermudagrass were estimated using the previously discussed quadratic equation (Table 2); however, a comparison of estimates is not possible due to the inability to predict confidence intervals. This is due to the highest confidence interval, sometimes being upward opening and never crossing the x-axis. Based on quadratic equation estimates, the base temperature for all cultivars is 13.1°C.

Base temperatures were also compared using extrapolations of the linear regression encompassing temperatures 16.9 through 30.3°C and excluding the highest temperature, 34.9 °C (data not shown). This method was chosen to avoid the effects of temperatures above the optimal. Base temperatures for MSB-285, Tifway, Latitude 36, and TifEagle, were 11.5, 8.0, 10.5, and 5.5, respectively (Table 2). Results were similar to those reported by Unruh et al. (1996) in that base temperatures among cultivars did not significantly differ. When pooled across cultivars,

the average base temperature was 9.2°C using our methods, which is consistent with temperatures reported to cause a decline in bermudagrass growth (Youngner, 1959) and those reported to induce chilling injury to warm-season species (< 12°C; Lyons, 1973). Alternatively, base temperatures determined by Unruh et al. (1996) using exponential and quadratic models were 3.1 or 4.9°C and 0.3 or 2.0°C, respectively. These differences may be due to the lower light conditions of Unruh et al. (1996), where the authors conducted a similar experiment in an artificially lit growth chamber providing PAR 20.2 mol m^{-2} d^{-1}. In contrast, PAR outside of the SPAR units averaged 39.5 mol m^{-2} d^{-1} during the present experiment. Results may also vary due to differences in response variables measured.

Total Root Dry Mass

Root dry mass declined linearly with an increase in temperature (Figure 1). MSB-285, Tifway, Latitude 36, and TifEagle root dry mass declined 2.4, 4.2, 4.1, and 1.7 g m^{-2} for every 1°C increase in temperature, respectively. Tifway and TifEagle root dry mass differed in response to increasing temperature, in that TifEagle root dry mass decline was less pronounced. These differences were slight, and results may simply be biased by dissimilar mowing heights. Mowing heights were chosen in order to simulate those of field conditions where these grasses are expected to be cultured. Additionally, dwarf and semi-dwarf growth habits, we felt, would have biased clipping yield data if grasses were maintained at similar heights.

For all bermudagrasses, there was more root dry mass at the lowest temperature treatment when compared to the highest temperature treatment. Similar results have been discussed by Reddy et al. (1994), Huang and Gao (2010), and Forbes (1997) in that temperature favoring shoot growth leads to a decline in root production. Reddy et al. (1994) determined the optimal temperature for root growth in cotton (*Gossypium hirsutum* L.) was 22.7°C and, at temperatures above that, root growth depended on how temperature affected the competition for assimilates between the roots and shoot. Huang and Gao (2010) determined that the root dry weight of creeping bentgrass decreased when exposed to higher temperatures due to an imbalance of photosynthesis and respiration, leading to a reduction in carbohydrate availability. It is likely a similar interaction occurred in our study, which caused the decline of root growth at higher temperatures. However, this response could be an artifact of root biomass accumulation before initiation of temperature treatments. Therefore, any differences observed may be due to the mobilization of root-stored carbohydrates in exchange for shoot growth (i.e., a decrease in roots as the experiment progressed).

CONCLUSIONS

In this study, temperature effects on bermudagrass cultivar shoot and root growth were quantified under optimal water and nutrient conditions in a sunlit environment similar to field conditions. The range of air temperatures imposed in this study represented the temperature variability of current conditions across the southern US. This is the first study to address temperature effects on several bermudagrass cultivars that are important for the turfgrass industry and to provide functional algorithms and base and optimal temperatures that could be useful to develop new models or improve existing models for management.

Optimal and base temperatures for clipping yield did not differ amongst bermudagrass cultivars. Results suggest that a single model reflects temperature response for all tested cultivars. Both linear and quadratic models have merits in predicting bermudagrass clipping yield responses to temperature with base temperatures of 9.2 and 13.1°C, respectively. The average optimal temperature for the bermudagrass clipping yield estimated from the quadratic function was 32.7°C. Unlike shoot biomass, the root biomass declined linearly with temperature in all cultivars, 1.7 to 4.2 g m^{-2} $1°C^{-1}$, depending on the cultivar. Base and optimal temperatures for bermudagrass growth are critical to more accurate modeling of bermudagrass growth for not only managed turfgrass scenarios but also for forage production. Future research should investigate the effects of other environmental factors individually and in interaction with temperature (ex. light, water and nutrient availability) to provide turfgrass managers with accurate predictive growth models.

CONFLICT OF INTEREST

There is no conflict of interest to declare

ACKNOWLEDGMENTS

The research was partially funded through a grant from the United States Golf Association.

LITERATURE CITED

Arnold CY. The determination and significance of the base temperature in a linear heat unit system. Proc. Amer. Soc. Hort. Sci. 1959; 74: 430-445.

Brosnan JT, Breeden GK, Elmore MT. Early and late postemergence control of Dallisgrass in tall fescue. Online. App. Turf. Sci. 2010; DOI 10.1094/ATS-2010-0312-02-RS.

Danneberger TK, Branham BE, Vargas Jr. JM. Mefluide applications for annual bluegrass seedhead suppression based on a growing degree-day accumulation. Agron. J. 1987; 79: 69-71.

Dudeck AE, Peacock CH. Shade and turfgrass culture. In D.V. Waddington et al. (ed.) Turfgrass. Agron. Monogr. 32. ASA, CSSA, and SSSA, Madison, WI, 1992; p. 269-284.

Fidanza MA, Dernoeden PH, Zhang M. Degree-days for predicting smooth crabgrass emergence in cool-season turfgrasses. Crop Sci. 1996; 36:9 90-996.

Forbes PJ, Black KE, Hooker JE. Temperature-induced alteration to root longevity in *Lolium perenne*. Plant Soil 1997; 190: 87-90.

Jordan GL, Haferkamp MR. Heat units for germination of several range grasses and shrubs. J. Range Manage. 1989; 42: 41-45.

Hewitt EJ. Sand and water culture: methods used in the study of plant nutrition. Technical Communication No. 22, Commonwealth bureau of horticulture and plantation, East Malling, Maidstone. Kent Publishers, Commonwealth Agricultural Bureaux, Farmham Royal, Bucks, England, 1952, pp. 187-190.

Huang B, Gao H. Growth and carbohydrate metabolism of creeping bentgrass cultivars in response to increasing temperatures. Crop Sci. 2010; 40: 1115-1120.

Kreuser WC, Soldat DJ. A growing degree day model to schedule Trinexapac-ethyl applications on *Agrostis stolonifera* golf putting greens. Crop Sci. 2011; 51:2228-2236.

Lyons JM. Chilling injury in plants. Ann. Rev. Plant Physio. 1973; 24:445-466.

McCullough P. Management practices and prediction models for controlling seedheads on warm-season turfgrasses. USGA TERO. 2014; 13:8-9.

McCullough PE, Yu J, Williams SM. Seedhead development of three warm-season turfgrasses as influenced by growing degree days, photoperiod, and maintenance regimens. Inter. Turf. Soc. Res. J. 2017; 13: 321-329.

McKinion JM, Hodges HF. Automated system for measurement of evapotranspiration from closed environmental growth chambers. Trans. ASAE 1985; 28: 1825-1828. doi:10.13031/2013.32526

McMaster GS, Wilhelm WW. Growing degree-days: one equation, two interpretations. Agric. For. Meteorol. 1997; 87: 291-300.

Patton AJ, Weisenberger DV, Breuninger JM. A growing degree day model is effective to schedule spring Defendor (florasulam) applications for suppressing dandelion flowers. Crop, Forage Turf. Manage. 2018; 4: 170088. doi:10.2134/cftm2017.12.0088.

Reddy KR, Hodges HF, McKinion JM. Cotton crop responses to a changing environment. Climate change and agriculture: Analysis of potential international impacts. Proceedings of a Symposium sponsored by the American Society of Agronomy in Minneapolis, 4-5 November 1992. Organized by Division A-3 (Agroclimatology and Agronomic Modeling) and Division A-6 (International Agronomy), 1995; pp. 3-30.

Reddy KR, Hodges HF, Read JJ, McKinion JM, Baker JT, Tarpley L, Reddy VR. Soil-Plant-Atmosphere-Research (SPAR) facility: a tool for

plant research and modeling. Biotronics 2001; 30: 27-50.

Reddy VR, Reddy KR, Acock MC, Trent A. Carbon dioxide enrichment and temperature effects on root growth in cotton. Biotronics 1994; 23: 47-57.

Ryan PR, Dernoeden PH, Grybauskas AP. Seasonal development of dollar spot epidemics in six creeping bentgrass cultivars in Maryland. HortScience 2012; 47: 422-426.

Timlin D, Fleisher D, Kim SH, Reddy VR, Baker J. Evapotranspiration measurement in controlled environment chambers. Agron. J. 2007; 99: 166-173. doi:10.2134/agronj2005.0344

Unruh JB, Gaussoin RE, Wiest SC. Basal growth temperatures and growth rate constants of warm-season turfgrass species. Crop Sci. 1996; 36: 997-999.

Wang JY. A critique of the heat unit approach to plant response studies. Ecology 1960; 41: 785-790.

Youngner VB. Growth of U-3 bermudagrass under various day and night temperatures and light intensities. Agron. J. 1959; 51: 557-559.

Factors Affecting *Listeria monocytogenes* Biofilm Formation in Food Processing Environments and Its Control

Mohit Bansal[1], Nitin Dhowlaghar[2], Ramakrishna Nannapaneni[2]*, Divya Kode[2], Sam Chang[2], Wen-Hsing Cheng[2], Tomi Obe[1] and Aaron Kiess[1]

[1]Poultry Science Department and [2]Department of Food Science, Nutrition and Health Promotion, Mississippi State University, Mississippi State, MS 39762, USA

***Corresponding author:** Ramakrishna Nannapaneni, E-mail: nannapaneni@fsnhp.msstate.edu

ABSTRACT

Listeria monocytogenes is widely present in biotic and abiotic surfaces, including manure, soil, and surface water samples. It is an environmentally persistent organism and can grow slowly even at refrigeration temperatures (4°C) in a variety of food products. This foodborne pathogen can attach firmly and form biofilms on any food-contact and non-food contact surface in almost all food processing conditions. It is still unclear what factors play a critical role in the food production facility in biofilm formation of *L. monocytogenes*. This review explores the known factors inducing the *L. monocytogenes* biofilm formation ability on food-contact and non-food contact surfaces and their elimination by disinfectant procedures in the food processing facilities.

Keywords: *Listeria monocytogenes*, biofilm formation, biofilm control, food processing environments, disinfectants

INTRODUCTION

Foodborne pathogens cause 48 million illnesses and 3,000 deaths annually in the United States (Scallan et al., 2011). Among them, *Listeria monocytogenes* (*L. monocytogenes*) is an important foodborne bacterial pathogen that causes listeriosis. Listeriosis accounts for 19% of all deaths related to foodborne diseases in the United States (Hamon et al., 2006). *L. monocytogenes* is an environmentally persistent organism and can grow slowly at refrigeration temperatures (4°C). It also survives in high salinity environments and a wide range of pHs. Due to its ubiquitous nature, different food products like fish, meat, coleslaw, cantaloupes, unpasteurized milk, and ice-cream are contaminated and known as sources of *L. monocytogenes* infection (Cartwright et al., 2013).

How *L. monocytogenes* survive and persist in food production facilities is still unclear as many factors are involved in it. Inadequate sanitation procedures of food contact surfaces can result in niches contaminated with organic content and higher water activity for bacteria to survive and to expose bacteria to the subinhibitory concentration of disinfectants (Bansal et al., 2018). Organic matter contamination in food processing facilities can cause subinhibitory levels of disinfectant exposure to bacteria. Exposure to subinhibitory levels of disinfectants can results in an increase in bacterial tolerance to disinfectants, an increase in disinfectant concentration or exposure time (Ortiz et al., 2014). This review explores the *L. monocytogenes* biofilm formation ability on food contact surfaces and the commonly used disinfectant procedures to reduce its persistence in food processing facilities.

Taxonomical and Ecological Characteristics of L. Monocytogenes

L. monocytogenes is a short rod-shaped (0.4-0.5 by 1-2 μm) non-spore forming and motile organism. *L. monocytogenes* cells have characteristic tumbling motility, expressed only in a narrow temperature range. The tumbling motility is characteristic of its peritrichous flagella. *L. monocytogenes* flagellin is expressed and produced more between 20 - 25°C than at 37°C (Peel et al., 1988). Based on the DNA homology and 16S rRNA cataloging results, the *Listeria* genus is classified into the following 7 species., *L. monocytogenes, L. innocua, L. seeligeri, L. welshimeri, L. ivanovii, L. grayi,* and *L. murrayi*

(Seeliger, 1984). *L. monocytogenes* has been classified into several serotypes based on the combinations of somatic (O) and flagellar antigens. There are at least 13 known serotypes for *L. monocytogenes* (1/2a, 1/2b, 1/2c, 3a, 3b, 3c, 4a, 4ab, 4b, 4c, 4d, 4e, and 7) where majorly three predominant serotypes (1/2a, 1/2b, and 4b) cause the vast majority of clinical listeriosis cases.

L. monocytogenes is widely present in biotic and abiotic surfaces, including plants, soil, and surface water samples. *L. monocytogenes* is an environmentally persistent organism and can grow slowly at refrigeration temperatures (4°C). *L. monocytogenes* has also been isolated from human and animal feces, silage, normal, and contaminated milk (Vasseur et al., 1999; Scallan et al., 2011). It is a facultative intracellular bacterium, often found in different kinds of foods as well as environments. There are two main clinical symptoms of human listeriosis: (1) invasive listeriosis caused by severe nervous infections; and (2) non-invasive mild listeriosis caused by gastroenteritis. Listerisosis occurs in susceptible populations such as elderly people, pregnant women, children and immunocompromised patients (Ooi and Lorber, 2005).

L. monocytogenes cells are motile with five to six peritrichous flagella. Extensive research over the past few decades has revealed that the flagella contribute to virulence in many foodborne pathogens, either as the effectors of motility, colonization, and invasion of the intestine or as mediators of toxin secretion inside the host (O'Neil and Marquis, 2006). The flagella participate in processes such as biofilm formation on surfaces of the external environment and modulation of the host immune response (Duan et al., 2013; Lemon et al., 2007). Flagella also facilitate intestinal epithelial cell invasion in the host (Bigot et al., 2005).

Despite the low listeriosis incidence of 0.25 case/100,000 population, *L. monocytogenes* contamination was considered as a notifiable disease (Schlech et al., 1983). Ready to eat products such as deli meats and hotdogs have also been implicated as a potential sources of *L. monocytogenes* in previous major outbreaks. Turkey deli meat was responsible for listeriosis outbreaks in the US in 2002 (Gottlieb et al., 2006) and Canada in 2008 (Currie et al., 2015). There were 111 illnesses, 32 adult deaths, and 3 fetal deaths associated with these two major listeriosis outbreaks. Listeriosis accounts for 19% of all deaths related to foodborne diseases in the United States (Scallan et al., 2015). Since *L. monocytogenes* can survive and multiply at low temperatures (< 4°C), it can contaminate food at any point in the processing plant, including during refrigerated storage. Despite multiple outbreaks from different food products, the transmission pathway and true reservoir of *L. monocytogenes* cells are still unclear.

L. monocytogenes Outbreaks in the USA and Canada

The first foodborne listeriosis case from meat was reported in England in 1988. Cooked chicken was found as the source of infection (Farber et al., 1989). Later, in the USA, the first foodborne *L. monocytogenes* case was reported in 1989, which was implicated by contaminated turkey frankfurter as the source of the outbreak (Wenger et al., 1990). *L. monocytogenes* serotype 1/2a was isolated from the contaminated turkey frankfurter and from the infected patient. The largest poultry associated listeriosis outbreak was reported in 1998-99. This outbreak was responsible for 108 listeriosis cases with 14 deaths and 4 stillbirths. It was found to be originated from contaminated turkey deli meat, and *L. monocytogenes* serotype 4b was found to be associated with this outbreak (Mead et al., 2006). Defective deli-meat handling, cutting, and insufficient sanitation practice can result in *L. monocytogenes* contamination. *L. monocytogenes* was frequently isolated from a variety of processed and raw food products. Some *L. monocytogenes* outbreaks are listed in Table 1.

Table 1. Examples of listeriosis outbreaks in the United States from 1998 to 2019.

Year	Food product implicated	No. infected	Reference
1998	Processed meat	101	(Frye et al., 2002)
1998	Hot dogs	4	(CDC, 1999)
2000	Delicatessen turkey	30	(Frye et al., 2002)
2009	Mexican style cheese	18	(Johnson et al., 1990)
2011	Whole cantaloupes	147	(CDC, 2011)
2012	Ricotta Salata cheese	22	(CDC, 2012)
2013	Crave brother's farmstead cheeses	6	(CDC, 2013)
2014	Wholesome soy products & sprouts	5	(CDC, 2014)
2015	Bluebell creameries products	10	(CDC, 2015)
2016	Frozen vegetables	9	(CDC, 2016)
2017	Soft milk cheese by Vulto creamery	8	(CDC, 2017)
2018	Deli ham	4	(CDC, 2018)
2019	Deli sliced meats and cheeses	10	(CDC, 2019)

Biofilm Concept

Bacteria prefer to live in communities or colonies under natural environmental conditions. They attach to different surfaces and protect themselves from harmful factors in the environment, such as desiccation, antimicrobials, and oxidative stress. The microbes that can freely float in liquid medium are considered as planktonic cells, while those which are attached to any surfaces are referred to as biofilms (Palková, 2004). Biofilms are comprised of the cellular and extracellular casing, which include extra polymeric compounds, proteins, and extracellular DNA (Vu et al., 2009). Biofilm was defined as "immobilized cells that grow, reproduce, and produce an extracellular polymer substance (EPS) that frequently extends from the cell, forming a tangled mass of fibers lending structure to the entire assemblage (Cooksey, 1992). *L. monocytogenes* can attach to any food or non-food contact surfaces such as polystyrene, stainless steel, or rubber to form a biofilm (Borucki et al., 2003). Later the biofilm was defined as a "structured multicellular bacterial communities' adherent to surfaces in man-made or natural environments" (Flemming and Wingender, 2010). These biofilms act as persistent sources of food contamination in the food processing plant.

Biofilm Formation and Stages

The majority of biofilms are composed of cells, which are approximately 10% dry mass surrounded by a matrix, which is around 90% (Flemming and Wingender, 2010). The matrix or extracellular component of biofilm is produced by cells that are entrenched and called extracellular polymeric substances (EPS). Previously, EPS was known as "the dark matter of biofilms" because of its complex and challenging to analyze the structure. This EPS consists of different kinds of biopolymer compounds such as polysaccharides, proteins, phospholipids, teichoic acids and extracellular DNA (Flemming et al., 2007). The EPS component of a biofilm provides physical strength for the development of the three-dimensional structure of a biofilm. EPS enhances the cell-cell interaction. It acts as a protection for the cells against bactericidal factors such as antibiotics, biocides, desiccation, UV rays, and water shear force. The chemical composition of biofilm and its function are provided in Table 2.

Table 2. Biofilm chemical composition and their functions

Components of EPS	Functions	Reference
eDNA	Hydrated hydrophilic molecules. Acts as an intercellular connector.	(Flemming and Wingender, 2010)
Surfactants and lipids	Hydrophobic molecules, initial microcolony formation; surface-associated bacterial migration; prevents colonization of channels and biofilm dispersion.	(Donlan et al., 2002)
Extracellular proteins enzymes	Biopolymers degrade and promote detachment of bacteria from biofilm to low-molecular-mass products. They act as virulence factors.	(Colagiorgi et al., 2016)
Structural proteins	Cell surface (Lectins) and extracellular; biofilm-associated protein (Bap) and appendages such as pili, fimbriae, and flagella.	(Fong and Yildiz, 2015)
Exopolysaccharides	Major fraction of the EPS matrix and structural component.	(Donlan et al., 2002)

Biofilm formation begins with planktonic cell attachment to an abiotic surface. It involves five main steps: (1) reversible attachment, (2) irreversible attachment, (3) micro-colony development, (4) production of exopolysaccharides (EPS); and (5) dispersal. Surface conditioning with organic matter contamination can enhance biofilm formation. Organic matter contamination reduces the hydrophobicity of surfaces and induces cell attachment. The reversible stage is when bacteria are loosely attached to surfaces by different physical forces such as van der Waals and gravitational forces (5-10 seconds) (Mittelman, 1998). Thus, the initial attachment of planktonic cells can be controlled by many surface charges such as the electrical charge of the bacteria, Van der Waals forces, electrostatic factors, hydrophobic interactions, and brownian motion (Donlan and Costerton, 2002). Following reversible attachment, the irreversible attachment occurs when bacteria firmly attach to the surfaces by

exopolysaccharides and other compounds that may take 20 min to 4 h (Mittelman, 1998). After the period of irreversible attachment, cells establish their micro-colonies and produce EPS in larger amounts, which helps in the formation of the three-dimension structure of biofilm. After complete formation, cells may disperse from the biofilm and may repeat production at another location. A similar process is followed by *L. monocytogenes* to form biofilms in food processing environments.

L. monocytogenes is regularly isolated from food processing and retail environments. The biofilms of *L. monocytogenes* act as a persistent source of cross-contamination of raw or cooked food products (Muhterem-Uyar et al., 2015). The prevalence of *L. monocytogenes* in certain poultry processing environments was as high as 16.4 - 20% of the samples collected (Chiarini et al., 2009). Until recently, nearly 83% of listeriosis cases and deaths were associated with deli meats (Endrikat et al., 2010). Due to its severe infection, the United States Department of Agriculture (USDA) has a zero-tolerance policy for *L. monocytogenes* in ready-to-eat (RTE) food products since the 1980s. The USDA-Food Safety Inspection Service (USDA-FSIS) zero-tolerance policy is applied to all RTE products irrespective of the distinction between levels of *L. monocytogenes* contamination.

Relation of the Phylogeny of L. Monocytogenes Strains with Its Biofilm Formation and Outbreaks

Biofilm acts as a persistent source of bacterial survival, multiplication, and transmission. It also has been hypothesized that the ability of *L. monocytogenes* to colonize both food or non-food contact surfaces may be a reason for the differences in the prevalence of the various serotypes (Valderrama, 2013). In other words, the isolates with a higher ability to colonize surfaces are likely to be found during environmental sampling, while those with a lower colonizing ability may be found less often. *L. monocytogenes* has been classified into two major and one minor phylogenetic divisions or lineages. Lineage I is comprised of serotype 1/2b and 4b, and lineage II is comprised of serotypes 1/2a and 1/2c. The third lineage has not been well characterized yet (Wu et al., 2015). Many studies have investigated the possible relationship of different serotypes, or lineages, with the prevalence of *L. monocytogenes* in the food processing environment with their colonizing and biofilm-forming ability. However, as of yet, there is no clear relationship between *L. monocytogenes* phylogeny prevalence and its biofilm formation ability (Doijad et al., 2015). Lineage I (mostly serotype 4b) is the cause of most listeriosis outbreaks, while lineage II serotypes 1/2a and 1/2c are commonly isolated in the food processing plants (Graves et al., 2007; Thévenot et al., 2005). *L. monocytogenes* cells are exposed to various environmental conditions in the processing plant, such as desiccation, lack of nutrients, moisture, and intermittent exposure to different antimicrobials (Taormina and Beuchat, 2001). Various studies have used these conditions to observe biofilm formation ability of *L. monocytogenes* under laboratory conditions and found differences in the relationship between lineage and their ability to form a biofilm (Borucki et al., 2003). *L. monocytogenes* biofilm-forming ability was found to be strongly correlated with its lineages in the presence of high nutrient conditions. Lineage II (serotypes 1/2a and 1/2c) were found to form stronger biofilms than lineage I (serotypes 4b and 1/2b) on polyvinyl chloride plates. Figure 1 shows the differences in biofilm-forming ability of *L. monocytogenes* ScottA (serotype 4b) and V7 (serotype 1/2a) on polystyrene surface after 48 h at 37°C. *L. monocytogenes* V7 formed denser biofilm at the bottom surface of the polystyrene well. In contrast, ScottA formed biofilm at the air-water inter-phase at the upper surface of the polystyrene well. Nonetheless, no association was established based on serotypes (Borucki et al., 2003; Doijad et al., 2015).

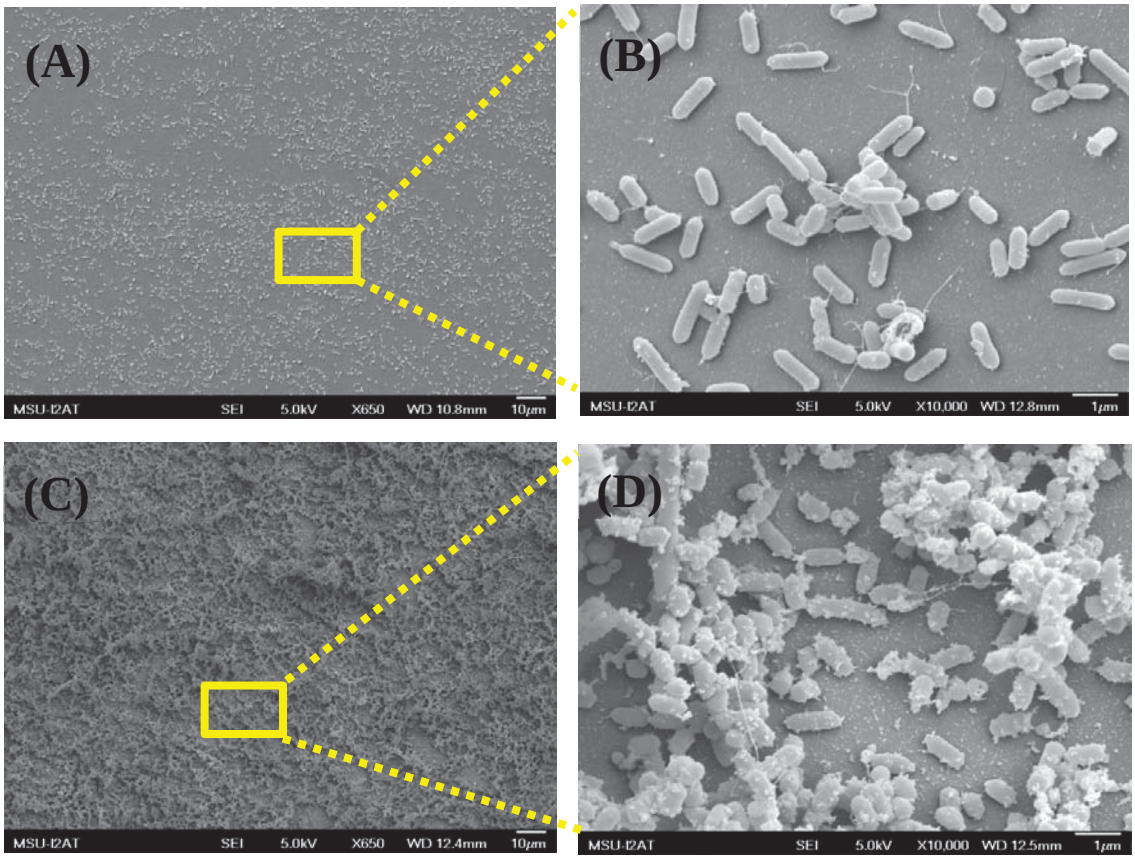

Figure 1. Differences in biofilm formation by two strains of *L. monocytogenes* representing two serotypes on the polystyrene surfaces after 48 h at 37°C: (A, B) Serotype 4b Scott A; and (C, D) Serotype 1/2a V7. Higher magnification images show dense EPS formation by *L. monocytogenes* 1/2a V7 strain (D) compared to 4b Scott A strain (B) during biofilm formation.

Influence of Environmental Factors on L. Monocytogenes Biofilm Formation

L. monocytogenes cells develop their biofilm in the processing plant in response to environmental conditions, such as a lack of nutrients, a low moisture level, or due to a wide range of pH. Bacteria in biofilms are found to be more resistant towards biocides than when in a planktonic state (Araújo et al., 2011). Sublethal stresses can induce physiological changes in bacterial physiology and morphology (Giotis et al., 2007), which in turn may influence the biofilm formation in pathogenic bacteria such as *L. monocytogenes*. Previous studies found *L. monocytogenes* is unable to form biofilms in the presence of plant-derived antimicrobials such as carvacrol, thymol, trans-cinnamaldehyde, eugenol (Upadhyay et al., 2013) and morin (Sivaranjani et al., 2016). The formation of a biofilm is known to be a stress response by bacterial cells (Oliveira et al., 2015). Along with lineages, other conditions such as biotic factors (eg., flagellation, motility, and disparity of cell structure) and abiotic factors (eg., hydrodynamics, temperature, pH, ionic composition, or nutrient availability) can influence the bacterial surface attachment and biofilm formation ability. These factors influence biofilm development individually or synergistically. *L. monocytogenes* cells are frequently exposed to different antimicrobials in a processing plant. Along with other factors, antimicrobials can also influence the ability of biofilm formation.

Influence of Temperature and Nutrient Condition

Temperature can modulate the virulence and environmental genes in *L. monocytogenes*, which can then induce changes in its cell surface. *L. monocytogenes* surface attachment is influenced by temperature, which is determined via growth patterns in polystyrene wells or on various food contact surfaces that mimic food processing conditions. Di Bonaventura et al. (2008) indicated that biofilm formation of various *L. monocytogenes* strains was significantly higher at 30-37°C as compared to 4-10°C or 42°C. Nilsson et al. (2011) observed that the clinical strains of *L. monocytogenes* produced more biofilm on polystyrene surfaces at high temperature (37°C) than the environmental (food factory) isolates at a lower temperature (10°C). Other studies also showed greater attachment at higher vs. low temperature for *L. monocytogenes* strains isolated from cantaloupe and catfish processing environment on four food contact surfaces (Abeysundara et al., 2017; Dhowlaghar et al., 2017).

Similarly, several studies indicated greater biofilm formation at higher temperatures (Dhowlaghar et al., 2018; Kadam et al., 2013; Ochiai et al., 2014; Pan et al., 2006). Differences in biofilm formation at various temperatures were attributed to altered cell surface properties of *L. monocytogenes*. At higher temperatures, *L. monocytogenes* flagellin expression is repressed. However, flagellum-mediated motility has been demonstrated in biofilm initiation in most of the strains (Lemon et al., 2007). In addition to temperature, biofilm formation by *L. monocytogenes* was greatly influenced by the nutrient medium. Even low nutrient media (1:10 tryptic soy broth or brain heart infusion broth) encouraged greater biofilm formation as compared to a 100% growth medium (Folsom et al., 2006). In some cases, type of media also influenced *L. monocytogenes* to form biofilm as an attachment on the plastic surface was greater in brain heart infusion broth followed by tryptic soy broth and then meat broth (Stepanović et al., 2004). Reports collectively indicated that greater temperature or nutrient medium encouraged a higher degree of attachment of *L. monocytogenes* on food contact surfaces, yet maintained a great attachment strength at low temperatures.

Influence of Strain and Serotype

L. monocytogenes biofilm formation varies among strains. Significant strain variations by *L. monocytogenes* to form biofilms among those collected from different food industries were reported. These strains include clinical (Nilsson et al., 2011), poultry and meat (Harvey et al., 2007; Rodrigues et al., 2010), milk and ice-cream (Lunden et al., 2000; Weiler et al., 2013), and seafood (Takahashi et al., 2009). A high variation among *L. monocytogenes* serotype and strain specificity biofilm formation were reported. Serotype 1/2a strains formed greater biofilm and increased EPS than serotypes 1/2b and 4b (Borucki et al., 2003). Another study demonstrated serotype 1/2c strains attached to a greater extent as compared to 1/2a, 1/2b, or 4b on stainless steel and glass surface (Di Bonaventura et al., 2008). In a nutrient-poor media, serotypes 1/2a and 4b were similar or lower than 1/2b (Kadam et al., 2013). On the other hand, biofilm formation was strain-specific rather than serotype-specific from those isolated from milk (Doijad et al., 2015; Weiler et al., 2013). No differences to form biofilm on stainless steel coupon surface among six *L. monocytogenes* catfish isolates were reported (Dhowlaghar et al., 2017). Altogether, *L. monocytogenes* forms biofilm among diverse food processing plants and processing conditions and various factors affected for its ability to form biofilms such as type of surface, poor or rich nutrient medium, incubation time/age (short/long time) and species specificity.

Influence of Surfaces and Its Characteristics on Attachment

L. monocytogenes can attach and form biofilms on numerous contact surfaces in almost all food processing conditions. Typically, most widely investigated studies on attachment behavior of *L. monocytogenes* was conducted on stainless surfaces (via determining CFU's), including the transfer of bacterial cells from food product to surface or surface to food product (Lunden et al., 2002; Vorst et al., 2006). The extent of attachment greatly varies by the type of surfaces. *L. monocytogenes* attachment on stainless steel, plastic (polyethylene & polyurethane)

was greater than Buna-N rubber (Abeysundara et al., 2017; Dhowlaghar et al., 2017; Ronner and Wong, 1993; Smoot and Pierson, 1998). *L. monocytogenes* attachment on wood was greater than stainless steel and glass surfaces (Adetunji and Isola, 2011). On the other hand, *L. monocytogenes* attachment was significantly greater on polyester floor sealant than nylon surface in nutrient-rich conditions (Blackman and Frank, 1996). The extent of biofilm attachment on different surfaces can be affected by contact angle, surface energies, surface tension, roughness, polishing, hydration or wettability, and hydrophilic/hydrophobicity (Dhowlaghar et al., 2017; Rodriguez et al., 2007; Rodriguez et al., 2008) and by designs such as joints, welding, and equipment (Bos et al., 2000; Guobjoernsdottir et al., 2005).

Influence of pH

The pH and ions greatly influence the growth of planktonic *L. monocytogenes* cells. Sodium chloride and an acidic pH significantly increased the lag and growth phase (>250 hours) of *L. monocytogenes* Scott A (Bereksi et al., 2002). Increased concentrations of NaCl (10%) along with a pH 5.0 has also been found to induce morphological changes in *L. monocytogenes* Scott A. However, at a pH of 5.0 with a 5% concentration of NaCl, short filaments were observed under the electron microscope. These properties showed *L. monocytogenes* can grow in altered environmental conditions but with modified surface properties. In addition, acidifying the pH of the basal growth medium can increase *L. monocytogenes* attachment to stainless steel and Buna N rubber (Smoot and Pierson, 1998).

Influence of Antimicrobials

Pre-exposure of subinhibitory concentrations (SICs) of a plant-derived antimicrobial, "morin" can inhibit the biofilm-forming ability of *L. monocytogenes* planktonic cells (Sivaranjani et al., 2016). This antibiofilm activity of morin against planktonic cells was observed to be dependent on concentration (6.25, 12.5, 25.0 µg/ml), temperature 32 °C and time (48 h) (Sivaranjani et al., 2016). *L. monocytogenes* flagellar mediated motility is essential for initial attachment to abiotic surfaces (Lemon et al., 2007). Subinhibitory concentrations of morin; modulate the motility (swimming and swarming) and cell to surface and cell to cell interactions of *L. monocytogenes*, which can further inhibit the formation of biofilm. However, morin is found to be inefficient in the eradication of mature biofilms at both sub MIC and MIC (minimum inhibitory concentration) (Sivaranjani et al., 2016). In another study, SICs of plant-derived antimicrobials (PDA) such as trans-cinnamaldehyde, carvacrol, thymol, and eugenol inhibited the biofilm-forming ability of *L. monocytogenes* on both polystyrene and stainless steel surfaces at 37, 25 and 4°C (Upadhyay et al., 2013). The SICs of PDAs down-regulated the genes responsible for the initial biofilm-forming steps (quorum sensing, initial attachment, and motility).

Genes and Protein Regulation for Biofilm Formation

Biofilm formation involves a set of stress factors and proteins where the respective expression of genes takes place. *L. monocytogenes* undergoes a considerable variation of protein expression during biofilm formation. For example, ribosomal proteins YvyD and RspB increase in the higher concentration of biofilm formation, and these proteins are responsible for detecting changes in environmental conditions. As *L. monocytogenes* synthesize biofilms, proteins such as SOD and Cysk are upregulated. Other essential proteins for *L. monocytogenes* to form biofilm are surface adhering protein (BapL), flagellar protein (FlaA), SOS-controller protein (YneA) and internalin (InlA) (Jordan et al., 2008; Kumar et al., 2009; van der Veen and Abee, 2010a). Studies also showed the involvement of a stress Sigma factor sigB (σB), which encodes a transcriptional regulating factors during the stress response and induction of biofilms. It was also shown that *sigB* is activated during static and continuous-flow biofilms and was resistant to quaternary ammonium compounds and peracetic acid (van der Veen and Abee, 2010b). The *agr* (accessory gene regulator) has an important role in biofilm formation of *L. monocytogenes*. Mutations caused in *agrA* and *agrD* among four *arg* regulators (*agrA*, *agrB*, *agrC* and *agrD*) have significantly reduced biofilm formation in *L. monocytogenes* as compared to wild type cells. This phenomenon was

observed when biofilms are produced on polystyrene and stainless steel surfaces (Rieu et al., 2007).

Control of L. Monocytogenes Biofilms

L. monocytogenes is a ubiquitous saprophytic organism, and it can enter a food processing plant at any place or point. *L. monocytogenes* biofilms can survive in their niche or harborage sites, which can provide protection from disinfectants (Mureddu et al., 2014). These sites are usually difficult to clean and sanitize. The niche also provides necessary optimal conditions such as temperature, organic content, and moisture, which are needed for multiplication and biofilm formation**.** The presence of organic matter and availability of sufficient moisture on food-contact or non-food contact surfaces in the food processing plants can provide a suitable microbial habitat for the development of biofilms. These surfaces must be cleaned regularly and disinfected with antimicrobials to avoid contamination of food products (Chmielewski and Frank, 2003).

L. monocytogenes is well known for surface attachment and biofilm formation in the food processing plants (Pan et al., 2006). However, there is no direct evidence available on the role of biofilms in foodborne outbreaks (Valderrama, 2013). The possible reason for this could be that the isolation and characterization of biofilms have not been a part of foodborne outbreak investigations. Cross-contamination of deli meat and mechanical cutting devices such as slicers and dicers are a potential source of *L. monocytogenes*. Proper cleaning and sanitation are key to prevent cross-contamination of ready-to-eat meat products (Johnson et al., 1990). As per the risk assessment study, proper cleaning and sanitation of all cross-contamination points, particularly, slicers, would decrease the predicted risk of listeriosis by approximately 34% (Lakicevic and Nastasijevic, 2017). Chemical disinfection is one of the commonly used methods for cleaning and sanitation. Chlorine is a widely used antimicrobial compound for the disinfection of food-contact surfaces. However, inadequate chlorine concentration applications would not help in the prevention of cross-contamination, but rather repeated exposure to such low concentrations might aid in *L. monocytogenes* sublethal adaptation.

Sodium Hypochlorite

Chlorine (sodium hypochlorite) is a widely used, low cost, antimicrobial compound for disinfection, and sanitation. Chlorine is a potent chemical oxidant and can transform or react with inorganic and organic compounds (Gray et al., 2013). Various species of chlorine (HOCl, ClO^-, Cl_2, etc.) may be present in solution depending upon the pH of the solution; however, HOCl (hypochlorous acid) is the major reactive chlorine species (Deborde and von Gunten, 2008). At neutral pH, sodium hypochlorite will form 50% HOCl and 50% ClO^-. The other chlorine reactive species do not have significant effects on microorganisms, as they are present in very low concentration in the solution. Hypochlorous acid induces structural changes in parent organic compounds and leads to the formation of chlorinated or oxidized compounds. Chlorine reacts with peptides and amino acids (only terminal amines) present in solutions, which leads to the formation of chloramines (oxidized proteins) (How et al., 2017).

The HOCl and ClO^- compounds react with organic compounds in culture broth solution like tryptic soy broth, which then leads to the formation of chloramines. These chloramines are also considered reactive chlorine species, as they are also capable of chlorinating and oxidizing compounds (Gray et al., 2013). However, chloramines are less active (four-five orders less) than HOCl and appear to have a higher affinity for cysteine and methionine oxidation. Oxidative stress by reactive chlorine species is generated when the concentration of these compounds (HOCl and chloramines, etc.) increases inside the bacteria, and the bacteria are not capable of displacing them (Sies, 1997). These reactive chlorine species induce the expression of the soxRS locus (superoxide or nitric oxide) promoter-reporter system. The soxRS region acts collectively to prevent oxidative damage or induces the repair system by different mechanisms such as scavenging for oxidants (superoxide dismutase), DNA repair (endonuclease IV), re-reduction of oxidized metals in prosthetic groups (flavodoxin and ferredoxin reductase),

reconstitution of the NADPH pool (glucose-6-phosphate dehydrogenase), reduced permeability and excretion of toxicants (efflux pumps). The soxRS activation can also induce heterologous adaptation by increasing the tolerance limits of macrophage-generated nitric oxide (NO), as well as increasing the bacteria's tolerance to antibiotics (Chou et al., 1993; Greenberg et al., 1990; Pomposiello and Demple, 2001). Generally, 50-200 ppm is recommended for chlorine concentration in food processing industries. There is a 2-log reduction on stainless steel surfaces when treated with 200 ppm of chlorine (Norwood and Gilmour, 2001). However, it is important to note that *L. monocytogenes* planktonic cells when exposed to sublethal concentrations of sodium hypochlorite on food contact surfaces, become more tolerant than its non exposed counterparts (Bansal et al., 2018).

Benzalkonium Chloride

Benzalkonium chloride (BAC) is an active cationic disinfectant belonging to the group of quaternary ammonium compounds. It penetrates the pathogens cell wall to disrupt the negatively charged cytoplasmic membrane, damages the structural integrity, and causes leakage of cytosol, nucleic acids, and protein from bacterial cells (Haubert et al., 2019). BAC is effective against foodborne pathogens, but *L. monocytogenes* showed adaptation to BAC. The BAC adaptation in *L. monocytogenes* can be due to a decrease in membrane fluidity or the presence of energy-dependent efflux systems such as *mdrL* (multidrug resistance *L. monocytogenes*) or *lde* (*L. monocytogenes* drug efflux) genes (Kraus and Peschel, 2006). BAC's are great instability; the recommended concentration is 200 ppm, and it differs based on the type of food processing plant.

Peracetic Acids

Peracetic acid (PAA) causes damage in bacterial DNA and cell death by the increase in free hydroxyl radicals (OH^-) and superoxide anions. PAA is more potent in removing biofilm-attached cells, compared with hydrogen peroxide. PAA is available as an aqueous solution mixed with acetic acid and hydrogen peroxide (Chmielewski and Frank, 2003). Similar to sodium hypochlorite and QACs, PAA solutions attenuate by organic contents. Hydrogen peroxide is a strong oxidizing antimicrobial that acts by damaging bacterial proteins, nucleic acids, and cellular membranes. The low molecular weight of hydrogen peroxide helps with the penetration of the biofilm matrix, and it causes a broad spectrum and intracellular effect (Finnegan et al., 2010). Peroxide based compounds are frequently applied in the food industries, and their recommended concentration range between 150 to 200 ppm. Biofilms formed in seafood processing surfaces are very challenging to eliminate despite combined treatments with sanitizers or disinfectants. Other strategies to control biofilms are the use of chitosan, bacteriophages, organic acids, plant extracts, surfactants and essential oils (Mizan et al., 2015). Several factors contribute to the efficacy of disinfection, such as food residue, sanitizing surface, temperature, nutrient, strain (single or mixed cocktail) and water availability (Chmielewski and Frank, 2003; Simões et al., 2010). Besides, food residues affect the efficacy of sanitizers. For example, conditioning of apple juice or diluted milk reduces the efficacy of disinfectants (Gram et al., 2007; Korany et al., 2018).

CONCLUSIONS

In summary, *L. monocytogenes* is a foodborne pathogen that causes life-threatening diseases in susceptible human populations. The biofilm formation ability of *L. monocytogenes* helps in its persistence in the processing plants and acts as a continuous cross-contamination source. Despite the availability of specific antibiotics for listeriosis treatment, emerging antibiotic resistance in *L. monocytogenes* is a matter of concern. Inadequate application of antimicrobials such as chlorine in the food processing environment can influence the *L. monocytogenes* biofilm formation and may create stress-resistant subpopulations with changes in susceptibility to biocides. Therefore, measures should be taken to ensure the application of appropriate concentrations of antimicrobials in the food processing plants that will prevent the development of biofilms and tolerant *L. monocytogenes* subpopulations.

CONFLICT OF INTEREST

There is no conflict of interest to declare.

ACKNOWLEDGEMENTS

This material is based upon the work that is supported by the Food Safety Initiative award to Nannapaneni from the Mississippi Agricultural and Forestry Experiment Station under project MIS-401210 with grant number USDA-ARS SCA No. 58-6402-2729.

LITERATURE CITED

Abeysundara PDA, Dhowlaghar N, Nannapaneni R, Schilling MW, Chang S, Mahmoud B, Sharma CS, Ma DP. Growth and biofilm formation by *Listeria monocytogenes* in cantaloupe flesh and peel extracts on four food-contact surfaces at 22° C and 10° C. Food Control. 2017; 80:131-142.

Araújo P, Lemos M, Mergulhão F, Melo L, Simões M. Antimicrobial resistance to disinfectants in biofilms. Science against microbial pathogens: Comm. Curr. Res. Tech. Adv. 2011; 3:826-834.

Adetunji VO, Isola TO. Crystal violet binding assay for assessment of biofilm formation by *Listeria monocytogenes* and *Listeria* spp on wood, steel and glass surfaces. Global Vet. 2011; 6: 6-10.

Bansal M, Nannapaneni R, Sharma CS, Kiess A. *Listeria monocytogenes* response to sublethal chlorine induced oxidative stress on homologous and heterologous stress adaptation. Front. Microbiol. 2018; 9:2050.

Bigot A, Pagniez H, Botton E, Fréhel C, Dubail I, Jacquet C, Charbit A, Raynaud C. Role of FliF and FliI of *Listeria monocytogenes* in flagellar assembly and pathogenicity. Infect. and Imm. 2005; 73:5530-5539.

Blackman IC, Frank J.F. Growth of *Listeria monocytogenes* as a biofilm on various food-processing surfaces. J. Food. Prot. 1996; 59:827-831.

Bereksi N, Gavini F, Benezech T, Faille C. Growth, morphology and surface properties of *Listeria monocytogenes* Scott A and LO28 under saline and acid environments. J Appl Microbiol. 2002; 92:556-565.

Borucki MK, Peppin JD, White D, Loge F, Call DR. Variation in biofilm formation among strains of *Listeria monocytogenes*. Appl. Environ. Microbiol. 2003; 69:7336-7342.

Bos R, Van der Mei H, Gold J, Busscher H. Retention of bacteria on a substratum surface with micro-patterned hydrophobicity. FEMS Microbiol. Lett. 2000; 189:311-315.

Cartwright EJ, Jackson KA, Johnson SD, Graves LM, Silk BJ, Mahon BE. Listeriosis outbreaks and associated food vehicles, United States, 1998–2008. Emerg. Infect. Dis. 2013; 19:1.

CDC. Update: multistate outbreak of listeriosis-United States, 1998-1999.MMWR. Morbidity and mortality weekly report. 1999; 47:1117.

CDC. Multistate outbreak of Listeriosis linked to whole cantaloupes from Jensen farms, Colorado (FINAL UPDATE). Center for Disease Control and Prevention, 2011; Available at https://www.cdc.gov/listeria/outbreaks/cantaloupes-jensen-farms/index.html; Accessed on 11/8/2019.

CDC. Multistate outbreak of Listeriosis Linked to imported frescolina marte brand ricotta salata cheese (Final Update). Center for Disease Control and Prevention, 2012; Available at https://www.cdc.gov/listeria/outbreaks/cheese-09-12/index.html; Accessed on 11/8/2019.

CDC. Multistate outbreak of listeriosis linked to crave brothers farmstead cheeses (Final Update). Center for Disease Control and Prevention, 2013; Available at https://www.cdc.gov/listeria/outbreaks/cheese-07-13/index.html; Accessed on 11/8/2019.

CDC. Wholesome soy products, Inc. sprouts and investigation of human listeriosis cases (Final Update). Center for Disease Control and Prevention, 2014; Available at https://www.cdc.gov/listeria/outbreaks/bean-sprouts-11-14/index.html; Accessed on 11/8/2019.

CDC. Multistate outbreak of listeriosis linked to blue bell creameries products (Final Update). Center for Disease Control and Prevention, 2015; Available athttps://www.cdc.gov/listeria/outbreaks/ice-cream-03-15/index.html; Accessed on 11/8/2019.

CDC. Multistate outbreak of listeriosis linked to frozen vegetables (Final Update). Center for Disease Control and Prevention, 2016; Available athttps://www.cdc.gov/listeria/outbreaks/frozen-vegetables-05-16/index.html; Accessed on 11/8/2019.

CDC. Multistate outbreak of listeriosis linked to soft raw milk cheese made by vulto creamery (Final Update). Center for Disease Control and Prevention, 2017; Available at https://www.cdc.gov/listeria/outbreaks/soft-cheese-03-17/index.html; Accessed on 11/8/2019.

CDC. Outbreak of *Listeria monocytogenes* infections linked to deli ham (Final Update). Center for Disease Control and Prevention, 2018; Available at https://www.cdc.gov/listeria/outbreaks/countryham-10-18/index.html; Accessed on 11/8/2019.

CDC. Outbreak of *Listeria monocytogenes* infections linked to deli-sliced meats and cheeses. Center for Disease Control and Prevention, 2019; Available at https://www.cdc.gov/listeria/outbreaks/deliproducts-04-19/index.html; Accessed on 11/8/2019.

Chou JH, Greenberg JT, Demple B. Posttranscriptional repression of *Escherichia coli* OmpF protein in response to redox stress: positive control of the micF antisense RNA by the soxRS locus. J Bacteriol. 1993; 175: 1026-1031.

Chiarini E, Tyler K, Farber JM, Pagotto F, Destro MT. *Listeria monocytogenes* in two different poultry facilities: manual and automatic evisceration. Poultry Sci. 2009; 88: 791-797.

Chmielewski R, Frank J. Biofilm formation and control in food processing facilities. Comp. Rev. Food. Sci. Food Saf. 2003; 2: 22-32.

Cooksey K. Extracellular polymers in biofilms, Biofilms—science and technology. Springer. 1992; pp.137-147.

Colagiorgi A, Di Ciccio P, Zanardi E, Ghidini S, Ianieri A. A look inside the *Listeria monocytogenes* biofilms extracellular matrix. Microorg. 2016; 4:22.

Currie A, Farber JM, Nadon C, Sharma D, Whitfield Y, Gaulin C, Galanis E, Bekal S, Flint J, Tschetter L, Pagotto F. Multi-province listeriosis outbreak linked to contaminated deli meat consumed primarily in institutional settings, Canada, 2008. Foodborne Path Dis. 2015; 12: 645-652.

Deborde M, Von Gunten UR. Reactions of chlorine with inorganic and organic compounds during water treatment-kinetics and mechanisms: a critical review. Water Res. 2008; 1; 42: 13-51.

Dhowlaghar N, Abeysundara PDA, Nannapaneni R, Schilling MW, Chang S, Cheng WH, Sharma CS. Growth and biofilm formation by *Listeria monocytogenes* in catfish mucus extract on four food contact surfaces at 22 and 10° C and their reduction by commercial disinfectants. J. Food. Prot. 2017; 81: 59-67.

Dhowlaghar N, Bansal M, Schilling MW, Nannapaneni R. Scanning electron microscopy of *Salmonella* biofilms on various food-contact surfaces in catfish mucus. Food. Microbiol. 2018; 74: 143-150.

Di Bonaventura G, Piccolomini R, Paludi D, D'orio V, Vergara A, Conter M, Ianieri A. Influence of temperature on biofilm formation by *Listeria monocytogenes* on various food-contact surfaces: relationship with motility and cell surface hydrophobicity. J. Appl. Microbiol. 2008; 104: 1552-1561.

Doijad SP, Barbuddhe SB, Garg S, Poharkar KV, Kalorey DR, Kurkure NV, Rawool DB, Chakraborty T. Biofilm-forming abilities of *Listeria monocytogenes* serotypes isolated from different sources. PLoS One. 2015; 10:e0137046.

Donlan RM, Costerton JW. Biofilms: survival mechanisms of clinically relevant microorganisms. Clin. Microbiol. Rev. 2002; 15: 167-193.

Duan Q, Zhou M, Zhu L, Zhu G. Flagella and bacterial pathogenicity. J. Bas Microbiol. 2013; 53: 1-8.

Endrikat S, Gallagher D, Pouillot R, Quesenberry HH, LaBarre D, Schroeder CM, Kause J. A comparative risk assessment for *Listeria monocytogenes* in prepackaged versus retail-sliced deli meat. J. Food. Prot. 2010; 73: 612-619.

Farber J, Sanders G, Johnston M. A survey of various foods for the presence of *Listeria* species. J. Food. Prot. 1989; 52: 456-458.

Finnegan M, Linley E, Denyer SP, McDonnell G, Simons C, Maillard JY. Mode of action of hydrogen peroxide and other oxidizing agents: differences between liquid and gas forms. J.of Antimicrob. Chem. 2010; 65:2108-2115.

Flemming HC, Wingender J. The biofilm matrix. Nature. Rev. Microbiol. 2010; 8: 623.

Flemming HC, Neu TR, Wozniak DJ. The EPS matrix: the "house of biofilm cells". J Bacteriol. 2007; 189: 7945-7947.

Fong JN, Yildiz FH. Biofilm matrix proteins. Microbiology spectrum. 2015; 10: 1128.

Folsom JP, Siragusa GR, Frank JF. Formation of biofilm at different nutrient levels by various genotypes of *Listeria monocytogenes*. J. Food. Prot. 2006; 69: 826-834.

Frye DM, Zweig R, Sturgeon J, Tormey M, LeCavalier M, Lee I, Lawani L, Mascola L. An outbreak of febrile gastroenteritis associated with delicatessen meat contaminated with *Listeria monocytogenes*. Cli. Infect. Dis. 2002; 35: 943-949.

Giotis ES, Blair IS, McDowell DA. Morphological changes in *Listeria monocytogenes* subjected to sublethal alkaline stress. International J Food Microbiol. 2007; 120: 250-258.

Gottlieb SL, Newbern EC, Griffin PM, Graves LM, Hoekstra RM, Baker NL, Hunter SB, Holt KG, Ramsey F, Head M, Levine P. Multistate outbreak of listeriosis linked to turkey deli meat and subsequent changes in US regulatory policy. Clin Infect Dis. 2006; 42: 29-36.

Gram L, Bagge-Ravn D, Ng YY, Gymoese P, Vogel BF. Influence of food soiling matrix on cleaning and disinfection efficiency on surface attached *Listeria monocytogenes*. Food Control. 2007; 18: 1165-1171.

Graves LM, Swaminathan B, Hunter SB. Subtyping *Listeria monocytogenes*, *Listeria*, listeriosis, and food safety. CRC Press. 2007; pp. 301-322.

Gray MJ, Wholey WY, Jakob U. Bacterial responses to reactive chlorine species. Ann Rev Microbiol. 2013; 67: 141-160.

Greenberg JT, Monach P, Chou JH, Josephy PD, Demple B. Positive control of a global antioxidant defense regulon activated by superoxide-generating agents in *Escherichia coli*. PNAS. 1990; 87: 6181-6185.

Guobjoernsdottir B, Einarsson H, Thorkelsson, G. Microbial adhesion to processing lines for fish fillets and cooked shrimp: influence of stainless steel surface finish and presence of gram-negative bacteria on the attachment of *Listeria monocytogenes*. Food Technol. Biotechnol. 2005; 43: 55-61.

Hamon M, Bierne H, Cossart P. *Listeria monocytogenes*: a multifaceted model. Nature Rev. Microbiol. 2006; 4: 423.

Harvey J, Keenan K, Gilmour A. Assessing biofilm formation by *Listeria monocytogenes* strains. Food Microbiol. 2007; 24: 380-392.

Haubert L, Zehetmeyr ML, Pereira YMN, Kroning IS, Maia DSV, Sehn CP, Lopes GV, de Lima AS, da Silva WP. Tolerance to benzalkonium chloride and antimicrobial activity of *Butia odorata* Barb. Rodr. extract in *Salmonella* spp. isolates from food and food environments. Food. Res. Int. 2019; 116: 652-659.

How ZT, Linge KL, Busetti F, Joll CA. Chlorination of amino acids: reaction pathways and reaction rates. Environ. Sci. Technol. 2017; 51: 4870-4876.

Johnson JL, Doyle MP, Cassens. *Listeria monocytogenes* and other Listeria spp. in meat and meat products a review. J. Food. Prot. 1990; 53: 81-91.

Jordan SJ, Perni S, Glenn S, Fernandes I, Barbosa M, Sol M, Tenreiro RP, Chambel L, Barata, B, Zilhao I. *Listeria monocytogenes* biofilm-associated protein (BapL) may contribute to surface attachment of *L. monocytogenes* but is absent from many field isolates. Appl. Environ. Microbiol. 2008; 74: 5451-5456.

Kadam SR, den Besten HM, van der Veen S, Zwietering MH, Moezelaar R, Abee T. Diversity assessment of *Listeria monocytogenes* biofilm formation:

impact of growth condition, serotype and strain origin. Int. J. Food Microbiol. 2013; 165: 259-264.

Korany AM, Hua Z, Green T, Hanrahan I, El-Shinawy SH, El-Kholy A, Hassan G, Zhu MJ. Efficacy of ozonated water, chlorine, chlorine dioxide, quaternary ammonium compounds and peroxyacetic acid against *Listeria monocytogenes* biofilm on polystyrene surfaces. Front. Microbiol. 2018; 9: 2296.

Kraus D, Peschel A. Molecular mechanisms of bacterial resistance to antimicrobial peptides, Antimicrobial Peptides and Human Disease. Springer. 2006; pp. 231-250.

Kumar S, Parvathi A, George J, Krohne G, Karunasagar I, Karunasagar I. A study on the effects of some laboratory-derived genetic mutations on biofilm formation by *Listeria monocytogenes*. World. J. Microbiol. Biotechnol. 2009; 25: 527-531.

Lakicevic B, Nastasijevic I. *Listeria monocytogenes* in retail establishments: Contamination routes and control strategies. Food. Rev. Int. 2017; 33: 247-269.

Lemon KP, Higgins DE, Kolter R. Flagellar motility is critical for *Listeria monocytogenes* biofilm formation. J. Bacteriol. 2007; 189: 4418-4424.

Lunden JM, Autio TJ, Korkeala H J. Transfer of persistent Listeria monocytogenes contamination between food-processing plants associated with a dicing machine. J. Food. Prot. 2002; 65: 1129-1133.

Lunden JM, Miettinen MK, Autio TJ, Korkeala HJ. Persistent *Listeria monocytogenes* strains show enhanced adherence to food contact surface after short contact times. J. Food. Prot. 2000; 63:1204-1207.

Mead PS, Dunne EF, Graves L, Wiedmann M, Patrick M, Hunter S, Salehi E, Mostashari F, Craig A, Mshar P, Bannerman T. Nationwide outbreak of listeriosis due to contaminated meat. Epidemiol Infect. 2006; 134: 744-751.

Mittelman MW. Structure and functional characteristics of bacterial biofilms in fluid processing operations. J. Dairy Sci. 1998; 81: 2760-2764.

Mizan MFR, Jahid IK, Ha SD. Microbial biofilms in seafood: a food-hygiene challenge. Food Microbiol. 2015; 49: 41-55.

Muhterem-Uyar M, Dalmasso M, Bolocan AS, Hernandez M, Kapetanakou AE, Kuchta T, Manios SG, Melero B, Minarovičová J, Nicolau AI, Rovira J. Environmental sampling for *Listeria monocytogenes* control in food processing facilities reveals three contamination scenarios. Food Control. 2015; 51: 94-107.

Mureddu A, Mazza R, Fois F, Meloni D, Bacciu R, Piras F, Mazzette R. *Listeria monocytogenes* persistence in ready-to-eat sausages and in processing plants. Italian J. Food Saf. 2014; 3: 1697.

Nilsson RE, Ross T, Bowman JP. Variability in biofilm production by *Listeria monocytogenes* correlated to strain origin and growth conditions. Int. J. Food Microbiol. 2011; 150: 14-24.

Norwood D, Gilmour A. The differential adherence capabilities of two *Listeria monocytogenes* strains in monoculture and multispecies biofilms as a function of temperature. Lett. Appl. Microbiol. 2001; 33: 320-324.

O'Neil HS, Marquis H. *Listeria monocytogenes* flagella are used for motility, not as adhesins, to increase host cell invasion. Infect Imm. 2006; 74: 6675-6681.

Ooi ST, Lorber B. Gastroenteritis due to *Listeria monocytogenes*. Clin Infect Dis. 2005; 40: 1327-1332.

Ochiai Y, Yamada F, Mochizuki M, Takano T, Hondo R, Ueda F. Biofilm formation under different temperature conditions by a single genotype of persistent *Listeria monocytogenes* strains. J.Food Prot. 2014; 77: 133-140.

Oliveira NM, Martinez-Garcia, E, Xavier J, Durham WM, Kolter R, Kim W, Foster KR. Biofilm formation as a response to ecological competition. PLoS Biol. 2015; 13: 1-23.

Ortiz S, López V, Martínez-Suárez JV. The influence of subminimal inhibitory concentrations of benzalkonium chloride on biofilm formation by *Listeria monocytogenes*. Int. J. Food Microbiol. 2014; 189:106-112.

Palková Z. Multicellular microorganisms: laboratory versus nature. EMBO reports. 2004; 5: 470–476

Pan Y, Breidt F, Kathariou S. Resistance of *Listeria monocytogenes* biofilms to sanitizing agents in a simulated food processing environment. Appl. Environ. Microbiol. 2006; 72: 7711-7717.

Peel M, Donachie W, Shaw A. Temperature-dependent expression of flagella of *Listeria manocytogenes* studied by electron microscopy, SDS-PAGE and Western blotting. Microbiol. 1988; 134: 2171-2178.

Pomposiello PJ, Demple B. Redox-operated genetic switches: the SoxR and OxyR transcription factors. Trends in Biotechnol. 2001; 19: 109-114.

Rieu A, Weidmann S, Garmyn D, Piveteau P, Guzzo J. Agr system of *Listeria monocytogenes* EGD-e: role in adherence and differential expression pattern. Appl. Environ. Microbiol. 2007; 73: 6125-6133.

Rodrigues LB, Santos LRd, Tagliari VZ, Rizzo NN, Trenhago G, Oliveira APd, Goetz F, Nascimento VPd. Quantification of biofilm production on polystyrene by *Listeria*, *Escherichia coli* and *Staphylococcus aureus* isolated from a poultry slaughterhouse. Braz. J. Microbiol. 2010; 41: 1082-1085.

Rodriguez A, Autio WR, McLandsborough LA. Effects of inoculation level, material hydration, and stainless steel surface roughness on the transfer of *Listeria monocytogenes* from inoculated bologna to stainless steel and high-density polyethylene. J. Food. Prot. 2007; 70: 1423-1428.

Rodriguez A, Autio WR, McLandsborough LA. Effects of contact time, pressure, percent relative humidity (% RH), and material type on *Listeria* biofilm adhesive strength at a cellular level using atomic force microscopy (AFM). Food. Biophys. 2008; 3: 305-311.

Ronner AB, Wong AC. Biofilm development and sanitizer inactivation of *Listeria monocytogenes* and *Salmonella* Typhimurium on stainless steel and buna-n rubber. J. Food Prot. 1993; 56: 750-758.

Scallan E, Hoekstra R, Mahon B, Jones T, Griffin P. An assessment of the human health impact of seven leading foodborne pathogens in the United States using disability adjusted life years. Epidemiol. Infect. 2015; 143: 2795-2804.

Scallan E, Hoekstra RM, Angulo FJ, Tauxe RV, Widdowson MA, Roy SL, Jones JL, Griffin PM. Foodborne illness acquired in the United States—major pathogens. Emerg. Infect. Dis. 2011; 17: 7-15.

Schlech III WF, Lavigne PM, Bortolussi RA, Allen AC, Haldane EV, Wort AJ, Hightower AW, Johnson SE, King SH, Nicholls ES, Broome CV. Epidemic listeriosis—evidence for transmission by food. New England J. Med. 1983; 308: 203-206.

Seeliger HP. Modern taxonomy of the *Listeria* group relationship to its pathogenicity. Clin. Invest. Med. 1984; 7: 217-221.

Sies H. Oxidative stress: oxidants and antioxidants. Experimental Physiology: Translation and Integration. 1997; 82: 291-295.

Sivaranjani M, Gowrishankar S, Kamaladevi A, Pandian SK, Balamurugan K, Ravi AV. Morin inhibits biofilm production and reduces the virulence of *Listeria monocytogenes*-An in vitro and in vivo approach. Int. J. Food Microbiol. 2016; 237: 73-82.

Simões M. Simões LC, Vieira MJ. A review of current and emergent biofilm control strategies. LWT-Food Sci. Technol. 2010; 43: 573-583.

Smoot LM, Pierson MD. Influence of environmental stress on the kinetics and strength of attachment of *Listeria monocytogenes* Scott A to Buna-N rubber and stainless steel. J. Food. Prot.1998; 61: 1286-1292.

Stepanović S, Ćirković I, Ranin L, S vabić-Vlahović M. Biofilm formation by *Salmonella* spp. and *Listeria monocytogenes* on plastic surface. Lett. Appl. Microbiol. 2004; 38: 428-432.

Takahashi H, Miya S, Igarashi K, Suda T, Kuramoto S, Kimura B. Biofilm formation ability of *Listeria monocytogenes* isolates from raw ready-to-eat seafood. J. Food Prot. 2009; 72: 1476-1480.

Taormina PJ, Beuchat LR. Survival and heat resistance of *Listeria monocytogenes* after exposure to alkali

and chlorine. Appl. Environ. Microbiol. 2001; 67: 2555-2563.

Thévenot D, Delignette-Muller ML, Christieans S, Vernozy-Rozand C. Fate of *Listeria monocytogenes* in experimentally contaminated French sausages. Int. J. Food. Microbiol. 2005; 101: 189-200.

Upadhyay A, Upadhyaya I, Kollanoor-Johny A, Venkitanarayanan K. Antibiofilm effect of plant derived antimicrobials on *Listeria monocytogenes*. Food Microbiol. 2013; 36: 79-89.

van der Veen S, Abee T. Dependence of continuous-flow biofilm formation by *Listeria monocytogenes* EGD-e on SOS response factor YneA. Appl. Environ. Microbiol. 2010a; 76: 1992-1995.

van der Veen S, Abee T. Importance of SigB for *Listeria monocytogenes* static and continuous-flow biofilm formation and disinfectant resistance. Appl. Environ. Microbiol. 2010b; 76: 7854-7860.

Valderrama WB, Cutter CN. An ecological perspective of *Listeria monocytogenes* biofilms in food processing facilities. Cri. Rev. Food Sci. Nut. 2013; 53: 801-817.

Vasseur C, Baverel L, Hebraud M, Labadie J. Effect of osmotic, alkaline, acid or thermal stresses on the growth and inhibition of *Listeria monocytogenes*. J. Appl. Microbiol. 1999; 86: 469-476.

Vorst KL, Todd EC, Ryser ET. Transfer of *Listeria monocytogenes* during mechanical slicing of turkey breast, bologna, and salami. J. Food. Protect. 2006; 69: 619-626.

Vu B, Chen M, Crawford RJ, Ivanova EP. Bacterial extracellular polysaccharides involved in biofilm formation. Molecules 2009; 14: 2535-2554.

Weiler C, Ifland A, Naumann A, Kleta S, Noll M. Incorporation of *Listeria monocytogenes* strains in raw milk biofilms. Int. J. Food. Microbiol. 2013; 161: 61-68.

Wenger JD, Swaminathan B, Hayes PS, Green SS, Pratt M, Pinner PW, Schuchat A, Broome CV. *Listeria monocytogenes* contamination of turkey franks: evaluation of a production facility. J. Food Prot. 1990; 53: 1015-1019.

Wu S, Wu Q, Zhang J, Chen M, Hu H. Listeria monocytogenes prevalence and characteristics in retail raw foods in China. PLoS One. 2015;10:e0136682.

Effect of Herbicide Additions on pH for Approved Dicamba Tank-Mixers in Cotton

J. Connor Ferguson*, Justin S. Calhoun, Kayla L. Broster, Luke H. Merritt, Michael T. Wesley, and Zachary R. Treadway

Department of Plant and Soil Sciences and Mississippi Agriculture and Forestry Experiment Station, Mississippi State University, Mississippi State, MS 39762, USA

*Corresponding author: J. Connor Ferguson, E-mail: connor.ferguson@msstate.edu

ABSTRACT

With the introduction of dicamba-tolerant cotton cultivars, the use of dicamba products tank-mixed with other herbicides has increased dramatically. pH is significant for herbicide efficacy, as changes to a pH can affect efficacy, especially when the pH of the tank-mixture is increased, thereby neutralizing weak acid herbicides like glyphosate. pH values of these mixtures are crucial to monitor, as pH can significantly increase the potential for volatilization and off-target movement of dicamba containing compounds. An experiment was conducted to determine the pH values of several commonly used tank-mixes involving dicamba. Studies were also conducted to assess the effect of glyphosate formulation and rate on the pH of dicamba tank-mixtures. Results indicate that any addition of glyphosate to a labeled dicamba herbicide, resulted in a pH lower than 5.0, except for Engenia® plus Credit Xtreme®. The addition of the 25 other labeled herbicides to dicamba resulted in a negligible change in pH. This research suggests that only the addition of glyphosate to tank-mixes with dicamba contributes to a significant reduction in pH.

Keywords: glyphosate, herbicide efficacy, off-target movement, adjuvant

Abbreviations: XMX, Xtendimax; FEX, Fexapan; ENG, Engenia; DRA, Drift reduction adjuvant; COC, Crop oil concentrate; NIS, Non-ionic surfactant, MSO, Methylated seed oil

INTRODUCTION

Over the past decade, herbicide resistance has been the driving factor in herbicide selection and use. In the midsouth, Palmer amaranth (*Amaranthus palmeri* S. Waats) control has been the focal point of weed management programs and research (Norsworthy et al., 2014, Schwartz-Lazaro et al., 2017, Ward et al., 2013). Multiple resistance among weed species has reduced herbicide options for cotton producers. However, the introduction of dicamba-tolerant cropping systems provided a resource to combat herbicide resistance for cotton and soybean producers. Incorporation of auxin herbicides into cotton weed management programs has resulted in satisfactory levels of control of *Amaranthus* spp. and has alleviated selection pressure for other modes of action (Meyer et al., 2019).

One significant issue of dicamba use in cotton is the exaggerated sensitivity of non-target broadleaf species, specifically soybean. This has led to increased concerns and extensive research into two forms of off-target movement: volatilization/vapor drift and physical/particle drift. Andersen et al. (2004) documented a 14% yield reduction when non-tolerant soybean was exposed to dicamba at the V3 stage of growth at 0.0056 kg ae ha^{-1} ($1/100^{th}$ of 1x labeled rate). At the sixth leaf and first square growth stages, dicamba has shown to reduce non-tolerant cotton yield by 30 and 41%, respectively, when applied at lower carrier volumes (Smith et al. 2017). In drift scenarios, non-target species are exposed to low carrier volume spray solutions with higher herbicide concentrations, thus increasing the potential for detrimental herbicidal effects (Smith et al., 2017). To reduce the potential for off-target movement, strict label guidelines have been implemented for the use of these products.

Instructions on how to avoid low pH tank-mixtures (defined as less than 5.0) were included in label

updates for dicamba re-registration beginning in 2019 (Anonymous, 2019a, 2019b, 2019c). The parent acid of dicamba (3,6-dichloro-2-methoxybenzoic acid) is categorized as a weak carboxylic acid with a pKa of 1.87 (Shaner, 2014). When dissolved in water, formulated dicamba salts dissociate into dicamba anions, which can bond with any available protons to form volatile dicamba acid. In higher pH spray solutions, the majority of dicamba is dissociated, and tiny amounts of dicamba acid are formed. However, in low pH solutions (less than 5.0) more protons are available for binding with dicamba anions to produce dicamba acid. To overcome this phenomenon, Bayer introduced VaporGrip® technology (VG). VG uses an acetic acid-acetate buffering system to conjugate any additional protons introduced to the spray solution by tank-mixed products or water, which reduces the potential of volatile dicamba acid formation (Witten 2019).

Understanding the pH of spray solutions and the effect it has on volatilization is crucial in managing mitigation of off-target movement of dicamba products. Unfortunately, little is known about specific pH values of individual tank-mixtures labeled for use with dicamba. Mueller and Steckel (2019) reported pH values for various combinations of dicamba and glyphosate formulations, water sources, and tank additives, including ammonium sulfate, drift reduction agents, and pH modifiers. Results showed that a number of these combinations resulted in a pH value lower than the 5.0 level recommended by dicamba labels to avoid volatility issues (Mueller and Steckel 2019, Anonymous 2019a, 2019b, 2019c).

The objective of this research was to assess the herbicide tank-mixture effect on pH for herbicides labeled for use with dicamba in cotton. Understanding the pH values of these solutions will play a crucial role in providing information as to which tank-mixture options will result in the most significant potential for volatility and off-target movement.

MATERIALS AND METHODS

Studies were conducted at Mississippi State University between January 2nd and January 16th, 2019, to quantify the effect of herbicides on pH for approved dicamba tank-mixtures. The pH was measured using an Oakton® pH 700 Benchtop Meter (Oakton Instruments, Vernon Hills, IL) equipped with an all-in-one electrode that measures both pH and temperature of solutions. Before each use, the meter was calibrated using Oakton pH buffer standards of 4.01, 7.0, and 10.00. By calibrating using these standards, the instrument could accurately measure any range of tank-mixture pH that resulted in the study. Temperatures for all tank-mixtures at each time interval ranged between 20 and 21.5°C; thus, repeatability of the mixtures was maintained. All herbicides were mixed for a 140 L ha^{-1} (15 GPA) application volume using only approved herbicide additions for each respective dicamba formulation. Tank-mixtures were measured out into beakers and mixed to a 300 mL volume. Water for the tank-mixture was the standard tap water in the laboratory, which recorded a pH of 7.57. In between tank-mixture pH readings, the probe was rinsed using a three-step wash process in beakers filled with deionized water. The probe was plunged into one beaker, wiped off, and this process continued until the third beaker. Beakers were changed out every three tank-mixtures and replaced with fresh deionized water. After initial pH measurement was conducted, tank-mixtures were stored in 473 mL HDPE plastic bottles until poured back into beakers for pH readings 24, and 48 hours after initial measurement. Replications of the mixtures were made in time at those three intervals (0, 24, and 48 hours). Before pouring into the beakers, each tank-mixture was agitated for 30 seconds, as several tank-mixtures settled out in the bottles.

Dicamba formulations used in the study included both commercially available diglycolamine salt + vapor grip™ formulations - Xtendimax® (Bayer Crop Science, St Louis, MO) and Fexapan® (Corteva Agriscience, Indianapolis, IN) and the *N*,*N*-Bis-(3-aminopropyl) methylamine salt formulation of dicamba - Engenia® (BASF, Research Triangle Park, NC). For ease of reading, the previous herbicides will be referred to as XMX, FEX, and ENG, respectively. Each dicamba herbicide was mixed at their field recommended rate of 561 g ae ha^{-1}. Two sub-studies were conducted as part of this project: one study assessing the effect of glyphosate formulation and

glyphosate addition rate on tank-mixture pH and the second study measuring the impact of approved herbicide combinations added to XMX, FEX, or ENG.

Glyphosate Formulation and Rate Study

Six formulations of glyphosate were mixed at two different rates, 863 and 1,261 g ae ha^{-1}. Four formulations were a potassium salt of glyphosate (K), one formulation was an isopropylamine salt (IPA), and one was a combination of K and IPA salts. The four K salt formulations were Roundup Powermax® (RUPM), Roundup Powermax II®(RUPM II), Roundup Weathermax® (WMAX) (Bayer Crop Sciences, St. Louis, MO) and Abundit Edge (Corteva Agriscience, Indianapolis, IN). The IPA salt formulation was Cornerstone® Plus (WinField United, River Falls, WI). The combination K and IPA salt formulation was Credit® Xtreme (Nufarm Inc., Alsip, IL). XMX and FEX were only labeled for use with the K salt formulations, so only four of the six formulations were added to both herbicides. Several of the tank-mixture herbicides labeled for use in cotton require the addition of glyphosate to be applied. The tank-mixtures without glyphosate were also recorded to better understand the effect of each approved tank-mixture herbicide on pH. For all tank-mixtures that included glyphosate across the three dicamba formulations, a drift reduction adjuvant (DRA) was added as per the label - Intact™ (Precision Labs, Waukegan, IL) at 0.5% v/v. This study included 28 total treatments, as listed in Table 1. For all tank-mixtures, the initial pH was recorded, and measurements were made at 24 and 48 hours after the initial reading. This was maintained +/- 30 minutes from the initial pH reading for the entirety of the study.

Approved Herbicide Tank-Mixture Study

Approved herbicides labeled for use with dicamba in cotton were selected to quantify their effect on tank-mixture pH. As with the glyphosate study, XMX, FEX, and ENG were mixed at 561 g ae ha^{-1} and mixed with other approved cotton herbicides for use with dicamba. Herbicides selected for use in the tank-mixture study and rates were: acetochlor at 1,680 g ai ha^{-1} (Warrant®, Bayer Crop Science, St. Louis, MO); acetochlor at 1,729 g ai ha^{-1} plus fomesafen at 386 g ai ha^{-1} (Warrant Ultra®, Bayer Crop Science, St. Louis, MO); clethodim at 280 g ai ha^{-1} (Section Three®, WinField United, River Falls, WI); clethodim at 272 g ai ha^{-1} (Select Max®, Valent U.S.A., Walnut Creek, CA); clethodim at 280 g ai ha^{-1} (Vaquero®, Wilbur-Ellis Company, Fresno, CA); dimethenamid-P at 1,100 g ai ha^{-1} (Outlook®, BASF, Research Triangle Park, NC); diuron at 1,800 g ai ha^{-1} (Direx 4L®, Adama, Raleigh, NC); diuron at 2,470 g ai ha^{-1} (Diuron 4L®, Adama, Raleigh, NC); fluazifop at 210 g ai ha^{-1} (Fusilade DX®, BASF Ag Products, Research Triangle Park, NC); flumioxazin at 71.5 g ai ha^{-1} (Valor SX®, Valent U.S.A., Walnut Creek, CA); fluometuron at 2,240 g ai ha^{-1} (Cotoran 4L®, Adama, Raleigh, NC); fomesafen at 420 g ai ha^{-1} (Reflex®, Syngenta Crop Protection, Greensboro, NC); fomesafen at 420 g ai ha^{-1} (Flexstar®, Syngenta Crop Protection, Greensboro, NC); lactofen at 220 g ai ha^{-1} (Cobra®, Valent U.S.A, Walnut Creek, CA); pendimethalin at 1,600 g ai ha^{-1} (Prowl H20®, BASF Ag Products, Research Triangle Park, NC); pendimethalin at 1,670 g ai ha^{-1} (Satellite Flex®, UPL NA, King of Prussia, PA); prometryn at 3,140 g ai ha^{-1} (Caparol 4L®, Syngenta Crop Protection, Greensboro, NC); pyrithiobac-sodium at 106 g ai ha^{-1} (Staple LX®, Corteva Agriscience, Indianapolis, IN); *S*-metolachlor at 1,420 g ai ha^{-1} (Cinch®, Corteva Agriscience, Indianapolis, IN); *S*-metolachlor at 1,420 g ai ha^{-1} (Everprex®, Corteva Agriscience, Indianapolis, IN); *S*-metolachlor at 1,420 g ai ha^{-1} (Dual Magnum®, Syngenta Crop Protection, Greensboro, NC); *S*-metolachlor at 1,417 g ai ha^{-1} plus fomesafen at 311 g ai ha^{-1} (Prefix®, Syngenta Crop Protection, Greensboro, NC); and saflufenacil at 25 g ai ha^{-1} (Sharpen®, BASF Ag Products, Research Triangle Park, NC). Only tank-mixtures approved on each respective dicamba formulation's label were included in the study. Additionally, two approved herbicides were tested with and without the addition of glyphosate as required by the label on www.engeniatankmix.com. Those herbicides and rates were fluridone at 337 g ai ha^{-1} (Brake®, SePro Corporation, Carmel, IN) and quizalofop at 93 g ai ha^{-1} (Assure II, Amvac Chemical Corporation, Newport Beach, CA). As with the glyphosate formulation study, pH measurements were taken initially (0 h), 24, and 48 hours after the initial reading, +/- 30 minutes. For all tank-mixture herbicides, the highest labeled

rate of the additional herbicide was selected to "stress" the system as much as possible. It was conjectured that if pH did not drop below 5 at the highest labeled rate of the addition, then it would not reduce pH below 5 at any labeled rate below that. For herbicides that were recommended for use with a crop oil concentrate (COC), methylated seed oil (MSO), or non-ionic surfactant (NIS), tank-mixtures were made to include all permutations of the above as additional mixtures – to ensure nothing was left undone from the study. The adjuvants used for the study were: COC (Penetrator Plus™, Helena, Collierville, TN), MSO (Noble™, WinField United, River Falls, WI), and NIS (Activate Plus™, WinField United, River Falls, WI). All three of the adjuvants are approved for use across all three dicamba formulations. The DRA added for these, and all tank-mixtures requiring a DRA was Intact™ (Precision Labs, Waukegan, IL) at 0.5% v/v. The study included 94 total tank-mixtures, measured at 0, 24, and 48 hours (h) after mixing for pH. Treatments are listed in Table 2. The pH measurements from the sub-component of this study that which examined herbicides required by the label at www.engeniatankmix.com to use approved glyphosate when tank-mixed with ENG are shown in Table 3.

Statistical Methods

For the glyphosate formulation and rate study, proper pH sample timings (0, 24, and 48 h) were used as replicates. Data were then subjected to ANOVA using R-studio (Version 1.2.1335, RStudio, Inc.) to investigate the main effect of glyphosate rate and formulation, as well as dicamba formulation. Where significance was observed, means were separated using Fisher's protected LSD (α=0.05).

RESULTS

Glyphosate Formulation and Rate Study

Glyphosate rate affected pH response; however, only the main effect of glyphosate rate was significant (*P*-value < 0.001). No interaction between glyphosate rate and glyphosate formulation nor dicamba formulation resulted in a significant response. Across all dicamba and glyphosate formulations, 867.7 g ae ha^{-1} rates of glyphosate produced a higher average pH value of 4.92 compared to 1,261 g ae ha^{-1} with an average pH value of 4.89. ANOVA also indicated that the interaction between dicamba formulation and glyphosate formulation was significant (*P*-value < 0.001). Resulting pH values for ENG, XMX, and FEX alone were 6.58, 5.64, and 5.55, respectively (Table 1). All dicamba formulations alone had a higher pH than any dicamba/glyphosate tank-mixture. ENG tank-mixed with Credit Xtreme® resulted in a pH value of 5.09, which was less than any dicamba formulation alone. This result was also higher than any other combination of dicamba and glyphosate (Table 1). RUPM, RUPM II, WMAX, and Abundit Edge® tank-mixed with FEX or XMX resulted in similar trends. When combined with either XMX or FEX, WMAX solutions resulted in a pH value of 4.98, which was higher than combinations of the same dicamba formulations with RUPM and Abundit Edge® (Table 1). Tank-mixtures of FEX or XMX with RUPM II resulted in pH values of 4.97 and 4.96, respectively, which was greater pH values compared to combinations of the same dicamba formulations mixed with Abundit Edge® (Table 1). Any combination of glyphosate with ENG resulted in significantly lower pH values except for Credit Xtreme. ENG mixed with WMAX or RUPM II resulted in a solution pH of 4.84 (Table 1). These were lower than any pH value for mixtures containing other forms of dicamba but greater than ENG mixed with Abundit Edge®, RUPM, and Cornerstone Plus® (4.78, 4.76, and 4.75, respectively). Within each dicamba formulation mixture, Abundit Edge® and RUPM were similar to RUPM II and WMAX.

Table 1. pH response to dicamba and glyphosate formulation.

Dicamba Formulation	Glyphosate Formulation	pH			
		Initial[x]	24HR[x]	48HR[x]	Average[w]
Engenia[z]	None	6.58	6.58	6.59	6.58 a
	Abundit Edge	4.79	4.8	4.76	4.78 j
	Roundup Powermax	4.79	4.75	4.74	4.76 j
	Roundup Powermax II	4.87	4.82	4.84	4.84 i
	Roundup Weathermax	4.91	4.81	4.81	4.84 i
	Credit Xtreme[y]	5.12	5.09	5.07	5.09 d
	Cornerstone Plus[y]	4.81	4.74	4.72	4.75 j
Xtendimax[z]	None	5.61	5.66	5.66	5.64 b
	Abundit Edge	5.01	4.89	4.91	4.93 fgh
	Roundup Powermax	4.94	4.94	4.92	4.93 gh
	Roundup Powermax II	4.98	4.98	4.95	4.97 ef
	Roundup Weathermax	5.04	4.95	4.96	4.98 e
Fexapan[z]	None	5.55	5.57	5.54	5.55 c
	Abundit Edge	4.95	4.93	4.92	4.93 gh
	Roundup Powermax	4.93	4.91	4.91	4.92 h
	Roundup Powermax II	4.99	4.97	4.94	4.97 efg
	Roundup Weathermax	5.05	4.95	4.95	4.98 e

[z] All dicamba herbicides were mixed at the 1x application rate of 561 g ae ha^{-1}.
[y] Credit Xtreme and Cornerstone Plus are only labeled for use with Engenia formulation of dicamba.
[x] Results averaged across two glyphosate rates (863 and 1,261 g ae ha^{-1}).
[w] pH values were subjected to ANOVA and means were separated using Fisher's protected LSD (α=0.05).

Approved Herbicide Tank-Mixture Study

The three dicamba herbicides, ENG, FEX, and XMX, each recorded an initial pH of 6.58, 5.55, and 5.61, respectively (Table 2). None of the dicamba herbicides experienced an increase or decrease in pH relative to time after mixing. Across all the herbicide additions, separations fell into three categories: increased pH, did not affect pH, and decreased pH but not below 5.0. Statistics were not calculated for this section; therefore, definitions for the three categories above will be met if a change in pH resulted in +/- 0.1. The herbicides that increased pH were: acetochlor, acetochlor plus fomesafen, pendimethalin (Prowl H_20® only), prometryn, and *S*-metolachlor plus fomesafen. The herbicides that did not affect pH were dimethenamid-P, diuron, fluazifop, flumioxazin, fluometuron, fomesafen, lactofen, pendimethalin (Satellite Flex® only), pyrithiobac sodium, *S*-metolachlor and saflufenacil.

The only herbicides that lowered the pH – but not below 5.0 were the three clethodim herbicides (Section Three®, Select Max®, and Vaquero®) for ENG only. The clethodim herbicides reduced pH for ENG by an average of 0.25 but did not affect the pH of FEX nor XMX.

When multiple adjuvants were approved for use in the tank-mixtures, NIS additions caused the pH to be higher than COC additions for the same herbicides. This was especially noticed with fomesafen herbicide additions (Reflex® and Flexstar®) where COC additions did not affect herbicide pH, but NIS additions caused the pH to increase by 0.1 (Table 2).

The only instance where COC, NIS, and MSO were used was for Select Max®, and MSO results matched more closely those of NIS than COC.

Table 2. pH measurements of tank mixture additions to dicamba at 0, 24, and 48 hours (h) after mixing.

			Adjuvant		Engenia[y]			Fexapan[y]			Xtendimax[y]		
Active ingredient(s)	Trade Name	Rate (g ai ha^{-1})	Type[z]	Rate	0 h	24 h	48 h	0 h	24 h	48 h	0 h	24 h	48 h
---	---	---	---		6.58	6.58	6.59	5.55	5.57	5.54	5.61	5.66	5.66
acetochlor	Warrant	1,680	---	---	6.78	6.88	6.86	5.94	6.17	6.12	6.02	6.37	6.35
acetochlor + fomesafen[x]	Warrant Ultra	1,729	COC	1% v/v	---	---	---	6.24	6.45	6.48	6.35	6.55	6.6
		386	NIS	0.5% v/v	---	---	---	6.35	6.53	6.57	6.44	6.68	6.7
	Section Three	280	COC	2.34 L ha^{-1}	6.22	6.02	6.13	5.44	5.35	5.43	5.53	5.4	5.49
			NIS	0.25% v/v	6.34	6.16	6.25	5.5	5.43	5.5	5.57	5.49	5.57
clethodim	Select Max	272	COC	2.34 L ha^{-1}	6.37	6.17	6.2	5.48	5.43	5.47	5.55	5.5	5.52
			MSO	1% v/v	6.44	6.25	6.28	5.53	5.45	5.48	5.59	5.51	5.57
			NIS	0.25% v/v	6.43	6.27	6.27	5.52	5.5	5.49	5.59	5.54	5.56
	Vaquero	280	COC	2.34 L ha^{-1}	6.19	6.11	6.2	5.37	5.31	5.4	5.44	5.42	5.47
			NIS	0.25% v/v	6.25	6.23	6.3	5.41	5.38	5.45	5.57	5.45	5.52
dimethenamid-P	Outlook	1,100	---	----	6.44	6.5	6.59	---	---	---	---	---	---
diuron	Direx 4L	1,800	---	---	6.55	6.58	6.58	5.56	5.66	5.61	5.67	5.67	5.71
	Diuron 4L	2,470	---	---	6.61	6.62	6.66	5.69	5.8	5.87	5.77	5.89	5.95
fluazifop	Fusilade DX	210	COC	1% v/v	6.47	6.52	6.62	5.52	5.49	5.58	5.6	5.61	5.71
			NIS	0.5% v/v	6.55	6.61	6.7	5.58	5.57	5.65	5.68	5.68	5.75
flumioxazin	Valor SX	71.5	COC	1% v/v	6.5	6.54	6.63	5.49	5.5	5.55	5.58	5.59	5.65
			NIS	0.25% v/v	6.6	6.68	6.76	5.57	5.58	5.65	5.64	5.66	5.73
fluometuron	Cotoran 4L	2,240	---	---	6.59	6.6	6.65	5.6	5.67	5.62	5.7	5.71	5.78
fomesafen	Flexstar	420	COC	1% v/v	6.55	6.54	6.56	5.66	5.65	5.67	5.7	5.73	5.75
			NIS	0.25% v/v	6.77	6.75	6.76	5.73	5.73	5.75	5.8	5.65	5.67
	Reflex	420	COC	1% v/v	6.55	6.55	6.53	5.59	5.57	5.56	5.67	5.64	5.66
			NIS	0.25% v/v	6.73	6.73	6.76	5.67	5.66	5.71	5.76	5.75	5.78
lactofen	Cobra	220	COC	2.34 L ha^{-1}	6.5	6.5	6.51	5.54	5.51	5.51	5.59	5.6	5.58
			NIS	0.25% v/v	6.56	6.58	6.59	5.58	5.54	5.56	5.64	5.64	5.65
pendimethalin	Prowl H20	1,600	---	---	7.15	7.2	7.21	6.1	6.28	6.47	6.22	6.42	6.74
	Satellite Flex	1,670	---	---	---	---	---	----	---	---	5.66	5.66	5.68
prometryn	Caparol	3,140	---	---	6.66	6.75	6.7	5.69	5.74	5.68	5.81	5.86	5.83
pyrithiobac sodium	Staple LX	106	NIS	0.25% v/v	6.59	6.6	6.65	5.54	5.58	5.58	5.7	5.71	5.78
	Cinch	1,420	---	---	---	---	---	5.54	5.57	5.61	---	---	---
S-metolachlor	Dual Magnum	1,420	---	---	6.54	6.57	6.65	5.54	5.58	5.57	5.61	5.64	5.67
	Everprex	1,420	---	---	6.54	6.61	6.66	5.58	5.6	5.61	5.61	5.67	5.67
S-metolachlor + fomesafen	Prefix	1,417	COC	1% v/v	6.67	6.64	6.67	6.09	6.06	6.09	6.14	6.15	6.16
		311	NIS	0.25% v/v	6.75	6.74	6.79	6.11	6.12	6.15	6.2	6.21	6.26
saflufenacil	Sharpen	25	MSO	1% v/v	6.43	6.37	6.44	5.56	5.51	5.54	5.62	5.61	5.64

z The adjuvants abbreviated COC, NIS, and MSO stand for: crop oil concentrate, non-ionic surfactant, and methylated seed oil, respectively.

y All dicamba herbicides were mixed at the 1x application rate of 561 g ae ha-1

x Treatments containing a "---" indicates that a given tank mixture herbicide was not labeled for a specific dicamba herbicide.

Table 3. Effect of glyphosate on tank-mix pH.

Herbicide[z]	Rate (g ai ha^{-1})	Glyphosate[z]	Adjuvant[y]	pH[x] Engenia[z]	pH[x] Xtendimax[z]
fluridone[w]	337	None	---	6.52 bc	---
		Roundup Powermax	---	4.79 ef	---
		Cornerstone Plus	---	4.76 ef	---
metolachlor	1,420	None	---	6.59 b	5.64 d
		Roundup Powermax	---	4.71 fg	4.86 e
pendimethalin	1,600	None	---	7.19 a	6.46 c
		Roundup Powermax	---	4.64 g	4.77 ef
quizalofop[w]	93	None	NIS	6.61 b	---
			COC	6.53 bc	---
		Roundup Powermax	NIS	4.72 fg	---
			COC	4.7 fg	---
		Cornerstone Plus	NIS	4.72 fg	---
			COC	4.7 fg	---

[z] All herbicides were mixed at a 1x application rate.
[y] Non-ionic surfactant (NIS) and crop oil concentrate (COC) mixed at 0.25 and 1% v/v, respectively.
[x] pH values were subjected to ANOVA and means were separated using Fisher's protected LSD (α=0.05).
[w] Treatments containing a "---" indicates that a given tank mixture herbicide was not labeled for a specific dicamba herbicide.

DISCUSSION

Glyphosate Formulation and Rate Study

Across the three dicamba formulations, all tank-mixture additions of glyphosate resulted in a pH below 5.0 except Credit Xtreme® mixed with ENG (Table 1). Unlike Mueller and Steckel (2019), differences in potassium salt (K) salt and isopropylamine salt (IPA) salt formulations were not observed – except for Credit Xtreme® which is a combination of K salt and IPA salt which produced a higher pH with ENG than all the other glyphosate additions. The glyphosates that resulted in the lowest pH were Cornerstone Plus® (IPA salt), RUPM (K salt) and Abundit Edge® (K salt), showing no clear distinction in salt type effects from this study. The impact of different water pH values was not examined in this study, but the water source averaged a pH of 7.57. Glyphosate additions reduced pH below 5.0 for all additions except Credit Xtreme® with ENG. Results of ENG or XMX with the addition of RUPM II or Cornerstone Plus® align with the low pH water data than the high pH water data observed by Mueller and Steckel (2019). Water with a pH of 7.57 is still noticeably similar in tank-mixture pH of water sources that are as low as 4.6 (Mueller and Steckel 2019), which underscores the greater effect of glyphosate additions than water source effect for tank-mixture pH.

Two herbicides, according to the www.engeniatankmix.com website, that were tested require the addition of approved glyphosate to be used with ENG - fluridone and quizalofop (Table 3). Those herbicides were tested for pH with and without the glyphosate to observe the effect further than adding glyphosate had on tank-mixture pH. For both quizalofop and fluridone, with all the permutations of adjuvants required with quizalofop, tank-mixture pH was significantly lower when glyphosate was added, independent of dicamba or glyphosate formulation. It was observed in the approved herbicide tank-mixture study that pendimethalin (Prowl H_20) raised pH by 0.6 for ENG and 0.8 for XMX (Table 2). When ENG or XMX were mixed with RUPM, tank-mixture pH fell to 4.64 for ENG and 4.77 for XMX (Table 3), pH values lower than mixtures of glyphosate plus dicamba alone. Applying glyphosate and dicamba in a burndown application and including a PRE like pendimethalin or *S*-metolachlor (Dual Magnum) pre-plant or at planting would be a common tank-mixture in cotton. With both PRE herbicides additions, the resulting pH was lower than dicamba mixtures with

only glyphosate (Tables 1 & 3). The implication that herbicides added to tank-mixtures of dicamba and glyphosate could further lower pH concerns, especially given that the two tested mixtures are commonly-used in cotton in the south, creating more questions perhaps than those answered.

Tank-mixture combinations of FEX and WMAX resulted in pH value (4.98) closest to the minimum value suggested by dicamba product labels. Mixtures of XMX with either WMAX or RUPM II, FEX with RUPM II, or WMAX, or ENG with Credit Xtreme were the only combinations to result in values similar to or greater than the 5.0 recommended minimum value. Therefore, growers should be cautious when combining these dicamba formulations with other glyphosate formulations included in this research.

Approved Herbicide Tank-Mixture Study

Across 94 different permutations of 23 herbicides, tank-mixture pH was not affected where growers need to be concerned about their use with any of the dicamba formulations (Table 2). This is especially useful given that growers may choose to utilize multiple modes of action, which would not affect tank-mixture pH. Tank-mixtures that require the addition of glyphosate, according to www.engeniatankmix.com - including fluridone and quizalofop did reduce tank-mixture pH below 5, but that is solely due to glyphosate. When those herbicides were mixed without glyphosate, the pH was not affected (Table 3). Overall, the effect of any herbicide addition other than glyphosate was negligible, which should provide some assurance for growers who are wanting to steward dicamba and ensure little to no off-target movement effectively.

CONCLUSIONS

Cotton growers are right to be concerned about the effect that tank-mixture herbicides have on the pH of tank-mixtures of dicamba, given the implications for off-target movement. The labels for all three dicamba herbicides refer to growers to local industry representatives or university extension services for further information. The present work was conducted to provide data for cotton growers to understand what effect that any labeled herbicide addition had on tank-mixture pH, but especially for additions of glyphosate. Results from this study showed that labeled herbicides for dicamba tank-mixtures in cotton do not affect mixture pH unless the mixture includes glyphosate. If growers add glyphosate to dicamba tank-mixtures they should presume a drop in pH below 5.0, thus requiring the addition of a pH buffer as listed on each herbicide's website. New herbicide technologies are needed to ensure effective weed control in cotton, especially given the increasing pressure placed on existing herbicide options. With new technology comes greater responsibility for stewardship by all involved in the research or production of cotton to work together to achieve success with any new technology or tool in agriculture.

CONFLICT OF INTEREST

There is no conflict of interest to declare.

ACKNOWLEDGEMENT

This work was supported through funding from the United States Department of Agriculture Hatch Project MIS-522070. This article is a contribution from the Department of Plant and Soil Sciences, Mississippi State University, Mississippi Agricultural and Forestry Experiment Station.

LITERATURE CITED

Andersen SM., Clay SA, Wrage LJ, Matthees D. Soybean foliage residues of dicamba and 2,4-D and correlation to application rates and yield. Agron. J. 2004; 96: 750-760.

Anonymous. Engenia herbicide label. 2019a. http://www.cdms.net/ldat/ldDG8028.pdf, Accessed: September 17th, 2019.

Anonymous. Fexapan herbicide plus vaporGrip technology label. 2019b. http://www.cdms.net/ldat/ldDJ1002.pdf, Accessed: September 17th, 2019.

Anonymous. XtendiMax with vaporGrip technology label. 20199c. http://www.cdms.net/ldat/ldDF9006.pdf, Accessed: September 17th, 2019.

Meyer CJ, Norsworthy JK, Young BG, Steckel LE, Bradley KW, Johnson WG, Loux MM, Davis

VM, Kruger GR, Bararpour MT, Ikley JT, Spaunhorst DJ, Butts TR. Herbicide program approaches for managing glyphosate-resistant Palmer amaranth (*Amaranthus palmeri*) and waterhemp (*Amaranthus tuberculatus* and *Amaranthus rudis*) in future soybean-trait technologies. Weed Technol. 2019; 29: 716-729.

Mueller TC, Steckel LE. Spray mixture pH as affected by dicamba, glyphosate, and spray additives. Weed Technol. 2019; 33: 547-554.

Norsworthy JK, Griffith G, Griffin T, Bagavathiannan M, Gbur EE. In-field movement of glyphosate-resistant Palmer amaranth (*Amaranthus palmeri*) and its impact on cotton lint yield: evidence supporting a zero-threshold strategy. Weed Sci. 2014; 62: 237-249.

Schwartz-Lazaro LM, Norsworthy JK, Scott RC, Barber LT. Resistance of two Arkansas Palmer amaranth populations to multiple herbicide sites of action. Crop Prot. 2017; 96:158-163.

Shaner DL. Dicamba. *In:* Shaner, DL., ed., Herbicide Handbook, 10th edn. Lawrence, KS: Weed Science Society of America, 2014; p. 139-141.

Smith HC, Ferrell, J.A, Fernandez JV, Webster TM. Cotton response to simulated auxin herbicide drift using standard and ultra-low carrier volumes. Weed Technol. 2017; 31:1-9.

Ward SM, Webster TM, Steckel LE. Palmer amaranth (*Amaranthus palmeri*): A review. Weed Technol. 2013; 27: 12-27.

Witten T. 2019. Understanding spray solution pH with XtendiMax with VaporGrip Technology. https://monsanto.com/app/uploads/2019/03/Understanding-Spray-Solution-pH-with-XtendiMax.pdf

Antifeedant Effect of Sickle Extract on Soybean Looper *Chrysodeixis includes* (Lepidoptera: Noctuidae)

Ziming Yue, Natraj Krishnan, and Te-Ming Tseng

Photo Credit: Ziming Yue

Antifeedant Effect of Sickle Extract on Soybean Looper *Chrysodeixis includens* (Lepidoptera: Noctuidae)

Ziming Yue[1], Natraj Krishnan[2], and Te-Ming Tseng*[1]

[1]Department of Plant and Soil Sciences and [2]Department of Biochemistry, Molecular Biology, Entomology, and Plant Pathology, Mississippi State University, Mississippi State, MS 39762

*Corresponding author: Te-Ming Tseng, E-mail: t.tseng@msstate.edu

ABSTRACT

Soybean is a major crop in the midsouth of the United States, and it is also the only major crop that suffers from heavy insect defoliation in this region, leading to significant economic loss. Soybean looper is one of the top three insect pests in soybean production in this region. Synthetic insecticides are often used in insect management. However, the environmental concerns and the potential of developing insecticide resistance stresses the need to identify natural compounds with the insecticidal property. This study proposed and tested sicklepod extract as an insecticide. The results were compared to the commercial synthetic insecticide bifenthrin (commercially; formulated as Bifen) and a natural plant product, neem oil. Sicklepod extract showed a similar antifeedant effect as bifenthrin where a 1.4 and 2 % leaf disc feeding was observed for sicklepod extract and bifenthrin treatments, respectively. Mortality experiments showed that the antifeedant effect of sicklepod extract was not effective when applied on the skin of the soybean loopers. The performance of sicklepod extract as an antifeedant to protect soybean was better than neem oil, and as a plant product, it is safe on humans and the environment.

Keywords: Natural insecticide, anthraquinone, anti-herbivory, leaf disc, bifenthrin, neem oil

Abbreviations: USDA, United States Department of Agriculture; US EPA, United States Environmental Protection Agency; HPLC, High-performance liquid chromatography; ANOVA, Analysis of variance

INTRODUCTION

Soybean, *Glycine max* (L.) Merr., is the most valuable row crop commodity in the mid-southern region of the United States in terms of planted area and total commodity value (Adams et al., 2016). Unfortunately, it is also the only major crop that suffers significant insect defoliation in this region, with peak insect infestation usually occurring in September. Although soybean can compensate insect defoliation to some extent, the soybean defoliation threshold in Mississippi and various other states is 35% during vegetative stages and 20% during reproductive stages (Owen, 2012). In field situations (especially during reproductive stages in September), the defoliation often exceeds the threshold, leading to significant yield reduction. Soybean looper (*Chrysodeixis includens* Walker) is one of the top three most expensive insect pests in the midsouth region of the United States (Musser et al., 2017). Synthetic chemicals such as bifenthrin are commonly used to control insects due to its effectiveness and ease of application; however, bifenthrin toxicity endangers farm operators, animals (Li et al., 2017), and food consumers (USDA, 2008). Hence US EPA has not authorized bifenthrin to be used on soybean (US EPA, 2015). Besides, soybean looper has developed resistance to most major classes of insecticides, including carbamates, cyclodienes, organophosphates, and pyrethroids (Boethel et al., 1992). There is interest in adopting botanically-derived insecticide as a simple plant extract for insect control (Jacobson, 1988; Hikal et al., 2017; Mbatchou et al., 2018). Sicklepod, *Senna obtusifolia* (L.) Irwin and Barneby, is one of the top ten troublesome weeds in agriculture in the southern and southeastern US (Webster et al., 2013). It is famous for its high anthraquinone derivative contents in its different plant parts and is widely used as herbal medicine as cathartics (van Gorkom et al., 1999) and health tea (Takahashi and Sakurai, 2014). Its active ingredients anthraquinone derivatives are shown to have a

repelling effect on birds (Avery et al., 1997), rodents (DeLiberto and Werner, 2016), and deer (Yue et al., 2018). In separate studies, anthraquinone and its derivatives were shown to have anti-insect properties (Vandeveer, 1935; Dave and Ledwani, 2012; Trial and Dimond, 1979). It was reported that anthraquinone was used as an insecticide as early as 1935 (Vanderveer, 1935). Dave and Lediwani (2012) found that anthraquinones isolated from *Cassia* species possessed insecticidal activity. Trial and Dimond (1979) reported an antifeedant property of emodin, a primary anthraquinone derivative in sicklepod, to gypsy moth (*Lymantria dispar*). During our field studies on evaluating the deer repelling effect of sicklepod extract, reduced insect damage was observed on soybean plants applied with the sicklepod extract compared to control plants applied with water. Therefore, based on our observation and other studies, the goal of this study was to determine the antifeedant property of sicklepod extract against soybean loopers, in comparison with commercial insecticides.

MATERIAL AND METHODS

Plant Materials

Roundup Extend soybean plants propagated in a standard nursery (planted in late May 2019) in RR Foil Plant Science Research Center, Mississippi State University, at the V5 to R1 stages were selected as leaf source. In June 2019, there was no leaf damage; hence no pesticide applied. Soybean leaves were selected below the third fully extended trifoliate. The leaf discs were perforated with a circular puncher of known diameter (5/8 inch) using the method described by Junior and Kawakami (2013). Each leaflet was perforated one to seven times, avoiding the central nervure.

Insecticide Preparations

Sicklepod fruits were dried at 50°C for one week. Dried sicklepod fruits were ground by Wiley Mill to -1 mm using a screen. Fifty grams of the sicklepod fruit meal was placed into a 2-L beaker with 1 L deionized water. The paste was boiled for 10 minutes, cooled to 40 °C, homogenized in a Hamilton Beach Blender with 10% (V/V) methanol for 5 minutes, and vacuum filtered through a No. 9 Whatman filter paper. The extraction was repeated three times, and the combined extract was concentrated on a hot plate to 10% of its original volume for application.

Commercial brands Bifen XTS concentrate and Garden Defense multi-purpose spray concentrate (neem oil) were used; the former is a pyrethroid insecticide (active ingredient is bifenthrin), and the latter is a plant product (active ingredient is triterpenoid). Finally, dilution and application of the commercial insecticides were according to their commercial label instructions, a dilution factor of 400 for bifenthrin, and 128 for neem oil. All applied insecticides and control treatment contained a 0.25% non-ionic surfactant.

Leaf Disc Feeding Assay

The soybean loopers were reared on Stonefly *Heliothis* Diet (Product No. 38-0600, Ward's Natural Science, Rochester, NY) in 40 mm transparent plastic cups with caps at the rearing facility in Clay Lyle Entomology Center at Mississippi State University for one week before being used in the soybean leaf disc experiment. The leaf discs were treated with different insecticides by dipping in the water control, sicklepod extract, neem oil emulsion, and bifenthrin emulsion for 5 seconds, in separate treatments. The soaked discs were taken out and laid on a Kimwipe for 1 minute, and then every two leaf discs were transferred to a 40 mm diameter plastic cup with two soybean loopers and enough alternate food source. The leaf-feeding data was measured as a feeding percentage after 48 hours.

Epidermis Penetration Assay

Soybean looper mortality was recorded in the above leaf disc feeding experiments. The looper mortality was calculated as follows:

Mortality (%) = no. of dead loopers within two days/total no. of loopers in the treatment x 100%

Looper deaths were assumed if no movement was observed when turned over. Besides, 4 μL of treatment solutions in acetone (same concentrations as above) of sicklepod extract, neem oil, bifenthrin, and acetone (control) were applied on the back of each of the 10 soybean loopers at the 2nd instar stage.

Their mortality was read and calculated after 12 hours.

HPLC Analysis of the Sicklepod Extract

The sicklepod extract was mixed well first, one mL of the extract mixed with 200 µL 6N H_2SO_4 in a 2 mL glass vial (sealed), and hydrolyzed in a water bath at 95°C for two hours. After cooling down, the product was transferred into a 2 mL plastic tube and freeze-dried. The dried product was homogenized with three beads on a Precellys Evolution Homogenizer for 2 minutes at 8,600 rpm. One mL of methanol was added and homogenized as above for an additional minute. The tube was rocked on a Roto Rocker for half an hour and then centrifuged at 16,100 × g for 1 min. The resulting supernatant was filtered through a 0.2 µm filter for HPLC analysis.

An Agilent 1100 series HPLC (Agilent, Santa Clara, CA, USA) was used to analyze the extracts for anthraquinone derivatives. The HPLC configuration used a diode array detector, an online vacuum degasser, a quaternary pump, an autosampler, and a thermostatted column compartment. A volume of 10 µL was injected and separated by an ACE Equivalence reverse phase C18 column (150 mm × 4.6 mm), with a particle size of 3 µm. Agilent Chemstation A.10.02 software with a spectral module (Agilent Technologies Inc., Wilmington, DE, USA) was used to process the data. Anthraquinone derivatives were detected at 254 nm, with a flow rate of 0.5 mL min^{-1}, and a column temperature of 30˚C. Peaks were identified using orantio-obtusin, chrysophanol, and emodin standards (Adooq Bioscience LLC (Irvine, CA, USA), BioVision (San Francisco, CA, USA), and TCI America (Portland, OR, US), respectively). The isocratic eluent was mixed with 40% acetonitrile and 60% water (modified with 0.2% acetic acid). The run stop time was 40 minutes.

Statistical Analysis

Each treatment was replicated at least seven times, and the experiment repeated three times. Leaf discs in each cup were visually evaluated for feeding on a 0 to 100% scale. The data were subjected to ANOVA using the student's t-test, and means were separated by the least significant differences at P≤0.05. The letters indicating statistical differences were obtained from the analyses. All analyses were conducted using JMP 14.0.0 (SAS Institute, Cary, NC, USA).

RESULTS

Leaf Disc Feeding Results

Sicklepod extract and bifenthrin had a similar antifeedant effect, with both exhibiting 2% feeding; neem oil and the untreated control showed higher feeding, 34 and 38%, respectively, and were statistically similar (Fig. 1 and Fig. 2). Based on personal observation, the impact of neem oil was much dependent on the level of emulsification. After about one-week of emulsification, the neem oil showed a better antifeedant effect but was still not different from the control treatment statistically.

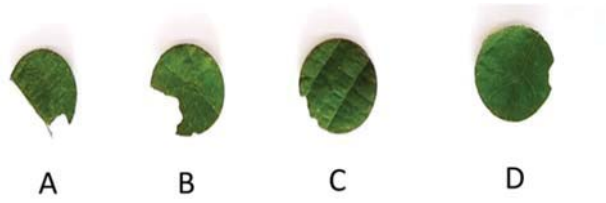

Figure. 1. Soybean leaf disc images after 48 hour-feeding with two loopers per cup and supplemented with an alternate food source. The treatments from left to right are: A, control; B, neem oil; C, sicklepod extract; and D, bifenthrin.

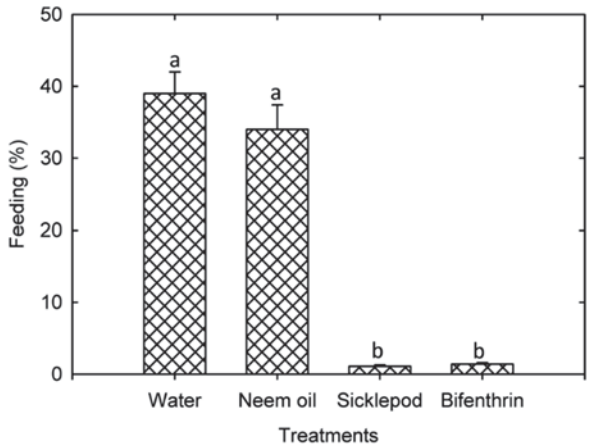

Figure. 2. Soybean leaf percentage fed after 48 hours. The statistical letters indicate sicklepod extract, and bifenthrin had the same antifeedant effect, while neem oil and water control had the same and higher insect feeding (n = 10). The letters a and b mean statistically different; the same letter means not statistically different.

Mortality Data

Looper mortality data showed bifenthrin having much higher mortality (50%), distantly followed by sicklepod extract (8.3%), neem oil (1%), and control (1%) (Fig. 3).

For epidermal penetration experiments, bifenthrin showed much higher mortality of 80%, while sicklepod extract and neem oil resulted in 10% mortality, 12 hours after application (Fig. 4).

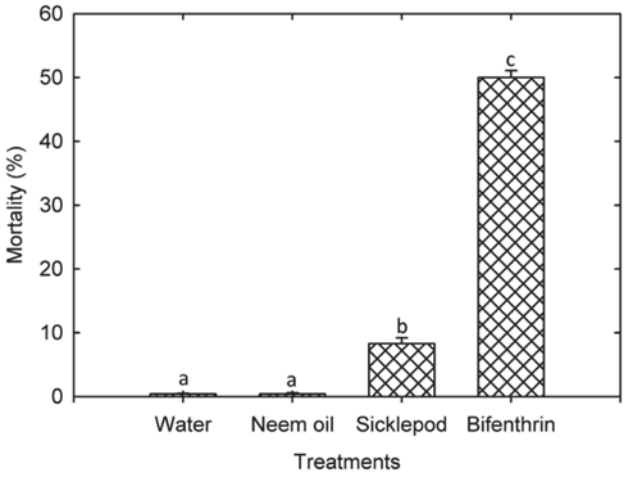

Figure. 3. Soybean looper mortality with different insecticide treatments in leaf disc assays, 48 hours after treatment. The letters a, b, and c mean statistically different; the same letter means not statistically different.

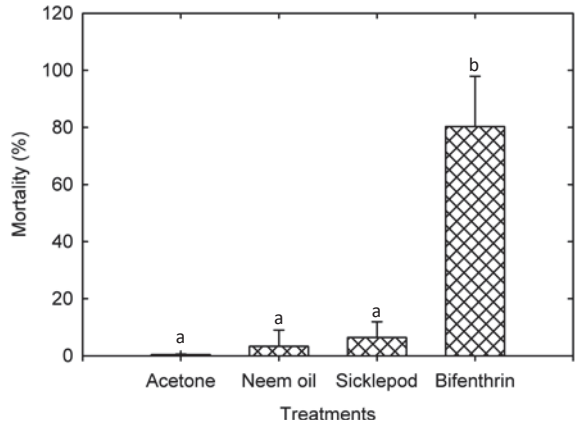

Figure. 4. Soybean looper mortality 12 hours after application of 4 μL of each insecticide treatment, in acetone, applied to looper epidermis. The letters a and b mean statistically different; the same letter means not statistically different.

Anthraquinone Derivative Contents in the Sicklepod Extract

The active ingredients of the sicklepod extract were dominated by orantio-obtusin (115 ppm), emodin (19 ppm), and chrysophanol (18 ppm) for hydrolyzed sample (Fig. 5).

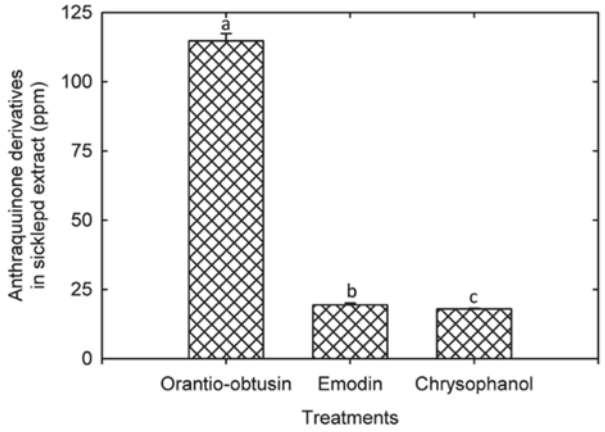

Figure. 5. Anthraquinone derivatives concentrations in the hydrolyzed sicklepod extract. The letters a, b, and c mean statistically different.

DISCUSSION

Comparing the Antifeedant Effects of Sicklepod Extract, Neem Oil, and Bifenthrin

Both the sicklepod extract and neem oil are plant products (Yue et al., 2018; Adnan et al., 2014). The active ingredients of sicklepod extract are anthraquinone derivatives (and their glycosides) (Yue et al., 2018), while the primary active ingredients of neem oil are tetranortriterpenoids, of which azadirachtin is the most effective (Saxena, 1988). The former is insoluble (solids) in water (Zhao et al., 2016), and the latter is a hydrophobic oil that requires emulsification (US EPA fact sheet); hence, surfactant was needed for their activity. A non-ionic surfactant of 0.25% was added for dispersion of both insecticides. The sicklepod extract reached a total anthraquinone derivative content of 150 mg/L. The neem oil concentration used in this experiment may be low as it was reported that a 3% neem oil was used to treat mango hopper (Adnan et al., 2014), which was

3.84 times the dose used in this study. In addition, it was found from our experiments that even fine-grain particles of anthraquinone derivatives on the leaf disc still showed antifeedant effects. Bifenthrin is a pyrethroid insecticide and is well emulsified according to the commercial label; hence, both sicklepod extract and bifenthrin achieved an antifeedant high impact.

Mode of Action of the Insecticides

Bifenthrin is a synthetic pyrethroid insecticide, a category of insecticide that originates from dried chrysanthemum flower head preparation. The active ingredients of the preparation were pyrethrins, which were not photostable (Spurlock and Lee, 2008). The synthetic counterpart of the group of insecticides is called pyrethroids, whose photostability was improved (Spurlock and Lee, 2008). Bifenthrin was designed to kill a broad spectrum of insects (Bifen XTS commercial label). Insects are killed upon contact with the insecticide, explaining the high mortality of loopers. Anthraquinone derivatives in sicklepod extract interact with vertebrate colon epithelial cells making the colon movement faster (van Gorkom et al., 1999), perhaps explaining why the soybean loopers feed less on the sicklepod extract-treated leaf discs as compared to the control treatment. These compounds need to be consumed to function, which is different from bifenthrin, where insects are killed upon contact.

For this reason, sicklepod extract leads to less mortality than bifenthrin, since consumption is a prerequisite for the sicklepod extract to work. The epidermal penetration experiments clearly showed sicklepod extract (anthraquinone derivatives) having a lesser effect on the looper when applied on the epidermis, while bifenthrin can kill the looper upon contact. This was in agreement with van Gorkom et al. (1999), where they found that anthraquinone derivatives usually target the digestive tract cells of animals. Neem oil also exhibited low mortality in the epidermis penetration test because it was an insect growth inhibitor and did not have much effect within 12 hours of application (Rembold, 1988).

Sicklepod extract required consumption to function on the digestive tract, and it was not possible for this consumption-dependent insecticides to achieve 0% defoliation with insect infestation. On the other hand, defoliation of less than 20% usually does not influence soybean yield (Owen, 2012); thus, if an insecticide provided less than 20% soybean defoliation, then there is no adverse effect on the crop yield. Sicklepod extract can, therefore, be used as an effective insecticide in soybean.

Insecticide Concentrations

The applied bifenthrin concentration was calculated as 625 ppm active ingredients. The total anthraquinone derivatives in the applied sicklepod extract were 169 ppm, which was the active ingredient. Both of them had the same antifeedant effect, but sicklepod extract had lower looper mortality. It was also observed that mortality increased with anthraquinone derivative concentrations, which was consistent with the emodin effect on gypsy moth larvae (Trial and Dimond 1979). Emodin is one of the major anthraquinone derivatives in our sicklepod extract (Fig. 5). Our current efforts are to reformulate the sicklepod extract to achieve higher anthraquinone derivative concentration. Once the goal realized, the sicklepod extract is expected to be a more effective insecticide.

Soybean Loopers vs. Mosquito Larvae

Mbatchou et al. (2017) tested the larvicidal effect of *Senna tora* extract on mosquito. *Sennna tora* is a similar species as sicklepod (*Senna obtusifolia*); it is hard to differentiate between them in phenology and chemistry. The results showed 100 ppm crude extract or orantio obtusin (the most dominant anthraquinone derivative in sicklepod) killed 100% mosquito larvae within 24 hours. This was a big contrast with our mortality results with even higher anthraquinone derivative concentrations. The reason might be that mosquito larvae lived in water, where the larvae had no way to avoid the 100 ppm anthraquinone derivatives, while the soybean loopers could avoid being killed by avoiding the touch of the treated leaf discs. The looper dipping (into sicklepod extract) experiments were conducted (the results not shown), much higher mortality resulted, similar to that of bifenthrin in the mortality experiments reported here.

Environmental Concern

As the third-generation pyrethroid insecticide, bifenthrin is famous for its strong environmental persistence and high insecticidal activity (Mokry and Hoagland, 1990). The frequent use of bifenthrin has led to ecological risks of different organisms, such as aquatic organisms, mammals, and earthworms (Li et al., 2017). Sicklepod extract, on the other hand, is often used as a herbal medicine commonly as herbal tea (Takahashi et al., 2014). Sicklepod extract is not only safe for contact with skin, for the applicators, but also nonlethal when consumed at a dose used in herbal medicines (Harry-O'kuru et al., 2012). It is, therefore, not expected to have any application restrictions on food crops from US EPA in contrast to the synthetic insecticide bifenthrin.

CONCLUSIONS

Leaf disc experiments showed sicklepod extract and bifenthrin having similar antifeedant effects on soybean loopers. But the looper mortality of sicklepod extract was lower than that of bifenthrin. Considering the active ingredients anthraquinone derivative concentration was more than three-time lower than that of bifenthrin in the experiments, an increase of anthraquinone derivative concentration might have the potential to increase looper mortality for sicklepod extract. If well formulated, sicklepod extract is expected to be a more effective insecticide. Reformulation of sicklepod extract is underway.

CONFLICT OF INTEREST

There is no conflict of interest to declare.

ACKNOWLEDGMENTS

Funding for this project was provided by the Mississippi Soybean Promotion Board. This publication is a contribution of the Mississippi Agricultural and Forestry Experiment Station and is based upon work that is supported by the National Institute of Food and Agriculture, US Department of Agriculture, Hatch project under accession number 230060. The authors would also like to express appreciation for the assistance provided by Dr. David Lang, Dr. Fred Musser, and Andrew Nuss.

LITERATURE CITED

Adnan SM, Uddin MM, Alam MJ, Islam MS, Kashem MA, Rafii MY, Latif MA. Management of Mango Hopper, *Idioscopus clypealis*, using chemical insecticides and neem oil, Sci. World J. 2014; 2014: 1-5.

Adams A, Gore J, Catchot A, Musser F, Cook D, Krishnan N, Irby T. Residual and Systemic efficacy of chlorantraniliprole and flubendiamide against corn earworm (Lepidoptera: Noctuidae) in soybean, J. Econ. Entomol. 2016; 109: 2411–2417, https://doi.org/10.1093/jee/tow210

Avery ML, Humphrey JS, Decker DG. Feeding deterrence of anthraquinone, anthracene, and anthrone to rice-eating birds. J. Wildl. Manag. 1997; 61: 1359-1365.

Board JE, Wier AT, Boethel DJ. Soybean yield reductions caused by defoliation during mid to late seed filling. Agron. J. 1994; 86: 1074-1079. doi:10.2134/agronj1994.00021962008600060027x

Boernel DJ, Mink JS, Wier AT, Thomas JD, Leonard BR. Management of Insecticide Resistant Soybean Loopers (*Pseudoplusia Includens*) in the Southern United States. In: R. Reeds, M. Green, and L. Copping (eds), Pest management in soybean. Society of the Chemical Industry. Elsevier Press, London, 1992; p66-87.

Dave H, Ledwani L. A review of anthraquinones isolated from *Cassia* species and their applications. Indian J. Nat. Prod. Resour. 2012; 3: 291-319.

DeLiberto ST, Werner SJ. Review of anthraquinone applications for pest management and agricultural crop protection. Pest Manag. Sci. 2016; 72:1813-1825.

Harry-O'kuru RE, Payne-Wahl KL, Busman M. Medicinal components recoverable from sicklepod (*Senna obtusifolia)* seed: Analysis of components by HPLC-MS. J. Chromatograph. Separat. Techniq. 2012; S2:001.

doi:10.4172/2157-7064.S1-001

Hikal WM, Baeshen RS, Said-Al Ahl. HAH. Botanical insecticide as simple extractives for pest control. Cogent Biol. 2017; 3: 1404274. https://doi.org/10.1080/23312025.2017.1404274

Jacobson M. Botanical pesticides-past, present, and future. In: Anason JT, Philogene and Morand P, editors, Insecticides of plant origin. ACS symposium series; 387, 1988; p1-10.

Junior, CP, Kawakami J. Efficiency of the leaf disc method for estimating the leaf area index of soybean plants. Maringá 2013; 35:487-493.

Li L. Yang D, Song Y, Shi Y, Huang B, Yan J, Dong X. Effects of bifenthrin exposure in soil on whole-organism endpoints and biomarkers of earthworm *Eisenia fetida*. Chemoshpere 2017; 168: 41-48.

Mbatchou VC, Dickson RA, Amponsah IK, Mensah AY, Habtemariam S. Protection effect of the anthraquinones, cassia torin and aurantio obtusin from seeds of *Senna tora* against cowpea weevil attack. Asian Pac. J. Trop. Biomed. 2018; 8: 98-105.

Mokry LE, Hoagland KD. Acute toxicities of five synthetic pyrethroid insecticides to Daphnia magna and Ceriodaphnia dubia. Environ. Toxicol. Chem. 1990; 9: 1045-1051.

Musser FR, Catchot AL, Davis JA, Lorenz GM, Reed T, Reisig DD, Stewart SD, Taylor S. 2016 soybean insect losses in the southern U.S. Midsouth. Entomol. 2017; 10: 1-13.

Owen LN. Effects of defoliation in soybean and susceptibility of soybean loopers to reduced risk insecticide, 2012; Ph.D. Dissertation, Mississippi State University, Mississippi State, MS.

Rembold H. Azadiractins-their structure and mode of action. In: Anason JT, Philogene, Morand P, editors, Insecticides of plant origin (ACS symposium series; 387), 1988; p150-163.

Saxena RC, Insecticides from neem. In: Anason JT, Philogene, Morand P, editors, Insecticides of plant origin (ACS symposium series; 387), 1988; p1-10.

Spurlock F, Lee M, Synthetic pyrethroid use patterns, properties and environmental effects. In: Gan J, Spurlock F, Hendley P, Weston DP, editors, Synthetic pyrethroids: occurrence and behavior in aquatic environments, ACS Symposium Series 991, 2008; p3-25.

Takahashi M, Sakurai K, Fujii H, Saito K. Identification of indicator components for the discrimination of *Cassia* plants in health teas and development of analytical method for the components. J. AOAC Int. 2014; 97: 1195-1201.

Trial H, Dimond J. Emodin in buckthorn: A feeding deterrent to phytophagous insects. Can. Entomol. 1979; 111: 207-212. doi:10.4039/Ent111207-2.

USDA. Pesticide data program annual summary, calendar year 2007. US Department of Agriculture, Agricultural Marketing Service: Washington, DC, 2008.

US EPA, Azadirachtin (121701) clarified hydrophobic extract of neem oil (025007) Fact Sheet. 2001. https://www3.epa.gov/pesticides/chem_search/reg_actions/registration/fs_G-127_01-Oct-01.pdf.

US EPA, Notice of pesticide registration. EPA Reg. Number: 89442-23, 2015

Vanderveer V. Light stable insecticide. 1935; U.S. patent no. US2011428A.

Van Gorkom BA, de Vries EG, Karrenbeld A., Kleibeuker JH. Anthranoid laxatives and their potential carcinogenic effects. Aliment Pharmacol. Ther. 1999; 13:443-452.

Webster TM, Patterson M, Everest J, Norsworthy J, Burgos N, Scott B, Barber T, Ferrell J, Leon R, Culpepper AS, Prostko EP, Moorhead D, Moore JM, Green JD, Martin JR, Stephenson D, Miller D, Sanders D, Griffin J, Bond J, Eubank T, Bradley K, York A, Jordan D, Fisher L. Weed survey. Proceedings of Southern Weed Science Society, 2013; 66: 275-287.

Yue Z, Tseng, TM, Lashley M. Characterization and deer-repellent property of chrysophanol and emodin from sicklepod weed. Am. J. Plant Sci. 2018; 9, 266-280. https://doi.org/10.4236/ajps.2018.92022

Zhao Y, Xu Z, Lin T. Barrier textiles for protection against microbes. In: Antimicrobial Textiles (Woodhead Publishing Series in Textiles), 2016; p225-245.

Soil Waterlogging and Nitrogen Fertilizer Source Effects on Soil Inorganic Nitrogen

Gurpreet Kaur[1], Peter P. Motavalli[2], Kelly A. Nelson[3], Gurbir Singh[1], and Taghi Bararpour[1]

[1]Delta Research and Extension Center, Mississippi State University, Stoneville, MS 38776, [2]School of Natural Resources, University of Missouri, Columbia, MO 65211, USA, [3]Division of Plant Sciences, University of Missouri, Novelty, MO 63460, USA

Corresponding Author: Gurpreet Kaur, E-mail: gk340@msstate.edu

ABSTRACT

Excessive soil moisture causes N loss through leaching, denitrification, runoff, and erosion. Three years (2013-2015) field experiment was conducted to assess the effects of early-season soil waterlogging, corn hybrids of varying flood tolerance and pre-plant N sources, and post-waterlogging rescue N applications on changes in soil properties, Urea-N release from PCU and soil NH_4^+-N and NO_3^--N concentrations. The experimental design was a randomized complete block split-split-split plot design and three replications. Main plots were waterlogging duration (non-waterlogged or 7-days waterlogged at the V3 growth stage of corn), and sub-plots included pre-plant fertilizer treatments: a non-treated control (CO), urea (NCU), urea plus nitrification inhibitor (NCU+NI), and polymer-coated urea applied at 168 kg N ha^{-1}. A post-waterlogging rescue N fertilizer application of 0 or 84 kg N ha^{-1} of urea plus urease inhibitor (NCU+UI) was applied at the V7 growth stage. Anaerobic soil conditions were developed during waterlogging, as indicated by the decrease in soil redox potential with each day of waterlogging. When averaged over waterlogging period, soil temperature was 1.1 and 1.4°C higher in 7-days waterlogged treatments compared to non-waterlogged treatments in 2013 and 2015, respectively. Soil NH_4^+-N concentrations were not affected by waterlogging duration in all three years. Soil NO_3^--N concentrations decreased by 69% and 30% in 2014 and 2015, respectively, due to 7-days waterlogging duration compared to non-waterlogged treatments. Differences in prevailing climatic conditions during the growing seasons caused variation in soil properties, PCU dissolution and soil N concentrations due to waterlogging and N fertilizer sources.

Keywords: Flood tolerance, polymer-coated urea, rescue nitrogen fertilizer, waterlogging

Abbreviations: NCU, Non-coated urea; PCU, Polymer-coated urea; NI, Nitrification inhibitor; UI, Urease inhibitor

INTRODUCTION

Extreme precipitation events causing flooding and excessive soil moisture conditions are significant contributors to crop production losses and may cause severe hazards in North America (Kozdrój and van Elsas, 2000; Kunkel, 2003). During June and July of 1993, extreme precipitation along with abnormal precipitation in the prior seven months created saturated soils and elevated stream flows that caused the Mississippi River to flood (Kunkel, 2003). The runoff of nutrients, such as nitrates, into the Mississippi River and Gulf of Mexico caused by flooding, may have contributed to the doubling of the Gulf's "Dead Zone" in 1993 (Rosenzweig et al., 2001).

Studies have shown that the incidence of extreme rainfall events in the Midwest region has increased from 1958 to 2007 and are expected to increase more in the future, especially during the spring (Kozdrój and van Elsas, 2000; Cubasch et al., 2001; Ban et al., 2015). Increases in precipitation in the Upper Midwest of the USA have caused extensive crop damage from excess water and off-farm loss of soil and nutrients

(Morton et al., 2015). There are approximately 4 million hectares of claypan soils in areas of Missouri, Kansas, and Illinois in the Midwestern USA that has limited drainage resulting in a perched water table and waterlogging of the topsoil layers after rainfall events (Jamison et al., 1968).

The combination of poorly-drained claypan soils and extreme rainfall events, mainly during spring, results in anoxic conditions which may limit aerobic N transformations in soil and lead to higher nutrient losses and reduced N uptake by plant roots (Huang et al., 1994; Urban et al., 2015). Nitrogen losses occur through leaching, denitrification, runoff, and erosion under waterlogged soil conditions (Hongprayoon, 1992; Kopyra, 2004). Soil waterlogging also reduces N mineralization rates (Pengthamkeerati et al., 2006; Haddad et al., 2013). The most important electron acceptor for the microbial decomposition of organic C compounds in soil and sediments is oxygen (Patrick and Jugsujinda, 1992). The reduction of O_2 is followed by NO_3^-, Mn^{+4} compounds, Fe^{+3} compounds, SO_2^- and CO_2 under anoxic conditions. Zurweller et al. (2015) concluded that a significant proportion of the cumulative soil surface N_2O emissions typically may occur during and shortly after soil waterlogging events on poorly-drained claypan soils in Northeast Missouri. The same study reported a rapid decline in soil NO_3^--N concentration with each day of waterlogging with 61% lower soil NO_3^--N concentration in waterlogged treatments than in non-waterlogged control when averaged across all pre-plant N fertilizer sources (Zurweller et al., 2015).

One possible approach for preventing N losses under waterlogged soil conditions is the use of enhanced efficiency fertilizers (EEFs). The EEFs include slow- (SRF) and controlled-release fertilizers (CRF), nitrification inhibitors (NI), and urease inhibitors (UI). Slow or controlled release fertilizers (such as polymer-coated urea, PCU) are formulated to regulate N release in soil by either delaying initial nutrient availability or extending nutrient availability for a longer period during the plant life cycle (Motavalli et al., 2008). Nitrification inhibitors (NI) can either slow down, delay, or restrict the nitrification process by four to ten weeks by inhibiting the metabolism of *Nitrosomonas* bacteria involved in the nitrification process (Motavalli et al., 2008; Halvorson et al., 2014). Some available NIs include nitrapyrin, DCD (dicyandiamide), and DMPP (3,4-dimethylpyrazole phosphate) (Huber et al., 1977). Urease inhibitors (UI), such as NBPT (N-(n-Butyl) thiophosphoric triamide), Agrotain, Koch Agronomic Services, Wichita, KS) inhibits urease activity and reduces the rate of urea conversion to ammonium, thereby lowering volatility losses of ammonia which occur primarily at the soil surface.

Studies have shown that higher crop yields and lower N losses can be achieved by EEF applications (Gagnon et al., 2012; Nash et al., 2013; Kaur et al., 2017). In eastern Canada, PCU and non-coated urea (NCU) with NI resulted in higher corn yields during wet years compared to urea but showed no differences in yields among fertilizer sources during dry years (Gagnon et al., 2012). The economic analysis revealed that despite 30% higher costs, PCU gave comparable net returns to UAN at an equivalent N rate in wet years (Gagnon et al., 2012). Polymer-coated urea may reduce subsoil NO_3^- concentrations early in the growing season compared to NCU, which can prevent N leaching losses and increase crop N use and yields (Nelson et al., 2009). However, the release of urea from PCU depends upon rainfall and soil temperature after its application (Nash et al., 2012a). Little is known about urea-N release from PCU and changes in soil NH_4^+-N and NO_3^--N content from different N fertilizer sources due to early-season soil waterlogging in corn fields. The objective of this study was to assess urea-N release from PCU, changes in soil properties, and soil inorganic N concentration from multiple N fertilizer sources due to 7-days waterlogging of cornfields planted with two different hybrids that have different levels of flood tolerance.

MATERIALS AND METHODS

Site Characterization

A field experiment was conducted for three years from 2013 to 2015 at the University of Missouri's Greenley Research Center (40° 1' 17" N, 92° 11'

24.9" W) near Novelty, MO (USA). Adjacent fields were used each year for corn, and the soil type at the experimental areas was Putnam silt loam (fine, smectitic, mesic Vertic Albaqualfs), which is a deep, poorly-drained claypan soil. The initial soil characterization data of the experimental fields are provided in Kaur et al. (2018). Daily weather monitoring, including air temperature and precipitation data, were obtained from a nearby automated weather station located at the Greenley Research Center.

Field Experiment

The experimental design was a randomized complete block with a split-split-split plot arrangement and three replications. Each block had two main plots that included waterlogging treatments of 0 or 7-days. The size of the main plots was 24 m x 24 m. The waterlogging was started at the V3 corn growth stage (Abendroth et al., 2011) and was accomplished by setting up earthen berms around the main plots, which allowed for the imposition of the flooding treatment. The depth of ponded water on the soil surface in the flooded treatment was approximately 4 to 8 cm causing only partial crop submergence, leaving the upper one or two leaves above the water surface. The berms were removed after the 7th day of waterlogging to allow ponded water to escape.

The subplots consisted of different pre-plant N fertilizer sources, and the sub-plot size was 6 m x 24 m. Each subplot was randomly planted with two different hybrids, which were selected from a greenhouse screening procedure for hybrids with differences in flood tolerance, creating a sub-sub plot (Kaur, 2016). Each sub-sub plot measured 3 x 24 m. There were 4 rows of corn in each sub-sub plot. After the waterlogging events, the sub-sub plots were divided into two parts of 12 m length each and one of them was treated with 84 kg N ha^{-1} of a rescue post-flood broadcast application of urea plus NBPT (N-(n-butyl) thiophosphoric triamide) urease inhibitor (4.2 L Mg^{-1} urea; Agrotain®, Koch Agronomic Services, Wichita, KS) while the other did not receive any additional N. The term 'rescue' is used for additional in-season N fertilizer applications when the previously applied N is lost due to excessive soil moisture conditions (Nelson et al., 2011).

Pre-plant N fertilizer sources included in this study were non-coated urea (NCU), polymer-coated urea (PCU; ESN®, Agrium, Inc., Calgary, AB, Canada) and non-coated urea plus a nitrification inhibitor (Instinct®, Dow AgroSciences, Indianapolis, IN, USA). A non-treated control (CO), which was not supplied with any pre-plant N fertilizer was also included in this study. All pre-plant N fertilizer sources were broadcast applied uniformly over the soil surface at a rate of 168 kg N ha^{-1} and were incorporated into the soil immediately after application to a depth of 15 cm using a Tilloll (Landoll Corp., Marysville, KS, USA).

The two corn hybrids, Hybrid #1 (P1360HR) and Hybrid #2 (P1498AM) (Pioneer Du Pont, Johnston, IA), used in this study were selected based on greenhouse screening results to provide one commercially-available hybrid that showed soil waterlogging tolerance and another that was less tolerant to soil waterlogging that was initiated at the V3 growth stage (Kaur, 2016; Kaur et al., 2019). Hybrid #2 was observed to be more tolerant of waterlogged soil conditions and Hybrid #1 less tolerant to waterlogging based on this screening of eight commercially-available corn hybrids subjected to 21 days of waterlogged soil conditions. The row spacing used for planting hybrids was 0.76 m, and the seeding rate was 81,512 seeds ha^{-1}. At the V7-V8 growth stage of corn, rescue N fertilizer was applied when corn plants were approximately 51 cm tall. The rate selected for the rescue N application was based on an estimate of an economical optimal N rate for yield response at the V7 corn growth stage determined by using the SPAD 502 chlorophyll meter (CM) readings (Konica Minolta, Hong Kong) taken after 7-days flooding in 2013 and from recommendation equations from Scharf et al. (2006). The sub-sub-sub plot size was 3 x 12 m. Other field treatments and crop management details are provided in Kaur (2016).

Changes in soil redox potential (E_h), soil pH, soil temperature, and bulk density at the soil surface were measured to determine soil conditions during waterlogging events. Portable ORP and

pH electrodes (Cole Palmer ORP/pH 91 cm long submersible, Vernon Hills, IL) attached to an Oakton 310 pH/ORP meter (Vernon Hills, IL) were used for taking soil redox potential and pH measurements. The portable ORP electrode consisted of a platinum wire and Ag/AgCl reference electrode saturated in 4 M KCl solution. Soil E_h values were converted to standard H_2 reference electrode values (Vepraskas, 2002). The soil surface pH and redox potential measurements were taken in the upper 5 cm of soil. Surface soil temperature was measured using an Oakton Temp 10 Thermocouple (Vernon Hills, IL) in the top 10 cm soil depth. These measurements were recorded during the day between 0900 and 1200 h. Bulk density samples were taken from 0-10 cm, 10-20 cm and 20-30 cm depths using the core method (Blake and Hartge, 1986) from the CO plots of each replication before and after waterlogging events to determine any effects of flooding on soil physical properties.

The weight-loss method was used for determining urea-N released from PCU due to waterlogging (Nash et al., 2012b). Standard mesh screen packets of PCU weighing 10 g each were placed on the soil surface before fertilizer application in the different treatments and then covered with some soil to about 5 cm to simulate soil incorporation. These PCU packets were removed at fertilization, waterlogging, 3 days after waterlogging, 1 month after fertilizer application, 1 week after waterlogging, 2 weeks after waterlogging, 1 month after waterlogging, 2 months after waterlogging, 3 months after waterlogging and 4 months after waterlogging. If corn harvest occurred before the last removal timings, then all remaining packets were removed on the day of harvest. The PCU packets were washed in ice to remove any sediment attached to them, then dried and allowed to re-solidify any released urea on PCU prills (Nash et al., 2012b). After washing, the PCU packets were dried and weighed for determining the percent urea-N release from PCU.

Soil samples (composite of 10 subsamples) were collected before (pre-waterlogging) and after waterlogging (post-waterlogging) events from 0-10, 10-20, and 20-30 cm depths using a stainless steel push probe. Post-waterlogging soil samples were collected approximately 7-10 days after the 7-days waterlogged plots were drained. The collected soil samples were air-dried, ground, passed through a 2 mm sieve and analyzed for soil inorganic N (NH_4^+-N and NO_3^--N) using a 2 M KCl extraction and analysis with a Lachat 8400 series II automated ion analyzer (Hach Corp., Loveland, CO) (QuikChem Method 12-107-06-2-A for ammonia analysis and QuikChem Method 12-107-04-1-B for nitrate analysis).

Statistical Analysis

The MIXED procedure of SAS v.9.4 statistical software (SAS Institute, 2013) was used for data analysis. Data normality was verified through UNIVARIATE procedure of SAS v9.4. Data were combined over factors when appropriate, as indicated by the ANOVA results. The ANOVA tables for results represented in this paper is provided in Kaur (2016). Means were separated using Fisher's Protected Least Significant Difference (LSD) at the $P < 0.10$ probability level.

RESULTS

Climatic Conditions During the Growing Seasons

The cumulative precipitation varied by year over the growing season from April to September (Fig. 1A-C). The cumulative precipitation over the growing season was highest in 2015 (911 mm), followed by 2014 (745 mm) and lowest in 2013 (673 mm). The flooding was initiated for the waterlogged treatments in May in 2014 and 2015 as compared to June in 2013. In 2013, about 199 mm of precipitation was received between planting and flooding initiation, with a major proportion of it falling a few days before the initiation of flooding events. The precipitation amounts that occurred in the period between planting and flood initiation in 2014 and 2015 were 83 and 48 mm, respectively. Besides, more precipitation occurred in a period of 30 days after the flooding treatment in 2014 and 2015 compared to 2013. The distribution of precipitation was highly variable in 2013 as extreme rains during the spring were followed by

an extended drought period in August and September. Comparatively, total precipitation was evenly distributed during the growing periods in 2014 and 2015 (Fig. 1B and 1C). Excessive moist soil conditions occurred for a more extended period during the 2015 growing season due to heavy precipitation after the waterlogging events.

Waterlogging treatments were initiated earlier in 2014 and 2015 during May with relatively lower air temperatures compared to higher air temperatures experienced during waterlogging in June during the 2013 growing season (Fig. 2A-C). The air temperature, when averaged over the 7-days flooding events, was 2.5°C lower in 2014 and 2015 compared to the 2013 growing season. The air temperature ranged from 15-20°C in 2013, 7.5-24.8°C in 2014, and 8-21°C in 2015 during waterlogging events. The air temperature during the 7-days flooding events was highly variable in 2014 and 2015 than in 2013. The air temperature in 2015 was 9.7 and 12.3°C lower than in 2013 on the 6th and 7th day of the waterlogging event. However, the air temperatures were 4.4 to 9.8°C lower for the first four days of waterlogging in 2014 compared to 2013. The air temperatures were higher during the remaining days of the waterlogging event in 2014 than in 2013.

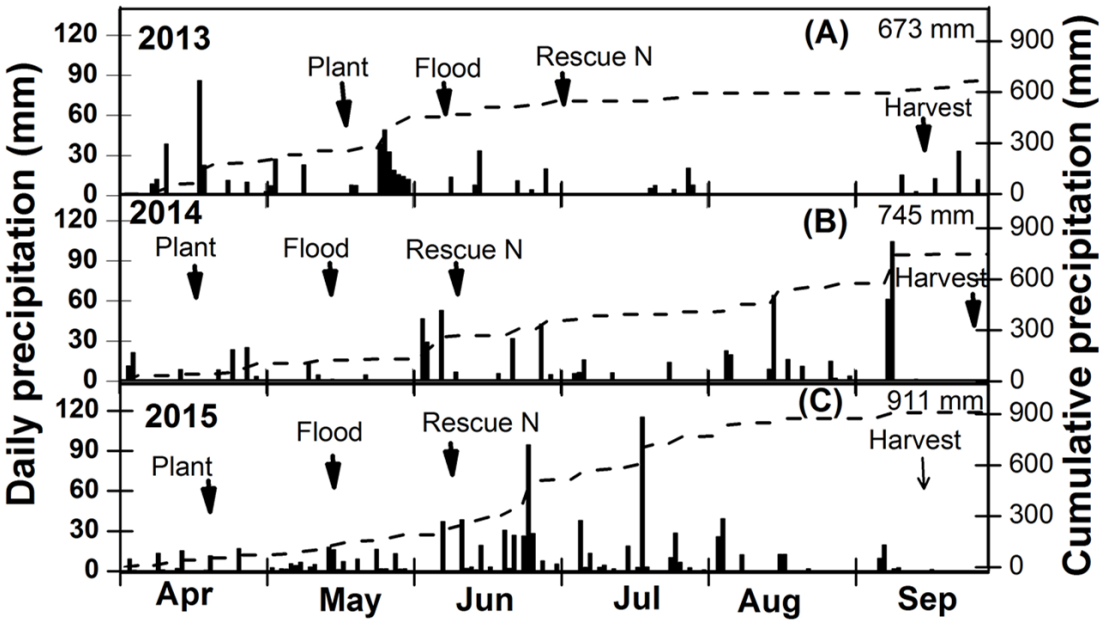

Figure 1. Daily (bars) and cumulative (line) precipitation during the 2013 (A), 2014 (B), and 2015 (C) growing seasons at the Greenley Research Center near Novelty, Missouri. Timings of major field events are indicated by arrows (Kaur et al., 2018)

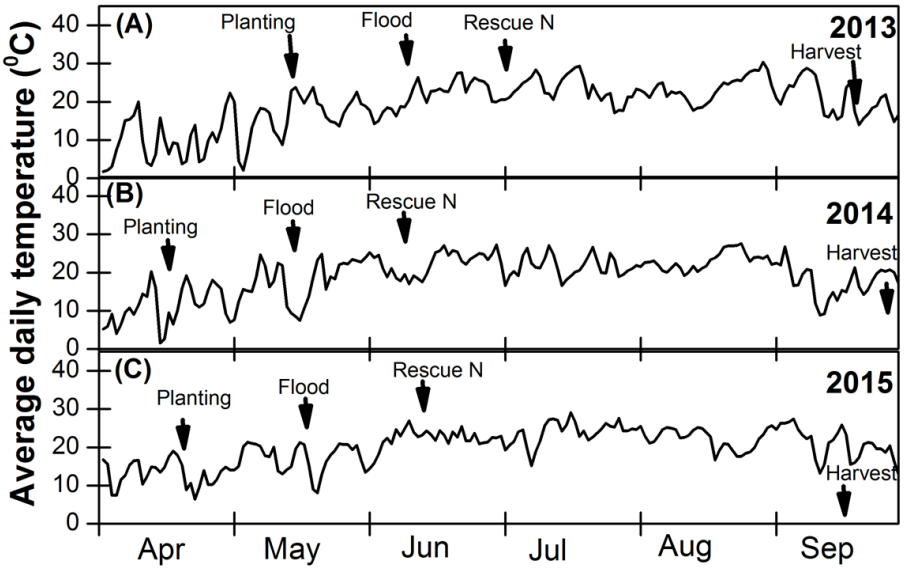

Figure 2. Average daily air temperature during the 2013 (A), 2014 (B), and 2015 (C) growing seasons at the Greenley Research Center near Novelty, Missouri. Timings of major field events are indicated by arrows (Kaur et al., 2018).

Soil Conditions During Soil Waterlogging

Soil E_h decreased with each day of soil waterlogging, indicating the development of reduced and anaerobic conditions in the soil over the duration of seven days (Fig. 3). Soil E_h decreased 136, 176, and 122 mV units by the third day of waterlogging compared to those of the first day of waterlogging in 2013, 2014, and 2015, respectively. Soil E_h was reduced 308, 306, and 294 mV units due to seven days of waterlogging compared to the first day of waterlogging in 2013, 2014, and 2015, respectively. Soil E_h decreased by 50 mV units per day of waterlogging in 2013 and 2015 (Fig. 3). In all three years of our experiment, soil E_h by the seventh day of soil waterlogging was in the range of 120 to 414 mV, indicating that the field soil was in a suboxic condition.

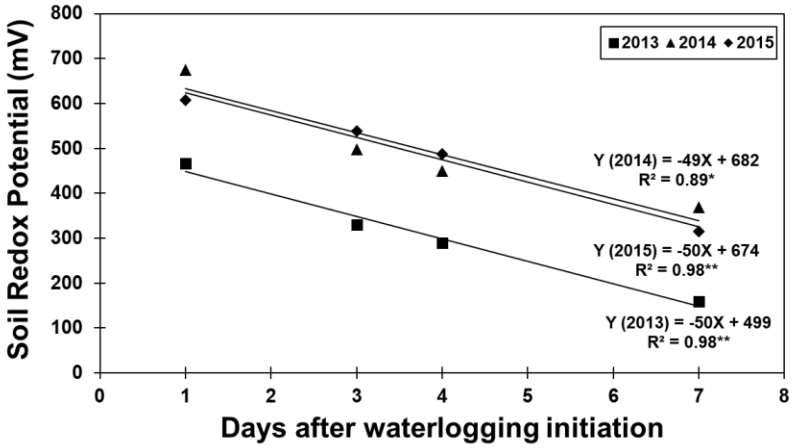

Figure 3. Changes in soil redox potential with waterlogging duration in 2013, 2014, and 2015 for field experiments conducted at the University of Missouri's Greenley Research Center near Novelty, MO.

*Significant at 0.1 probability level; ** Significant at 0.01 probability level.

Table 1. Soil surface pH (0-10 cm) as affected by soil waterlogging in 2013, 2014, and 2015 growing seasons for field exeperiment conducted at the University of Missouri's Greenley Research Center near Novelty, MO.

Days after waterlogging initiation	Soil surface pH		
	2013	2014	2015
1	6.2a[†]	5.6b	5.2a
3	6.1a	6.1a	5.3a
4	6.2a	5.9ab	5.4a
7	6.2a	5.9ab	5.8a

[†]Means followed by the same letter within a column do not differ significantly (P<0.10) based on Fisher's least significant difference test.

No significant changes were observed for soil pH due to soil waterlogging in 2013 and 2015 for this research experiment (Table 1). Soil surface pH measured during waterlogging increased significantly by 0.5 units from 5.6 to 6.1 after 3 days of waterlogging and then decreased to 5.9 on the seventh day of waterlogging at the end of the flooding treatment in 2014 (Table 1). The soil surface pH was similar on the first and seventh days of waterlogging in 2014.

Soil temperature was higher in the waterlogged treatments compared to non-waterlogged treatments in 2013 and 2015 by 1.4 and 1.1^{o}C, respectively, when averaged over the 7-days of the waterlogging period (Fig. 4). The heat capacity of water in soil is higher than air, which makes the waterlogged soils more resistant to change in soil temperature. Once the soils were heated up in waterlogged treatments, the heat capacity of soil water can resist further changes in soil temperature. However, variation in soil temperature each day depends upon differences in the air temperature and solar radiation among different days. Soil temperature increased during the 7-days of waterlogging events in 2013 and 2014. However, soil temperatures decreased throughout 7-days waterlogging events in 2015.

The mean soil bulk density values for upper 30 cm depth in 2013, 2014, and 2015 were 1.38, 1.34, and 1.37 Mg m^{-3}. The 7-days soil waterlogging did not significantly affect soil bulk density. In 2014, the bulk density in the 0-10 cm depth was 0.15 and 0.11 Mg m^{-3} lower compared to the soil bulk density at 10-20 cm (1.40 Mg m^{-3}) and 20-30 cm (1.36 Mg m^{-3}) depth. Soil bulk density was 0.20 and 0.17 Mg m^{-3} higher in the 10-20 cm (1.45 Mg m^{-3}) and 20-30 cm (1.42 Mg m^{-3}) soil depths, respectively, compared to the 0-10 cm soil depth in 2015.

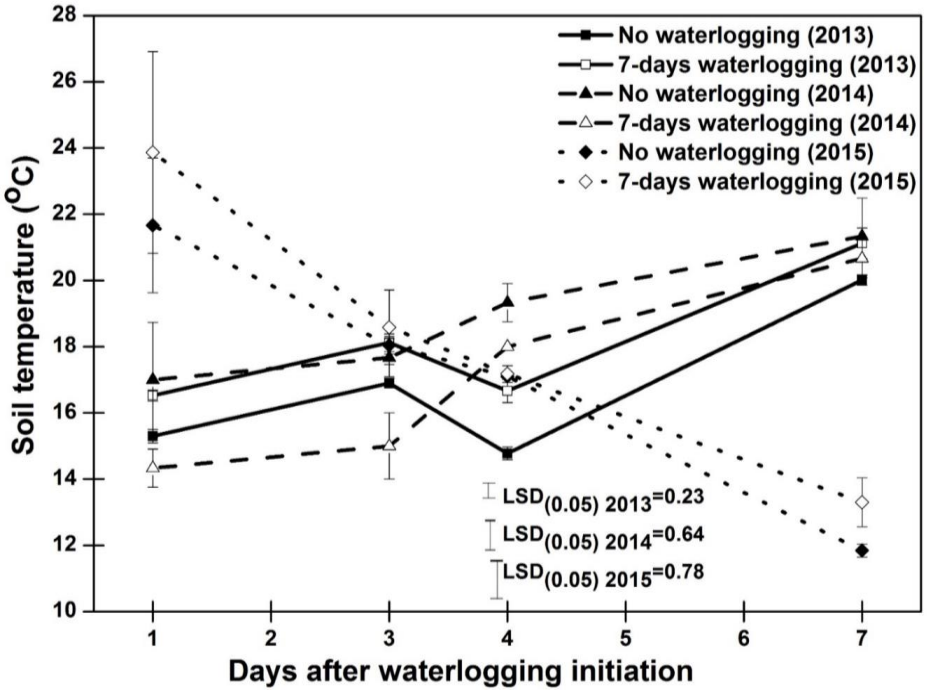

Figure 4. Soil surface temperature in non-waterlogged and waterlogged soil during waterlogging event in 2013, 2014 and 2015 for field experiment conducted at the University of Missouri's Greenley Research Center near Novelty, MO.

Urea-N Fertilizer Release from Polymer Coated Urea

When data was averaged overtime for the whole growing season, the mean urea-N release from PCU over the growing period in the 7-days waterlogging treatments was significantly higher than the non-waterlogged treatments in 2013 and 2014 (Fig. 5A & B). However, no differences were found between the non-waterlogged and 7-days waterlogged treatments in 2015 (Fig. 5C). The urea-N release from the waterlogged and non-waterlogged treatments two weeks after waterlogging was 78% and 72% in 2013 and 59 and 52% in 2015, respectively. However, urea-N release between waterlogged and non-waterlogged treatments two weeks after waterlogging initiation was not significantly different. After waterlogging started in 2014, the urea-N release from 7-days waterlogging treatments was comparatively higher than non-waterlogged treatments, but it was not significantly different. The urea-N release at the time of waterlogging was 38% in 7-days waterlogged treatments and 36% in non-waterlogged treatments in 2014. The urea-N release increased up to 56% by the first week after waterlogging in 7-days waterlogged treatments, whereas it was 49% in treatments that were not waterlogged in 2014. In 2014, the urea-N release was 13% higher in 7-days waterlogged plots compared to non-waterlogged treatments two weeks after waterlogging (Fig. 5B). About 70% of urea-N from PCU was released two weeks after waterlogging in 7-days waterlogged treatments in 2014 (Fig. 5B).

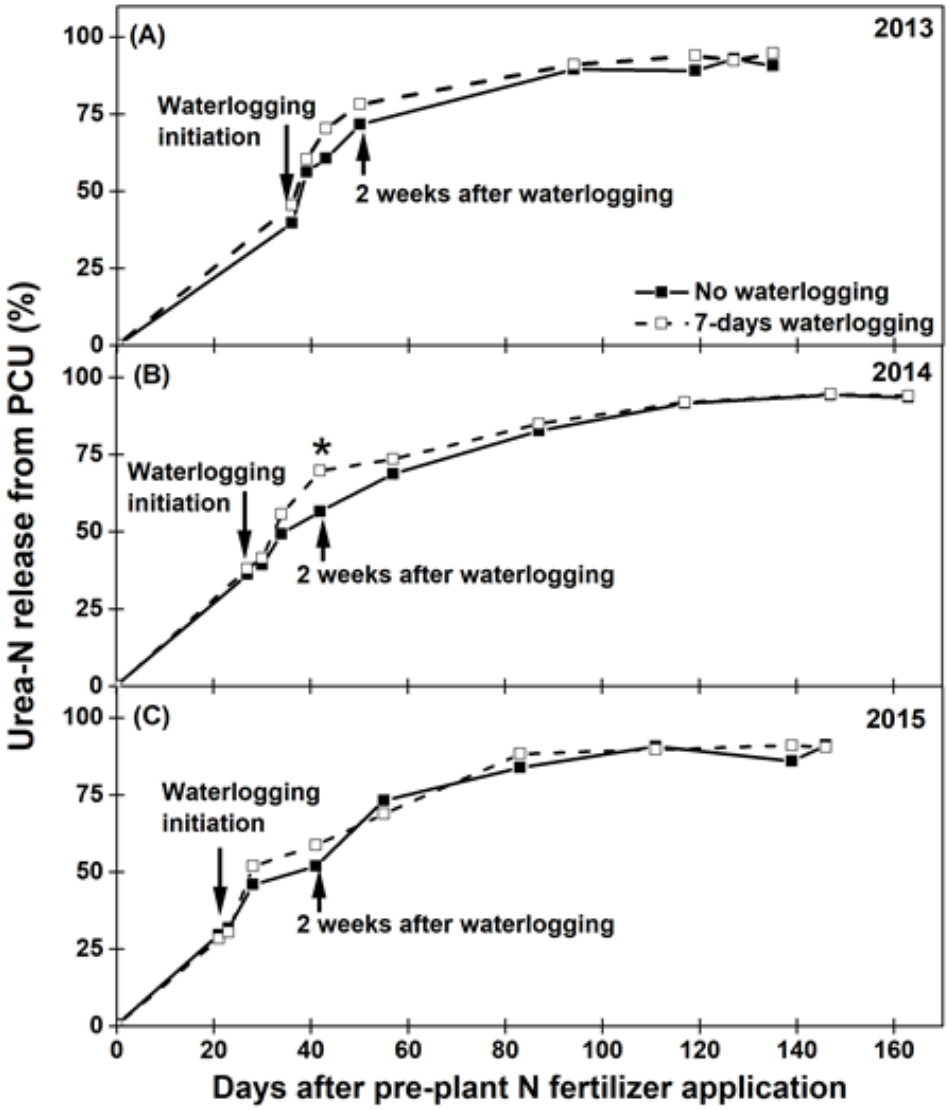

Figure 5. Urea-N release from polymer-coated urea in non-waterlogged and 7-days waterlogged treatments during the growing season in 2013 (A), 2014 (B), and 2015 (C) for field experiments conducted at the University of Missouri's Greenley Research Center near Novelty, MO.

Pre-waterlogging Soil N Concentrations

In 2013, pre-waterlogging soil NH_4^+-N concentrations were 33.13 to 43.47 mg kg^{-1} higher at the 0-10 cm depth in NCU+NI compared to PCU, NCU, and CO at all three depths in plots planted with the less flood tolerant Hybrid #1 (Table 2). At 0-10 cm depth among NCU+NI plots, the less flood tolerant Hybrid #1 treatments had 21.97 mg kg^{-1} higher soil NH_4^+-N than treatments with the more flood-tolerant Hybrid #2 (Table 2). The soil NH_4^+-N concentration was significantly higher at the 0-10 cm depth compared to the 10-20 cm and 20-30 cm depths in 2013. All pre-plant N fertilizer sources including PCU, NCU, and NCU+NI resulted in 34 to 43 mg kg^{-1} higher soil NO_3^--N concentration at 0-10 cm soil depth than the CO in 2013 (Table 3). At the 0-10 cm depth, the more flood-tolerant Hybrid #2 had 8.45 mg kg^{-1} lower soil NO_3^--N concentration than the less flood tolerant Hybrid #1 treatments in 2013 when data was averaged over all pre-plant N sources (Table 4). Less flood-tolerant Hybrid #1 had higher soil

NH_4^+-N and NO_3^--N concentrations before waterlogging initiation than more flood-tolerant Hybrid #2 in 2013, indicating that Hybrid #2 had comparatively more N uptake early in the season than Hybrid #1. The plots planted with less flood tolerant Hybrid #1 are susceptible to higher N losses due to waterlogging through leaching or denitrification, as they have higher pre-waterlogging soil NH_4^+-N and NO_3^--N concentrations.

Table 2. Pre-waterlogging soil inorganic N concentration at different depths as affected by the pre-plant N fertilizer sources and corn hybrids in 2013 and 2015 for field experiments conducted at the University of Missouri's Greenley Research Center near Novelty, MO.

Pre-plant N fertilizer sources†	Corn hybrids	Depth	Pre-waterlogging Soil Inorganic N	
			NH_4^+-N 2013	NO_3^--N 2015
		---cm---	----------mg kg^{-1} ----------	
CO	P1360HR (Hybrid #1)	0-10	8.01bc‡	52.53cde
PCU		0-10	11.37bc	74.79bcd
NCU		0-10	5.89bc	71.38bcd
NCU+NI		0-10	44.50a	98.90bc
CO		10-20	3.55c	13.38e
PCU		10-20	8.47bc	14.35e
NCU		10-20	3.96c	15.54e
NCU+NI		10-20	2.83c	16.59e
CO		20-30	8.59bc	11.11e
PCU		20-30	1.03c	11.90e
NCU		20-30	3.29c	13.38e
NCU+NI		20-30	6.32bc	12.41e
CO	P1498AM (Hybrid #2)	0-10	3.59c	44.32de
PCU		0-10	16.77bc	168.12a
NCU		0-10	4.46c	117.44b
NCU+NI		0-10	22.53b	99.84bc
CO		10-20	6.91bc	17.13e
PCU		10-20	4.28c	18.25e
NCU		10-20	1.60c	14.62e
NCU+NI		10-20	8.29bc	20.52e
CO		20-30	5.22bc	8.62e
PCU		20-30	2.03c	10.19e
NCU		20-30	2.60c	10.40e
NCU+NI		20-30	2.97c	7.62e

†Abbreviations: CO, non-fertilized control; NCU, non-coated urea; PCU, polymer-coated urea; NCU+NI, non-coated urea + nitrification inhibitor (Instinct).

‡Means followed by the same letter within a column do not differ significantly (P<0.10) based on Fisher's least significant difference test.

In 2014, PCU treatments resulted in 31.92 and 32.97 mg kg^{-1} higher soil NH_4^+-N concentrations than CO and NCU at the 0-10 cm depth (Table 3). No significant differences were found for soil NH_4^+-N concentration between the CO and NCU treatments at all three depths. The soil NH_4^+-N concentration at the 0-10 cm depth in the NCU+NI treatment was not significantly different from the PCU or NCU treatments (Table 2). The PCU treatment at the 0-10 cm depth had 33.23 and 34.90 mg kg^{-1} higher NH_4^+-N concentration than at 10-20 cm and 20-30 cm. The soil NH_4^+-N concentration at lower depths from 10-20 cm and 20-30 cm was not significantly different among all pre-plant N fertilizer sources. No differences were observed among corn hybrids for soil NH_4^+-N concentrations. In 2014, PCU and NCU+NI had 35.26 and 28.93 mg kg^{-1} higher soil NO_3^--N concentrations than the CO at the 0-10 cm depth (Table 3). The soil NO_3^--N concentrations from NCU was similar to the CO and PCU or NCU+NI at the 0-10 cm depth (Table 2).

Table 3. Pre-waterlogging and post-waterlogging soil inorganic N concentration at different soil depths as affected by pre-plant N fertilizer sources in 2013, 2014 and 2015 for field experiment conducted at the University of Missouri's Greenley Research Center near Novelty, MO. .

		Soil inorganic N concentration					
Pre-plant N fertilizer†	Depth	Pre-waterlogging			Post-waterlogging§		
		NH_4^+-N 2014	NO_3^--N 2013	NO_3^--N 2014	NH_4^+-N 2013	NH_4^+-N 2015	NO_3^--N 2013
	--cm--	mg kg^{-1}					
CO	0-10	10.10b‡	5.22b	16.71bc	9.54ab	4.08bc	39.14b
PCU	0-10	42.02a	43.98a	51.98a	9.28b	5.55abc	74.05a
NCU	0-10	9.04b	47.85a	38.35ab	9.51ab	6.52a	69.38a
NCU+NI	0-10	20.52ab	39.72a	45.64a	11.31a	6.07ab	83.22a
CO	10-20	8.62b	9.76b	13.03c	6.15c	3.90bc	18.53c
PCU	10-20	8.79b	11.84b	9.30c	5.42cd	3.96bc	21.06c
NCU	10-20	6.91b	12.54b	8.39c	5.94cd	3.95bc	23.00bc
NCU+NI	10-20	7.46b	10.59b	8.12c	5.16cd	3.59c	21.23c
CO	20-30	9.24b	10.47b	9.22c	4.38d	4.41abc	16.57c
PCU	20-30	7.11b	11.96b	8.27c	4.77cd	4.10bc	19.30c
NCU	20-30	8.77b	13.60b	8.93c	4.74cd	3.71c	21.27c
NCU+NI	20-30	8.39b	11.11b	7.40c	5.02cd	3.29c	18.99c

†Abbreviations: CO, non-fertilized control; NCU, non-coated urea; PCU, polymer-coated urea; NCU+NI, non-coated urea + nitrification inhibitor (Instinct).

‡Means followed by the same letter within a column do not differ significantly (P <0.10) based on Fisher's least significant difference test.

§ Data was averaged over waterlogging duration and corn hybrids to show the interaction of pre-plant N fertilizer sources with soil depth.

Pre-plant N fertilizers and corn hybrids did not cause any differences in soil NH_4^+-N concentration at all depths in 2015 (data not presented). The pre-waterlogging soil NO_3^--N concentrations were higher at the 0-10 cm depth than at the 10-20 cm or 20-30 cm depths for PCU, NCU, and NCU+NI treatments in all three years (Table 2 & 3). When compared within individual

soil depths, no significant differences were found for soil NO_3^--N concentration between pre-plant N fertilizer sources and the CO in treatments planted with the less flood tolerant Hybrid #1 in 2015. However, the PCU resulted in 123.8, 50.68, and 68.23 mg kg^{-1} more soil NO_3^--N concentration than the CO, NCU, and NCU+NI, respectively, at the 0-10 cm depth in treatments planted with the more flood-tolerant Hybrid #2 in 2015 (Table 2). Among PCU plots at the 0-10 cm depth in 2015, the less flood tolerant Hybrid #1 treatments had 93 mg kg^{-1} lower soil NO_3^--N concentration than the more flood-tolerant Hybrid #2 (Table 3). This indicates differences in N uptake among hybrids in PCU plots, which is contrary to results obtained for soil NO_3^--N concentration for both hybrids in 2013.

Post-Waterlogging Soil N Concentrations

About 7-10 days after the water from waterlogged main plots was drained, post-waterlogging soil samples were collected from both waterlogged and non-waterlogged main-plots and compared for post-waterlogging soil NH_4^+-N and NO_3^--N concentrations. In all three years of this research, soil NH_4^+-N concentrations measured after waterlogging were similar between 7-days waterlogged and non-waterlogged plots. However, the post-waterlogging soil NO_3^--N concentrations were significantly different between waterlogged and non-waterlogged treatments in 2014 and 2015. In general, the post-waterlogging soil NH_4^+-N and NO_3^--N concentrations were higher at the 0-10 cm depth than at 10-20 cm and 20-30 cm depths (Table 3 & 5).

Averaged over waterlogging duration treatments and corn hybrids, post-waterlogging soil NH_4^+-N concentrations in 2013 and 2015, and soil NO_3^--N concentrations in 2013 showed no significant differences between pre-plant N sources at the 10-20 cm and 20-30 cm depths (Table 3). The NCU+NI post-waterlogging soil NH_4^+-N concentration was 2.03 mg kg^{-1} higher than the PCU treatment at a 0-10 cm depth in 2013 (Table 3). In 2013, post-waterlogging soil NH_4^+-N concentrations in the CO and NCU were similar to PCU and NCU+NI (Table 3). No significant differences between NCU+NI and NCU for post-waterlogging soil NH_4^+-N concentration indicates that NI was no longer active when soils were waterlogged for seven days in this research.

Table 4. Pre-waterlogging soil inorganic N concentration at different depths in 2013 as affected by corn hybrids for field experiment conducted at the University of Missouri's Greenley Research Center near Novelty, MO.

Corn Hybrids†	Depth	Pre-waterlogging NO_3^--N§
	--cm--	---------mg kg^{-1}------
P1360HR (Hybrid #1)	0-10	38.41a‡
P1360HR (Hybrid #1)	10-20	11.56c
P1360HR (Hybrid #1)	20-30	11.62c
P1498AM (Hybrid #2)	0-10	29.97b
P1498AM (Hybrid #2)	10-20	10.80c
P1498AM (Hybrid #2)	20-30	11.95c

†Based on a screening trial, Hybrid #1 (P1360HR) was assessed as less tolerant of soil waterlogging and Hybrid#2 (P1498AM) was more tolerant of waterlogging at the V2 growth stage. ‡Means followed by the same letter within a column do not differ significantly (P <0.10) based on Fisher's least significant difference test. § Data was averaged over pre-plant N fertilizer sources to show the interaction of corn hybrids with soil depth.

Table 5. Post-waterlogging soil NO_3^--N concentration at different depths as affected by the waterlogging duration, pre-plant N fertilizer sources and corn hybrids in 2014 and 2015.

			Waterlogging duration (in days)			
			0		7	
Year	Pre-plant N Fertilizer†	Depth	Hybrid #1 (P1360HR)	Hybrid #2 (P1498AM)	Hybrid #1 (P1360HR)	Hybrid #2 (P1498AM)
		---cm---	----------NO_3^--N (mg kg^{-1})----------			
2014	CO	0-10	19.37ghi§	19.69ghi	14.59hi	10.94hi
	PCU	0-10	63.34bcde	87.76abc	53.86cdefg	33.58efghi
	NCU	0-10	96.75ab	113.15a	45.23defgh	38.64efghi
	NCU+NI	0-10	79.89abcd	59.98cdef	39.08efghi	40.71 efghi
	CO	10-20	14.13hi	11.00hi	8.72i	8.62i
	PCU	10-20	28.33fghi	17.76ghi	16.07hi	13.45hi
	NCU	10-20	17.93ghi	20.88ghi	18.50ghi	16.97hi
	NCU+NI	10-20	20.62ghi	22.05ghi	17.77ghi	16.80hi
	CO	20-30	14.27hi	9.40i	9.61i	8.66i
	PCU	20-30	16.28hi	25.96fghi	13.31hi	12.71hi
	NCU	20-30	20.43ghi	22.92ghi	15.16hi	15.74hi
	NCU+NI	20-30	15.36hi	29.28efghi	14.31hi	17.86ghi
2015	CO	0-10	38.79defg	65.16cd	43.33efg	36.07defg
	PCU	0-10	139.43a	93.80bc	65.94cd	65.11cd
	NCU	0-10	95.00bc	90.46bc	62.20cde	83.23bc
	NCU+NI	0-10	100.74b	93.40bc	83.01bc	78.29bc
	CO	10-20	19.51fg	20.09fg	14.45fg	17.15fg
	PCU	10-20	22.00fg	25.57fg	22.31fg	23.22fg
	NCU	10-20	29.47efg	27.97fg	22.74fg	25.84fg
	NCU+NI	10-20	24.99fg	27.69fg	22.15fg	24.12fg
	CO	20-30	10.47fg	12.22fg	10.08g	9.67g
	PCU	20-30	15.45fg	14.61fg	13.44fg	13.84fg
	NCU	20-30	19.72fg	17.50fg	15.37fg	18.04fg
	NCU+NI	20-30	17.56fg	12.98fg	15.13fg	12.71fg

Abbreviations: CO, non-fertilized control; NCU, non-coated urea; PCU, polymer coated urea; NCU+NI, non-coated urea + nitrification inhibitor (Instinct). ‡Based on a screening trial, Hybrid #1 was assessed as less tolerant of soil waterlogging and Hybrid#2 was more tolerant of waterlogging at the V2 growth stage. §Means followed by the same letter do not differ significantly ($P<0.10$) based on Fisher's least significant difference test. Mean comparisons within a year are valid.

In contrast to 2013 and 2015, no interaction was found between pre-plant N fertilizer sources and soil depth for post-waterlogging soil NH_4^+-N concentrations in 2014. When data was averaged over waterlogging duration, soil depth, and corn hybrids, the PCU treatments had 4.69 mg kg^{-1} higher post-waterlogging NH_4^+-N concentration than the CO in 2014, which might be due to higher PCU dissolution due to waterlogging as indicated by the urea-N release (Fig. 5). The soil NH_4^+-N concentration from NCU (8.92 mg kg^{-1}) and NCU+NI (10.28 mg kg^{-1}) was not significantly different from either PCU or CO. At the 0-10 cm depth, NCU treatments had 2.45 mg kg^{-1} higher soil NH_4^+-N concentration post-waterlogging than CO in 2015 (Table 3).

All pre-plant N fertilizer sources had higher post-waterlogging soil NO_3^--N concentration compared to the CO at a 0-10 cm depth when data was averaged over other treatments in 2013

(Table 4). The post-waterlogging soil NO_3^--N concentrations in CO treatments were 34.91, 30.25, and 44.08 mg kg^{-1} lower than PCU, NCU, and NCU+NI, respectively, in 2013 (Table 3). In 2013, the post-waterlogging soil NO_3^--N concentrations were not significantly different between waterlogged and non-waterlogged treatments when data were averaged over other treatments. An interaction was found between the waterlogging duration, pre-plant N fertilizer sources, corn hybrids, and soil depth for post-waterlogging NO_3^--N concentration in 2014 and 2015 (Table 5). At the 0-10 cm depth in 2014, the 7-days waterlogging reduced soil NO_3^--N concentrations compared to the non-waterlogged treatments in NCU sub-plots by 51.52 and 74.51 mg kg^{-1} for less flood tolerant Hybrid #1 and more flood-tolerant Hybrid #2, respectively; PCU treatments planted with the more flood-tolerant Hybrid #2 by 54.18 mg kg^{-1}; and NCU+NI treatments planted with the less flood tolerant Hybrid #1 by 40.81 mg kg^{-1} (Table 5).

In 2014, no significant differences were obtained for post-waterlogging soil NO_3^--N concentrations between all pre-plant N fertilizer sources at individual soil depths in 7-days waterlogged treatments, except that PCU treatments planted with the less flood tolerant Hybrid #1 had 39.27 mg kg^{-1} higher soil NO_3^--N concentrations than the CO at the 0-10 cm depth. In non-waterlogged plots, all pre-plant N sources had significantly higher post-waterlogging soil NO_3^--N concentration at a 0-10 cm depth than CO in 2014 irrespective of corn hybrids used (Table 5).

Soil NO_3^--N concentrations decreased by 69% and 30% in 2014 and 2015, respectively, due to 7-days waterlogging duration compared to non-waterlogged treatments. When data was averaged over pre-plant N sources and corn hybrids, the post-waterlogging NO_3^--N concentration in 2014 and 2015 was 20.87 and 33.23 mg kg^{-1} in 7-days waterlogged treatments and 35.27 and 43.11 mg kg^{-1} in non-waterlogged treatments.

In 7-day waterlogged treatments at depth 0-10 cm, soil NO_3^--N concentrations from PCU and NCU+NI treatments planted with the less flood tolerant Hybrid #1 as well as NCU and NCU+NI planted with the more flood-tolerant Hybrid #2 were significantly higher than the CO in 2015 (Table 5). In non-waterlogged plots planted with the less flood tolerant Hybrid #1 in 2015, PCU had 100.64, 44.43, and 38.69 mg kg^{-1} higher soil NO_3^--N concentrations than the CO, NCU, and NCU+NI treatments (Table 5). At depth 10-20 cm, post-waterlogging soil NO_3^--N concentrations were not different between pre-plant N fertilizer sources, soil waterlogging and corn hybrids.

DISCUSSION

Environmental and Soil Conditions During Soil Waterlogging

Annual variation in precipitation, air and soil temperatures resulted in different times for planting of corn, and the initiation of the waterlogging treatments and may account for some of the observed differences among years for urea release from PCU and changes in soil inorganic N content.

The soil E_h measurements were recorded to quantify the reducing conditions in the soil to determine whether the soil was aerobic or anaerobic and whether chemical compounds such as nitrate were present in their oxidized form or they were chemically reduced through denitrification process resulting in N losses as N_2O emissions (Vepraskas, 2002). The E_h of reduced soils varies between +400 to -300 mV, and E_h of soil normally fluctuates between −300 and +900 mV (Sahrawat, 2005; Husson, 2013). At pH 7, the redox potentials for oxic (aerobic), suboxic and anoxic (anaerobic) soil conditions were >414 mV, 414-120 mV and <120 mV (Essington, 2004). Fageria et al. (2011) reported that nitrate reduction to dinitrogen takes place at a soil E_h of 220 to 280 mV. Soil waterlogging decreased soil Eh as the waterlogging duration increased in our study. Soil Eh was by the last day of waterlogging was in the suboxic range. Similar to our study, previous studies have reported a decrease in soil E_h due to waterlogging. Decreases in soil E_h (at a depth of 5 cm) and dissolved oxygen within three to five weeks of flooding, with the development of anaerobic soil conditions within 12 days of inundation in five-weeks flooding treatments was also reported by

Unger et al. (2009). Variation in soil E_h among different years might be due to factors including the kind and amount of soil organic matter, the nature, and content of electron acceptors, soil temperature, and soil pH (Ponnamperuma, 1972). Soil E_h decreased sharply from its initial value ranging between 450-500 mV in a lysimeter experiment, and soil E_h was 343, 294,156, and 119 mV in alkali soil at pH 7.5, pH 8.2, pH 9.0 and pH 9.4, respectively, after 15 days of waterlogging (Yaduvanshi et al., 2010).

In our study, waterlogging did not cause any changes in soil pH in two out of three years. Similarly, no significant trends for soil pH at a depth of 5 cm were found by Unger et al. (2009) following three or five weeks of flooding treatments or over time compared to the non-flooded treatments. In flooded soils, soil pH changes along with redox potential, and it increases in acid soils due to proton consumption during the reduction of Fe and Mn oxides (Sahrawat, 2005; Kögel-Knabner et al., 2010; Fageria et al., 2011). It usually takes a few days to several weeks for changes to occur in soil pH due to waterlogging, depending on the soil type, organic matter sources and amounts, soil microbial population, temperature, and other soil chemical properties (Kongchum, 2005).

Soil temperature varied due to waterlogging in different years. These differences in soil temperature might be caused by fluctuations in solar radiation during the waterlogging event. A field-laboratory study conducted by Unger et al. (2009) found that soil temperatures (measured at depths of 5 cm and 15 cm) of non-flooded soils were lower than the three or five weeks flooded soils, with gradual increases over the monitored period in both flooded and non-flooded treatments. In contrast, Zurweller et al. (2015) found no differences in soil temperature at a 10 cm depth between non-waterlogged and three-days waterlogged soils. Still, yearly variations in soil temperature were obtained as higher air temperature caused a 4.2^{o}C warmer soil temperature, one out of the two years of the study.

Changes in bulk density because of flooding occurs due to swelling/drying of clay particles and weakening or breaking of soil aggregates. Previous studies in rice production systems have shown that waterlogging changes and creates bulk density gradient with depth as the soil particles settle down, with small values for bulk density at the interface between the soil and overlying floodwater and significant values in compacted layers at depth (Kirk et al., 2003). No changes found in bulk density in our study might be due to comparatively shorter waterlogging duration, depth of water ponding, stagnant water ponding, or differences caused by crop management practices and plant root characteristics.

Urea-N Fertilizer Release from Polymer Coated Urea

The release of N from PCU is mainly affected by soil temperature and moisture (Trenkel, 1997). Differences in N release from PCU among the three years of this research might have been caused by variation in rainfall amount and distribution as well as air and soil temperatures (Nash et al., 2012b; Nelson et al., 2014). The urea-N release rate from PCU in claypan soils of northeast Missouri can be increased by extreme wet soil conditions and/or higher soil temperatures (Nash et al., 2012b; Nelson et al., 2014). Higher rainfall amounts and uniform distribution in 2015 compared to 2013 and 2014 might have caused equally wet soil conditions even in non-waterlogged treatments resulting in no differences between non-waterlogged and waterlogged treatments for urea-N released in 2015. However, the urea-N release values two weeks after waterlogging events were higher in 2013 and 2014 than in 2015. Higher air and soil temperatures at the time of waterlogging and two weeks after waterlogging in 2013 and 2014 compared to 2015 might have resulted in the higher urea-N release from PCU when measured at two weeks after waterlogging (Fig. 4).

Pre-waterlogging Soil N Concentrations

In our study, NCU+NI had higher pre-waterlogging soil NH_4^+-N concentrations compared to PCU, NCU, and CO in 2013. In contrast, Zurweller et al. (2015) reported higher NH_4^+-N concentration at depth 0-10 cm before waterlogging at the V6 growth stage in PCU

treatments in poorly-drained soils in Northeast Missouri in 2013. The higher soil NH_4^+-N concentration resulting from the NCU+NI treatment might be due to inhibition of the nitrification process by NI that prevented the conversion of NH_4^+-N to nitrate-N. Lower NH_4^+-N concentration in PCU plots might be due to less release of urea-N from PCU prills or conversion of released N into nitrate forms by the time of this soil sampling. All N fertilizer sources resulted in higher pre-waterlogging NO_3^--N concentrations than the non-treated control plots at 0-10 cm soil depth in 2013. Zurweller et al. (2015) also found similar results for soil NO_3^--N concentrations at 10 cm depth when corn was flooded at the V6 growth stage and about 15 days later than the waterlogging initiation in this study. Differences between the hybrids in soil N concentrations may be due to differences in their N uptake patterns, root growth, or root architecture. The interaction of corn hybrids with pre-plant N fertilizer sources for pre-waterlogging soil NH_4^+-N and NO_3^--N concentration varied among year in our study. These responses might have depended upon the rainfall received and air or soil temperatures before initiation of waterlogging at the V3 growth stage that affected plant growth and development.

Post-Waterlogging Soil N Concentrations

Post-waterlogging soil NH_4^+-N concentrations were not affected by waterlogging treatments in all three years of this research, which could be due to the incorporation of all urea treatments. Similarly, Unger et al. (2009) also reported that soil NH_4^+-N concentration increased more in five weeks waterlogged treatments than the control or three weeks flooded treatments, with no significant differences between waterlogged and non-waterlogged treatments. Unger et al. (2009) concluded that observed soil NH_4^+-N concentration increases were possibly due to ammonification and nitrate reduction processes occurring under waterlogged soils (Unger et al., 2009).

Similar to our study, Unger et al. (2009) reported that soil NO_3^--N concentrations decreased significantly as a result of five weeks of continuous flooding treatment as compared to the no flood control. However, the non-flooded and three weeks of flowing water flooded treatments showed an increase in soil NO_3^--N concentrations in their study. Zurweller et al. (2015) reported that soil NO_3^--N concentration decreased rapidly with each day of waterlogging for three days at the V6 growth stage of corn across all pre-plant N fertilizer treatments including PCU, NCU and NCU+NI used in their study and soil NO_3^--N concentration was 32.3 mg kg^{-1} lower in three-days waterlogged soils compared to non-waterlogged soil. Lower soil NO_3^--N concentrations in the waterlogged plots were probably due to N losses through denitrification. Previous studies in northeast Missouri have shown that significant N loss pathways on poorly-drained claypan soils were denitrification and runoff (Udawatta et al., 2006; Nash et al. 2012a; Zurweller et al., 2015). Zurweller et al. (2015) reported, about 1.1% and 2.6% of N fertilizer was lost as soil N_2O emissions due to three days of waterlogging during and up to four days after waterlogged plots were drained on poorly drained soils of Northeast Missouri. They concluded that most of soil N_2O emissions occurred during and shortly after soil waterlogging events in these poorly-drained claypan soils.

CONCLUSIONS

Soil waterlogging for 7-days at the V3 growth stage of corn induced the development of anaerobic conditions in soil and resulted in higher surface soil temperatures compared to non-waterlogged treatments in two out of three years of this research. The urea-N release from PCU varied by year and depended upon annual variability in precipitation and soil temperature. In general, soil NH_4^+-N and NO_3^--N concentrations were higher at the 0-10 cm soil depth compared to the 10-20 cm and 20-30 cm depths, and no differences were obtained for soil inorganic N concentrations at depths 10-30 cm due to different treatments. In a relatively dry year (2013), the NI worked effectively in delaying the conversion of ammonium to nitrate up to three weeks, as indicated by the pre-waterlogging soil NH_4^+-N concentrations. No significant differences were observed between non-waterlogged and 7-days waterlogged

treatments for post-waterlogging soil NH_4^+-N concentrations in all three years as well as for soil NO_3^--N in 2013. In comparatively wet years (2014 and 2015), soil NO_3^--N was reduced due to 7-days waterlogging. However, no significant differences were obtained between PCU, NCU, and NCU+NI for post-waterlogging soil NO_3^--N concentrations, which could be due to the incorporation of all urea treatments. The interaction of corn hybrids with pre-plant N fertilizer sources for pre-waterlogging soil NH_4^+-N and NO_3^--N concentration varied among years. The PCU dissolution and soil NH_4^+-N and NO_3^--N concentrations due to waterlogging and applied N fertilizer sources depended upon changes in soil properties with waterlogging and varied by growing season climatic conditions, including precipitation and air/soil temperature.

CONFLICTS OF INTEREST

Authors have no conflicts to declare.

ACKNOWLEDGMENTS

The authors wish to acknowledge the Missouri Fertilizer and Aglime program for generously providing funding for this research project.

LITERATURE CITED

Abendroth LJ, Elmore R Boyer M, Marlay S. Corn growth and development, Iowa State University, University Extension. 2011. Available at: http://store.extension.iastate.edu/Product/Corn-Growth-and-Development

Ban N, Schmidli J, Schär C. Heavy precipitation in a changing climate: Does short-term summer precipitation increase faster? Geophys. Res. Lett. 2015; 42: 1165-1172.

Blake GR, Hartge KH. Bulk density. In: Methods of Soil Analysis: part 1. Physical and Mineralogical Methods, 2nd ed. (Ed.): A. Klute, ASA, Madison, Wisconsin. 1986; 363-375 pp.

Cubasch U, Meehl G, Boer G, Stouffer R, Dix M, Noda A, et al., Projections of future climate change, In: Climate change 2001: the scientific basis: contribution of working group I to the third assessment report of the intergovernmental panel. (Ed.): J.T. Houghton, Y. Ding, D.J. Griggs, M. Noguer, P.J. Van der Linden, X. Dai, K. Maskell, C.A. Johnson, 2001; 526-582 pp.

Essington ME. 2004. Soil and water chemistry: an integrative approach. CRC Press, Boca Raton, FL.

Fageria N, Carvalho G, Santos A, Ferreira E, Knupp A. Chemistry of lowland rice soils and nutrient availability. Comm. Soil Sci. Plant Anal. 2011; 42: 1913-1933.

Gagnon B, Ziadi N, Grant C. Urea fertilizer forms affect grain corn yield and nitrogen use efficiency. Can. J. Soil Sci. 2012; 92: 341-351.

Haddad S, Tabatabai M, Loynachan T. Biochemical processes controlling soil nitrogen mineralization under waterlogged conditions. Soil Sci. Soc. America J. 2013; 77: 809-816.

Halvorson AD, Snyder CS, Blaylock AD, Del Grosso SJ. Enhanced-efficiency nitrogen fertilizers: Potential role in nitrous oxide emission mitigation. Agron. J. 2014; 106: 715-722.

Hongprayoon C. 1992. Urea transformations in flooded soil. Louisiana State University, Baton Rouge, LA.

Huang B, Bridges DC, Nesmith S, Johnson JW. 1994. Growth, physiological and anatomical responses of two wheat genotypes to waterlogging and nutrient supply. J. Exp. Bot. 45: 193–202.

Huber D, Warren H, Nelson D, Tsai C. Nitrification inhibitors-new tools for food production. BioSci. 1977; 27: 523-529.

Husson O. Redox potential (E_h) and pH as drivers of soil/plant/microorganism systems: A transdisciplinary overview pointing to integrative opportunities for agronomy. Plant Soil 2013; 362: 389-417.

Jamison VC, Smith DD, Thornton JF. 1968. Soil and water research on a claypan soil. USDA-ARS Tech. Bull. 1379.

Kaur G. 2016. Use of nitrogen fertilizer sources to enhance tolerance and recovery of corn

hybrids to excessive soil moisture. Ph.D. diss. University of Missouri, Columbia, MO.

Kaur G, Zurweller BA, Nelson KA, Motavalli PP, Dudenhoeffer CJ. Soil waterlogging and nitrogen fertilizer management effects on corn and soybean yields. Agron. J. 2017; 109: 97-106.

Kaur G, Zurweller B, Motavalli PP, Nelson KA Screening Corn hybrids for soil waterlogging tolerance at an early growth stage. Agric. 2019; 9:33-44.

Kaur G, Nelson KA, Motavalli PP. Early-Season soil waterlogging and N fertilizer sources impact on corn N uptake and apparent N recovery efficiency. Agron. 2018; 8: 102-124.

Kirk GJD, Solivas JL, Alberto MC. Effects of flooding and redox conditions on solute diffusion in soil. European J. Soil Sci. 2003; 54: 617-624.

Kögel-Knabner I, Amelung W, Cao Z, Fiedler S, Frenzel P, Jahn R, Kalbitz K, Kolbl A, Schloter M. Biogeochemistry of paddy soils. Geoderma 2010; 157: 1-14.

Kongchum M. 2005. Effect of plant residue and water management practices on soil redox chemistry, methane emission, and rice productivity. Ph.D. diss. Khon Kaen University, Thailand.

Kopyra M. The role of nitric oxide in plant growth regulation and responses to abiotic stresses. Acta Physiologiae Plantarum 2004; 26: 459-473.

Kozdrój J, van Elsas JD. Response of the bacterial community to root exudates in soil polluted with heavy metals assessed by molecular and cultural approaches. Soil Biol. Biochem. 2000; 32: 1405-1417.

Kunkel KE. North American trends in extreme precipitation. Nat. Hazards. 2003; 29:291-305.

Morton LW, Hobbs J, Arbuckle JG, Loy A. Upper midwest climate variations: Farmer responses to excess water risks. J. Environ. Qual. 2015; 44: 810-822.

Motavalli PP, Goyne KW, Udawatta RP. 2008. Environmental impacts of enhanced-efficiency nitrogen fertilizers. Crop Manage. doi:10.1094/CM-2008-0730-02-RV.

Nash PR, Nelson KA, Motavalli PP. Corn yield response to polymer and non-coated urea placement and timings. Int. J. Plant Prod. 2013; 7: 373–392.

Nash PR, Motavalli PP, Nelson KA. Nitrous oxide emissions from claypan soils due to nitrogen fertilizer source and tillage/fertilizer placement practices. Soil Sci. Soc. Am. J. 2012a; 76: 983-993.

Nash PR, Nelson KA, Motavalli PP, Meinhardt CG. Effects of polymer-coated urea application ratios and dates on wheat and subsequent double-crop soybean. Agron. J. 2012b; 104: 1074-1084.

Nash PR, Nelson KA, Motavalli PP. Reducing nitrogen loss in subsurface tile drainage water with managed drainage and polymer-coated urea in a river bottom soil. J. Water Resour. Prot. 2014; 6: 988-997.

Nelson KA, Motavalli PP, Dudenhoeffer CJ. Cropping system affects polymer-coated urea release and corn yield response in claypan soils. J. Agron. Crop Sci. 2014; 200: 54-65.

Nelson KA, Paniagua SM, Motavalli PP. Effect of polymer coated urea, irrigation, and drainage on nitrogen utilization and yield of corn in a claypan soil. Agron. J. 2009; 101:681-687.

Nelson KA, Scharf PC, Stevens WE, Burdick BA. Rescue nitrogen applications for corn. Soil Sci. Soc. Am. J. 2011; 75: 143–151.

Patrick W, Jugsujinda A. Sequential reduction and oxidation of inorganic nitrogen, manganese, and iron in flooded soil. Soil Sci. Soc. Am. J. 1992; 56: 1071-1073.

Pengthamkeerati P, Motavalli PP, Kremer R, Anderson S. Soil compaction and poultry litter effects on factors affecting nitrogen availability in a claypan soil. Soil Tillage Res. 2006; 91: 109-119.

Ponnamperuma FN. The chemistry of submerged soils. Adv. Agron. 1972; 24: 29-96.

Rosenzweig C, Iglesias A, Yang X, Epstein PR, Chivian E. Climate change and extreme weather events; implications for food production, plant diseases, and pests. Global Change Human Health. 2001; 2: 90-104.

Sahrawat K. Fertility and organic matter in submerged rice soils. Curr. Sci. 2005; 88: 735-739.

Scharf PC, Brouder SM, Hoeft RG. Chlorophyll meter readings can predict nitrogen need and yield response of corn in the north-central USA. Agron. J. 2006; 98: 655-665.

Trenkel ME. 1997. Improving fertilizer use efficiency: controlled-release and stabilized fertilizers in agriculture. International Fertilizer Industry Association, Paris, France.

Udawatta RP, Motavalli PP, Garrett HE, Krstansky JJ. Nitrogen losses in runoff from three adjacent agricultural watersheds with claypan soils. Agric. Ecosyst. Environ. 2006; 117: 39-48.

Unger IM, Motavalli PP, Muzika RM. Changes in soil chemical properties with flooding: A field laboratory approach. Agric. Ecosyst. Environ. 2009; 131: 105-110.

Urban DW, Roberts MJ, Schlenker W, Lobell DB. The effects of extremely wet planting conditions on maize and soybean yields. Climatic Change 2015; 130: 247-260.

Vepraskas M. Redox potential measurements. NC State University. 2002. Available online: http://citeseerx.ist.psu.edu/viewdoc/download?doi=10.1.1.630.1755&rep=rep1&type=pdf.

Yaduvanshi NPS, Setter TL, Sharma SK, Singh KN, Kulshreshtha N. Waterlogging effects on wheat yield, redox potential, manganese and iron in different soils of India. Proceedings of the World Congress of Soil Science, Soil Solutions for a Changing World, Brisbane, Australia. 1–6 August. 2010; 45-48 pp.

Zurweller BA., Motavalli PP, Nelson KA, Dudenhoeffer CJ. Short-term soil nitrous oxide emissions as affected by enhanced efficiency nitrogen fertilizers and temporarily waterlogged conditions. J. Agric. Sci. 2015; 7: 1-14.

Evaluation of Rice Genotypes for Early- and Mid-season Vigor Using Morphological and Physiological Traits

Salah H. Jumaa[1,2], Akanksha Sehgal[1], Naqeebullah Kakar[1], Edilberto D. Redoña[3], Daryl Chastain[3], Marilyn L. Warburton[4] and K. Raja Reddy[1*]

[1]Department of Plant and Soil Sciences, Mississippi State University, Mississippi State, MS 39762, USA, [2]Department of Field Crop Science, Tikrit University, Salah Al Deen Governorate, Tikrit 34001, Iraq, [3]Delta Research and Extension Center, Mississippi State University, 82 Stoneville Road, Stoneville, MS 38776, USA, and [4]Corn Host Plant Resistance Research Unit, USDA-ARS, Mississippi State, MS 39762, USA

Corresponding author: K. Raja Reddy, Email: krreddy@pss.msstate.edu

ABSTRACT

Rice (Oryza sativa L.) is a major staple crop consumed by more than half of the world's population. Production of rice must be increased quantitatively and improved qualitatively to meet the requirements of the growing population in the twenty-first century and to maintain global food security. Early season vigor is a summation of the genotype's ability to germinate uniformly, synchronize emergence, and grow rapidly. Developing quantitative methods and identifying traits for screening and classification of rice genotypes with early-season vigor could be valuable both for breeding as well as commercial rice production. We hypothesized that rice genotypes vary for seedling vigor, and relative scores could be used to identify genotypes with superior early stand establishment and canopy development. Therefore, a study was conducted using a sunlit pot-culture set-up to assess genetic variation among 36 rice genotypes for the shoot and root traits, and several physiological parameters at the seedling growth stage (26 DAS) and mid-grain filling stage (95 DAS). Individual (IVRI) and cumulative response indices (CVRI) were estimated for each trait for all genotypes. Genotypes were classified into different categories using CVRI values. Three genotypes, RU1204197 (inbred breeding line), XL753 (hybrid), and THAD (inbred released variety) showed the highest vigor indices and three genotypes (inbred varieties CL142-AR and SABINE and breeding line RU1304146) showed the lowest vigor indices at 26 DAS. Seven genotypes, including inbred breeding lines RU1204197 and RU1304122, hybrids CLX 745 and XL 753, and cultivars CLIZMN, LAKAST, and THAD, showed the highest vigor indices among the 36 genotypes at 95 DAS. There appeared to be no specific differences among hybrids and inbreds for early season vigor. Based on the results from the present study, rice producers could select either inbred varieties or hybrids to maximize rice production in their specific growing environments.

Keywords: Early-season vigor, Genotypes, Photosynthesis, Rice, Root growth, Screening tools

Abbreviations: CTD, Canopy temperature depression; CVRI, Cumulative vigor response index; DAS, Days after sowing; DMSO, Dimethyl sulphoxide; Fv'/Fm', Fluorescence; gs, Stomatal conductance; IVRI, Individual vigor response index; LA, Leaf area; LN, Leaf number of main tiller; LW, Leaf dry weight; PAR, Photosynthetically active radiation; PCA, Principal component analysis; PH, Plant height; Pn, Photosynthesis; RAD, Root average diameter; RC, Root crossings; RF, Root forks; RI, Relative injury; RL, Root length; RN, Root number; RS, Root: shoot ratio; RSA, Root surface area; RT, Root tips; RV, Root volume; RW, Root dry weight; SHW, Aboveground dry weight; SW, Stem dry weight; Ta, Air temperature; Tc, Canopy temperature; TCh, Total chlorophyll; TDW, Total dry weight; TL, Total leaves; TN, Tiller number; Tr, Transpiration; TVRI, Total vigor response index; WUE, Water use efficiency

INTRODUCTION

As population and incomes rise, the demand for both food quantity and quality increases, and global food security becomes a growing challenge. Increasing population and growing prosperity are accompanied by changing human diets that will claim more natural resources per capita. This reality could raise the global demand for food crops two- to four-fold within two generations (Godfray and Garnett, 2014). Worldwide, the pressures on agriculture to produce more food will increase beyond 2050, as global agricultural production must continue to grow at 0.4

% per year from 2050 to 2080, i.e., less than half the growth rate projected for the period 2005/2007–2050 (Alexandratos and Bruinsma, 2012; Bandumula et al., 2019).

Rice is the staple food for over half of the global population and has significant cultural and historical roots. It is the second most cultivated cereal after wheat. About 90% of the global rice harvest is produced and consumed in Asia, where rice production is key to global food security. Sustained growth in rice production is needed to achieve food security, especially in developing countries (Bandumula et al., 2019). With the world population likely growing to 10 billion by 2050, mostly in Asia, the demand for rice will increase faster than for other crops. There are already many challenges to achieving higher rice productivity (Krishnan et al., 2011). Yield growth is expected to remain modest in the next few decades as high-yielding varieties continue to face high input costs and low consumer prices. The increase in rice area is expected to continue to slow, as the risk of crop diseases discourages multiple cropping, and new investments in irrigation infrastructure have not expanded. World rice consumption continues to rise, but at a reduced pace (Alexandratos and Bruinsma, 2012). Any fluctuations in rice production and changes in rice trade policies can have outsized effects on international prices. For the expansion of international trade, governments will need to adopt measures that reduce supply chain losses, improve supply response time, and reduce the market costs and post-harvest damages. High food prices have a disproportionate impact on global food security (Bandumula et al., 2019). Hence, efforts in research and extension should be made to break the trend of yield stagnation and close the yield gap to increase rice production and ensure global food security (Bandumula et al., 2019).

Over the past two decades, the size of U.S. rice farms and the methods of rice production have changed substantially. As the total number of farms growing rice declined (from 9,627 in 1997 to 5,591 in 2012), the total US planted rice acres also dropped at an annual average rate of about 0.75 percent between 1995 and 2017 (McBride et al., 2018). During this time, rice producers adopted several new technologies that improved the economic efficiency of rice production. Economically sound rice production has specific agronomic requirements, such as a plentiful supply of water applied in a timely fashion (via rain or irrigation from groundwater or surface water sources); high average temperatures during the growing season; a smooth land surface to facilitate uniform flooding and drainage; and a subsoil hardpan that inhibits the percolation of water. Thus, rice production in the United States is limited to certain areas meeting these conditions (McBride et al., 2018).

Early vigor determines uniform emergence and rapid development of seedlings under a wide range of field conditions (AOSA, 1983). Crop varieties with early seedling vigor and good stand establishment tend to maximize the use of available soil water, resulting in increased dry matter accumulation and improved grain yield. Early vigor is associated with rapid crop establishment, which is important in increasing the ability of rice to compete against weeds. Rice competitiveness with weeds, the ability to suppress weeds or the ability to avoid being suppressed by weeds (Goldberg and Landa, 1991; Namuco et al., 2009), or both (Jannink et al., 2000; Namuco et al., 2009), would be a valuable tool for increasing yields in many rice production systems. For the drought-prone rainfed ecosystem, rapid early growth reduces water loss through reduced evapotranspiration loss by early canopy closure, thereby allowing a greater soil water reservoir available for plant growth. In rice, high early vigor or rapid biomass accumulation has been reported to be associated with weed suppression and yield under weed competition in a direct-seeded situation in the uplands (Zhao et al., 2006 a, b, c). Improving early-season vigor is considered the most relevant and useful strategy to mitigate poor, uneven crop stands establishment, thus combating one of the major constraints in direct-seeded rice systems. (Okami et al., 2015; Kumar et al., 2009; Singh et al., 2017a, 2017b; Jumaa et al., 2019). Producing quantitative values and identifying important traits to screen and classify rice genotypes for early season vigor will be valuable to select current varieties and develop new genotypes better suited for the production system.

The objectives of this study were to: (1) evaluate the morphology, growth, and physiology of 36 rice inbred breeding lines and cultivars, and hybrid cultivars, during seedling growth and grain-filling stages; (2) develop a method to identify vigor variability among the rice genotypes; and (3) classify and rank rice genotypes, based on vigor response indices, during seedling (26 DAS) and mid-grain filling (95 DAS) stages.

MATERIALS AND METHODS

Planting Material

An experiment, comprised of 36 rice genotypes (including 18 released inbred varieties, 3 hybrids, and 15 inbred breeding lines (Table S1) was sown on 30 July, 2014 at the Rodney Foil Plant Science Research Center, Mississippi State University, Mississippi State (lat. 33°28`N, long. 88°47`W). The experiment was arranged in a randomized complete block design with five pots per variety. Polyvinyl chloride pots with 15cm diameter by 30cm height were filled with the soil medium consisting of 3:1 sand: loam (clay) with 500 g of gravel at the bottom of each pot. One hundred eighty pots were planted per line in four rows with 45 pots per row. Plants were irrigated with full-strength Hoagland's nutrient solution, three times a day, through an automated and computer-controlled drip irrigation system. Initially, eight seeds per pot were sown and gradually thinned to one plant per pot over the next 10 days after sowing (DAS). Standard cultural practices were applied according to guidelines specified by the Mississippi State Extension service for commercial rice production.

Growth Parameters

Plant height, leaf number of the main tiller, tiller number, and total leaves were measured on plants at 26 and 95 days after sowing (DAS). Leaf area was measured using the LI-3100 leaf-area meter (LI-COR, Inc.) at 26 DAS and 95 DAS (final harvest). Panicle initiation and panicle number were recorded at the final harvest (95 DAS). Plant component dry weights (leaf dry weight, stem dry weight, root dry weight, aboveground dry weight, and total dry weight) were measured from all plants after oven drying at 75° C until a constant weight was reached.

The roots were cut and separated from the stem at 26 DAS. The roots were then scanned using WinRHIZO Pro optical scanner software (Regent Instruments, Inc., Quebec, Canada). Roots were washed, cleaned, and untangled for scanning to acquire root images of 800 dpi resolution. Root images were then analyzed to study root morphology with a computer linked to WinRHIZO optical scanner and software analysis system. The system provided the analysis of the root parameters, including root: shoot ratio (RS), root length (RL), root surface area (RSA), average root diameter (RAD), root volume (RV), number of tips (RT), the number of forks (RF), and number of crossings (RC). Roots that had length more than 5 cm were counted and recorded as root number (RN).

Gas Exchange Parameters

Leaf net photosynthesis (Pn), stomatal conductance (g_s), transpiration (Tr), and fluorescence (Fv'/Fm') parameters were measured on the third or fourth recently fully expanded leaf from the top between 1000 and 1400 h on cloud-free days, 65–75 days after sowing, using a portable photosynthesis system (LiCOR Inc., Lincoln, Nebraska, USA). When measuring photosynthesis, the photosynthetically active radiation (PAR) provided by a 6400-02 LED light source was set at 1500 µmol m^{-2} s^{-1}, the temperature inside the leaf cuvette was set to 30 °C, relative humidity was adjusted to near-ambient level (50%), and leaf chamber [CO_2] was set to 420 µL L^{-1}. The chlorophyll fluorescence was measured using the built-in leaf chamber fluorometer, which used two red LEDs (center wavelength lies on 630 nm, and detector radiation lies at 715 nm in the photosystem II (PS II) fluorescence band). The Fv'/Fm', which is the efficiency of energy harvested by oxidized (open) PSII reaction centers in light, was calculated using Eq. 1,

$$\frac{Fv'}{Fm'} = \frac{Fm' - Fo'}{Fm'} \qquad \text{[Eq. 1]}$$

where Fo' is the minimum fluorescence of a light-adapted leaf that has momentarily been darkened, Fm' is the maximum fluorescence during a saturating light flash estimated by providing a saturating flash intensity of >6000 µmol m^{-2} s^{-1} and flash duration of 0.8 s and Fv' is the variable frequency (Surabhi et

al., 2008).

Relative Injury (RI)

The technique to determine RI used was similar to that developed by Martineau et al. (1979) with some minor modifications. Fully expanded leaves were collected from five replicates of all the genotypes at 65-75 DAS. Two sets (control and treatment) of 2.5 cm^2 leaf discs from approximately five randomly selected leaves were placed in the test tubes containing 10 mL of de-ionized water. The leaf segments were thoroughly rinsed thrice with de-ionized water to remove adhering electrolytes and those released from the cut surface of the segments. After final rinsing, the treatment set of tubes were drained, capped with aluminum foil to prevent dehydration of tissue during heat treatment. In contrast, the control set of tubes was kept at 25° C.

After incubation, treatment sets of tubes were brought to 25° C, and then both sets of tubes were incubated at 10° C for 18 h. After they were brought to 25° C, conductance was measured in control (CEC1) and treatment (TEC1) set of tubes. Tubes were then placed in an autoclave at 0.1MPa for 12 min to kill the tissue completely, releasing all the electrolytes. The tubes were then cooled to 25° C, and final conductance was measured in both control (CEC2) and treatment (TEC2) test tubes. The RI to the tissues was measured following with Eq. 2 Martineau et al. (1979):

$$RI\ (\%) = 1 - \{[1-(TEC1/TEC2)/(1-CEC1/CEC2)]x100\} \quad [Eq.\ 2]$$

Canopy Temperature Depression (CTD)

The CTD measurements were made during the mid-flowering period (65-75 DAS), where leaf temperature and the respective air temperature of fully expanded leaves from each replicate of each cultivar were measured between 1200 and 1300 h (on cloudless, bright days) using a handheld infrared thermometer (Model OMEGASCOPE; OMEGA Engineering, OS533E-Inc., Stamford, CT). Canopy temperature depression was estimated using Eq. 3 as follows:

$$CTD = Ta - Tc \quad [Eq.\ 3]$$

where Ta and Tc refer to air and canopy temperature of the target leaf, respectively.

Leaf Pigment Estimation

For pigment extraction, leaf samples were collected at 65-75 DAS from five replicates of each cultivar. Five leaf discs (2.0 cm^2) from each sample were placed in vials containing 5 mL of dimethyl sulphoxide (DMSO). To permit the complete extraction of pigments, the sample vials were incubated at room temperature in the dark for 24 h. After incubation, the absorbance of the extract was measured at 470, 648, and 663 nm using a Bio-Rad ultraviolet/VIS spectrophotometer (Bio-Rad Laboratories, Hercules, CA) to calculate the concentrations of carotenoid content, chlorophyll a and chlorophyll b (Chapple et al., 1992). From these values, total chlorophyll content was calculated and expressed on a leaf area basis (µg cm^{-2}).

Vigor Response Index

The individual vigor index (I) for each cultivar was calculated by dividing the value of each variety (Vi) by the maximum value (Vx) among the genotypes for a particular parameter (Eq. 4).

$$I = Vi/Vx \quad [Eq.\ 4]$$

The cumulative vigor response indices were then estimated as the sum of all the parameters for each cultivar at two different stages of growth; early seedling (26 DAS) and mid-grain filling stage (95 DAS) (Eq. 5).

$$CVRI\ (1) = (PHi/PHx) + (TNi/TNx) + (LNi/LNx) + (TLi/TLx) + (LAi/LAx) + (LWi/LWx) + (SWi/SWx) + (RWi/RWx) + (SHWi/SHWx) + (RSi/RSx) + (TWi/TWx) + (RLi/RLx) + (RSAi/RSAx) + (ADi/ADx) + (RVi/RVx) + (Ti/Tx) + (RLi/RLx) + (RNi/RNx) + (Pni/Pnx) + (Tri/Trx) + (RIi/RIx) + (TChi/TChx) + (Fv'/Fm'i/ Fv'/Fm'x) + (CTi/CTx) \quad [Eq.\ 5]$$

The cumulative vigor response indices and standard deviation were used to classify genotypes into different groups; very low, low, moderate, and very high at both stages of crop growth. The total vigor response index (TVRI) was determined as the sum of all cumulative vigor response indices from each experiment (Eq. 6).

CVRI (1) + CVRI (2) = TVRI [Eq. 6]

Statistical Analysis

Standard statistical protocols, ANOVA using the general linear model "PROC GLM" procedure in SAS software (Cary, NC), were employed to test the significance of differences among the genotypes for the growth and developmental parameters. Regression analysis was used to identify the relationships between the combined vigor response index and major growth and developmental traits. Sigma Plot 13 (Systat Inc., Santa Clara, CA) was used to plot the box-plots and relationships. Principal component analysis (PCA) is a statistical technique for multivariate data analysis and is useful in separating experimental units into subgroups. PCA was performed using the means of all the measured parameters in all genotypes at 26 and 95 DAS to understand the variations among the genotypes and to detect the contribution of each of the traits.

RESULTS AND DISCUSSION

Developing a reliable and effective screening tool is one of the essential strategies for recognizing cultivar superiority for enhanced field performance. In the present experiment, parameters related to the morphology, physiology, and vigor index of 36 rice genotypes, including inbred and hybrid cultivars, were measured and compared. Overall, rice inbred breeding lines and inbred and hybrid varieties differed for morphological and physiological parameters as well as various vigor response indices.

Genetic variation among genotypes for vigor related traits in seedlings including plant height, tiller number, canopy ground cover, and early crop biomass can be selected for breeding gain, and quantified in existing genotypes to aid farmers in deciding what cultivars to plant (Caton et al., 2003; Zhao et al., 2006c; Deseo, 2012; Lone et al., 2019). Indicators of early vigor including shoot length, shoot biomass, leaf area, the number of roots, root biomass, and growth rates measured in a screening experiment by Cairns et al. (2009) showed phenotypic correlations that could be used to define early vigor. In another study conducted by Saito et al. (2010), genotypes with high mean values for the morphological or growth parameters also possessed desirable vigor status for best survival and competition.

Morpho-physiological Parameters

Root system architecture plays a vital role in plant growth, development, and ultimately crop yield. Plant roots optimize their architecture to acquire water and essential nutrients. The number of root tips, number of forks, and the number of crossings play essential roles in root architecture because they have the potential to enhance penetration through soil layers, increasing plant nutrient uptake. Rice is a model cereal plant that possesses a fibrous root system with crown roots that emerge post-embryonically from the stem nodes. Early emergence of a vigorous crop stand provides better root anchorage and improves nutrient absorptive capacity (Farooq et al., 2011).

The mean values of each root parameter among 36 rice genotypes are shown in Additional file: Table S1. Root parameters such as root tips (RT), root forks (RF), and root crossings (RC) were significantly different among all the genotypes with hybrids showing the maximum values for all root traits (Table 1; Fig. 1a, b, c). Major root growth parameters, including root length (RL), root surface area (RSA), and root volume (RV) were significantly different among the 36 rice genotypes at 26 DAS whereas there were no significant variations observed in root average diameter (Fig. 2a, b, c; Fig. 3a, b). The root number (RN) ranged from 27 plant^{-1} to 45.2 plant^{-1} among all the 36 genotypes, with an overall mean of 38.94 plant^{-1}. Root length among the genotypes ranged from 3274 cm plant^{-1} to 7155 cm plant^{-1} with an overall average of 5079 cm plant^{-1}. The highest values were recorded by the released inbred variety THAD whereas the least value was recorded with the inbred released variety CL 142-AR as compared to the rest of the genotypes (Fig. 2b). Root surface area ranged from 323 cm^2 plant^{-1} (CL 142-AR) to 742 cm^2 plant^{-1} (THAD) with an overall mean of 552 cm^2 plant^{-1}. CL 163, an inbred released variety, showed 58% more root volume in comparison to CL 151, another inbred released variety with minimum root volume.

Table 1. Mean and LSD values of root growth and developmental traits; root/shoot ratio (RS), root length (RL, cm plant^{-1}), root surface area (RSA, cm^2 plant^{-1}), average root diameter (RAD, mm plant^{-1}), root volume (RV, cm^3 plant^{-1}), root tips (RT, no. plant^{-1}), root forks (RF, no. plant^{-1}), root crossing (RC, no. plant^{-1}), and root number (RN, no. plant^{-1}), and shoot growth traits; plant height (PH, cm plant^{-1}), leaf number of the main tiller (LN, no. tiller^{-1}), tiller number (TN, no. plant^{-1}), total leaves (TL, no. plant^{-1}), leaf area (LA, cm^2 plant^{-1}), and dry weight traits; leaf dry weight (LW, g plant^{-1}), stem dry weight (SW, g plant^{-1}), root dry weight (RW, g plant^{-1}), aboveground dry weight (SHW, g plant^{-1}), and total dry weight (TW, g plant^{-1}) for 36 rice genotypes measured during the seedling stage, 26 days after sowing.

Genotypes	Root growth and developmental traits									Shoot growth and dry weight traits									
	RS	**RL**	**RSA**	**RAD**	**RV**	**RT**	**RF**	**RC**	**RN**	**PH**	**LN**	**TN**	**TL**	**LA**	**LW**	**SW**	**RW**	**SHW**	**TW**
Mean	0.33	4978.67	533.82	0.33	4.46	30412.06	56297.12	6866.78	38.16	11.80	2.98	7.44	29.70	100.98	0.76	0.64	0.45	1.40	1.86
LSD of cultivars	N.S.	1492***	193***	0.03***	1.52***	9536*	20446***	25225***	7.50***	1.81***	N.S.	2.29***	9.81**	42.9**	0.31*	0.34*	0.19***	0.63*	0.78**
Mean	0.29	5151.22	587.72	0.34	4.92	33466	66824.2	8062.4	39.40	11.56	3.40	8.20	32.33	115.96	0.87	0.81	0.46	1.69	2.15
LSD of hybrids	N.S.	N.S.	N.S.	N.S.	N.S.	N.S.	N.S.	N.S.	9.6*	N.S.	N.S.	3.68*	9.89**	N.S.	0.35*	N.S.	N.S.	0.80*	0.97*
Mean	0.34	5086.77	533.23	0.35	4.67	28943.48	56204.56	6584.55	39.25	11.84	3.03	7.32	29.03	102.95	0.74	0.61	0.44	1.34	1.80
LSD of breeding lines	0.07*	N.S.	N.S.	0.03*	N.S.	N.S.	N.S.	N.S.	5.9*	1.2**	N.S.	2.6**	8.9***	38.1***	0.27**	0.29**	0.16*	0.55**	0.69**
Grand Mean	**0.32**	**5079**	**552**	**0.34**	**4.69**	**31018**	**59859**	**7164**	**38.94**	**11.73**	**3.13**	**7.65**	**30.35**	**106.63**	**0.79**	**0.69**	**0.45**	**1.48**	**1.94**
LSD	**0.10****	**1604****	**195*****	**0.03*****	**1.75*****	**9115****	**20730*****	**2540*****	**7.21*****	**1.82*****	**N.S.**	**2.58*****	**9.28*****	**4.96*****	**0.30*****	**0.33****	**0.19*****	**6.187***	**0.768*****

*** Significant at P < 0.001, ** Significant at P <0.01, * Significant at P <0.05, and N.S = not significant.

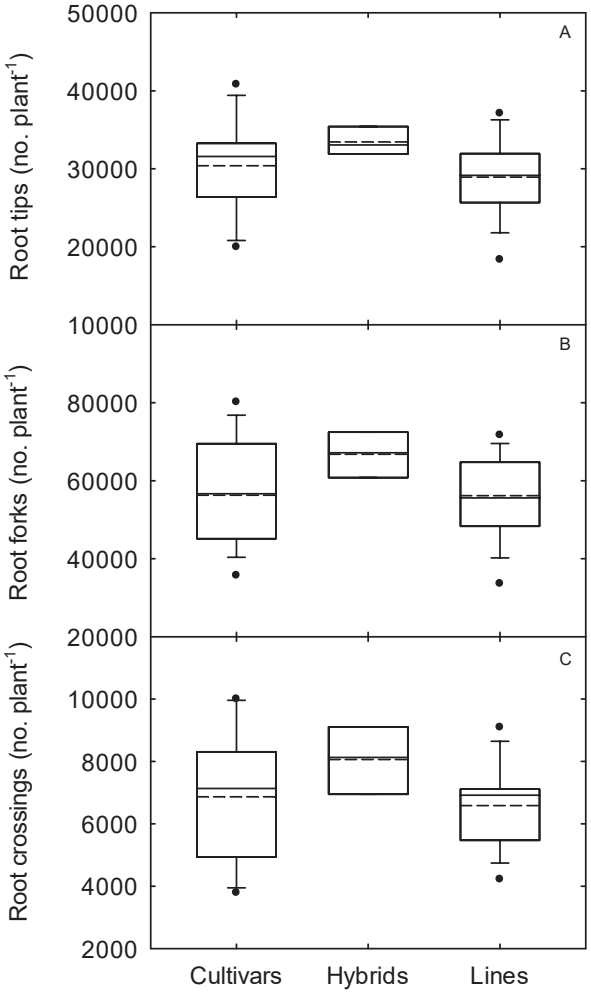

Figure 1. Box and whisker plots for the root growth traits showing variations among 36 rice genotypes in (a) root tips, no. plant^{-1}; (b) root forks, no. plant^{-1}; and (c) root crossings, no. plant^{-1}; at 26 DAS. The middle line indicates the median, the box indicates the range of the 25th to 75th percentiles of the total data. The whiskers indicate the interquartile range, and the outer dots are outliers.

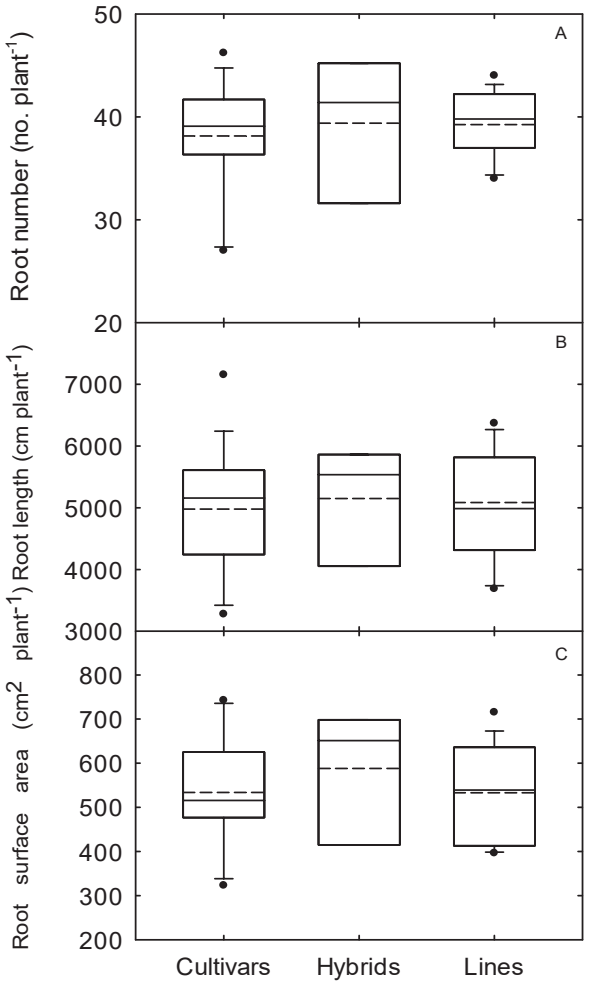

Figure 2. Box and whisker plots for the root growth traits showing variations among 36 rice genotypes in (a) root number, no. plant^{-1}; (b) root length, cm plant^{-1}; and (c) root surface area, cm^2 plant^{-1}; at 26 DAS. The middle line indicates the median, the box indicates the range of the 25th to 75th percentiles of the total data. The whiskers indicate the interquartile range, and the outer dots are outliers.

Root growth and development parameters like root length, root volume, root surface area, and root thickness are useful in determining the root hydraulic conductance that can potentially enhance water uptake by rice under drought conditions (Henry et al., 2012; Singh et al., 2017b; Kakar et al., 2019). Root length is associated with the ability of the crop to provide greater area for nutrient absorption that is needed for rapid shoot growth, indicating that it is another vital trait that can define early vigor (Redoña and Mackill, 1996). In the present study, rice genotypes with higher values for RL, RV, and RSA could be desirable and might show higher potential productivity under water-limited growth conditions. Regan et al. (1992) identified shoot growth traits such as plant height and dry weight as useful indicators of

seedling and early vigor. All shoot parameters recorded at the seedling growth stage (26 DAS), except leaf number of the main tiller (LN), showed significant variation among the 36 rice genotypes (Additional file: Table S2; Fig. 4a, b, c, d). Plant height ranged from 10.04 cm plant^{-1} to 14.56 cm plant^{-1} with an overall average of 11.73 cm plant^{-1} at 26 DAS. The highest values of tiller number (TN) and total leaves (TL) were recorded in THAD, whereas the lowest values were recorded in RU1304100 (an inbred breeding line) at 26 DAS. Leaf area (LA) at 26 DAS ranged from 61.54 cm^2 plant^{-1} (SABINE) to 169.51 cm^2 plant^{-1} (RU1201102) among all the 36 genotypes with an overall mean of 106.63 cm^2 plant^{-1}

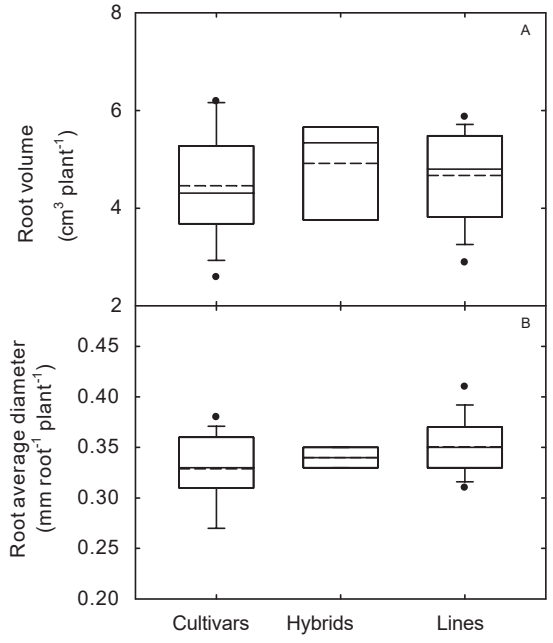

Figure 3. Box and whisker plots for the root growth traits showing variations among 36 rice genotypes in (a) root volume, cm^3 plant^{-1}, and (b) root average diameter, mm plant^{-1}; at 26 DAS. The middle line indicates the median, and the box shows the range of the 25th to 75th percentiles of the total data. The whiskers indicate the interquartile range, and the outer dots are outliers.

All the dry weight traits at the seedling stage (26 DAS) varied significantly among all 36 rice genotypes (Table 1; Fig. 5a, b, c). The leaf dry weight (LW) at 26 DAS ranged from 0.49 g plant^{-1} to 1.18 g plant^{-1}. The highest and lowest values for stem dry weight (SW) were 1.17 g plant^{-1} (THAD) and 0.33 g plant^{-1} (RU1304156), respectively, with an overall average of 0.69 g plant^{-1}at 26 DAS. Root dry weight (RW) varied significantly at 26 DAS, ranging from 0.23 g plant^{-1} to 0.78 g plant^{-1}. THAD showed 62% more aboveground dry weight (SHW) and 65% total dry weight (TDW) in comparison to inbred line RU1304156 (with least values of SHW and TDW) at 26 DAS. Maximum values for TN, TL, SW, RW, and SHW, were recorded in THAD at 26 DAS. However, the minimum values for TN, TL, LW, and SHW were recorded in RU1304100, and for SW and TDW were recorded in RU1304156 at 26 DAS. Root: shoot ratio (RS) measured at the seedling stage as well as mid-grain filling stage did not show any significant genotypic differences (Fig. 6 a, b). The mean value of all the breeding lines was highest at 26 DAS, whereas 95 DAS hybrids showed the maximum mean value for root: shoot ratio (Tables 1, 3, S2 and S4).

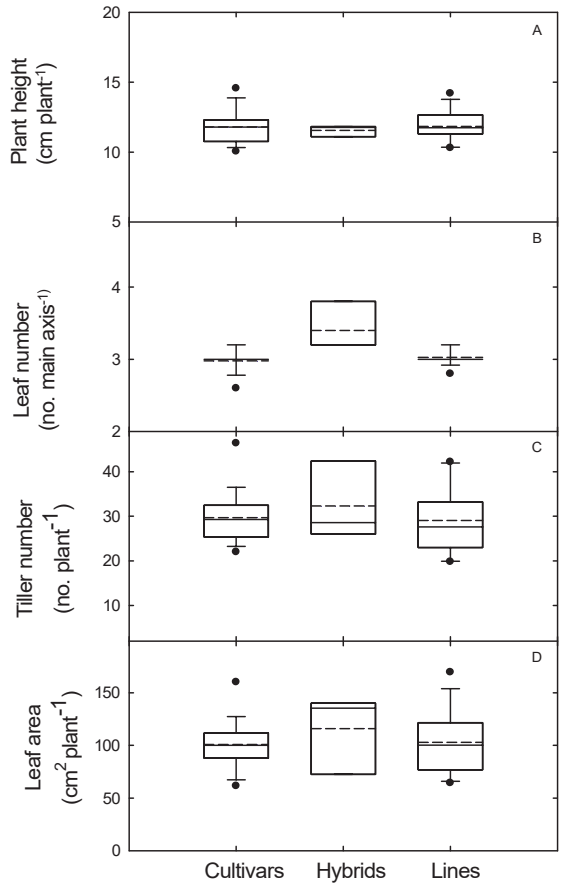

Figure 4. Box and whisker plots for the shoot growth and developmental traits showing variations among 36 rice genotypes in (a) plant height, cm plant^{-1}; (b) leaf number, no. main axis^{-1}; (c) tiller number, no. plant^{-1}; and (d) leaf area, cm^2 plant^{-1}; at 26 DAS. The middle line indicates the median, the box indicates the range of the 25th to 75th percentiles of the total data. The whiskers indicate the interquartile range, and the outer dots are outliers.

Table 2. Mean and LSD values of photosynthesis characteristics; photosynthesis (Pn, µmol CO_2 m^{-2} s^{-1}), transpiration (Tr, mol H_2O m^{-2} s^{-1}), water use efficiency (WUE, mmol CO2 mol^{-1} H_2O), stomatal conductance (g_s, mmol m^{-2} s^{-1}), and fluorescence (Fv'/Fm'); relative injury (RI, %), and canopy-air temperature differential (CTD, °C); pigment characteristics chlorophyll a (Chl a, µg cm_{-2}), chlorophyll b (Chl b, µg cm_{-2}), carotenoids (Caro, µg cm_{-2}), total chlorophyll (TCh, µg cm_{-2}) for 36 rice genotypes measured at flowering stage, 65-75 days after sowing.

Genotypes	Photosynthesis characteristics					Relative injury, canopy-air temperature, and pigment characterstics					
	Pn	Tr	WUE	g_s	Fv'/Fm'	RI	CTD	Chl a	Chl b	Caro	TCh
Mean	23.19	9.02	2.61	0.45	0.56	38.01	-1.43	25.83	13.24	7.21	39.07
LSD of cultivars	N.S.	N.S.	0.4**	N.S.	N.S.	N.S.	N.S.	5.2***	4.4***	2.67**	9.6**
Mean	24.39	8.91	2.76	0.41	0.59	36.05	-1.70	25.26	12.21	6.37	37.47
LSD of hybrids	2.5*	N.S.	0.20*	N.S.	N.S.	N.S.	N.S.	N.S.	3.0*	N.S.	7.0*
Mean	22.37	8.89	2.51	0.46	0.57	33.78	-1.62	25.42	13.11	6.94	38.53
LSD of breeding lines	N.S.	N.S.	N.S	N.S.	0.13*	16.9*	1.12***	5.8*	5.0*	2.4*	10.7*
Grand Mean	**23.32**	**8.94**	**2.62**	**0.44**	**0.57**	**35.95**	**-1.59**	**25.51**	**12.85**	**6.84**	**38.36**
LSD	**4.8***	**1.99***	**0.41***	**N.S.**	**0.13***	**20.42***	**1.33****	**5.34****	**4.62****	**2.49****	**9.87****

*** Significant at P < 0.001, ** Significant at P <0.01, * Significant at P <0.05, and N.S = not significant.

Table 3. Mean and LSD values of shoot growth and developmental traits, and dry weight traits for cultivars, hybrids and breeding lines at mid-grain filling stage (95 DAS), plant height (PH, cm $plant^{-1}$), leaf number of the main tiller (LN, no. $tiller^{-1}$), tiller number (TN, no. $plant^{-1}$), total leaves (TL, no. $plant^{-1}$), leaf area (LA, cm^2 $plant^{-1}$), and combined dry weight, leaf dry weight (LW, g $plant^{-1}$), stem dry weight (SW, g $plant^{-1}$), root dry weight (RW, g $plant^{-1}$), aboveground dry weight (SHW, g $plant^{-1}$), and total dry weight (TW, g $plant^{-1}$) of 36 rice genotypes measured during the seedling stage, 26 days after sowing.

Genotypes	Shoot growth traits				Panicle initiation and panicle number		Dry weigh traits					
	PH	LN	TN	LA	PI	TP	LW	SW	RW	SHW	RS	TW
Mean	58.52	5.60	29.00	4808	72.51	23.04	25.30	62.59	24.15	87.89	0.28	112.03
LSD of cultivars	2.7*	N.S.	N.S.	1418*	N.S.	N.S.	5.89**	14.2*	5.6*	19.5*	N.S.	21.9*
Mean	59.03	5.57	37.75	5427	73.69	27.84	23.92	68.95	26.83	92.87	0.29	119.70
LSD of hybrids	2.0*	N.S.	N.S.	N.S.	N.S.	N.S.	N.S.	N.S.	N.S.	N.S.	N.S.	N.S.
Mean	59.33	5.57	29.81	4780	73.39	22.53	26.51	61.39	22.56	87.90	0.26	110.46
LSD of breeding lines	3.9***	N.S.	7.9*	1349*	5.2*	6.8*	6.0*	13.8*	4.8*	19.4*	N.S.	20.8*
Grand Mean	**58.96**	**5.58**	**32.18**	**5005**	**73.20**	**24.47**	**25.24**	**64.31**	**24.51**	**89.55**	**0.28**	**114.06**
LSD	**3.71*****	**N.S.**	**8.21***	**1355***	**5.01***	**7.2***	**6.01*8**	**13.93**	**5.53***	**19.37***	**N.S.**	**21.19****

*** Significant at P < 0.001, ** Significant at P <0.01, * Significant at P <0.05, and N.S = not significant.

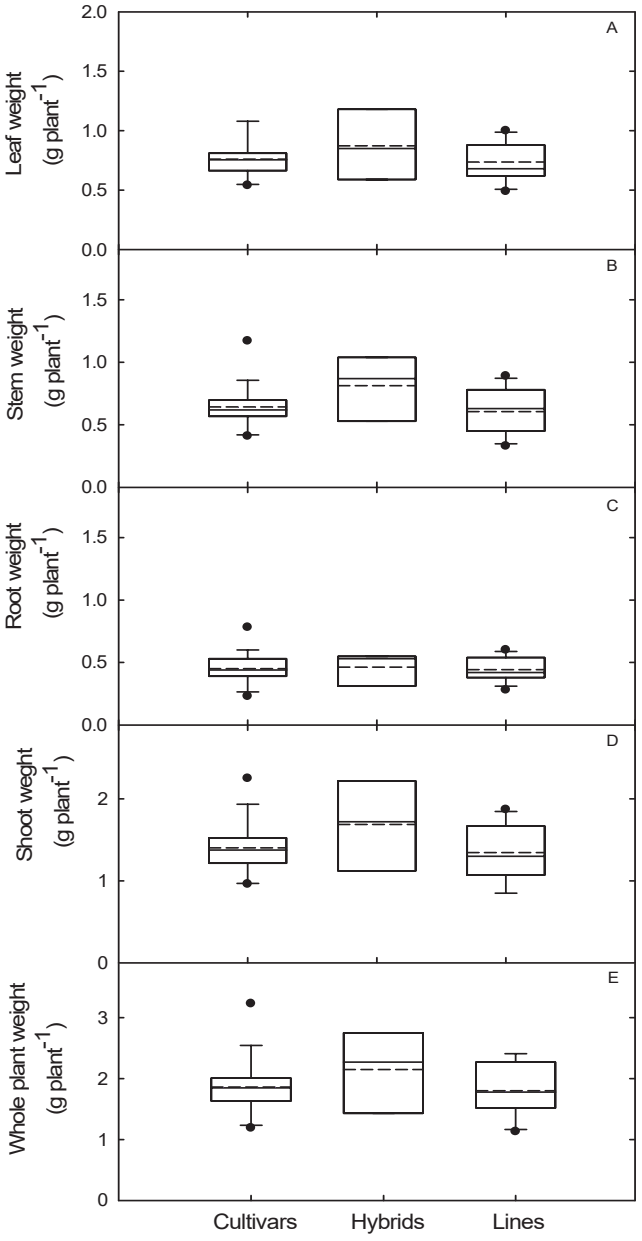

Figure 5. Box and whisker plots for the dry weight traits showing variations among 36 rice genotypes in (a) leaf weight, g plant^{-1}; and (b) stem weight, g plant^{-1}; (c) root weight, g plant^{-1}; (d) shoot weight, g plant^{-1}; and (e) whole plant weight, g plant^{-1}; at 26 DAS. The middle line indicates the median, and the box shows the range of the 25th to 75th percentiles of the total data. The whiskers indicate the interquartile range, and the outer dots are outliers.

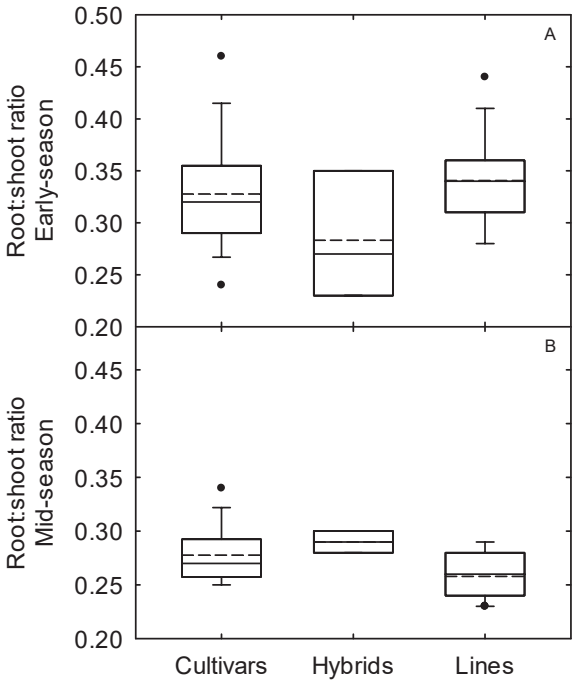

Figure 6. Box and whisker plots for the root: shoot ratio showing variations among 36 rice genotypes at (a) early-season (26 DAS); and (b) mid-season (95 DAS). The middle line indicates the median, and the box shows the range of the 25th to 75th percentiles of the total data. The whiskers indicate the interquartile range, and the outer dots are outliers.

The use of ecophysiologically based remote-sensing/infrared techniques such as CTD, vapor pressure deficit (VPD), chlorophyll fluorescence, and pigment characterization parameters including chlorophyll a and b content and chlorophyll a:b ratio is gaining popularity to screen efficiently and quickly with reliability. The association between CTD and leaf conductance with each other and with yield extends the possibility of coupled selection for both traits (Singh et al., 2007). None of the photosynthetic characteristics, except the transpiration rate (Tr), showed significant differences among 36 genotypes (Table 2 and Table S3). The transpiration rate ranged from 7.83 mol H_2O m^{-2} s^{-1} (MERMENTAU) to 10.03 mol H_2O m^{-2} s^{-1} (RU1204194) with an overall average of 8.94 mol H_2O m^{-2} s^{-1} during the flowering stage (65-75 DAS) (Fig. 7c). The difference between air and foliage temperatures, designated as canopy temperature depression (CTD), a

measure of a plant's ability to lower canopy temperature through transpiration cooling, varied significantly among the 36 genotypes. The maximum and minimum CTD (°C) of 1.20 °C and -3.17 °C were recorded in the inbred released varieties BOWMAN and CLIZMN, respectively (Fig. 8c). The values for total chlorophyll (TCh) also differed significantly among the 36 rice genotypes. The lowest TCh value was recorded for RU1204114 (30.03 µg cm^{-2}), while THAD (52.19 µg cm^{-2}) exhibited the highest value with an overall mean of 38.36 µg cm^{-2} (Fig. 9c).

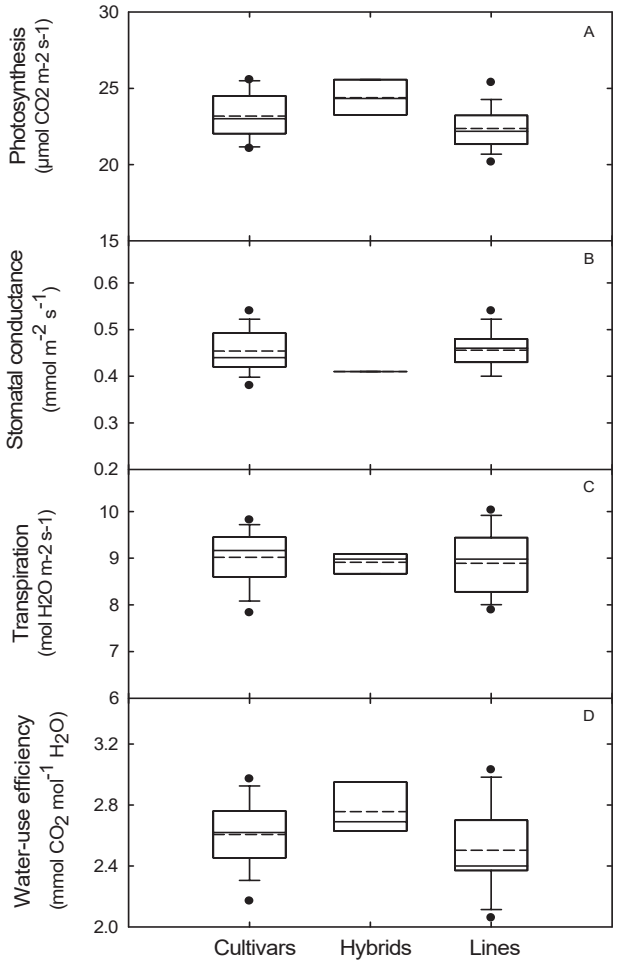

Figure 7. Box and whisker plots for the physiological traits showing variations among 36 rice genotypes in (a) photosynthesis, µmol CO_2 m^{-2} s^{-1}; and (b) stomatal conductance, mmol m^{-2} s^{-1}; (c) transpiration, mol H_2O m^{-2} s^{-1}; and (d) water-use efficiency, mmol CO_2 mol^{-1} H_2O; at 65-75 DAS. The middle line indicates the median, the box shows the range of the 25th to 75th percentiles of the total data. The whiskers indicate the interquartile range, and the outer dots are outliers.

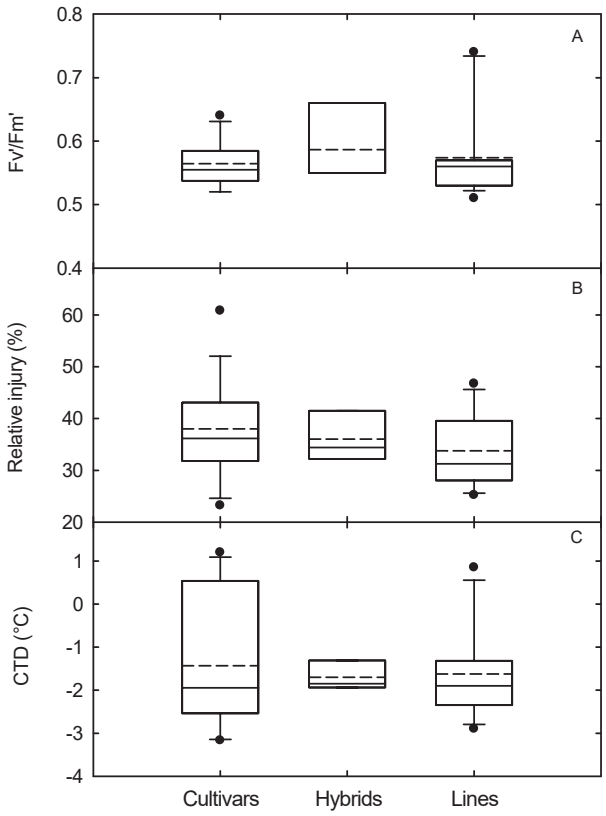

Figure 8. Box and whisker plots for the physiological traits showing variations among 36 rice genotypes in (a) fluorescence; and (b) relative injury, %; and (c) canopy-air temperature differential, °C; at 65-75 DAS. The middle line indicates the median, and the box shows the range of the 25th to 75th percentiles of the total data. The whiskers indicate the interquartile range, and the outer dots are outliers.

At mid-grain filling stage (95 DAS), except for leaf number (LN) and root dry weight (RW), all shoot growth and dry weight traits varied significantly among the 36 rice genotypes. The mean value for all hybrids for most of the shoot and dry weight parameters was higher than the inbred cultivars and breeding lines (Table 3). The highest number of panicles (TP) was recorded in the hybrid CLXL729 (29.58 $plant^{-1}$) and lowest in inbred breeding line RU1204156 (18.96 $plant^{-1}$). There were no significant genotypic differences in days to panicle initiation at 95 DAS (Fig. 10a, b). Among the 36 rice genotypes, maximum values for LA, SW, SHW, and TW were recorded in LAKAST whereas the least values for LW, SHW, and TW were recorded in SABINE (Additional file: Table S4; Fig. 11a, b, c, d; Fig. 12a, b, c, d, e).

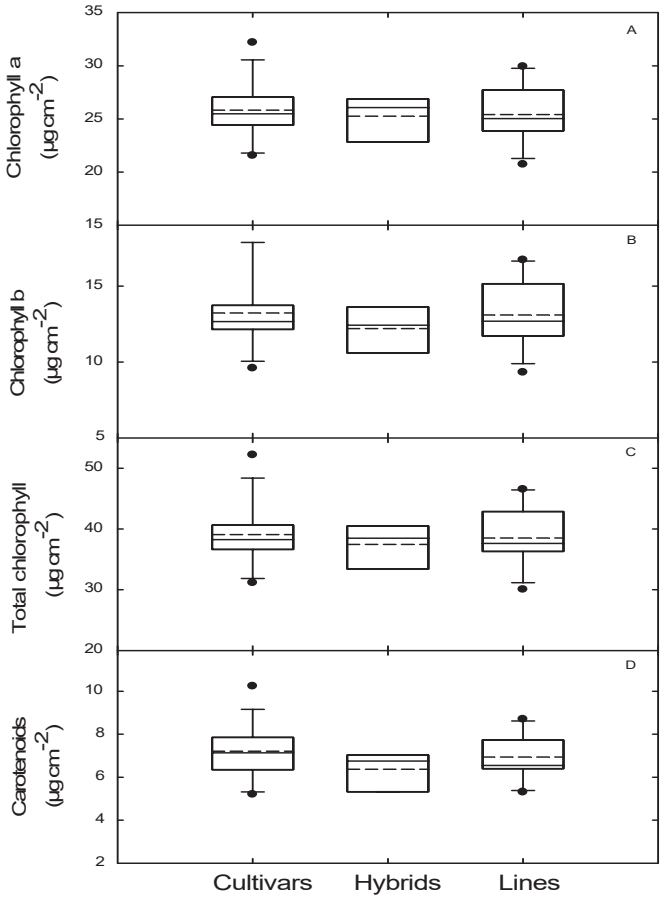

Figure 9. Box and whisker plots for the pigment characteristics showing variations among 36 rice genotypes in (a) chlorophyll a, µg cm^{-2}; and (b) chlorophyll b, µg cm^{-2}; (c) total chlorophyll, µg cm^{-2}; and (d) carotenoids, µg cm^{-2}; at 65-75 DAS. The middle line indicates the median, the box indicates the range of the 25th to 75th percentiles of the total data. The whiskers indicate the interquartile range and the outer dots are outliers.

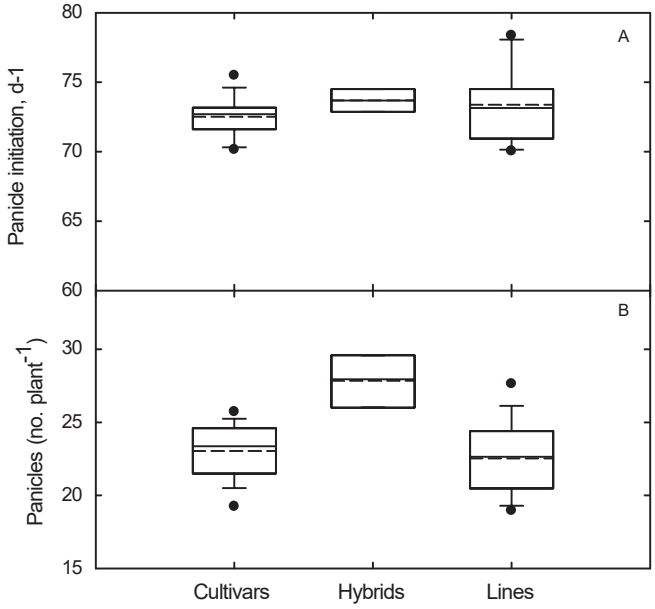

Figure 10. Box and whisker plots for (a) panicle initiation, d^{-1}; and (b) panicle number, no. plant-1, showing variations among 36 rice genotypes at mid-grain filling stage (95 DAS). The middle line indicates the median, the box indicates the range of the 25th to 75th percentiles of the total data. The whiskers indicate the interquartile range and the outer dots are outliers.

Seedling vigor is the plant's ability to emerge rapidly from soil or water and establish itself before its competitors (Fukai and Cooper 1995; Bastiaans et al., 2011). Several parameters closely associated with seedling vigor were considered relevant in determining the crop's vigor. Rapid emergence is a key trait for successful crop establishment (Namuco et al., 2009). According to Bastiaans et al. (2011), the seedling dry weight could be used as a basis in defining early vigor. In association with seedling dry matter, leaf area of the plants during the vegetative stage plays an essential role in the accumulation of greater biomass. In rice, early vigor is mainly attributed to the high leaf area index (LAI) during the vegetative stage (Okami et al., 2011). The rate of early leaf area development (early vegetative vigor) is a determinant for resource colonization and yield competitiveness of the rice seedling (Zhao et al., 2006c) and yield potential (Dingkuhn et al., 1999). In this experiment, the inbred breeding line RU1201102 at the seedling stage and inbred released variety LAKAST at the mid-grain filling stage had the highest LA.

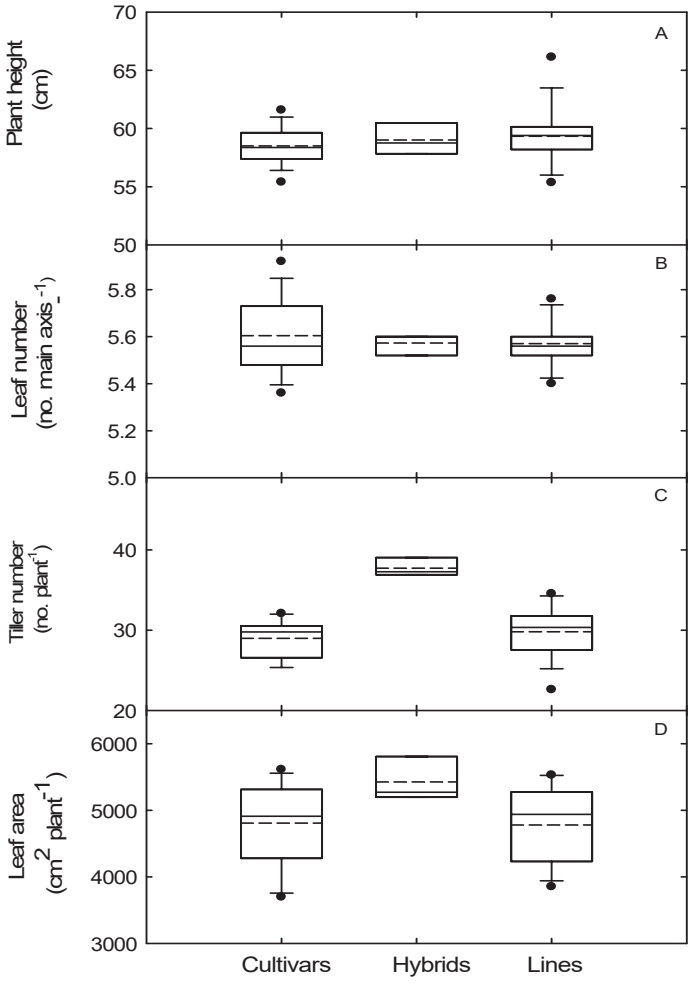

Figure 11. Box and whisker plots for the shoot growth traits showing variations among 36 rice genotypes in (a) plant height, cm plant^{-1}, and (b) leaf number, no. main axis^{-1}; (c) tiller number, no. plant^{-1}; and (d) leaf area, cm^2 plant^{-1}; at 95 DAS. The middle line indicates the median, the box indicates the range of the 25th to 75th percentiles of the total data. The whiskers indicate the interquartile range, and the outer dots are outliers.

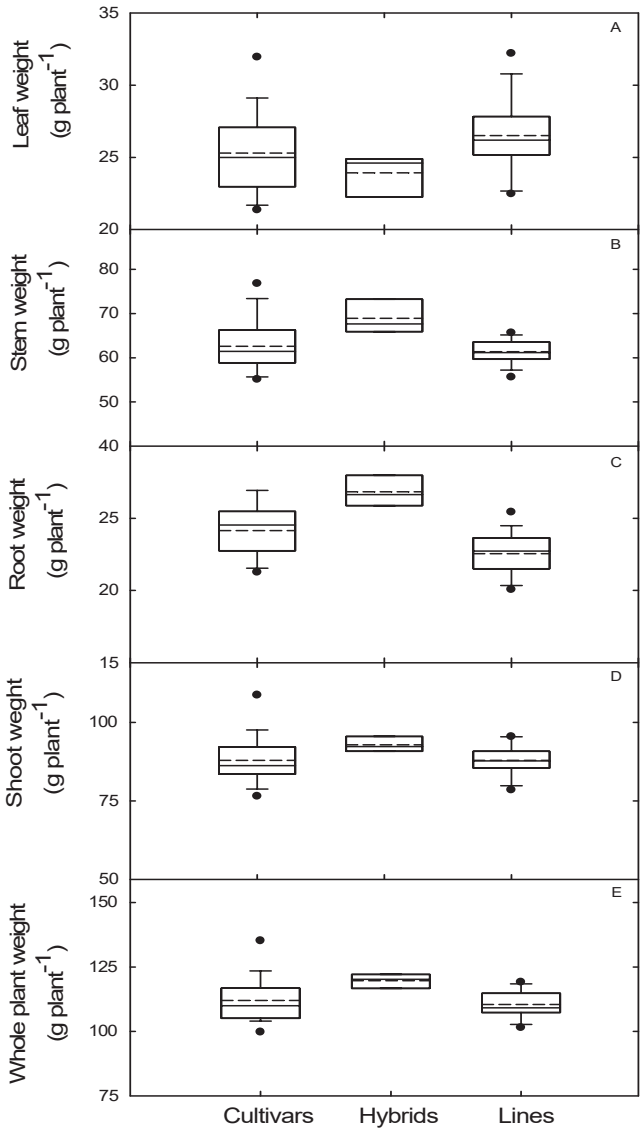

Figure 12. Box and whisker plots for dry weight traits showing variations among 36 rice genotypes in (a) leaf weight, g plant^{-1}; and (b) stem weight, g plant^{-1}; (c) root weight, g plant^{-1}; (d) shoot weight, g plant^{-1}; and (e) whole plant weight, g plant^{-1} at 95 DAS. The middle line indicates the median, and the box shows the range of the 25th to 75th percentiles of the total data. The whiskers indicate the interquartile range, and the outer dots are outliers.

Vigor Response Indices and Principal Component Analysis

Vigor indices provide information about the growth rate and uniform development of genotypes under varied environmental conditions (Powell and Matthews, 2005), which is crucial for the growth and development of the crop when competing for limited resources. Plants with high vigor usually compete successfully under limited environmental resources, influencing stand establishment and, ultimately, grain yield. The use of the combined vigor response index (CVRI) to examine the relationship between growth, physiological, and yield-related parameters is an additional tool for breeders to understand physiological changes during variety development, and could be a useful basis for selection in plant breeding.

Our study revealed that traits such as root number, average root diameter, and plant height contributed the maximum to combined vigor response at 26 DAS. In contrast, leaf number and panicle initiation contribute maximum at 95 DAS (Table 4). Fluorescence and pigment characterization traits were among the least contributing traits to the combined vigor response index at 95 DAS. This indicated that root traits are essential in screening genotypes for better performance, whereas physiological genotypes do not contribute much in seedling vigor.

In the present study, CVRI values for each rice genotype were calculated by summing individual vigor response indices for all root and shoot morphological features at 26 DAS and root, shoot, and physiological traits at 95 DAS as evaluated among the 36 rice genotypes (presented in Tables 5 and 6). The CVRI-based technique helped classify the genotypes into five vigor groups (very low, low, moderate, high and very high) during the seedling growth stage and into four vigor groups (low, moderately low, moderately high and high) at mid-grain filling stage (Tables 5 and 6). At 26 DAS, 3 genotypes were classified under the very low vigor index group, 6 genotypes were classified as having a low vigor index, 16 genotypes were classified as moderately vigorous, 8 genotypes as having a high vigor index and 3 genotypes as having a very high vigor index. The highest CVRI value (15.881) was recorded for THAD and least (9.888) for CL142-AR among all the genotypes at 26 DAS.

At mid-grain filling stage (95 DAS), 5 genotypes were classified as having a low vigor index, 10 genotypes had moderately low vigor, 14 genotypes were classified as having moderately high vigor, and 7 genotypes as highly vigorous. The highest CVRI value (18.692) was recorded for THAD and LAKAST, whereas the least (16.334) was recorded for CL152 at 95 DAS (Table 6). Rice genotypes with high CVRI values display excellent productivity and can be selected for sowing and future breeding purposes and, in the case of released varieties, used directly in commercial rice production.

In the present study, scanner-based image analysis was used to unravel the root architecture of rice genotypes. Fig. 13 represents the scanned root images for selected rice genotypes based on the cumulative vigor response index (CVRI) at 26 DAS. Rice genotypes with high CVRI values in this study had larger, more robust, and branched root systems with higher values for root parameters. In contrast, rice genotypes with lower CVRI values showed less organized root structures with low values for root parameters. Improving the root systems with deep roots and high-water uptake ability will improve future elite rice varieties suitable for water-limited and water use-efficient farming systems.

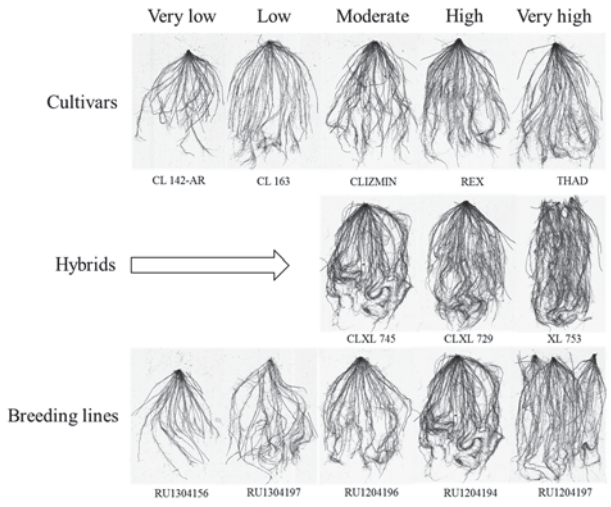

Figure 13. Representative scanned root images for selected rice genotypes based on cumulative vigor response index (CVRI), harvested at 26 days after planting.

A Principal component analysis (PCA) was used to elucidate relationships among rice genotypes using the shoot, root, and physiological traits. The genotypes were classified into four categories. Based on the PCA analysis, more than 68% of total variation among genotypes was explained by the first three PCs at 26 DAS as well as at 95 DAS (Fig. 14). BOWMAN and the hybrid CLXL 729, which were classified as highly vigorous, were grouped under the high tolerance category and CL142-AR, which had the lowest CVRI value, and CHENIERE, which was classified as having low vigor index, were grouped under low tolerance category at 26 DAS. CL152 and RU1204154, which were identified as low vigor

genotypes using the CVRI approach, were grouped under the low tolerance category and REX and the hybrid XL753, which had high CVRI values, were grouped under the high tolerance group at 95 DAS. CL142-AR, which was classified as having a moderately low vigor, was grouped under the high tolerance group at 95 DAS. This indicated that both methods generally gave similar results, and together, PCA and CVRI approaches allowed a clear identification of the high and low vigor rice genotypes.

Table 4. A contribution of sum of each root, shoot, and morpho-physiological vigor response indices to combined vigor response index of 36 rice genotypes measured during seedling and flowering stages, 26 and 95 days after sowing, respectively.

Traits	26 DAS		95 DAS	
	Sum of all traits of given cultivars	Contribution, %	Sum of all traits of given cultivars	Contribution, %
Plant height, cm plant^{-1}	29.17	6.21	32.07	5.01
Leaf, no. tillers^{-1}	28.79	6.12	33.98	5.31
Tillers, no. plant^{-1}	23.14	4.92	27.72	4.33
Total leaves, no. plant^{-1}	23.00	4.89	-	-
Leaf area, cm^2 plant^{-1}	20.45	4.35	30.05	4.69
Leaf dry weight, g plant^{-1}	23.26	4.95	28.72	4.49
Stem dry weight, g plant^{-1}	19.72	4.19	29.72	4.59
Root dry weight, g plant^{-1}	20.74	4.41	30.52	4.77
Aboveground dry weight, g plant^{-1}	22.45	4.78	29.25	4.57
Total dry weight, g plant^{-1}	20.77	4.42	29.83	4.66
Root/shoot ratio	25.87	5.50	29.03	4.53
Root length, cm plant^{-1}	26.32	5.60	-	-
Root surface area, cm^2 plant^{-1}	23.00	4.89	-	-
Root average diameter, mm plant^{-1}	29.73	6.32	-	-
Root volume, cm^3 plant^{-1}	26.58	5.65	-	-
Tips, no. plant^{-1}	26.81	5.70	-	-
Forks, no. plant^{-1}	25.52	5.43	-	-
Crossings, no. plant^{-1} Primary	24.64	5.24	-	-
roots number Panicle, no. plant^{-1}	30.17	6.42	-	-
Panicle initiation, d^{-1}	-	-	28.27	4.41
Net photosynthesis, µmol CO_2 m^{-2} s^{-1}	-	-	33.53	5.24
	-	-	32.31	5.05

Stomatal conductance, mmol m^{-2} s^{-1}	-	-	30.07	4.70
Transpiration, mol H_2O m^{-2} s^{-1}	-	-	32.16	5.02
Water use efficiency, mmol CO_2 mol^{-1} H_2O	-	-	30.62	4.78
Fluorescence	-	-	27.85	4.35
Relative injury, %	-	-	21.36	3.34
Chlorophyll a, µg cm^{-2}	-	-	28.65	4.47
Chlorophyll b, µg cm^{-2}	-	-	23.56	3.68
Carotenoids, µg cm^{-2}	-	-	24.71	3.86
Total chlorophyll, µg cm^{-2}	-	-	26.70	4.17
Combined vigor response index	470.11	100.00	640.33	100.00

Table 5. Classification of 36 rice genotypes based on combined vigor response indices for root and shoot morphological features during the seedling growth stage, 26 days after sowing.

Very low (9.888 - 11.155)	Low (11.156-12422)	Moderate (12.422-13.689)	High (13.690-14.957)	Very high (14.958-16.22)
CL142-AR (9.888)	CL 163 (11.625)	CLXL745 (12.433)	RU1304157 (13.700)	RU1204197 (15.299)
SABINE (10.849)	CHENIERE (11.682)	COCODRIE (12.533)	COLORADO (13.981)	XL753 (15.550)
RU1304156 (11.056)	RU1204156 (11.955)	RU1304122 (12.626)	RU1204122 (13.990)	THAD (15.881)
	RU1204154 (11.980)	CL111 (12.735)	REX (14.038)	
	MERMENTAU (12.182)	RU1304114 (12.747)	BOWMAN (14.130)	
	RU1304197 (12.241)	RU1304154 (12.787)	RU1201102 (14.160)	
		RU1304100 (12.837)	CLXL729 (14.191)	
		RU1204114 (12.924)	RU1204194 (14.420)	
		CL151 (12.967)		
		ANTONIO (12.972)		
		NIPONBARE (13.014)		
		LAKAST (13.130)		
		RU1204196 (13.329)		
		ROYJ (13.354)		
		CL152 (13.357)		
		CLIZMN (13.548)		

Table 6. Classification of 36 rice genotypes based on combined vigor response indices of growth developmental and physiological traits measured at mid grain filling stage, 95 days after sowing.

Low (16.334-17.004)	Moderately low (17.005-17.674)	Moderately high (17.675-18.334)	High (18.335-19.015)
CL152 (16.334)	CL151 (17.150)	RU1304197 (17.738)	RU1204197 (18.370)
RU1204114 (16.484)	CHENIERE (17.303)	ANTONIO (17.823)	CLXL745 (18.505)
RU1204156 (16.565)	COCODRIE (17.340)	MERMENTAU (17.825)	CLIZMN (18.526)
SABINE (16.671)	RU1304156 (17.410)	NIPONBARE (17.825)	RU1304122 (18.528)
RU1204154 (16.949)	RU1304157 (17.410)	RU1304100 (17.947)	XL753 (18.793)
	RU1204194 (17.468)	CL111 (17.977)	LAKAST (18.962)
	RU1204196 (17.479)	RU1201102 (18.007)	THAD (18.962)
	RU1304114 (17.523)	ROYJ (18.019)	
	CL142-AR (17.541)	CLXL729 (18.089)	
	RU1304154 (17.547)	REX (18.198)	
		CL 163 (18.206)	
		COLORADO (18.256)	
		RU1204122 (18.256)	
		BOWMAN (18.258)	

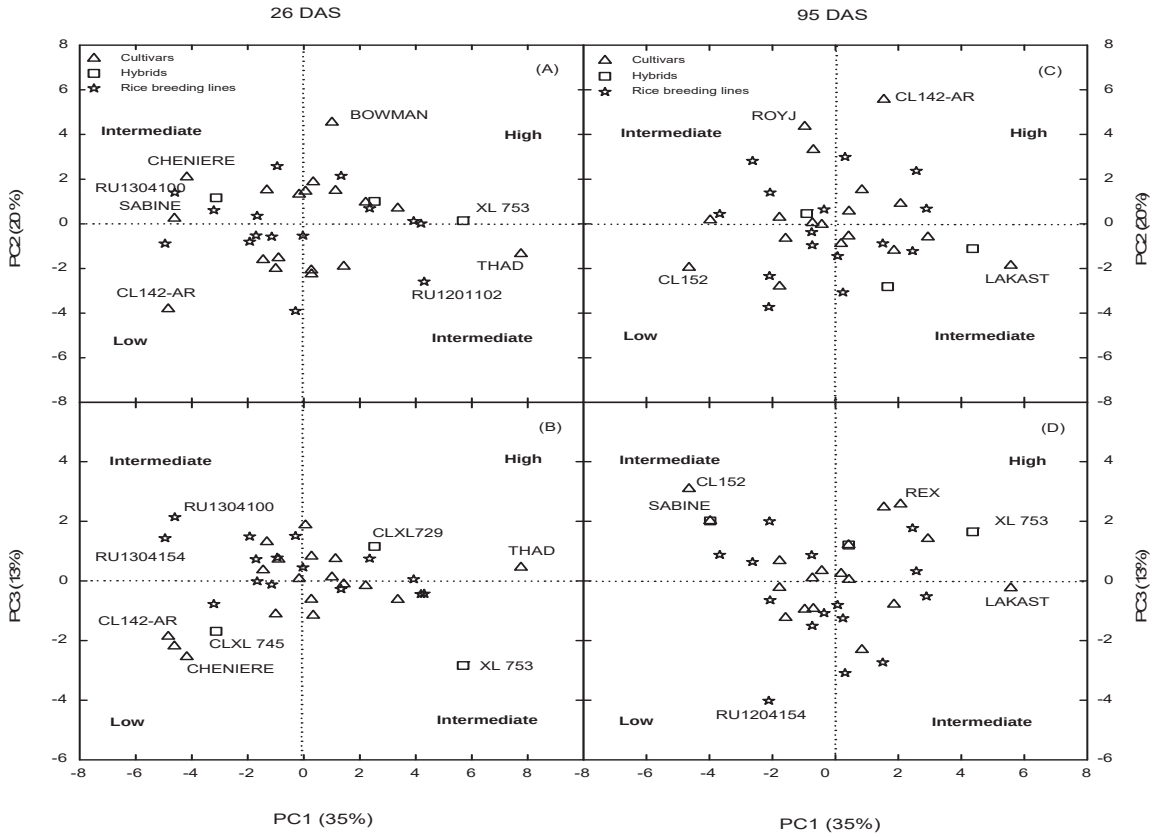

Figure 14. Principal component analysis for the first three principal component (PC) scores, PC1, PC2, and PC3 related to the classification of 36 rice genotypes for seedling and mid-grain filling stages, at 26 and 95 days after sowing, respectively. Cultivars that ranked high or low scores in each tolerance category are identified in the figure.

The correlation coefficient between the combined vigor response index and root vigor indices ($r^2 = 0.71$) and the correlation coefficient between the combined vigor response index and shoot vigor indices ($r^2 = 0.69$) were similar at 26 DAS (Fig. 15). This suggests that either root or shoot parameters might be sufficient in evaluating early vigor, and selection based on either may be enough for classification. Because it is much easier to measure shoot traits, this would be the more efficient choice. The correlation coefficient between the total vigor response index and early-season vigor response index ($r^2 = 0.88$) was much higher in comparison to the correlation coefficient between the total vigor response index and mid-season vigor response index ($r^2 = 0.58$) at 26 DAS and 95 DAS (Fig. 16). This suggests that the early-season traits are more important in the evaluation and classification of early vigor genotypes. The correlation coefficient between the combined vigor response index and physiology vigor response index ($r^2 = 0.74$) was higher in comparison to the correlation coefficient between combined vigor response index and morphology vigor response index ($r^2 = 0.45$) at 95 DAS (Fig. 17). This indicates no significant relationship between morphological traits and the combined vigor response index during the mid-grain filling stage (95 DAS). This further implies the greater importance of physiological parameters in identifying high vigor rice genotypes using these indices during mid-grain filling stages.

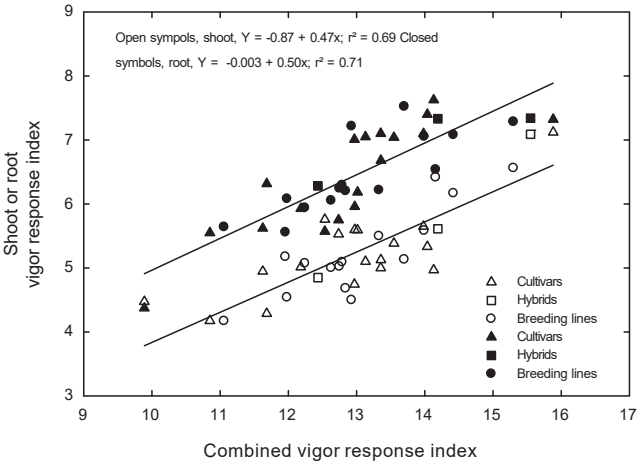

Figure 15. The relationship between combined vigor response index and shoot or root vigor response indices of 36 rice genotypes measured during seedling stage, 26 days after sowing.

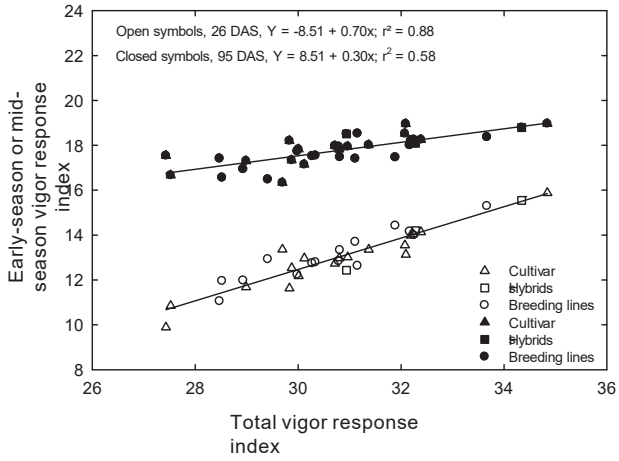

Figure 16. The relationship between total vigor response index and early-season or mid-season vigor response indices of 36 rice genotypes measured during seedling and mid-grain filling stages, at 26 and 95 days after sowing, respectively.

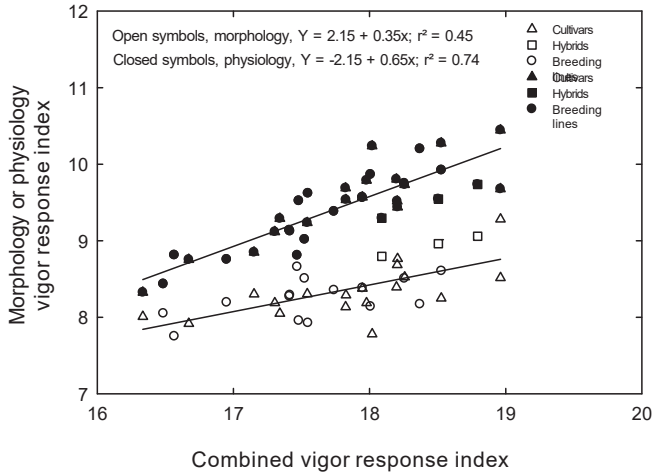

Figure 17. The relationship between combined vigor esponse index and morphological and physiological vigor response indices of 36 rice genotypes measured during the mid-grain filling stage, 95 days after sowing.

CONCLUSIONS

The pot culture screening is a simple and efficient technique for screening rice genotypes with high precision. Traits such as root length, root surface area, leaf area, plant height, tiller numbers, leaf weight, stem weight, root weight, aboveground weight, and

total weight displayed significant genetic variability during the seedling stage and mid-grain filling stage. Genotypes with deep, well developed, and extensive root systems cope well under stressful conditions by maintaining efficient water and nutrient supply and storing them for a more extended period for plant survival in comparison to genotypes with the poorly developed and less vigorous root system. The inbred variety THAD, hybrid XL753, and inbred breeding line RU1204197, with the highest values for the vigor indices, were the best among the 36 genotypes tested at early-season (26 DAS) and mid-grain filling (95 DAS) stages and could be used both for breeding as well as commercial production in the case of THAD and XL753. The increasing importance of direct seeding in many countries has also made it critical to improve the seedling vigor of rice genotypes. The principal component analysis (PCA) and CVRI methods that were used in the present study helped to identify low, moderate, and high vigor rice genotypes. The cumulative vigor response index (CVRI) calculated from the morphological and physiological parameters revealed variability among the 36 rice genotypes. The two analysis methods (Vigor response indices and PCA) are equally reliable but work better together to confirm the accuracy of the experimental results. The correlation studies also showed that shoot and root morphological traits are both useful in identifying genotypes with high early vigor. The physiological traits, however, did not reveal any significant variations among the rice genotypes. Selected high vigor rice genotypes could help rice breeders to screen and choose rice genotypes for various development and related research, and serve as valuable resources for the enhancement of rice production across a wide range of growing conditions.

CONFLICT OF INTEREST

There is no conflict of interest to declare.

ACKNOWLEDGMENTS

We thank David Brand for technical assistance and graduate students at the Environmental Plant Physiology Laboratory for their help during data collection. We also thank the Mississippi Rice Promotion Board and the National Institute of Food and Agriculture, NIFA 2016-34263-25763, and NIFA Hatch 1024293 for partial funding to carry out this research.

LITERATURE CITED

Alexandratos N, Bruinsma J. 2012. World agriculture towards 2030/2050: the 2012 revision. 11 June 2012. http://www.fao.org/3/a-ap106e.pdf.

AOSA (Association of Official Seed Analysts). Seed vigor testing handbook. Contribution no. 32. Association of Official Seed Analysts, Lincoln. 1983; 89 pp.

Bandumula N, Neeraja CN, Waris A, SanjeevaRao D, Muthuraman P. An economic analysis of biofortified rice varieties. Oryza. 2019; 56: 405-410.

Bastiaans L, Ast AV, Zhao D. 2011. What is the basis of early vigour, being an important trait of weed competitiveness in rice. 23 Aug 2011. *http://www.ewrs.org/pwc/pwc_Samsun/Bastiaans.pdf.*

Cairns JE, Namuco OS, Torres R, Simborio FA, Courtois B, Aquino GA, Johnson, DE. Investigating early vigour in upland rice (*Oryza sativa* L.): Part II. Identification of QTLs controlling early vigour under greenhouse and field conditions. Field Crops Res. 2009; 113: 207-217.

Caton BP, Cope AE, Mortimer M. Growth traits of diverse rice cultivars under severe competition: implications for screening for competitiveness. Field Crops Res. 2003; 83: 157-172.

Chapple CCS, Vogt T, Ellis BE, Somerville CR. An Arabidopsis mutant defective in the general phenylpropanoid pathway. Plant Cell. 1992; 4: 1413-1424.

Deseo NB. Early vigor traits in selected upland and rainfed lowland rice (*Oryza sativa* L.) genotypes. Bachelor thesis. 2012; University of the Philippines.

Dingkuhn M, Johnson DE, Sow A, Audebert AY. Relationships between upland rice canopy characteristics and weed competitiveness. Field Crops Res. 1999; 61: 79-95.

Farooq M, Siddique KH, Rehman H, Aziz T, Lee DJ, Wahid A. Rice direct seeding: experiences, challenges and opportunities. Soil Till. Res. 2011; 111: 87-98.

Fukai S, Cooper M. Development of drought-resistant cultivars using physio-morphological traits in rice. Field Crops Res. 1995; 40: 67-86.

Godfray HCJ, and Garnett T. Food security and sustainable intensification. Philos. T. R. Soc. B. 2014; 369: 1-10.

Goldberg DE, Landa K. Competitive effect and response: hierarchies and correlated traits in the early stages of competition. J. Ecol. 1991; 79: 1013-1030.

Henry A, Cal AJ, Batoto TC, Torres RO Serraj R. Root attributes affecting water uptake of rice (*Oryza sativa*) under drought. J. Exp. Bot. 2012; 63: 4751-4763.

Jannink JL, Orf JH, Jordan NR, Shaw RG. Index selection for weed suppressive ability in soybean. Crop Sci. 2000; 40: 1087-1094.

Jumaa S, Redoña E, Walker T, Gao W, Reddy KR. Developing screening tools for early-season high- and

low-temperature stress tolerance in rice. Sabrao J. Breed. Genet. 2019; 51: 12-36.

Kakar N, Jumaa SH, Redoña ED, Warburton ML, Reddy KR. Evaluating rice for salinity using pot-culture provides a systematic tolerance assessment at the seedling stage. Rice 2019; 12: 57-71.

Krishnan P, Ramakrishnan B, Reddy KR, Reddy VR. High-temperature effects on rice growth, yield, and grain quality. In Advances in Agronomy. (Ed.): D.L. Sparks, Academic Press, Massachusetts. 2011; 87-206 pp.

Kumar A, Verulkar S, Dixit S, Chauhan B, Bernier J, Venuprasad R, Zhao D, Shrivastava MN. Yield and yield-attributing traits of rice (*Oryza sativa* L.) under lowland drought and suitability of early vigor as a selection criterion. Field Crops Res. 2009; 114: 99-107.

Lone AA, Jumaa SH, Wijewardana C, Taduri S, Redoña ED, Reddy KR. Drought stress tolerance screening of elite American breeding rice genotypes using low-cost pre-fabricated mini-hoop modules. Agronomy 2019; 9: 199-25.

Martineau JR, Specht JE, Williams JH, Sullivan CY. Temperature tolerance in soybeans. I. Evaluation of a technique for assessing cellular membrane thermostability 1. Crop Sci. 1979; 19: 75-78.

McBride WD, Skorbiansky SR, Childs N. US Rice Production in the New Millennium: Changes in Structure, Practices, and Costs. Econ. Res. Bull. 2018; 202: 1-62.

Namuco OS, Cairns JE, Johnson DE. Investigating early vigor in upland rice (*Oryza sativa* L.): Part I. Seedling growth and grain yield in competition with weeds. Field Crops Res. 2009; 113: 197-206.

Okami M, Kato Y, Yamagishi J. Role of early vigor in adaptation of rice to water-saving aerobic culture: Effects of nitrogen utilization and leaf growth. Field Crops Res. 2011; 124: 124-131.

Okami M, Kato Y, Kobayashi N, Yamagishi J. 2015 Morphological traits associated with vegetative growth of rice (*Oryza sativa* L.) during the recovery phase after early-season drought. Eur. J. Agron. 2015; 64: 58-66.

Powell AA, Matthews S. Towards the validation of the controlled deterioration vigour test for small seeded vegetables. Seed Testing International. 2005; 129: 21-24.

Redoña ED, Mackill DJ. Mapping quantitative trait loci for seedling vigor in rice using RFLPs. Theor. Appl. Genet. 1996; 92: 395-402.

Regan KL, Siddique KHM, Turner NC, Whan BR. Potential for increasing early vigour and total biomass in spring wheat. II. Characteristics associated with early vigour. Aust. J. Agric. Res. 1992; 43: 541-553.

Saito K, Azoma K, Rodenburg J. Plant characteristics associated with weed competitiveness of rice under upland and lowland conditions in West Africa. Field Crops Res. 2010; 116: 308-317.

Singh B, Reddy KR, Redoña ED, Walker T. Developing a screening tool for osmotic stress tolerance classification of rice cultivars based on in vitro seed germination. Crop Sci. 2017a; 57: 387-394.

Singh B, Reddy KR, Redoña ED, Walker T. Screening of rice cultivars for morpho-physiological responses to early-season soil moisture stress. Rice Sci. 2017b; 24: 322-335.

Singh RP, Prasad PV, Sunita K, Giri SN, and Reddy KR. Influence of high temperature and breeding for heat tolerance in cotton: a review. Adv. Agron. 2007; 93: 313-385.

Surabhi GK, Reddy KR, Singh SK. Photosynthesis, fluorescence, shoot biomass and seed weight responses of three cowpea (*Vigna unguiculata* (L.) Walp.) cultivars with contrasting sensitivity to UV-B radiation. Environ. Exp. Bot. 2009; 66: 160-171.

Zhao DL, Atlin, GN, Bastiaans L, Spiertz JHJ. Cultivar weed-competitiveness in aerobic rice: heritability, correlated traits, and the potential for indirect selection in weed-free environments. Crop Sci. 2006a; 46: 372-380.

Zhao DL, Atlin, GN, Bastiaans L, Spiertz JHJ. Developing selection protocols for weed competitiveness in aerobic rice. Field Crops Res. 2006b; 97: 272-285.

Zhao DL, Atlin, GN, Bastiaans L, Spiertz JHJ. Comparing rice germplasm groups for growth, grain yield and weed-suppressive ability under aerobic soil conditions. Weed Res. 2006c; 46: 444-452.

SUPPLEMENTARY FILES:

Table S1. Root growth and developmental traits, root: shoot ratio (RS), root length (RL, cm plant^{-1}), root surface area, cm^2 plant^{-1}), average root diameter (RAD, mm plant^{-1}), root volume (RV, cm^3 plant^{-1}), root tips (RT, no. plant^{-1}), root forks (RF, no. plant^{-1}), root crossing (RC, no. plant^{-1}), and root number (RN, no. plant^{-1}) of 36 rice genotypes measured during the seedling stage, 26 days after sowing.

Cultivar name	Root growth and developmental traits								
	RS	RL	RSA	RAD	RV	RT	RF	RC	RN
ANTONIO	0.33	5287	513	0.35	3.83	26268	41131	4362	40.80
BOWMAN	0.41	5529	609	0.27	6.16	40839	76488	9721	43.00
CHENIERE	0.27	3689	340	0.36	4.83	33035	80220	9950	28.60
CL 163	0.31	4297	487	0.33	2.59	20922	40937	8144	36.20
CL111	0.32	4280	447	0.33	5.51	25445	45412	3966	36.40
CL142-AR	0.24	3274	323	0.33	2.97	19989	35721	3793	27.00
CL151	0.37	5057	517	0.36	6.19	33147	60663	7046	37.60
CL152	0.46	4973	514	0.32	5.20	33629	59347	7018	38.20
CLIZMN	0.33	5995	735	0.29	4.12	31870	58101	7219	42.60
COCODRIE	0.29	4128	497	0.27	3.44	26406	50383	4594	39.80
COLORADO	0.35	6140	628	0.32	4.35	36278	69299	7530	39.00
LAKAST	0.29	5313	536	0.37	5.86	31605	70124	8803	39.20
MERMENTAU	0.30	4520	489	0.37	4.21	26544	46128	5046	41.40
NIPONBARE	0.32	5852	624	0.31	3.23	27568	44460	5563	38.60
REX	0.34	5430	670	0.38	5.19	32522	75111	7654	40.20
ROYJ	0.32	5261	579	0.33	4.27	39251	58040	10007	46.20
SABINE	0.28	3437	359	0.31	4.54	30519	55349	7268	27.40
THAD	0.37	7155	742	0.32	3.76	31580	46434	5919	44.60
Mean	*0.33*	*4978.67*	*533.82*	*0.33*	*4.46*	*30412.06*	*56297.12*	*6866.78*	*38.16*
LSD of cultivars	*N.S*	*1492****	*193****	*0.03****	*1.52****	*9536**	*20446****	*25225****	*7.50****
CLXL729	0.35	5537	651	0.35	5.66	33069	60821	6950	45.20
CLXL745	0.27	4054	415	0.33	5.34	31902	67169	8129	31.60
XL753	0.23	5863	698	0.34	3.76	35428	72483	9108	41.40
Mean	*0.29*	*5151.22*	*587.72*	*0.34*	*4.92*	*33466*	*66824.2*	*8062.4*	*39.40*
LSD of hybrids	*N.S*	*N.S*	*N.S*	*N.S*	*N.S*	*N.S*	*N.S*	*N.S*	*9.6**
RU1201102	0.28	6202	715	0.36	3.50	25935	44656	5468	40.80
RU1204114	0.39	4888	539	0.35	5.49	33551	68095	9099	39.80
RU1204122	0.36	5653	645	0.33	4.80	31504	58612	7114	42.20

RU1204154	0.34	3772	396	0.34	4.78	31953	55527	7153	34.60
RU1204156	0.31	6159	557	0.41	2.89	18383	33619	4225	40.40
RU1204194	0.33	5817	636	0.33	3.82	35722	62947	6977	44.00
RU1204196	0.35	4987	554	0.33	3.64	30268	53143	6156	42.40
RU1204197	0.32	5541	630	0.35	5.48	31147	66369	6947	42.60
RU1304100	0.44	3685	400	0.37	5.61	28271	64736	6918	34.60
RU1304114	0.34	4960	471	0.35	4.56	25463	55641	6089	39.00
RU1304122	0.37	5232	488	0.38	4.98	25895	48376	5093	37.00
RU1304154	0.36	4315	413	0.35	5.09	29175	58958	7036	38.40
RU1304156	0.33	3904	409	0.38	5.26	24087	47987	5254	34.00
RU1304157	0.31	6368	637	0.32	5.87	37113	71725	8340	40.00
RU1304197	0.28	4819	508	0.31	4.28	25683	52678	6898	39.00
Mean	*0.34*	*5086.77*	*533.23*	*0.35*	*4.67*	*28943.48*	*56204.56*	*6584.55*	*39.25*
LSD of breeding lines	*0.07**	*N.S*	*N.S*	*0.03**	*N.S*	*N.S*	*N.S*	*N.S*	*5.9**
Grand Mean	0.32	5079	552	0.34	4.69	31018	59859	7164	38.94
LSD	0.10**	1604**	195***	0.03***	1.75***	9115**	20730***	2540***	7.21***

*** Significant at P < 0.001, ** Significant at P <0.01, * Significant at P <0.05, and N.S = not significant.

Table S2. Shoot growth, plant height (PH, cm plant^{-1}), leaf number of the main tiller (LN, no. tiller^{-1}), tiller number (TN, no. plant^{-1}), total leaves (TL, no. plant^{-1}), leaf area (LA, cm^2 plant^{-1}), and combined dry weight, leaf dry weight (LW, g plant^{-1}), stem dry weight (SW, g plant^{-1}), root dry weight (RW, g plant^{-1}), aboveground dry weight (SHW, g plant^{-1}), and total dry weight (TW, g plant^{-1}) of 36 rice genotypes measured during the seedling stage, 26 days after sowing.

Cultivar name	Growth traits					Dry weight traits				
	PH	LN	TN	TL	LA	LW	SW	RW	SHW	TDW
ANTONIO	12.10	3.00	7.80	33.20	123.72	0.75	0.61	0.46	1.37	1.82
BOWMAN	10.40	3.00	6.00	24.00	92.55	0.80	0.62	0.58	1.42	2.00
CHENIERE	10.60	3.00	5.60	23.80	68.07	0.55	0.47	0.27	1.01	1.29
CL 163	11.70	3.00	7.20	28.80	87.52	0.76	0.62	0.43	1.38	1.80
CL111	12.34	3.00	8.00	29.40	111.15	0.73	0.63	0.43	1.36	1.79
CL142-AR	11.48	2.80	6.80	27.40	70.23	0.54	0.42	0.23	0.96	1.19

CL151	12.14	3.20	6.40	23.40	97.01	0.65	0.58	0.44	1.22	1.66
CL152	12.30	3.00	6.80	29.40	111.50	0.73	0.62	0.53	1.35	1.88
CLIZMN	10.36	3.00	7.00	28.20	108.95	1.08	0.82	0.58	1.90	2.47
COCODRIE	14.56	3.20	8.60	29.20	108.06	0.81	0.72	0.44	1.53	1.98
COLORADO	13.08	2.60	9.00	35.40	112.09	0.91	0.69	0.50	1.59	2.09
LAKAST	13.80	3.00	8.00	25.80	88.03	0.81	0.66	0.41	1.47	1.88
MERMENTAU	11.70	3.00	6.80	31.40	97.51	0.67	0.53	0.36	1.20	1.55
NIPONBARE	12.26	3.00	8.40	35.20	123.26	0.81	0.68	0.47	1.49	1.96
REX	11.88	3.00	7.20	29.40	102.82	0.79	0.73	0.53	1.52	2.04
ROYJ	10.04	3.00	7.20	32.20	93.44	0.67	0.60	0.40	1.27	1.67
SABINE	10.90	2.80	5.60	22.00	61.54	0.57	0.41	0.27	0.97	1.24
THAD	10.82	3.00	11.60	46.40	160.16	1.08	1.17	0.78	2.25	3.23
Mean	*11.80*	*2.98*	*7.44*	*29.70*	*100.98*	*0.76*	*0.64*	*0.45*	*1.40*	*1.86*
LSD of cultivars	*1.81***	*N.S*	*2.29****	*9.81***	*42.9***	*0.31**	*0.34**	*0.19****	*0.63**	*0.78***
CLXL729	11.82	3.20	7.40	28.60	135.33	0.85	0.87	0.55	1.72	2.27
CLXL745	11.76	3.20	6.00	26.00	72.50	0.59	0.53	0.31	1.12	1.43
XL753	11.10	3.80	11.20	42.40	140.06	1.18	1.04	0.53	2.22	2.75
Mean	*11.56*	*3.40*	*8.20*	*32.33*	*115.96*	*0.87*	*0.81*	*0.46*	*1.69*	*2.15*
LSD of hybrids	*N.S*	*N.S*	*3.68**	*9.89***	*N.S*	*0.35**	*N.S*	*N.S*	*0.80**	*0.97**
RU1201102	10.46	3.00	9.40	42.20	169.51	0.98	0.89	0.54	1.87	2.41
RU1204114	11.40	3.00	5.60	23.00	76.89	0.72	0.57	0.50	1.29	1.79
RU1204122	11.38	3.20	6.60	33.20	121.51	0.88	0.78	0.60	1.67	2.27
RU1204154	10.30	3.00	6.20	27.60	73.07	0.57	0.44	0.33	1.02	1.35
RU1204156	11.96	3.00	8.20	27.20	114.08	0.66	0.64	0.42	1.30	1.72
RU1204194	11.78	3.00	9.60	41.40	142.82	1.00	0.83	0.58	1.83	2.41
RU1204196	11.74	3.00	7.00	28.20	110.68	0.68	0.65	0.44	1.34	1.78
RU1204197	11.70	3.00	10.60	41.80	143.51	0.97	0.86	0.57	1.83	2.41
RU1304100	12.92	3.20	5.20	19.80	67.13	0.49	0.36	0.34	0.85	1.19
RU1304114	11.90	3.00	6.80	23.00	100.37	0.68	0.50	0.39	1.18	1.57
RU1304122	11.30	3.00	7.80	24.60	78.89	0.64	0.48	0.41	1.12	1.52
RU1304154	10.38	3.20	8.20	32.00	92.13	0.62	0.45	0.38	1.07	1.66

RU1304156	13.50	3.00	5.40	20.00	64.43	0.52	0.33	0.28	0.85	1.13
RU1304157	12.66	2.80	7.60	30.20	104.25	0.84	0.67	0.45	1.51	1.96
RU1304197	14.20	3.00	5.60	21.20	84.98	0.81	0.63	0.41	1.44	1.85
Mean	*11.84*	*3.03*	*7.32*	*29.03*	*102.95*	*0.74*	*0.61*	*0.44*	*1.34*	*1.80*
LSD breeding lines	*1.2***	*N.S*	*2.6***	*8.9****	*38.1****	*0.27***	*0.29***	*0.16**	*0.55***	*0.69***
Grand mean	11.73	3.13	7.65	30.35	106.63	0.79	0.69	0.45	1.48	1.94
LSD	1.82***	N.S	2.58***	9.28***	4.96***	0.30***	0.33**	0.19***	6.187*	0.768***

*** Significant at P < 0.001, ** Significant at P <0.01, * Significant at P <0.05, and N.S = not significant.

Table S3. Photosynthesis characteristics, net photosynthesis (Pn, µmol CO_2 m^{-2} s^{-1}), transpiration (Tr, mol H_2O m^{-2} s^{-1}), water use efficiency (WUE, mmol CO_2 mol^{-1} H_2O), stomatal conductance (g_s, mmol m^{-2} s^{-1}), and fluorescence (Fv'/Fm'); relative injury (RI, %), and canopy-air temperature differential (CTD, °C); pigment characterization, chlorophyll a (µg cm^{-2}), chlorophyll b (µg cm^{-2}), carotenoids (µg cm-2) of 36 rice genotypes measured during flowering stage, 65-75 days after sowing.

Cultivar name	Photosynthesis characteristics					Relative injury, canopy-air temperature, and pigment characterization					
	Pn	Tr	WUE	g_s	Fv'/Fm'	RI	CT	Chl a	Chl b	Caro	TCh
ANTONIO	23.66	9.46	2.53	0.42	0.63	60.81	-2.01	24.69	11.98	6.51	36.67
BOWMAN	22.78	9.82	2.35	0.52	0.56	43.74	1.20	26.92	13.22	7.31	40.14
CHENIERE	24.24	9.29	2.64	0.42	0.54	23.23	-1.81	24.50	12.45	7.61	36.95
CL 163	23.44	9.61	2.65	0.49	0.58	30.84	1.00	25.65	12.80	6.67	38.45
CL111	22.36	8.41	2.72	0.54	0.60	51.05	-3.14	25.46	12.21	6.73	37.67
CL142-AR	23.24	8.89	2.53	0.43	0.56	35.10	-2.48	25.00	12.66	6.01	37.66
CL151	22.24	9.35	2.40	0.48	0.55	34.77	1.08	21.83	10.11	5.33	31.94
CL152	21.17	9.25	2.32	0.43	0.57	24.81	-2.89	21.55	9.59	5.20	31.14
CLIZMN	24.78	9.17	2.67	0.50	0.64	43.04	-3.17	28.63	15.12	8.06	43.75
COCODRIE	24.42	8.69	2.85	0.45	0.53	36.21	-1.96	24.28	12.32	6.47	36.60
COLORADO	25.50	8.63	2.92	0.38	0.53	36.14	-2.46	25.37	12.94	7.45	38.32
LAKAST	25.00	9.03	2.79	0.43	0.63	39.50	0.50	25.50	12.68	6.97	38.18
MERMENTAU	22.10	7.83	2.97	0.41	0.57	35.21	-1.85	25.71	12.60	9.04	38.32
NIPONBARE	21.06	9.71	2.17	0.48	0.55	41.92	-1.93	25.71	13.44	7.79	39.15

REX	25.56	9.45	2.60	0.46	0.52	31.97	0.65	27.49	14.60	7.49	42.09
ROYJ	22.56	9.16	2.47	0.50	0.54	43.35	-2.11	30.37	17.63	8.92	48.00
SABINE	21.44	8.51	2.58	0.40	0.54	31.39	-1.73	24.06	11.91	6.00	35.96
THAD	21.82	8.11	2.75	0.43	0.52	41.12	-2.72	32.19	20.01	10.24	52.19
Mean	*23.19*	*9.02*	*2.61*	*0.45*	*0.56*	*38.01*	*-1.43*	*25.83*	*13.24*	*7.21*	*39.07*
LSD of cultivars	*N.S*	*N.S*	*0.4***	*N.S*	*N.S*	*N.S*	*N.S*	*5.2****	*4.4****	*2.67***	*9.6***
CLXL729	24.34	9.09	2.69	0.41	0.55	41.49	-1.94	22.83	10.59	5.33	33.42
CLXL745	23.26	8.98	2.63	0.41	0.66	34.41	-1.85	26.07	12.42	6.75	38.49
XL753	25.57	8.67	2.95	0.41	0.55	32.24	-1.31	26.88	13.62	7.03	40.50
Mean	*24.39*	*8.91*	*2.76*	*0.41*	*0.59*	*36.05*	*-1.70*	*25.26*	*12.21*	*6.37*	*37.47*
LSD of hybrids	*2.5**	*N.S*	*0.20**	*N.S*	*N.S*	*N.S*	*N.S*	*N.S*	*3.0**	*N.S*	*7.0**
RU1201102	21.34	9.10	2.38	0.43	0.53	39.59	-2.02	29.93	16.60	8.57	46.54
RU1204114	21.68	8.28	2.69	0.43	0.57	28.44	-1.32	20.72	9.32	5.59	30.03
RU1204122	23.54	8.08	3.03	0.43	0.73	30.50	-1.90	26.82	14.88	7.47	41.70
RU1204154	20.16	9.41	2.15	0.54	0.56	29.56	0.85	21.66	10.27	5.43	31.92
RU1204156	22.54	8.98	2.06	0.40	0.56	31.28	-1.78	24.92	12.69	6.44	37.61
RU1204194	23.22	10.03	2.20	0.47	0.57	28.07	-2.19	22.25	10.28	5.31	32.53
RU1204196	23.18	9.66	2.40	0.51	0.53	37.38	0.02	25.48	13.15	7.66	38.63
RU1204197	22.18	9.44	2.37	0.48	0.56	44.86	-1.80	29.66	16.72	8.70	46.38
RU1304100	21.32	8.29	2.60	0.46	0.74	25.86	-2.37	25.83	13.24	7.28	39.07
RU1304114	21.04	8.28	2.37	0.44	0.51	42.70	-2.35	24.39	12.27	6.49	36.67
RU1304122	22.96	8.62	2.70	0.40	0.55	46.72	0.36	28.49	15.68	7.98	44.17
RU1304154	21.54	9.19	2.37	0.46	0.53	36.10	-2.73	27.71	15.16	7.73	42.87
RU1304156	23.40	7.89	2.95	0.45	0.56	25.24	-2.32	23.88	12.69	6.47	36.57
RU1304157	22.06	8.29	2.70	0.46	0.54	27.30	-1.90	25.03	11.91	6.55	36.93
RU1304197	25.38	9.85	2.59	0.48	0.57	33.16	-2.90	24.60	11.71	6.40	36.31
Mean	*22.37*	*8.89*	*2.51*	*0.46*	*0.57*	*33.78*	*-1.62*	*25.42*	*13.11*	*6.94*	*38.53*
LSD breeding lines	*N.S*	*N.S*	*N.S*	*N.S*	*0.13**	*16.9**	*1.12****	*5.8**	*5.0**	*2.4**	*10.7**
Grand mean	23.32	8.94	2.62	0.44	0.57	35.95	-1.59	25.51	12.85	6.84	38.36
LSD	4.8*	1.99*	0.41*	N.S	0.13*	20.42*	1.33**	5.34**	4.62**	2.49**	9.87**

*** Significant at P < 0.001, ** Significant at P <0.01, * Significant at P <0.05, and N.S = not significant.

Table S4. Shoot growth, plant height (PH, cm plant^{-1}), leaf number of the main tiller (LN, no. tiller^{-1}), tiller number (TN, no. plant^{-1}), leaf area (LA, cm^2 plant^{-1}), panicle initiation, d^{-1}, and panicle, no. plant^{-1}; combined dry weight, leaf dry weight (LW, g plant^{-1}), stem dry weight (SW, g plant^{-1}), root dry weight (RW, g plant^{-1}), aboveground dry weight (SHW, g plant^{-1}), and root shoot ratio, and total dry weight (TW, g plant^{-1}) of 36 rice genotypes measured during mid-grain filling stage 95 days after sowing.

Cultivar name	Growth traits				Panicle initiation and panicle number		Dry weight traits					
	PH	LN	TN	LA	PI	TP	LW	SW	RW	SHW	RS	TW
ANTONIO	60.92	5.76	28.00	4683	72.56	21.62	25.71	55.73	23.11	81.44	0.28	104.54
BOWMAN	59.62	5.56	30.44	5259	73.12	21.68	28.23	59.04	24.54	87.28	0.28	111.82
CHENIERE	56.52	5.84	30.76	5439	70.34	22.32	24.40	58.43	21.84	82.82	0.26	104.66
CL 163	59.56	5.52	30.12	5159	71.68	24.58	28.79	66.51	24.81	95.29	0.26	120.10
CL111	57.68	5.44	30.40	4092	70.60	25.18	24.04	62.24	24.71	86.28	0.29	110.98
CL142-AR	59.44	5.48	25.36	4732	74.52	24.06	24.92	66.23	24.53	91.15	0.27	115.68
CL151	55.40	5.40	32.08	4809	70.16	24.74	23.03	62.15	25.08	85.18	0.30	110.26
CL152	57.52	5.68	26.68	3697	72.84	19.24	21.73	57.27	26.13	79.00	0.34	105.13
CLIZMN	57.60	5.76	29.88	5285	71.48	24.40	25.07	63.10	21.57	88.16	0.25	109.73
COCODRIE	60.48	5.68	26.32	4340	75.48	21.12	26.88	60.30	21.66	87.19	0.25	108.85
COLORADO	61.58	5.56	28.52	5402	73.08	22.74	27.68	68.64	25.27	96.32	0.27	121.59
LAKAST	57.16	5.72	31.90	5612	73.10	23.98	31.94	76.75	26.50	108.68	0.25	135.18
MERMENTAU	57.08	5.36	32.00	5091	72.38	24.44	26.61	59.08	23.07	85.69	0.27	108.76
NIPONBARE	58.36	5.52	30.20	5551	72.36	24.66	25.71	60.15	23.41	85.86	0.27	109.27
REX	57.48	5.64	25.36	4019	73.16	25.72	22.21	73.04	26.93	95.25	0.28	122.18
ROYJ	58.40	5.48	29.72	3761	73.48	20.96	22.79	60.94	21.26	83.73	0.25	104.99
SABINE	58.80	5.92	26.24	4606	71.66	20.64	21.36	55.10	23.28	76.46	0.31	99.74
THAD	59.72	5.56	28.04	5013	73.20	22.70	24.25	61.94	26.93	86.19	0.32	113.12
Mean	*58.52*	*5.60*	*29.00*	*4808*	*72.51*	*23.04*	*25.30*	*62.59*	*24.15*	*87.89*	*0.28*	*112.03*
LSD of cultivars	*2.7**	*N.S*	*N.S*	*1418**	*N.S*	*N.S*	*5.89***	*14.2**	*5.6**	*19.5**	*N.S*	*21.9**
CLXL729	58.76	5.60	36.92	5273	74.52	29.58	24.90	65.91	25.88	90.80	0.29	116.68
CLXL745	57.84	5.60	37.28	5198	73.68	26.00	24.61	67.68	27.97	92.29	0.30	120.26
XL753	60.48	5.52	39.04	5809	72.88	27.94	22.26	73.26	26.64	95.52	0.28	122.16
Mean	*59.03*	*5.57*	*37.75*	*5427*	*73.69*	*27.84*	*23.92*	*68.95*	*26.83*	*92.87*	*0.29*	*119.70*
LSD of hybrids	*2.0**	*N.S*	*N.S*	*N.S*	*N.S*	*N.S*	*N.S*	*N.S*	*N.S*	*N.S*	*N.S*	*N.S*
RU1201102	56.44	5.72	27.56	4969	71.84	22.64	25.84	59.60	22.60	85.44	0.26	108.04
RU1204114	61.74	5.40	27.68	3851	72.88	20.10	24.11	61.19	23.87	85.30	0.28	109.17
RU1204122	66.12	5.52	29.04	4231	74.52	20.48	32.20	63.15	22.74	95.35	0.24	118.09
RU1204154	58.20	5.56	34.10	4505	70.04	25.12	25.32	64.89	20.98	90.21	0.23	111.18

RU1204156	60.24	5.60	22.60	4001	73.50	18.96	22.46	58.29	22.83	80.75	0.28	103.58
RU1204194	60.12	5.52	30.96	5529	73.16	23.38	29.59	63.58	23.67	93.17	0.25	116.84
RU1204196	57.52	5.76	26.96	4197	76.52	19.52	25.42	59.98	21.90	85.41	0.26	107.30
RU1204197	59.40	5.60	30.36	5293	72.24	23.88	27.00	60.73	20.06	87.73	0.23	107.79
RU1304100	58.52	5.56	34.54	5521	70.96	27.62	26.40	64.39	20.54	90.79	0.23	111.33
RU1304114	58.86	5.60	27.38	5061	73.80	21.70	27.49	61.89	25.43	89.38	0.29	114.81
RU1304122	58.34	5.52	32.08	4803	78.36	21.32	29.83	65.63	23.65	95.46	0.25	119.11
RU1304154	55.36	5.52	31.56	4335	77.88	20.98	22.81	55.63	23.03	78.45	0.29	101.48
RU1304156	60.16	5.56	31.40	5184	70.94	24.40	25.18	60.79	22.35	85.97	0.26	108.32
RU1304157	59.52	5.68	31.80	5278	73.96	25.08	26.19	59.67	21.50	85.86	0.25	107.36
RU1304197	59.44	5.44	29.08	4938	70.24	22.72	27.83	61.40	23.18	89.23	0.27	112.41
Mean	*59.33*	*5.57*	*29.81*	*4780*	*73.39*	*22.53*	*26.51*	*61.39*	*22.56*	*87.90*	*0.26*	*110.46*
LSD of breeding lines	*3.9****	*N.S*	*7.9**	*1349**	*5.2**	*6.8**	*6.0**	*13.8**	*4.8**	*19.4**	*N.S*	*20.8**
Grand mean	58.96	5.58	32.18	5005	73.20	24.47	25.24	64.31	24.51	89.55	0.28	114.06
LSD	3.71***	N.S	8.21*	1355*	5.01*	7.2*	6.01*8	13.93	5.53*	19.37*	N.S	21.19**

*** Significant at P < 0.001, ** Significant at P <0.01, * Significant at P <0.05, and N.S = not significant.

Cover Crops and Landscape Positions Impact Infiltration and Anion Leaching in Corn-Soybean Rotation

Gurbir Singh[1], Gurpreet Kaur[1], Karl Williard[2], Jon Schoonover[2], and Taghi Bararpour[1]

[1]Delta Research and Extension Center, Mississippi State University, Stoneville, MS 38776, USA, and
[2]Department of Forestry, Southern Illinois University, Carbondale, IL 62901, USA

Corresponding Author: Gurbir Singh, E-mail: gs1064@msstate.edu

ABSTRACT

Cover crops (CCs) provide multiple benefits, including improving infiltration, decreasing soil compaction, building soil aggregates, and provide cover for reducing erosion. Several of the benefits of using CCs were reported from plot-scale studies. The variability in the performance of CCs due to the inclusion of landscape positions (LPs) is not well understood. Therefore, our objective was to study the effects of LPs (shoulder, backslope, and footslope) and crop rotations with and without CCs on cumulative infiltration rate, steady-state infiltration rate, sorptivity, and soil solution anion concentrations (sulfur, chloride, fluoride, and bromide). Cereal rye (*Secale cereal* L.) and hairy vetch (*Vicia villosa* Roth.) CCs were planted in a rotation with corn (*Zea mays* L.)-soybean (*Glycine max* [L.] Merr.) on three LPs in three watersheds (CC treatment) whereas non-treated control watersheds (noCC treatment) had corn-soybean rotation without CCs. Cover crops increased cumulative infiltration at shoulder, backslope, and footslope LPs by 2.9, 2.1, and 2.2 mm compared to noCC treatment, respectively. The steady-state infiltration rate for noCC treatment was 23 to 41% lower than CC treatment at shoulder and footslope positions. In CC treatment, anion concentrations measured using suction cup lysimeters at footslope LP were generally higher compared to footslope LP of noCC treatment. Increased anion concentrations in CC treatments at footslope LP was due to increased infiltration rates. Overall, anion leaching increases if higher anion concentrations are present in the soil solution, and it is possible that theses anions could be vulnerable to leaching or deep percolation loss in fields planted with CCs.

Keywords: bromide, chlorine, fluoride, sulfur, topographic positions
Abbreviations: CC, Cover crop; LP, Landscape position

INTRODUCTION

The addition of cover crops (CCs) in the cropping system can significantly affect soil physical, chemical, and biological properties. Cover crops improve water infiltration (Williams, 1966; McVay et al., 1989; Meek, 1990; Martens and Frankenberger, 1992; Gulick et al., 1994; Haruna, 2018a), increase soil water retention (Haruna, 2018b; Keisling et al., 1994; Yoo et al., 1996) and soil aggregate stability (McVay, 1989; Villamil et al., 2006; Hubbard et al., 2013; Acuña and Villamil, 2014), reduce soil bulk density (Keisling et al., 1994; Blanco-Canqui et al., 2011; Steele et al., 2012) and promote soil stabilization by reducing runoff sediment loss and discharge (Blanco-Canqui, 2018; Singh et al., 2018a). Singh et al. (2018a) reported that CCs established at a watershed scale reduced total suspended solids and discharge by 33% and 34%, respectively. Cover crop species and their root structure impact nutrient concentrations in the soil solution (Kristensen and Thorup-Kristensen, 2004; Singh et al., 2018b). Reductions in soil solution nutrient concentration and leaching have been reported previously with nitrate-N concentrations in soil solution being reduced between 12 to 95% (Blanco-Canqui, 2018; Singh et al., 2019). Cover crops can scavenge excess nutrients from the soil profile and can temporarily fix it in their biomass. Nitrogen accumulation in CC biomass depends on CC species, residual N in the soil, and biomass of the CCs at the time of termination (Odhiambo and Bomke, 2001; Dean and Weil, 2009; Komatsuzaki and Wagger, 2015). Cover crops use water for their growth, thereby reducing water

availability to leach out nitrates, as leaching is a function of water present in the soil profile (Heinrich et al., 2014; Singh et al., 2018b).

Landscape positions (LP) impacts spatial variability in a watershed and affects erosion, deposition, runoff, distribution of soil particles, soil organic matter, bulk and labile pools of carbon, nutrient availability, hydrologic properties, biomass accumulation and crop yields (Zhu and Lin, 2011; Muñoz et al., 2014; Negassa et al., 2015; Singh et al., 2018c; Adler et al., 2020). Infiltration and soil water retention properties of a toposequence without the inclusion of CCs have been studied previously. Soil water storage and water redistribution are directly affected by LP (McGee et al., 1997; Tomer et al., 2006). Water redistribution in a soil profile interacts with crop management practices (da Silva et al., 2001). In a cropped landscape with different tillage systems, da Silva et al. (2001) found that soil moisture was significantly affected by the spatial distribution of clay content and organic matter along a slope. Saturated hydraulic conductivity (K_{sat}) of fields under hay and conservation reserve program were reported to have 10 to 16 times higher K_{sat} compared to fields under mulch till corn-soybean rotation at backslope LP (Jiang et al., 2007). Guzman and Al-Kaisi (2011) reported that root biomass, soil organic carbon, and water-stable aggregates decreased whereas bulk density increased in a reconstructed prairie at the backslope compared to the summit and footslope positions which resulted in lower infiltration rates at backslope LP. Summit and footslope LPs had similar soil properties; however, infiltration rates were much greater at the footslope position, which was attributed to higher water-stable aggregates, due to greater soil organic carbon concentrations (Guzman and Al-Kaisi, 2011).

There is limited research on the LPs effects on CC performance. Munoz et al. (2014) reported that biomass accumulation of red clover (*Trifolium pretense* L.), a legume CC, was 15 to 28% higher at depression LPs compared to the summit and slope LP (Muñoz et al., 2014) whereas biomass of cereal rye (a grass CC) was significantly lower at depression LP compared to the summit and slope LPs (Negassa et al., 2015). Beehler et al. (2017) reported that summit and slope LP had 0.7 mg g^{-1} of greater particulate organic carbon content in the treatments with CCs compared to noCCs, and depression slopes did not show any significant differences. Additionally, CCs' effect on bulk organic carbon pool and soil water retention was not significant (Beehler et al., 2017). Singh et al. (2019) studied nitrogen dynamics in a watershed with CCs and reported a reduction in nitrate-N leaching loss at the footslope position by using CCs. Reductions in nitrate leaching at footslope position were attributed to nitrogen fixed in CC biomass, immobilized, or lost through denitrification, which might have been stimulated by higher water availability at the footslope position.

Limited published research is available on CCs impact on anion leaching at different LPs (phosphate-P, sulfate-S, fluoride, chloride, bromide) (Miller et al., 1994; Aronsson et al., 2016; Couëdel et al., 2018). Previous studies have reported that water-soluble sulfur concentration in soil was dependent on the crops grown in the rotations, carbon to sulfur (CS) ratio of the decomposing biomass, soil arylsulphatase activity in rhizosphere, and temperature during the growing season (Vong et al., 2004; Ryant, 2014). Cover crops and LP interaction effects on infiltration and soil solution concentrations of essential and non-essential nutrients are not well understood. Therefore, our objective was to study the effects of LP (shoulder, backslope, and footslope) and crop rotations with and without CCs on cumulative infiltration rate, steady-state infiltration rate, sorptivity, and soil solution concentration of anions (sulfur, chloride, fluoride, and bromide). We hypothesized that CCs would increase the infiltration rate at all LPs, and soil solution concentrations of essential elements (sulfates and chlorides) will decrease. In contrast, non-essential elements such as fluoride and bromide will increase in the soil profile.

MATERIALS AND METHODS

Site Description and Experimental Design

This study was established in 2015 at the Southern Illinois University research farms (37°42’34” N, -89°16’08” W). The research field was split into 12 watersheds with an area of <4.9 ha of each watershed. Watersheds in the research field were delineated

using a digital elevation model developed from LIDAR data with a raster resolution of 1.219 by 1.219 m obtained from the Illinois geospatial clearing house (Illinois Geospatial Data Clearinghouse, 2019). Out of twelve watersheds, six watersheds were randomly selected for this study. Further, three watersheds out of six watersheds were randomly assigned with CC treatment, and the other three watersheds had noCC. Each watershed was further split into three LPs (shoulder, backslope, and footslope). Landscape positions were developed using a topographic position index (TPI) tool created by Jenness et al. (2006) in ArcMap (Version 10.4.1). Details of classifying LPs and the baseline soil properties that were collected in spring 2015 from the six watersheds are provided in Singh et al. (2016). Dominant soil series on shoulder and backslope LP was Hosmer silt loam soil series (Fine-silty, mixed, active, mesic Oxyaquic Fragiudalfs). The footslope position had Bonnie silt loam (Fine-silty, mixed, active, acid, mesic Typic Fluvaquents) soil series. The 20-year average annual total rainfall was 1067 mm.

Crop Management, Lysimeter Installation, and Data Collection

From 2006, the research site was under a two-year corn-soybean rotation with no-tillage. The research site was under corn-soybean production with conventional tillage before 2006. Starting the year 2015, a watershed in the fields assigned to CC rotation followed corn-cereal rye-soybean-hairy vetch (legume) rotation, whereas noCC fields in the watersheds had a corn-noCC-soybean-noCC rotation. Table 1 provides the dates for field operations and data collection. A pre-plant fertilizer application to corn averaged around 222 kg N ha^{-1} as anhydrous ammonia, 34 kg P ha^{-1} as diammonium phosphate and 56 kg K ha^{-1} as Muriate of potash (KCl).

Additionally, on average, soybean received 160 kg K ha^{-1} as KCl in spring before planting. Cereal rye CC was drilled at a seeding rate of 88 kg ha^{-1} after corn harvest in fall 2015 and 2017. Hairy vetch was planted after soybean harvest in 2016 at a seeding rate of 28 kg ha^{-1} and then terminated in May 2017 (Table 1). Corn and soybean were planted with a 76.2-cm row spacing. Soybean cultivar Asgrow AG3334 and corn hybrid DKC58-06RIB were planted in the watersheds.

Table 1. Dates of field operations and data collection.

Crop	N Fertilizer Application	Planting	Harvest/Termination[1]	Soil Sampling	Soil Solution Sampling Events
Corn	30 Apr. 2015	3 May 2015	1 Oct. 2015	8 Oct. 2015	8
Cereal rye	-	5 Oct. 2015	18 Apr. 2016	13 Apr. 2016	16
Soybean	-	16 Jun. 2016	25 Oct. 2016	25 Oct. 2016	10
Hairy vetch	-	26 Oct. 2016	12 May 2017	12 Apr. 2017	16
Corn	3 May 2017	19 May 2017	6 Oct. 2017	9 Oct. 2017	7
Cereal rye	-	13 Oct. 2017	10 May 2018	18 Apr. 2018	13

[1]Cover crop before corn was terminated using glyphosate, *N*-(phosphonomethyl)glycine at 1.27 kg a.e. ha^{-1} plus 2,4-D, (2,4-Dichlorophenoxyacetic acid) at 4.21 kg a.e. ha^{-1} plus diammonium sulfate (DAS) at 2% v/v. Cover crop prior to planting soybean was terminated using glyphosate at 0.95 kg a.e. ha^{-1} plus saflufenacil (N′-[2-chloro-4-fluoro-5-(3-methyl-2,6-dioxo-4-(trifluoromethyl)-3,6-dihydro-1(2H)-pyrimidinyl)benzoyl]-N-isopropyl-N-methylsulfamide) at 0.04 kg a.i. ha^{-1} plus methylated seed oil (MSO) at 1% v/v plus DAS at 1.5% v/v.

Soil solution data at each LP within a watershed was collected using a suction cup lysimeter installed at 46-cm soil depth. Soil Moisture Equipment Corp. (Santa Barbara, CA, USA) supplied the Lysimeter model 1920F1. Each watershed had three lysimeters, one at each LP. Suction cup lysimeters were installed according to the procedure outlined by the model manual and Singh et al. (2018d). The negative pressure of 0.6 bars was used in the lysimeters for soil solution extraction. The lysimeters were sampled for

soil solution starting in June 2015 until the conclusion of the study in May 2018. Soil solution samples from suction cup lysimeters were collected following significant storm events (i.e., >12 mm of precipitation). In total, 70 soil solution sampling events were collected during the study period of three years. After collecting soil solution samples from the field, the samples were transferred to the Southern Illinois University water quality lab, where they were fine-filtered through 0.45 μm filters using vacuum filtration. After filtration, soil solution samples were refrigerated below 4°C until further analysis. Filtered soil solution samples were analyzed within a week for anions (Chloride, Cl^-; Flouride, Fl^-; Bromide, Br^-; Sulfate, SO_4^-) on an ion chromatograph (2000isp, Dionex, Thermo Fisher Scientific, Waltham, MA, USA).

Soil infiltration was measured using Cornell Sprinkler Infiltrometer (Cornell University, NY) during the fall of 2017 (Ogden et al., 1997). In total, 18 infiltration measurements were taken in six watersheds (one at each LP, three LPs, and six watersheds). Infiltration field test locations were near each suction cup lysimeter. The Cornell Sprinkler Infiltrometer consists of a portable rainfall simulator that is placed on an infiltration ring, which has a diameter of 241 mm. The single ring of infiltrometer was inserted to a depth of 70 mm. For every infiltration measurement, the sprinkler vessel was placed on the ring, and the initial water level in the vessel was measured. Rainfall simulator intensity rates of 0.4 to 0.5 cm (0.15 to 0.20 in) min^{-1} was used for each infiltration measurement. Every three minutes, the runoff was measured until steady infiltration occurred. Rainfall simulation or precipitation rate (r) was measured by the following equation:

$$r = [H1 - H2] / T_f$$

where H1 was the beginning water level, H2 was the ending water level in the infiltrometer vessel; and T_f was the time required for lowering down water level from H1 to H2. The runoff rate (ro_t, cm min^{-1}) was determined by the following equation:

$$ro_t = Vt / (457.30*t)$$

where 457.30 cm^2 was the area of the ring, Vt was the runoff volume, and t was the time interval for which runoff water was collected. Finally, the infiltration rates (i_t) was determined by the difference between the rainfall rate and runoff rate:

$$i_t = r - ro_t$$

Additionally, the steady-state infiltration rate was measured from 10 consecutive infiltration measurements recorded during the infiltration tests and was scaled to mm hr^{-1}. Sorptivity (S), a measure of hydraulic soil property that describes initial infiltration rate independent of rainfall rate was estimated using the following equation:

$$S = (2T_{RO})^{0.5} * r$$

where time-to-runoff (T_{RO}) is dependent on the rainfall rate (r) as well as the antecedent soil moisture conditions. The runoff will occur earlier if r is higher, and the soil is wetter (Kutilek, 1980).

Statistical Analysis

Soil solution and infiltration data were analyzed using the SAS Statistical software v9.4 (SAS Institute, Cary, NC, USA). Watersheds planted with and without CCs and LPs were treated as independent variables, whereas anion concentrations collected using suction cup lysimeters and infiltration data collected using Cornell infiltrometer were treated as dependent variables. All data were tested for normality using univariate procedure before analyses, and where ever needed, data were log-transformed for analyses and back-transformed for presenting results. Due to the two-year cropping rotation, the crops in the field changed with every season. Therefore, soil solution data were split by season. For example, eight soil solution collection events that were collected during corn season 2015 were analyzed together using a repeated measure model in the Glimmix procedure. Additionally, an exponential spatial or temporal covariance structure type = SP (EXP(c-list)) selected based on the lowest Akaike's Information Criteria (AIC) was also added in the model for analyses of anion concentrations. Tukey–Kramer grouping was used for a mean separation at alpha = 0.05.

RESULTS

Infiltration

Cover crops increased cumulative infiltration at shoulder, backslope, and footslope LP by 2.9, 2.1, and 2.2 mm compared to noCC treatments, respectively (Figure 1). Steady-state infiltration rate for noCC treatment was 23% and 41% lower than CC treatment at the shoulder (17.7±1.1 mm vs 23.0±3.9 mm) and footslope (10.4±2.2 mm vs. 17.7.0±2.9 mm) positions, respectively (Figure 2). There were no significant differences in the steady-state infiltration rates at the backslope LP between CC and noCC treatments. Within the CC treatment, a steady-state infiltration rate for backslope position was 38% lower compared to shoulder LP; however, within the noCC treatment, footslope LP had 41% lower infiltration rate compared to the shoulder LP. Additionally, no significant differences were present in the sorptivity between treatments and among LPs (Figure 2).

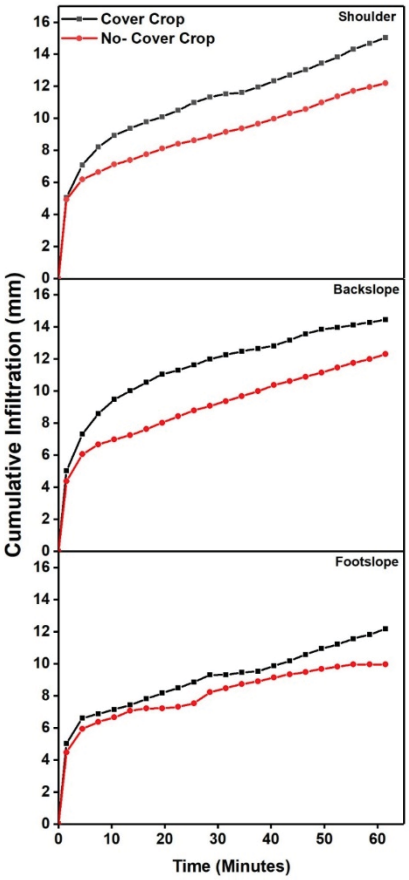

Figure 1. Cumulative infiltration measured in cover crop and no cover crop treatments on landscape positions.

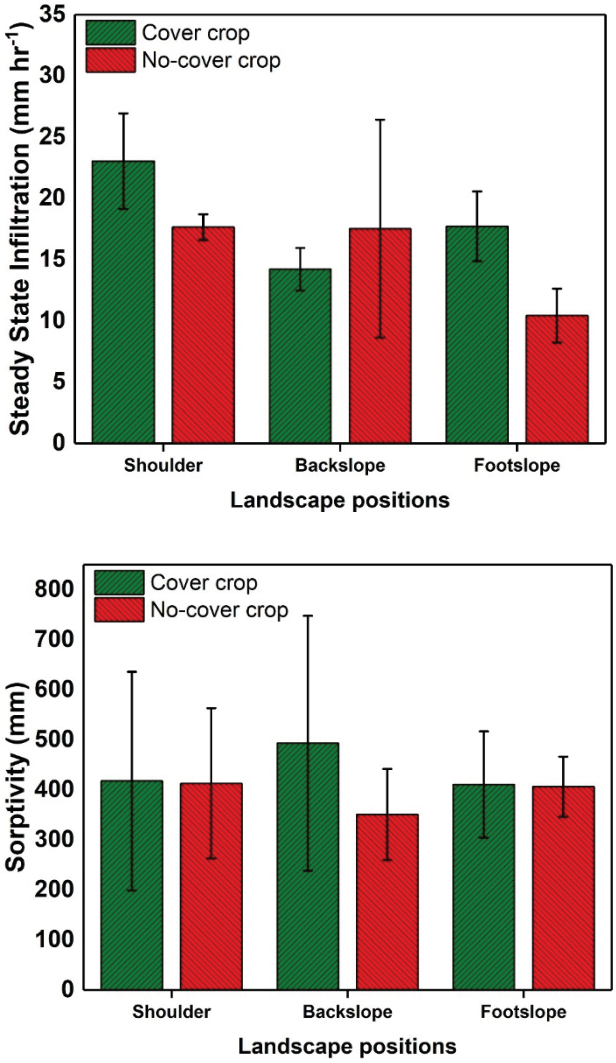

Figure 2. Steady-state infiltration and sorptivity in cover crop and no cover crop treatments on three landscape positions. Error bars indicate ± 95% confidence interval.

Anion Leaching

The Cl^- leaching was significantly affected by the LP during the soybean 2016, corn 2017, and cereal rye 2017-2018 (Table 2). Averaged over CC treatments, the Cl^- concentrations were higher at the footslope position than the shoulder position by 43.17, 48.80, and 102.20 mg L^{-1} during the soybean 2016, corn 2017, and cereal rye 2017-2018 growing seasons,

respectively (Table 2). Chloride leaching was also significantly affected by the interaction of LP and treatment during the corn and cereal 2015-2016, and hairy vetch 2016-2017. At the backslope position, CC treatments had 149 mg L^{-1} lower Cl^- concentration in soil solution compared to the noCC treatment during the corn 2015 growing season (Table 2). During hairy vetch 2016-2017 season, CC treatments had 69 mg L^{-1} higher Cl^- concentrations in soil solution than the noCC treatments at the footslope position. Within CC treatment, the footslope position had 74 to 87 mg L^{-1} higher Cl^- concentration compared to shoulder position during the corn 2015, cereal rye 2015-2016, and hairy vetch 2016-2017 seasons.

The soil solution SO_4-S concentration was significantly affected by the interaction of LPs and treatments during all growing season except corn 2015-2016 (Table 2). Averaged over treatment, soil solution SO_4-S concentration during the corn 2015 season was higher at footslope position than shoulder and backslope position by 42.44 and 43.77 mg L^{-1}. Inclusion of CC treatments at the footslope position resulted in higher soil solution SO_4-S concentration by 49 and 48 mg L^{-1} as compared to noCC, during soybean and hairy vetch 2016-2017 season, respectively (Table 2). Soil solution SO_4-S concentrations at footslope positions were 48 to 84 mg L^{-1} higher compared to shoulder LP for cereal rye 2015-2016, soybean 2016-2017, hairy vetch 2016-2017, corn 2017-2018, cereal rye 2017-2018 seasons within CC treatment. Within noCC treatment, soil solution SO_4-S concentrations at footslope position were 24 to 33 mg L^{-1} higher compared to shoulder for cereal rye 2015-2016, soybean 2016-2017, hairy vetch 2016-2017, corn 2017-2018, cereal rye 2017-2018 seasons.

Table 2. Comparison of mean chloride (Cl^-) and sulfate-S (SO_4-S) concentrations collected using suction cup lysimeters in cover crop (CC) and no cover crop (noCC) treatments. Within a column and a given factor or combination of factors, means followed by the same letter are not statistically different ($\alpha = 0.05$).

Treatment	Topography	2015–2016				2016–2017				2017–2018			
		Corn		Cereal Rye		Soybean		Hairy Vetch		Corn		Cereal Rye	
		Cl^-	SO_4-S	Cl^-	SO_4-S	Cl^-	SO_4-S	Cl^-	SO_4-S	Cl^-	SO_4-S	Cl^-	SO_4-S
		mg L^{-1}											
CC		91.48	37.7	96.39	46.05	118.03	39.95	121.83	35.98	88.71	34.56	93.71	28.73
noCC		137.66	23.87	113.65	28.61	109.58	18.47	100.42	17.45	74.77	17.73	110.83	12.85
	Shoulder	59.92b	17.08b	38.81c	25.77b	80.98b	9.44b	65.15c	6.79c	45.64b	2.87b	43.01c	2.21b
	Backslope	151.91a	15.75b	170.11a	20.60b	136.29a	15.05b	160.29a	17.36b	105.14a	15.44b	118.59b	9.67b
	Footslope	131.98a	59.52a	106.15b	65.63a	124.15a	63.15a	107.94b	55.99a	94.44a	60.11a	145.21a	50.49a
CC	Shoulder	55.02c	27.17	38.56c	34.94bc	81.18	12.89bc	68.61b	8.39bc	51.57	0.81b	30.03	0.95b
CC	Backslope	77.05bc	16.52	130.85ab	19.67bc	135.36	19.29bc	154.5a	19.33bc	122.39	17.67b	112.03	11.24b
CC	Footslope	142.38ab	69.41	119.78ab	83.26a	137.56	87.66a	142.37a	80.22a	92.17	85.2a	139.06	74.02a
noCC	Shoulder	64.82bc	7.00	39.07c	16.59c	80.78	5.99c	61.68b	5.18c	39.71	4.94b	55.98	3.47b
noCC	Backslope	226.58a	14.98	209.38a	21.23bc	137.21	10.8c	166.08a	15.39bc	87.89	13.22b	125.16	8.1b
noCC	Footslope	121.58bc	49.63	92.51b	47.99ab	110.74	38.63b	73.5b	31.77b	96.71	35.02a	151.35	26.98a

Temporal variation in soil solution concentrations of Cl^- and SO_4-S concentration is provided in figures 3 and 4. At backslope position, Cl^- concentrations during corn 2015 were lower in CC treatment compared to noCC; however, these differences disappeared later in the growing season (Figure 3). At the footslope position, Cl^- concentrations were generally higher for CC treatment compared to noCC treatment during cereal rye 2015-2016 and hairy vetch 2016-2017 growing season (Figure 3). Temporal variation in soil solution SO_4-S concentrations (Figure 4) indicates that SO_4-S concentrations were higher for CC treatment compared to noCC at footslope position, and no difference was observed among the treatments at shoulder LP.

Fluoride concentrations in soil solution were affected by the interaction of LPs and treatment for all season except corn 2015, and hairy vetch 2016-2017. Fluoride concentrations in soil solution were 94%

higher (0.16 mg L^{-1}) in CC treatment compared to noCC treatment at the footslope during cereal rye 2015-2016. In contrast, no significant difference was present in Br^- concentrations at the footslope position (Table 3). Bromide concentrations were 0.06 mg L^{-1} higher for noCC treatment compared to CC treatment during cereal rye 2015-2016 season at backslope position. During soybean 2016-2017 and corn 2017-2018 growing seasons, Fl^- concentrations at footslope LP were 0.2 to 0.3 mg L^{-1} higher in CC compare to noCC treatment. Fluoride concentrations at the shoulder and backslope positions for CC treatment during corn 2017-2018 were 0.1 to 0.3 mg L^{-1} higher compared to the shoulder and backslope positions for noCC treatment, respectively. Bromide concentration of soil solution for CC treatment was 0.04 mg L^{-1} higher compared to noCC treatment in corn 2017-2018 growing season. Within CC treatment, soil solution concentrations for Fl^- anion was 0.13 to 0.18 mg L^{-1} higher at footslope compared to shoulder LP during cereal rye (2015-2016 and 2017-2018) and corn 2017-2018 growing seasons. Similarly, soil solution Br^- concentrations were 0.05 to 0.15 mg L^{-1} higher at footslope LP compared to shoulder position within CC treatment.

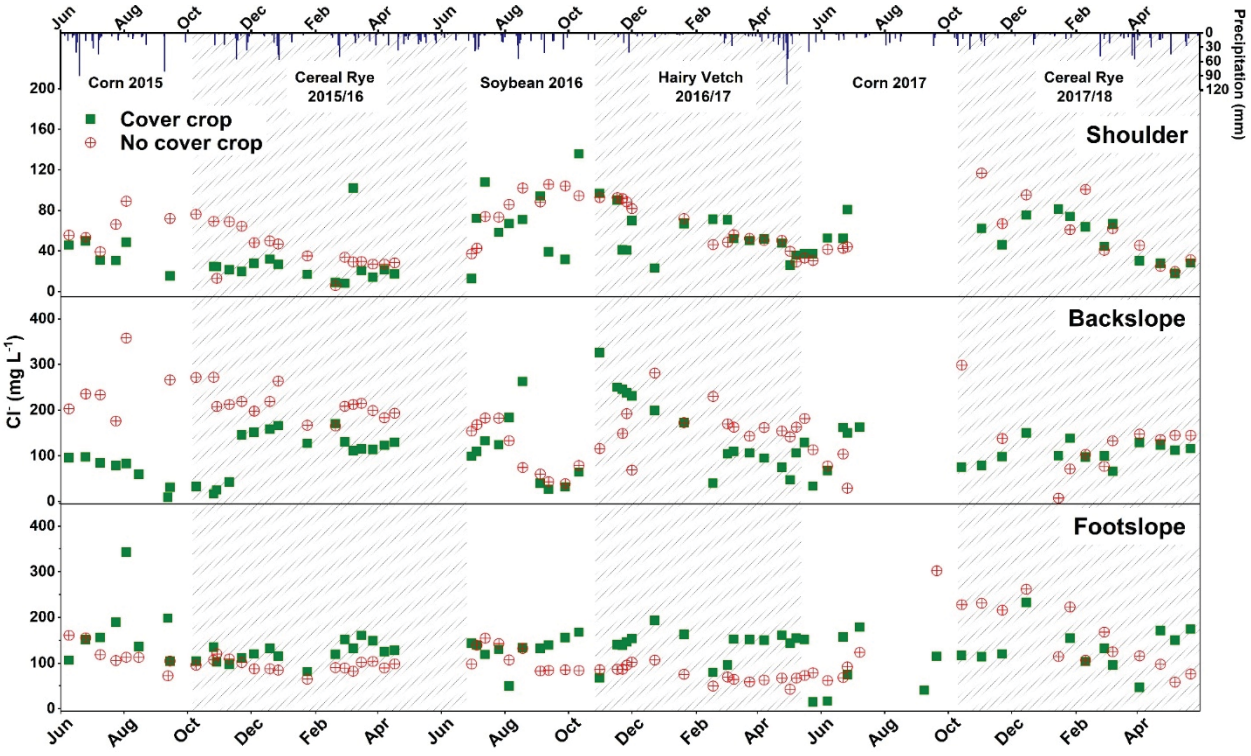

Figure 3. Soil solution Chloride (Cl^-) concentrations for cover crop and no-cover crop treatments at shoulder, backslope, and footslope topographic positions. Shaded areas indicate the cover crop growing season. Bars at the top of the figure represent daily precipitation received at the research site.

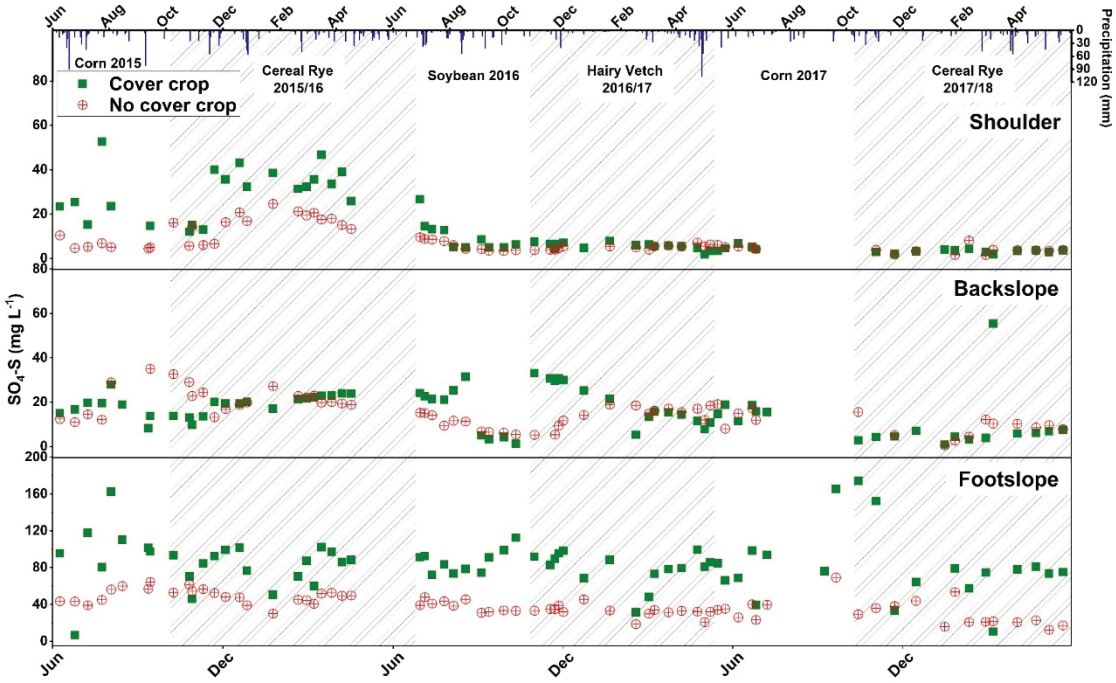

Figure 4. Soil solution Sulfate-S (SO_4-S) concentrations for cover crop and no-cover crop treatments at shoulder, backslope, and footslope topographic positions. Shaded areas indicate the cover crop growing season. Bars at the top of the figure represent daily precipitation received at the research site.

Table 3. Comparison of mean fluoride (F^-) and bromide (Br^-) concentrations collected using suction cup lysimeters in cover crop (CC) and no cover crop (noCC) treatments. Within a column and a given factor or combination of factors, means followed by the same letter are not statistically different ($\alpha = 0.05$).

Treatment	Topography	2015–2016				2016–2017				2017–2018			
		Corn		Cereal Rye		Soybean		Hairy Vetch		Corn		Cereal Rye	
		F^-	Br^-	F^-	Br^-	F^-	Br^-	F^-	Br^-	F^-	Br^-	F^-	Br^-
		mg L^{-1}											
CC		0.24	0.46	0.24	0.05	0.31	0.1	0.43	0.06	0.32a	0.08a	0.24	0.03
noCC		0.14	0.42	0.15	0.07	0.17	0.06	0.30	0.05	0.08b	0.04b	0.17	0.04
	Shoulder	0.12b	0.44	0.15c	0.03b	0.20b	0.04b	0.45a	0.04	0.14b	0.02b	0.15b	0.02b
	Backslope	0.14b	0.42	0.19b	0.08a	0.23b	0.07b	0.40a	0.05	0.23a	0.06b	0.22a	0.03b
	Footslope	0.30a	0.46	0.25a	0.06a	0.29a	0.13a	0.26b	0.07	0.23a	0.11a	0.23a	0.06a
CC	Shoulder	0.14	0.48	0.17b	0.02c	0.22ab	0.04b	0.55	0.04b	0.19b	0.03	0.16b	0.01
CC	Backslope	0.17	0.40	0.24b	0.05bc	0.31ab	0.08a	0.43	0.04b	0.38a	0.08	0.27ab	0.02
CC	Footslope	0.41	0.51	0.33a	0.07ab	0.39a	0.19a	0.32	0.09a	0.37a	0.14	0.29a	0.06
noCC	Shoulder	0.11	0.41	0.13b	0.03bc	0.18b	0.04b	0.34	0.05ab	0.09c	0.02	0.15b	0.02
noCC	Backslope	0.11	0.44	0.14b	0.11a	0.15b	0.07ab	0.38	0.05ab	0.07c	0.05	0.17ab	0.03
noCC	Footslope	0.19	0.40	0.17b	0.05bc	0.19b	0.07ab	0.19	0.05ab	0.08c	0.07	0.18ab	0.06

DISCUSSION

Topography in an agricultural landscape influences upslope and downslope soil's physical and chemical properties, including soil nutrient concentrations, organic matter, redistribution of soil particles, and water availability due to both vertical and horizontal water redistribution (Kravchenko and Bullock, 2000; Singh et al., 2019). Soil erosion from higher LPs results in soil organic matter and moisture accumulation at the lower LPs (Sariyildiz et al., 2005). These might have resulted in a higher infiltration rate at the shoulder position than the other

two LPs in our study. Similarly, Guzman and Al-Kaisi (2011) found that midslope positions have lower infiltration rates as compared to the summit and toe slope position due to decreased root biomass, soil organic carbon, and water-stable aggregate at this LP.

Many studies report an increase in cumulative infiltration and steady-state infiltration with the use of CCs (Folorunso et al., 1992; Haruna et al., 2018a; Haruna et al., 2018b). Al-Kaisi and Wilson (2009) also reported a higher steady-state infiltration rate with CCs compared to noCCs. Cover crop improves soil structure and aggregate stability, resulting in improvement of water infiltration (Al-Kaisi and Wilson, 2009). Cover crops increase soil organic matter content through the decomposition of their root biomass and incorporation of aboveground biomass into soil. Increases in soil organic matter can improve soil structure and, consequently, improves water infiltration in soil. In addition to this, CCs maintain aggregate stability during rainfall events by reducing rain droplet's kinetic energy and splash detachment. Haruna et al. (2018b) reported that CCs increased macropores in soil by 24% compared to noCCs treatments, which can potentially increase infiltration, saturated hydraulic conductivity, and reduce runoff from agricultural fields.

Sulfur and chloride are essential plant nutrients and needed by plants for their growth, development, and completion of the life cycle. The plant absorbs most of its sulfur from soils in the form of sulfate ion. Sulfate is the most common form of inorganic sulfur in soil and is usually present either in soil solution or adsorbed to soil particles. Sulfate leaching from agricultural soils can result in S deficiency in the crop and thus, reducing the crop yields (Barber, 1995). Sulfur leaching can be affected by climate, soil properties, crop management practices, and crop growth (Riley et al., 2002). The risk of sulfur leaching is higher when the sulfur uptake by plants is lower or when there is higher sulfur released by the decomposition of organic matter (Ercoli et al., 2012). Sulfate retention in soil by adsorption is dependent upon the soil pH, nature of the colloidal system, concentration of sulfate, and other ions in the solution (Harward and Reisenauer, 1966).

Leaching of anions will also be affected by soil moisture content and volume of water, leaving the soil profile. Higher infiltration rates in the CC treatments in our study might have resulted in higher leaching of anions in CC treatments compared to noCC treatments. Ercoli et al. (2012) reported that sulfur leaching increased during winter as the rainfall increases. Al-Kaisi and Wilson (2009) reported that cereal rye CC reduced bromide leaching during the CC season compared to noCC treatments due to a reduction in the amount of water moving through soil profile as CCs used the soil water for their growth. Fluoride and Br^- are not essential plant nutrients. Bromide and $C1^-$ are biologically and chemically stable, and they do not undergo microbial transformations and gaseous losses (Kessavalou et al., 1996). Therefore, these anions have a higher chance of their loss via leaching in the soil in the presence of excess water. Smith and Cassel (1991) reported that high infiltration rates and water permeability in coarse to medium textured soils resulted in excess water passing through the soil and, consequently, higher bromide leaching. Similarly, our results indicated that footslope LP had higher infiltration rates in CC treatment compared to noCC treatment and therefore had higher Fl^- and Br^- soil solution concentrations in CC treatments. It is possible that CCs might have created a higher number of biopores or macropores that promoted infiltration at footslope positions and resulted in greater soil solution anion concentrations in the soil profile.

CONCLUSION

This study evaluated the effects of LP (shoulder, backslope, and footslope) and crop rotation (CC and noCC) on cumulative infiltration rate, steady-state infiltration rate, sorptivity, and soil solution concentration of essential and non-essential anions. We hypothesized that CCs would increase the infiltration rate at all LPs, and soil solution concentration of essential elements (sulfates and chlorides) will decrease whereas non-essential elements (fluoride and bromide) will increase in the soil profile. Our results indicated that infiltration rates were only increased at the footslope LP of CC treatment when compared with similar LP of noCC treatment. Steady-state infiltration rate followed

shoulder>footslope>backslope for CC treatment. Steady-state infiltration rate for noCC treatment was 23% and 41% lower than CC treatment at the shoulder and footslope positions, respectively. In general, higher infiltration rates at footslope LP resulted in higher soil solution concentrations of all anions. It is possible that higher anion concentrations along with higher availability of water and a greater number of biopores created by CC might have resulted in a higher soil solution concentration of anions observed in suction cup lysimeters. Due to the variability in a toposequence, CC planted at large scale might not show improvement in increased infiltration at all LPs. Additionally, reduction in anion leaching by CC planted in a toposequence will depend on anion substrate, amount of water, and several other factors that need further research.

ACKNOWLEDGMENT

We acknowledge Jackie Crim and Randy Lange for their assistance in maintaining the cover crops project site at Carbondale, IL. Also, we thank Shelly Williard and all the undergraduate students who provided help in sample collection and analyses. This project was partially funded by the Illinois Nutrient Research and Education Council (ILNREC), Award No. 2014-11-002, Agronomic Science Foundation, and Bayer.

LITERATURE CITED

Acuña J, Villamil MB. Short-term effects of cover crops and compaction on soil properties and soybean production in Illinois. Agron. J. 2014; 106: 860-870.

Adler, RL, Singh, G, Nelson, KA, Weirich J, Motavalli PP, Miles RJ. Cover crop impact on crop production and nutrient loss in a no-till terrace topography. J. Soil Water Conserv. 2020; 75: 153-165.

Al-Kaisi M, Wilson G. Tillage and cover crop effects on productivity, soil properties, and nitrate leaching. Proceedings of the Integrated Crop Management Conference. 2009; 2.

https://lib.dr.iastate.edu/icm/2009/proceedings/2.
doi:10.31274/icm-180809-2

Aronsson H, Hansen EM, Thomsen IK, Liu J, Øgaard A, Känkänen H, Ulén B. The ability of cover crops to reduce nitrogen and phosphorus losses from arable land in southern Scandinavia and Finland. J. Soil Water Conserv. 2016; 71: 41-55.

Barber SA. Soil nutrient bioavailability: a mechanistic approach, 2nd ed. John Wiley & Sons, New York. 1995; 384 pp.

Beehler J, Fry J, Negassa W, Kravchenko A. Impact of cover crop on soil carbon accrual in topographically diverse terrain. J. Soil Water Conserv. 2017; 72: 272-279.

Blanco-Canqui H. Cover crops and water quality. Agron. J. 2018; 110: 1633-1647.

Blanco-Canqui H, Mikha MM, Presley DR, Claassen MM. Addition of cover crops enhances no-till potential for improving soil physical properties. Soil Sci. Soc. Am. J. 2011; 75: 1471-1482.

Couëdel A, Alletto L, Justes É. Crucifer-legume cover crop mixtures provide effective sulphate catch crop and sulphur green manure services. Plant Soil 2018; 426: 61-76.

da Silva AP, Nadler A, Kay B. Factors contributing to temporal stability in spatial patterns of water content in the tillage zone. Soil Till. Res. 2001; 58: 207-218.

Dean JE, Weil RR. Brassica cover crops for nitrogen retention in the Mid-Atlantic Coastal Plain. J. Environ. Qual. 2009; 38: 520-528.

Ercoli L, Arduini I, Mariotti M, Lulli L, Masoni A. Management of sulphur fertiliser to improve durum wheat production and minimise S leaching. Euro. J. Agron. 2012; 38: 74-82.

Folorunso O, Rolston D, Prichard T, Loui D. Soil surface strength and infiltration rate as affected by winter cover crops. Soil Tech. 1992; 5: 189-197.

Gulick S, Grimes D, Goldhamer D, Munk D. Cover-crop-enhanced water infiltration of a slowly permeable fine sandy loam. Soil Sci. Soc. Am. J. 1994; 58: 1539-1546.

Guzman J, Al-Kaisi M. Landscape position effect on selected soil physical properties of reconstructed prairies in southcentral Iowa. J. Soil Water Conserv. 2011; 66: 183-191.

Haruna S, Nkongolo N, Anderson S, Eivazi F, Zaibon S. In situ infiltration as influenced by cover crop and tillage management. J. Soil Water Conserv. 2018a; 73: 164-172.

Haruna SI, Anderson SH, Nkongolo NV, Zaibon S. Soil hydraulic properties: Influence of tillage and cover crops. Pedosphere 2018b; 28: 430-442.

Harward M, Reisenauer HM. Reactions and movement of inorganic soil sulfur. Soil Sci. 1966; 101: 326-335.

Heinrich A, Smith R, Cahn M. Winter-killed cereal rye cover crop influence on nitrate leaching in intensive vegetable production systems. HortTech. 2014; 24: 502-511.

Hubbard RK, Strickland TC, and Phatak S. Effects of cover crop systems on soil physical properties and carbon/nitrogen relationships in the coastal plain of southeastern USA. Soil Till. Res. 2013; 126: 276-283.

Illinois Geospatial Data Clearinghouse 2019. Illinois height modernization: LIDAR Data. https://clearinghouse.isgs.illinois.edu/data/elevation Accessed 10-14-2019.

Jenness J, Enterprises, J, Site, W NAME: Topographic Position Index (TPI) v. 1.3. 2006.

Jiang P, Anderson S, Kitchen N, Sadler E, Sudduth K. Landscape and conservation management effects on hydraulic properties of a claypan-soil toposequence. Soil Sci. Soc. Am. J. 2007; 71: 803-811.

Keisling T, Scott H, Waddle B, Williams W, Frans R. Winter cover crops influence on cotton yield and selected soil properties. Commun. Soil Sci. Plant Anal. 1994; 25: 3087-3100.

Kessavalou A, Doran JW, Powers WL, Kettler TA, Qian JH. Bromide and nitrogen-15 tracers of nitrate leaching under irrigated corn in central Nebraska. J. Environ. Qual. 1996; 25: 1008-1014.

Komatsuzaki M, Wagger M. Nitrogen recovery by cover crops in relation to time of planting and growth termination. J. Soil Water Conserv. 2015; 70: 385-398.

Kravchenko AN, Bullock DG. Correlation of corn and soybean grain yield with topography and soil properties. Agron. J. 2000; 92: 75-83.

Kristensen HL, Thorup-Kristensen K. Root growth and nitrate uptake of three different catch crops in deep soil layers. Soil Sci. Soc. Am. J. 2004; 68: 529-537.

Kutilek M. Constant-rainfall infiltration. J. Hydrol. 1980; 45: 289-303.

Martens D, Frankenberger W. Modification of infiltration rates in an organic-amended irrigated. Agron. J. 1992; 84: 707-717.

McGee E, Peterson G, Westfall D. Water storage efficiency in no-till dryland cropping systems. J. Soil Water Conserv. 1997; 52: 131-136.

McVay K, Radcliffe D, Hargrove W. Winter legume effects on soil properties and nitrogen fertilizer requirements. Soil Sci. Soc. Am. J. 1989; 53: 1856-1862.

Meek BD, DeTar WR, Rechel E, Carter L, Rolph D. Infiltration rate as affected by an alfalfa and no-till cotton cropping system. Soil Sci. Soc. Am. J. 1990; 54: 505-508.

Miller M, Beauchamp E, Lauzon J. Leaching of nitrogen and phosphorus from the biomass of three cover crop species. J. Environ. Qual. 1994; 23: 267-272.

Muñoz JD, Steibel JP, Snapp S, Kravchenko AN. Cover crop effect on corn growth and yield as influenced by topography. Agric. Eco. Environ. 2014; 189: 229-239.

Negassa W, Price RF, Basir A, Snapp SS, Kravchenko A. Cover crop and tillage systems effect on soil CO_2 and N_2O fluxes in contrasting topographic positions. Soil Till. Res. 2015; 154: 64-74.

Odhiambo JJO, Bomke AA. Grass and legume cover crop effects on dry matter and nitrogen accumulation. Agron. J. 2001; 93: 299-307.

Ogden C, Van Es H, Schindelbeck R. Miniature rain simulator for field measurement of soil infiltration. Soil Sci. Soc. Am. J. 1997; 61: 1041-1043.

Riley N, Zhao F, McGrath S. Leaching losses of sulphur from different forms of sulphur fertilizers: a field lysimeter study. Soil Use Manage. 2002; 18: 120-126.

Ryant P. Changes in the content of water-soluble sulphur in the soil after an application of straw and elemental sulphur. Acta Universitatis Agriculturae et Silviculturae Mendelianae Brunensis 2014; 55: 195-204.

Sariyildiz T, Anderson J, Kucuk M. Effects of tree species and topography on soil chemistry, litter quality, and decomposition in Northeast Turkey. Soil Biol. Biochem. 2005; 37: 1695-1706.

Singh G, Schoonover J, Williard K. Cover crops for managing stream water quantity and improving stream water quality of non-tile drained paired watersheds. Water 2018a; 10: 521.

Singh G, Williard KW, Schoonover JE. Cover crops and tillage influence on nitrogen dynamics in plant-soil-water pools. Soil Sci. Soc. Am. J. 2018b; 82: 1572-1582.

Singh G, Schoonover JE, Williard KW, Kaur G, Crim J. Carbon and nitrogen pools in deep soil horizons at different landscape positions. Soil Sci. Soc. Am. J. 2018c; 82: 1512-1525.

Singh G, Kaur G, Williard K, Schoonover J, Kang J. Monitoring of water and solute transport in the vadose zone: A review. Vadose Zone J. 2018d; 17:160058. doi:10.2136/vzj2016.07.0058

Singh G, Williard KW, Schoonover JE. Spatial relation of apparent soil electrical conductivity with crop yields and soil properties at different topographic positions in a small agricultural watershed. Agron. 2016; 6: 57.

Singh G, Williard K, Schoonover J, Nelson KA, Kaur G. Cover crops and landscape position effects on nitrogen dynamics in plant-soil-water pools. Water 2019; 11: 513-531.

Smith SJ, and Cassel DK. Estimating nitrate leaching in soil materials. *In* Follett et al., (ed.) Managing nitrogen for groundwater quality and farm profitability. SSSA, Madison, WI. 1991; p. 165–188.

Steele M, Coale F, Hill R. Winter annual cover crop impacts on no-till soil physical properties and organic matter. Soil Sci. Soc. Am. J. 2012; 76: 2164-2173.

Tomer M, Cambardella C, James D, Moorman T. Surface-soil properties and water contents across two watersheds with contrasting tillage histories. Soil Sci. Soc. Am. J. 2006; 70: 620-630.

Villamil MB, Bollero GA, Darmody R, Simmons F, Bullock D. No-till corn/soybean systems including winter cover crops. Soil Sci. Soc. Am. J. 2006; 70: 1936-1944.

Vong P, Dedourge O, Guckert A. Immobilization and mobilization of labelled sulphur in relation to soil arylsulphatase activity in rhizosphere soil of field-grown rape, barley and fallow. Plant Soil 2004; 258: 227-239.

Williams, WA. Management of nonleguminous green manures and crop residues to improve the infiltration rate of an irrigated soil 1. Soil Sci. Soc. Am. J. 1966; 30: 631-634.

Yoo K, Dane J, Missildine B. Soil-water content changes under three tillage systems used for cotton. J. Sustain. Agric. 1996; 7: 53-61.

Zhu Q, Lin H. Influences of soil, terrain, and crop growth on soil moisture variation from transect to farm scales. Geoderma 2011; 163: 45-54.

Molecular and Physiological Response to Dicamba in Dicamba-Tolerant Wild Tomato

Rouzbeh Zangoueinejad[1,2], Mohammad Taghi Alebrahim[2], and Te Ming Tseng[1]

[1]Department of Plant and Soil Sciences, Mississippi State University, Mississippi State, MS 39762, USA, [2]Department of Agronomy and Plant Breeding, Faculty of Agriculture and Natural Resources, University of Mohaghegh Ardabili, Ardabil, Iran.

Corresponding Author: Te Ming Tseng, Email: t.tseng@msstate.edu

ABSTRACT

Auxin-like herbicides such as dicamba, in low concentration, plays a role close to phytohormones in promoting plant growth. On the other hand, with an increase in auxin compound concentration, their activity is gradually changed to an abiotic stressor, thus disrupting normal plant processes. From our previous study, we identified three wild tomato accessions to be tolerant of the simulated drift rate of dicamba. Understanding the mechanism of tolerance in these accessions to dicamba will, therefore, be crucial in breeding for auxin tolerant tomato. This information will also shed light on auxin tolerance/ resistance mechanisms in plants since much of this is unknown. The objective of this study was, therefore, to investigate the molecular and biochemical basis of dicamba tolerance in three wild tomato accessions. We conducted gene expression analysis to determine the potential role of F-box$^{TIR1/AFB}$ in dicamba tolerance. Besides, levels of H_2O_2 and HCN in response to dicamba application were measured and compared between dicamba-tolerant and susceptible tomato accessions. Based on the greenhouse study, all wild accessions were confirmed tolerant to dicamba at the simulated drift rate (0.001X; 2.8 g ae ha^{-1}). Association analysis using SSR markers revealed that dicamba tolerance trait might be associated with drought stress-induced gene, *1e16*. Expression study of *TIR1*, *AFB1,* and *AFB2* genes using qPCR showed relative differential expression of *TIR1* between tolerant accessions and susceptible cultivars. No difference was observed between tolerant accessions and cultivars in the relative expression of *AFB1* and *AFB2* genes. Biochemical compounds quantified were related to auxin herbicide activity and correlated with gene expression data; the levels of H_2O_2 and HCN were increased in susceptible cultivars over time, but not in tolerant accessions.

Keywords: Auxin herbicides, Gene expression, Herbicide drift, Herbicide resistance mechanism, Herbicide tolerance

Abbreviations: ABA, abscisic acid; ACC, 1-aminocyclopropane-1-carboxylic acid; AFB, auxin-related F-box; Aux/IAA, auxin/indole-3-acetic acid; DAA, days after application; ETH, ethylene; HAA, h after application; HCN, hydroxide cyanide; H_2O_2, hydrogen peroxide; MCPA, 2-methyl-4-chlorophenoxyacetic acid; NCED, 9-cis-epoxycarotenoid dioxygenase; ROS, reactive oxygen species; TIR1, transport inhibitor response 1; WAP, weeks after planting

INTRODUCTION

Tomato (*Solanum lycopersicum* L.) is highly sensitive to herbicides, particularly auxin-like herbicides (Hemphill and Montgomery, 1981; Jordan and Romanowski, 1974; Kruger et al., 2012; Lovelace et al., 2007a; Zangoueinejad et al., 2019). Auxin-like herbicides cause severe damage to tomato even at low concentrations, such as at drift rate (Hemphill and Montgomery, 1981; Jordan and Romanowski, 1974; Kruger et al., 2012; Fagliari and Oliveira Jr., 2005). Plants exposed to auxinic herbicides or natural auxins at high concentrations exhibit symptoms such as leaf epinasty and tissue swelling, and consequently, horizontal stem curvature, stem narrowing, chlorosis, and necrosis (Cobb, 1992; Grossmann, 2000; Sterling and Hal, 1997).

By increasing the concentration of auxinic compounds (synthetic or phytohormone) in plant tissues, numerous biochemical pathways are triggered, including the activation of 1-aminocyclopropane-1-carboxylic acid (ACC) synthase, overproduction of ethylene (ETH), abscisic acid (ABA) biosynthesis, xanthophyll cleavage,

overproduction of H_2O_2 (hydrogen peroxide), and production of HCN (hydroxide cyanide), which eventually leads to plant death (Cobb, 1992; Grossmann, 2000; Raghavan et al., 2006; Romero-Puertas et al., 2004a; Valenzuela-Valenzuela et al., 2001). Pea plants (*Pisum sativum*L.) treated with 2,4-D showed increased oxidative stress due to the overproduction of superoxide radicals (O_2-) and H_2O_2 (Romero-Puertas et al., 2004a). Meanwhile, Ivanchenko et al. (2013) reported that exposure of tomato to auxinic compounds increased the concentration of H_2O_2 in root tips. Similarly, the HCN content was three times higher in quinclorac treated *Echinochloa cross-galli* L. compared to untreated plants (Grossmann and Kwiatkowski, 1995). By increasing the concentration of the auxinic compound, the level of HCN was increased in plant tissues. Because HCN results in increased ethylene concentration, plant growth is severely retarded, resulting in plant death (Grossmann and Kwiatkowski, 1993, 1995). The measure of HCN in plant tissue, therefore, provides a general view of the concentration of ethylene present in plant tissues. Additionally, numerous molecular mechanisms are affected by the presence of high levels of auxinic compounds (Grossmann, 2010; Mithila et al., 2011). The F-box transport inhibitor response 1 (TIR1) protein and auxin/indole-3-acetic acid (Aux/IAA) receptors recognize auxinic compounds in plant tissues and control transcriptional responses to auxins (Grossmann, 2010; Mithila et al., 2011; Kepinski and Leyser, 2005). Aux/IAA repressor proteins after binding to the promoters of auxin-responsive genes at a low concentration of auxinic compounds prevent the expression of these genes (Grossmann, 2010; Mithila et al., 2011; Kepinski and Leyser, 2005; Chapman, 2009). By increasing the concentration of auxinic compounds, the expression of auxin-responsive genes is induced via the ubiquitin-mediated degradation of transcriptional repressors. The Aux/IAA transcriptional repressor proteins bind to SCFTIR1/AFBs E3 ligase, followed by degradation through the ubiquitin-proteasome pathway (Grossmann, 2010; Mithila et al., 2011; Ludwig-Müller, 2011; Tromas et al., 2013; Dharmasiri and Dharmasiri, 2005; Parry et al., 2009).

All the molecular and biochemical pathways described above occur in auxin herbicide susceptible plants (Mithila et al., 2011; Kern et al., 2005; Lovelace et al., 2007b), and a modification in any of these mechanisms may result in tolerance to auxin herbicides, such as in auxin-tolerant plants (Gleason et al., 2011; Walsh et al., 2006). A single dominant gene is associated with resistance to 2,4-D, dicamba, and picloram in wild mustard (*Sinapis arvensis* L.) (Jugulam et al., 2005); resistance to clopyralid and picloram in yellow starthistle (*Centaurea solstitialis* L.) is due to a single recessive gene (Sabba et al., 2003); while resistance to MCPA (2-methyl-4-chlorophenoxyacetic acid; a selective phenoxy herbicide) is attributed to two additive genes in common hemp nettle (*Galeopsis tetrahit* L.) (Weinberg et al., 2006). As proposed, the incidence of resistance to auxin herbicides in dicot weeds may appear via mutations at several loci syllogism (Gressel et al., 1982).

The objective of the current study was to identify the molecular and biochemical basis of dicamba tolerance in three wild tomato accessions identified from our previous research (Zangoueinejad et al., 2019). A gene expression analysis was conducted to determine the potential role of F-boxTIR1/AFB in dicamba tolerance. Moreover, the levels of H_2O_2 and HCN in response to dicamba application were measured and compared between dicamba-tolerant and susceptible tomato accessions.

MATERIALS AND METHODS

In our previous greenhouse and field studies, TOM199, TOM198, and TOM300 was approximately 7, 7, and 6.5-fold more tolerant to dicamba (at drift rate; 2.8 g ae ha^{-1}) compared to susceptible commercial cultivars (Money Maker and Better Boy). In this current study, we conducted a greenhouse experiment to confirm the previous results.

Greenhouse Screening Study

The experiment was conducted at the R.R. Foil Plant Science Research Center, Mississippi State University, Mississippi State, MS, in 2018. Tomato seeds were sown in 72-cell trays (size of each tray: 50.8 × 25.4 × 6.7 cm) filled with potting mix (SunGro

Horticulture Sunshine Mix #2 Basic). All wild tomato accessions (TOM199, TOM198, and TOM300) were obtained from the Tomato Genetic Resource Center at the University of California in Davis, CA. Meanwhile, two commercial cultivars (Money Maker and Better Boy) were obtained from a commercial seed company (Burpee Seed Co., Warminster, PA). All three wild accessions belong to *Solanum lycopersicum*. Plants were watered once a day to field capacity after the emergence of seedlings and were fertilized [20:20:20 formulated fertilizer (MiracleGro)] twice a week from seedling emergence until the end of the experiment. Dicamba (Clarity®; BASF Corporation) was applied at the simulated drift rate of 2.8 g ae ha^{-1} (0.01X) (Kruger et al., 2012), at 4 weeks after planting (WAP) (15 cm height), using a single-tip spray chamber fitted with a TP8002VS Flat spray tip (TeeJet®, Wheaton, IL). The spray boom was calibrated to deliver 186 L ha^{-1} at 275.79 kPa while maintaining a constant speed of 4.8 KPH. Tomato plants were rated for visual injury (using a scale of 0 to 100%; 0 means no injury symptoms and 100% for plant death) and plant height at 7, 14, 21, and 28 days after application (DAA) of dicamba. All foliage tissues were harvested from the soil surface (at 28 DAA), oven-dried at 50°C for 72 h, and then weighed (g $plant^{-1}$). Also, for the gene expression study and H_2O_2 and HCN analysis, tomato leaf tissues were harvested at 0, 6, 12, 24, and 48 h after application (HAA) of dicamba using liquid nitrogen and stored in -80ºC until analysis.

Hydrogen Peroxide (H_2O_2) Content Assay

The concentration of H_2O_2 in leaf tissues of dicamba treated tomato plants was measured using spectroflurometric method, as described previously by Guilbault et al. (1967). Briefly, crude extracts were filtered through two nylon layers after homogenizing leaf tissues (0.4 g) in 1.2 mL 25 mM HCl. The resulting crude extract was mixed with 15 mg of charcoal (Sigma-Aldrich, St Louis, MO, USA) to remove pigments, and centrifuged at 5000 *g* for 5 min. The supernatant was clarified by passing through a 0.22-mm filter unit (Whatman 7402-001 Filter Circles, Maidstone, United Kingdom). After adjusting the pH of leaf extracts to 7.0 using NaOH, the extracts were used to measure the H_2O_2 concentration. The reaction mixtures (3 mL) contained 50 mM Hepes buffer (pH 7.6), 5 mM homovanillic acid, and 100 mL of extract, and the reaction was started by adding 40 mM horseradish peroxidase in a spectrofluorophotometer (NanoDrop-ND-10000, Thermo Scientific, Waltham, MA) at excitation and emission wavelengths of 315 and 425 nm, respectively. The H_2O_2 concentration was determined from a calibration curve of H_2O_2 (Merck, Darmstadt, Germany) in the range of 0.5–20 mM. All operations were carried out at 4ºC.

Colorimetric Determination of Hydrogen Cyanide (HCN)

According to Lambert et al. (1975), tomato leaf tissues (1 g) were presoaked in 2% KCI solution in a blotted dry (50-mL flask) for 2 h. Then a 10-mL flask was used to incubate previous blotted dry at 25°C. The released HCN was trapped in each flask containing a plastic center well with 200 µL of 0.1 N NaOH. Finally, 200 µL of the trap solution (0.1 N NaOH) was added to a mixture consisting of 100 µL 1 M acetic acid, 1 mL 0.25% succinimide/0.025% n-chlorosuccinimide reagent, and 200 µL 3% barbituric acid in 30% pyridine. Finally, all ingredients were mixed by shaking, and the sample absorbance was read at 580 nm after 10 min.

Identification of Homologous Gene Sequence (S) Associated with Dicamba Tolerance Using SSR Markers

All herbicide-tolerant and susceptible tomato plants were propagated at the R.R. Foil Plant Science Research Center greenhouse of Mississippi State University. Seeds were planted in 8-in pots filled with Sunshine #1 (Sun Gro Horticulture Canada Ltd, Vancouver, Canada) and the experiment was designed in a completely randamozied design with four replications. Leaf tissues were harvested from each plant (tolerant and susceptible) at the four-leaf stage, and total genomic DNA was extracted using a modified hexadecyl trimethylammonium bromide (CTAB) protocol. The genomic DNA was quantified using a NanoDrop spectrophotometer (NanoDrop-ND-10000, Thermo Scientific, Waltham, MA), diluted to 100 ng μL^{-1} with deionized water, and used as a template in the polymerase chain reaction (PCR). Nineteen most polymorphic (locus-specific

and abundant) SSR markers for tomato were selected: 7 from Benor et al. (2008), and 12 from Korir et al. (2014) (Table 1). Benor et al. (2008) used the 7 SSR markers to assess the genetic variation in tomato (*Solanum lycopersicum* L.) inbred lines, while Korir et al. (2014) investigated genetic diversity and relationships among different tomato varieties using the 12 SSR markers. Amplification reactions were carried out in a total volume of 25 µL, which consisted of 2 µL DNA template, 12.5 µL Mastermix (M0270L, New England Biolabs, Ipswich, Massachusetts 1938 United States), 1 µL of each primer (1 µM), and 8.5 µL nuclease-free water (B1500S, New England Biolabs, Ipswich, Massachusetts 1938 United States). Reactions were run in a 96-well plate in Thermal Cycler (MyCycler™ Thermal Cycler System #1709703, Bio-Rad, California, USA) with the following cycling conditions: initial denaturation of one cycle of 94ºC for 5 min; 35 cycles of denaturation, annealing, and extension at 94°C for 40 s, 55ºC for 1 min, and 72°C for 1 min, respectively, and a final extension of 72ºC for 10 min. The PCR amplification products were verified by polyacrylamide gel electrophoresis (8%). Bands were detected using ethidium bromide (X328, VWR, Ireland) staining, and allele sizes were determined using a 100 bp ladder (N3231S, New England Biolabs, Ipswich, MA, USA).

To confirm the SSR reproducibility, each marker was amplified with the same tomato accession twice. Then, Nucleotide BLAST (Web BLAST, NCBI) was used to identify the gene(s) that the SSR markers were associated with, specifically the genes related to abiotic stress tolerance since herbicide is also a form of abiotic stress.

Gene Expression Analysis

The expression level of *TIR1*, *AFB1*, and *AFB2* were examined to determine the expression pattern of F-box$^{TIR1/AFB}$ in tolerant and susceptible tomato lines at 0, 6, 12, 24, and 48 HAA (2.8 g ae ha^{-1}). Total RNA from samples was isolated using Trizol, according to Portillo et al. (2006). The first-strand cDNA synthesis was performed using 2 ng of total RNA by Reverse Transcription System (A5000, Promega, USA). Quantitative PCR (qPCR) was performed using cDNAs corresponding to 2.5 ng of total RNA in a 10 µL reaction volume using SYBR GREEN PCR Master Mix (Probe-Based Real-Time qPCR-Promega) on a real-time PCR system (CFX96 Touch™ Real-Time PCR Detection System, Bio-Rad, USA). The forward (F) and reverse (R) primers used in qPCR are listed in Table 2. The qPCR machine was programmed as follows: 50ºC for 2 min; 95ºC for 10 min; followed by 40 cycles of 95ºC for 15 s, and 60ºC for 1 min; and, one cycle of 95ºC for 15 s, and 60ºC for 15 s. Four biological replicates were included for all qPCR experiments and each reaction was run in duplicate. The Ct (cycle threshold) is defined as the number of cycles required for the fluorescent signal to cross the threshold (i.e., exceeds background level). Relative fold differences were calculated based on the comparative Ct method using the *Actin* as an internal standard. Additionally, relative fold differences for each sample in each experiment were determined using the Ct value for the transcripts *TIR1*, *AFB1*, and *AFB2*. Then those were normalized to the Ct value for *Actin* and was calculated relative to a calibrator using the formula $2^{-\Delta\Delta Ct,}$ according to Livak and Schmittgen (2001).

Table 1. Simple sequence repeat markers used in the genetic study.

Primer Name	Primer Sequence	Annealing Temperature (℃)	Reference
AI773078 55	F: GAT GGA CAC CCT TCA ATT TAT GGT R: TCC AAG TAT CAG GCA CAC CAG C	55	Benor et al., 2008
AW034362	F: CCG CCT CTT TCA CTT GAA C R: CCA GCG ATA CGA TTA GAT ACC	55	Benor et al., 2008
AI895126	F: GCT CTG TCC TTA CAA ATG ATA	55	Benor et

	CCT CC R: CAA TGC TGG GAC AGA AGA TTT AAT G		al., 2008
SSR50	F: CCG TGA CCC TCT TTA CAA GC R: TTG CTT TCT TCT TCG CCA TT	55	Benor et al., 2008
Tom236-237	F: GTT TTT TCA ACA TCA AAG AGC T R: TGC AAA GAA CAA AGA CCG TG	55	Benor et al., 2008
SLR4	F: ACT GCA TTT CAG GTA CAT ACT CTC R: ATA AAC TCG TAG ACC ATA CCC TC	56	Korir et al., 2014
SLR10	F: AGA ATT TTT TCA TGA AAT TGT CC R: TAT TGC GTT CCA CTC CCT CT	58	Korir et al., 2014
SLR13	F: GCC ACG TAG TCA TGA TAT ACA TAG R: GCC TCG GAC AAT GAA TTG	60	Korir et al., 2014
SL16	F: CGG CGT ATT CAA ACT CTT GG R: GCG GAC CTT TGT TTT GGT AA	58	Korir et al., 2014
SLR18	F: CGA TTA GAG AAT GTC CCA CAG R: TTA CAC ATA CAA ATA TAC ATA GTC TG	58	Korir et al., 2014
SLR19	F: AGC CAC CCA TCA CAA AGA TT R: GTC GCA CTA TCG GTC ACG TA	58	Korir et al., 2014
SLR2	F: TGT TGG TTG GAG AAA CTC CC R: AGG CAT TTA AAC CAA TAG GTA GC	56	Korir et al., 2014
SLR21	F: CCT TGC AGT TGA GGT GAA TT R: TCA AGC ACC TAC AAT CAA TCA	58	Korir et al., 2014
SLR22	F: TTG GTA ATT TAT GTT CGG GA R: TTG AGC CAA TTG ATT AAT AAG TT	52	Korir et al., 2014
SLR23	F: ACA AAC TCA AGA TAA GTA AGA GC R: GTG AAT TGT GTT TTA ACA TGG	54	Korir et al., 2014
SLR26	F: AAC GGT GGA AAC TAT TGA AAG G R: CAC CAC CAA ACC CAT CGT C	60	Korir et al.,2014
SLR27	F: ATT GCT CAT ACA TAA CCC CC R: GGG ACA AAA TGG TAA TCC AT	60	Korir et al., 2014
TMS37	F: CCT TGC AGT TGA GGT GAA TT R: TCA AGC ACC TAC AAT CAA TCA	55	Benor et al. 2008
U81996	F: AGG TTG ATG AAA GCT AAA TCT GGC R: CAA CCA CCA ATG TTC ATT ACA AGA C	55	Benor et al. 2008

Table 2. Primer sequences used for qPCR amplification.

Primer	Primer sequences
TIR1-F	5#-AGG GGT CCT CCA GAT ACA AG-3#
TIR1-R	5#-CGC TAA TAC CTG CCC ATC TTT-3#
AFB1-F	F 5#-ACT GCG AGA ACT GAG GGT GT-3#
AFB1-R	5#-TCA CAC AGA GAC GGA AGC AC-3#
AFB2-F	F 5#-CGC AGC TGA GAT TCA TGG TA-3#
AFB2-R	5#-TTG CCT CCA CCG AGT AAA TC-3#
Actin-F	5#-TGT CCC TAT TTA CGA GGG TTA TGC-3#
Actin-r	R 5#-CAG TTA AAT CAC GAC CAG CAA GAT-3#

Statistical Analysis

The greenhouse study was arranged in a completely randomized design with four replications in a factorial arrangement of three factors including herbicide options (dicamba and untreated control), tomato line types (three wild accessions, TOM199, TOM198, and TOM300; and two tomato commercial cultivars, Money Maker and Better Boy), and four-time points (7, 14, 21, and 28 DAT). However, the plant dry weight was only evaluated at 28 DAT, thus, only two factors (tomato line types and herbicide options) were included in the analysis. Meanwhile, for H_2O_2 and HCN assay and *AFB1*, *AFB2*, and *TIR1* **gene expression study, t**wo factors, tomato accession types and different time points (0, 6, 12, 24, and 48 HAA) were included. The experiments were repeated twice. The homogeneity was checked based on the Levene's test. After plotting the Q-Q. (quantile-quantile) plots in GraphPad Prism 8 (GraphPad Software, San Diego, CA, USA), it was revealed that the residual effects were normally distributed. The experimental run or run by factor (treatment) interactions were not significant for either experiment, so data were combined across experimental runs (in each experiment). All data were subjected to ANOVA using PROC MIXED SAS 9.4 (SAS Institute, Cary, NC, USA), and means were separated using LSD's-test at $P \leq 0.05$.

The concentration of H_2O_2 and HCN, in addition to relative expression levels of *TIR1*, *AFB1*, and *AFB2* were plotted using linear regression (Eq. 1) against time points to compare these traits among tomato lines over time.

$$Y=ax+b \quad \text{Eq. [1]}$$

In the linear regression equation, Y was the value of H_2O_2 and HCN in leaf tissue samples of tomato lines or the level of relative expression of *TIR*1, *AFB1*, and *AFB2* in foliage samples of wild and commercial cultivars. Independent variable, x, is the h after the application of dicamba at the drift rate (2.8 g ae ha^{-1}). Furthermore, a and b are the slope and intercept of the equation, respectively. The fitted linear regression curves based on the different independent variables during all time points were compared among tomato lines by contrasting the best-fit values using one-way ANOVA. All graphs were generated using GraphPad Prism 8 (GraphPad Software, San Diego, CA, USA) and Microsoft Excel (Microsoft Redmond, WA, USA).

RESULTS

Greenhouse Study

The results presented in Table 3 indicate that all treatments and their combinations were significant ($P < 0.01$) based on visible injury and dry weight. The percentage of visual damages for TOM199, TOM198, and TOM300 were significantly lower than commercial cultivars (Money Maker and Better Boy) at 7, 14, 21, and 28 DAA (Figure 1). The levels of visual injury were 1, 0, 1, 63, and 69 % for TOM199, TOM198, TOM300, Money Maker, and Better Boy, respectively, at 7 DAA (Figure 1). The level of visual injury was gradually increased over time so that it was higher for all accessions and cultivars at 14, 21, and 28 DAA compared to the first observation at 7 DAA. Nevertheless, wild accessions survived at 28 DAA

(Figure 1). Meanwhile, the dry weight of TOM199, TOM198, TOM300, Money Maker, and Better Boy was 0.8, 0.77, 0.825, 0.33, and 0.3 g plant^{-1}, respectively (Figure 1). This suggests that the reduction in the dry weight of TOM199, TOM198, and TOM300 compared with their control plots was lesser than both Money Maker and Better Boy (Figure 1). Thus, all three wild accessions TOM199, TOM198, and TOM300 showed tolerance against dicamba application at the drift rate (2.8 g ae ha^{-1}) (Figure 1).

Table 3. Analysis of variance (ANOVA) for the effects of tomato accession types, time points, and herbicide, on visible injury and dry weight.

		Mean of square	
Source of variation	df	Visible injury	Dry weight
Tomato accession	4	1270601×10^{-2}**	779×10^{-2}**
Time	3	88473×10^{-2} **	-
Herbicide	1	4882515×10^{-2} **	39753×10^{-2}**
Tomato accession*time	12	4216×10^{-2}**	-
Tomato accession*herbicide	4	1270601×10^{-2}**	2256×10^{-2}**
Time*herbicide	3	88474×10^{-2}**	-
Tomato accession*time*herbicide	12	4216×10^{-2}**	-
C.V		1389×10^{-2}	542×10^{-2}

** P < 0.01, LSD's test.

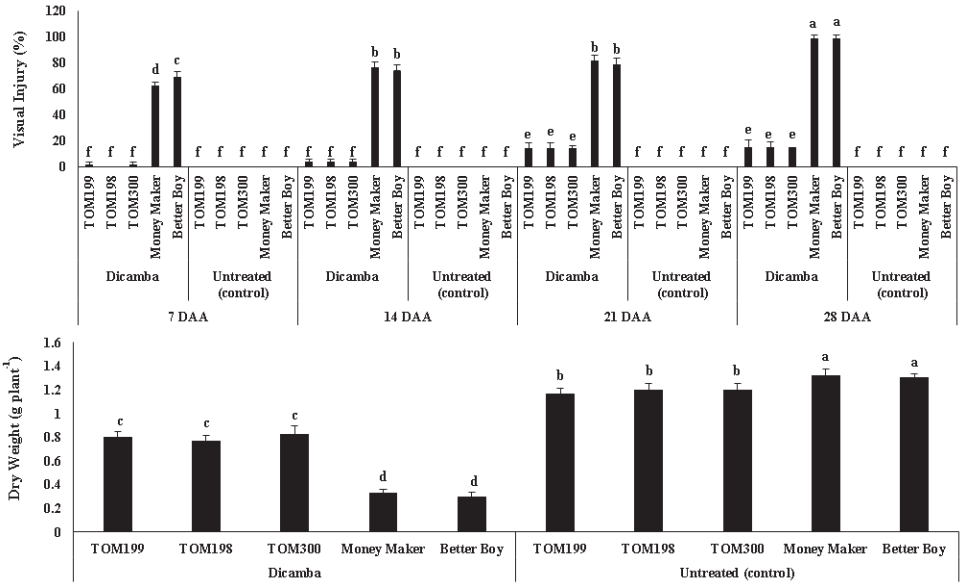

Figure 1. Comparison of the level of visible injury at 7, 14, 21, and 28 DAA and plant dry weight at 28 DAA among TOM199, TOM198, TOM300, Better Boy, and Money Maker. The S.E. of the mean is represented by vertical bars (n=8). Different letters indicate significant differences within each column at P≤0.05 based on the LSD test.

Immediately before dicamba treatment (0 HAA),

H2O2 and HCN Content Assay

Immediately before dicamba treatment (0 HAA), all accessions and cultivars contained similar levels of H_2O_2 (Figure 2A). At 6 HAA, the concentration of H_2O_2 increased in both the cultivars and continued to grow until the final time point (48 HAA) (Figure 2A). The level of H_2O_2 increased from 6 to 12 HAA in all three accessions, after which it decreased from 24 to 48 HAA (Figure 2A). The concentration of H_2O_2 was 86, 94, 85, 383, and 391 nmol (g FW)^{1} in TOM199, TOM198, TOM300, Money Maker, and Better Boy, respectively, at 48 HAA (Figure 2A). Additionally, across all time points, the highest (391 nmol (g FW) $^{-1}$) and the lowest (85 nmol (g FW) ^{1}) concentration of H_2O_2 was recorded for Better Boy and TOM300, respectively, at 48 HAA (Figure 2A). No differences were observed among the fitted linear regression equations based on the H_2O_2 content in the foliage samples of tomato accessions (Figure 2B); however, TOM199, TOM198, and TOM300 were different compared to Money Maker and Better Boy ($P \leq 0.05$) over time (Figure 2B).

The HCN measurements demonstrated that at the initial time point (0 HAA), all tomato accessions were significantly different in comparison to the cultivars (Figure 3A). Although the quantity of HCN was higher in all accessions from 0 to 6 HAA, it remained constant, with only a few variations from 12 to 48 HAA (Figure 3A). The concentration of HCN in TOM199, TOM198, and TOM300 was 9.02, 10.53, and 9.13 nmol (g FW)^{1}, respectively, at 48 HAA (Figure 3A). The quantity of HCN in Money Maker, and Better Boy was 3.2 and 2.7 times higher, respectively, at 48 HAA than at 0 HAA (Figure 3A). The highest (26.37 nmol (g FW) $^{-1}$) and lowest (9.02 nmol (g FW) $^{-1}$) concentration of HCN were observed in Money Maker and TOM199, respectively, at 48 HAA (Figure 3A). Overall, the level of HCN in both cultivars was increased over time but stayed constant in all the three tolerant accessions from 6 to 48 HAA (Figure 3A). Moreover, there were no significant differences among the linear regression equations of dicamba-tolerant tomato wild accessions in terms of HCN content over time (Figure 3B). On the other hand, according to the fitted linear regression equations, the HCN was lower in TOM199 and TOM300 compared to both Money Maker and Better Boy ($P \leq 0.01$) (Figure 3B). The accession TOM198 was different compared to Money Maker ($P \leq 0.05$) and Better Boy ($P \leq 0.01$) (Figure 3B).

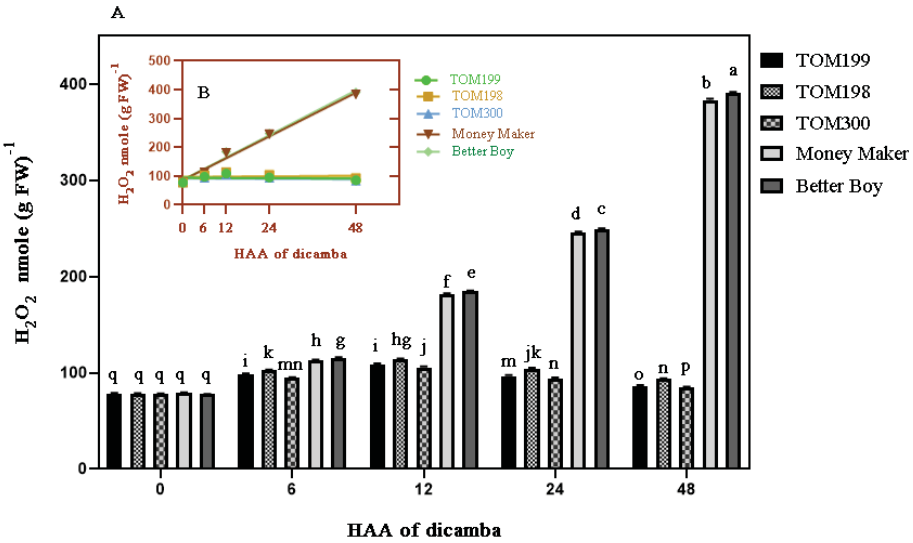

Figure 2. A. Comparison of the concentration of H_2O_2 for tomato accessions and cultivars among all time points (0, 6, 12, 24, and 48 HAA). The S.E. of the mean is represented by vertical bars (n=8). Different letters indicate significant differences within each column at $P \leq 0.05$ based on the LSD test. B. Comparison of the relationship between the level of H_2O_2 content against time points using linear regression equations among tomato accessions and cultivars. The S.E. of the mean is represented by vertical bars (n=8).

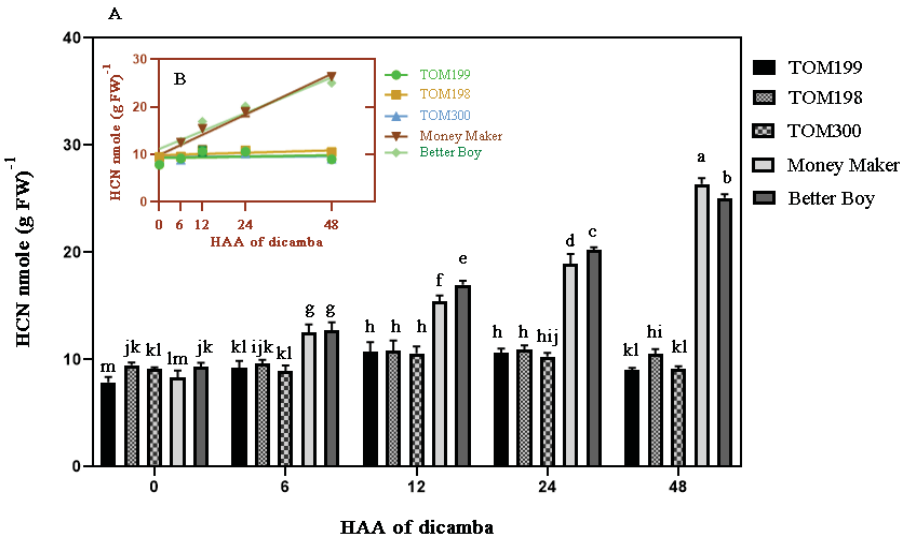

Figure 3. A. Comparison of the concentration of HCN for tomato accessions and cultivars among all time points (0, 6, 12, 24, and 48 HAA of dicamba at a rate of 2.8 g ae ha^{-1}). The S.E. of the mean is represented by vertical bars (n=4). Different letters indicate significant differences within each column at P≤0.05 based on the LSD test. B. Comparison of the relationship between the level of HCN content against time points using linear regression equations among tomato accessions and cultivars. The S.E. of the mean is represented by vertical bars (n=4).

Identify Homologous Sequences of Gene/Genes Which Can Donate Tolerance against Dicamba using SSR Markers

Among all the nineteen SSR markers, only SLR21, TMS37, Tom236-237, and U81996 produced band with the genomic DNA of wild tomato accessions. According to Figure 4, SLR21 produced a band with TOM300 and was 100 bp in size, while TMS37 produced a 100 and 120 bp band with TOM300 and TOM199, respectively (Figure 4). Moreover, Tom236-237 generated a band only with TOM300, and its size was approximately 110 bp (Figure 4). Finally, U81996 displayed a 100 bp band with two wild tomato accessions, TOM300, and TOM198 (Figure 4). After blasting the sequence of each primer (SLR21, TMS37, Tom236-237, and U81996) using NCBI Nucleotide Blast, the *le16* gene [(GenBank: U81996.1; *Lycopersicon esculentum* nonspecific lipid transfer protein (*le16*) mRNA)] (Plant et al., 1991) was found to be associated with the U81996 primer. The percentage of both coverage and identity for *le16* was 100%. No other genes were found to be associated with the other primer sequences.

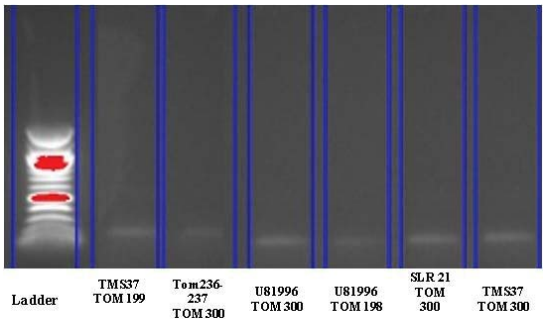

Figure 4. Agarose gel electrophoresis showing banding patterns of the tomato accessions using the simple sequence repeat markers.

Expression Patterns of F-Box$^{tir1/AFB}$

The different time points had a significant effect on the expression level of *AFB1*, *AFB2*, and *TIR1* genes (Table 4). However, two other factors, tomato accession types and time x tomato accession type interaction, showed a significant impact on the expression level of the *TIR1* gene (Table 4). Analysis of real-time qPCR indicated that there were differences in the relative expression of *TIR1* among the three tolerant wild tomato accessions at all time points (Figure 5A). At the first time point (0 HAA), no differences were observed between accessions and cultivars in the expression level of *TIR1* (Figure 5A). Accessions TOM199 and TOM300 expressed 0.029 and 0.027-fold relative expression of *TIR1* at 6 HAA, respectively, and were lower than TOM198 and both cultivars (Figure 5A). Money Maker and Better Boy were different in their relative expression of *TIR1* at 6 HAA, but were not different at other time points (Figure 5A); TOM199 and TM198 were not different at 12 and 24 HAA (Figure 5A). The relative expression of *TIR1* in TOM199, TOM198, TOM300, Money Maker, and Better Boy was 0.02, 0.024, 0.016, 0.046, and 0.046-fold, respectively, at 48 HAA (Figure 5A). TOM300 presented the lowest relative expression of *TIR1* at 12, 24, and 48 HAA and was 0.022, 0.018, and 0.016-fold low, respectively (Figure 5A). Meanwhile, the relative expression of *TIR1* in TOM198 was higher than TOM300 at 6, 12, 24, and 48 HAA by 20, 26, 43, and 48%, respectively (Figure 5A). Interestingly, the relative expression of TIR1 in both cultivars was higher than all accessions at 6, 12, 24, and 48 HAA (Figure 5A). In comparison to TOM300 (lowest relative expression of *TIR1*), both cultivars had 1.5, 2, 2.5, and 2.8-fold higher relative expression of *TIR1* at 6, 12, 24, and 48 HAA, respectively (Figure 5A). On comparing the relative expression of TIR1 in all accessions and cultivars across all time points, the relative expression of *TIR1* in all three accessions was found to be reduced over time (Figure 5A). In other words, the relative expression of *TIR1* in accessions TOM199, TOM198, and TOM300 at 48 HAA was lower than at 0 HAA by 1.55, 1.29, and 1.94 times, respectively (Figure 5A). On the other hand, the relative expression of *TIR1* in Money Maker and Better Boy was increased from 0 to 48 HAA (Figure 5A), so that both cultivars, Money Maker and Better Boy, displayed 0.032 and 0.046-fold of relative *TIR1* expression, respectively, at 0 and 48 HAA (Figure 5A). Moreover, it was determined that there were no differences among the fitted linear regression equations of the dicamba-tolerant wild tomato accessions (Figure 5B); however, TOM199 and TOM198 were different in comparison to Money Maker and Better Boy ($P \leq 0.0001$) (Figure 5B). The fitted linear regressions based on the recorded expression level of *TIR1* for Money Maker and Better Boy were different compared to TOM300 ($P \leq 0.001$ and $P \leq 0.0001$, respectively) (Figure 5B). Differences in the relative expression of *AFB1* and *AFB2* were not significant between cultivars and accessions at each time point (Figs. 6A and 7A). However, the relative expression levels of *AFB1* and *AFB2* was increased in the accessions and cultivars over time (Figs. 6A and 7A). The fitted linear regressions based on the expression level of *AFB1* and *AFB2* were not different among tomato accessions and cultivars (Figs. 6B and 7B).

Table 4. Analysis of variance (ANOVA) for the effects of tomato accession types and time points on H_2O_2 and HCN content and expression level of *AFB1*, *AFB2*, and *TIR1*.

Source of variation	df	Mean of square				
		H_2O_2	HCN	Expression of *AFB1*	Expression of *AFB2*	Expression of *TIR1*
Tomato accession	4	6884009×10^{-2}**	27693×10^{-2}**	39×10^{-8}NS	54×10^{-8}NS	3.72**
Time	1	5292926×10^{-2}**	16398×10^{-2}**	14572×10^{-8}**	14402×10^{-8}**	5512×10^{-8}**
Tomato accession*time	4	1710568×10^{-2}**	4668×10^{-2}**	2×10^{-7}NS	48×10^{-8}NS	13843×10^{-8}**
C.V		159×10^{-2}	402×10^{-2}	134×10^{-2}	26×10^{-1}	372×10^{-2}

** $P < 0.01$, NS Non-significant, LSD's test.

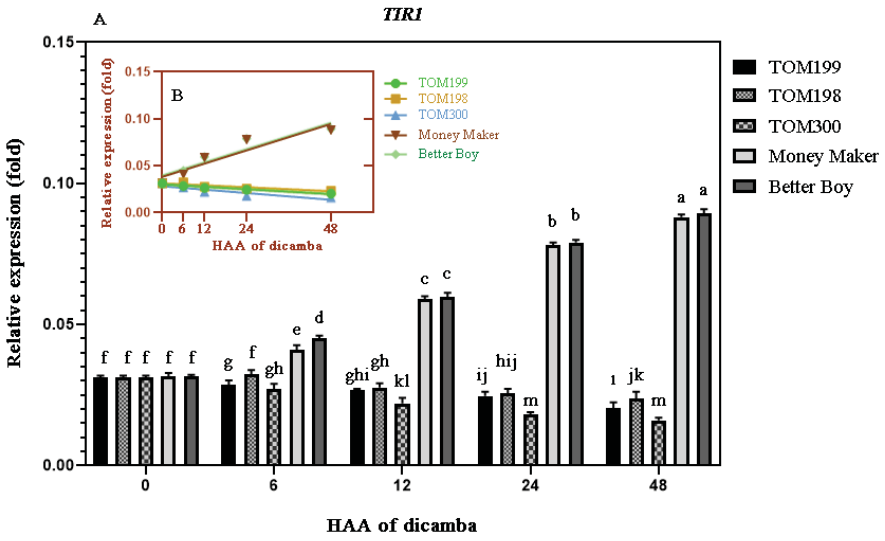

Figure 5. A. Comparison of relative expression of *TIR1* in tomato accessions and cultivars leaf tissues among all time points (0, 6, 12, 24, and 48 HAA of dicamba at rate 2.8 g ae ha^{-1}). The analysis was performed with three biological repeats, each in duplicate with similar results. The S.E. of the mean is represented by vertical bars (n=4). Different letters indicate significant differences within each column at P≤0.05 based on the LSD test. B. Comparison of the relationship between the expression level of *TIR1* against time points using linear regression equations among tomato accessions and cultivars. The S.E. of the mean is represented by vertical bars (n=4).

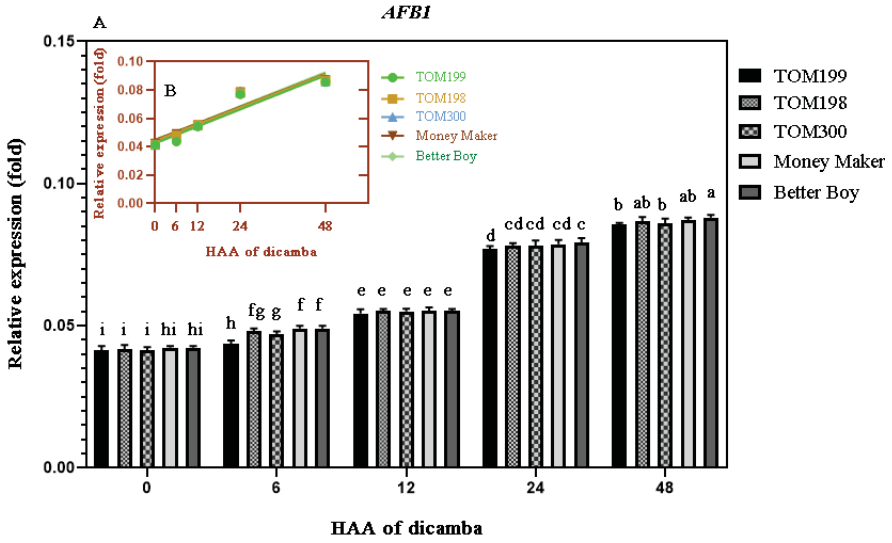

Figure 6. A. Comparison of relative expression of AFB1 in tomato accessions and cultivars leaf tissues among all time points (0, 6, 12, 24, and 48 HAA of dicamba at a rate of 2.8 g ae ha^{-1}). The analysis was performed with three biological repeats, each in duplicate with similar results. The S.E. of the mean is represented by vertical bars (n=4). Different letters indicate significant differences within each column at P≤0.05 based on the LSD test. B. Comparison of the relationship between the expression level of AFB1 against time points using linear regression equations among tomato accessions and cultivars. The S.E. of the mean is represented by vertical bars (n=4).

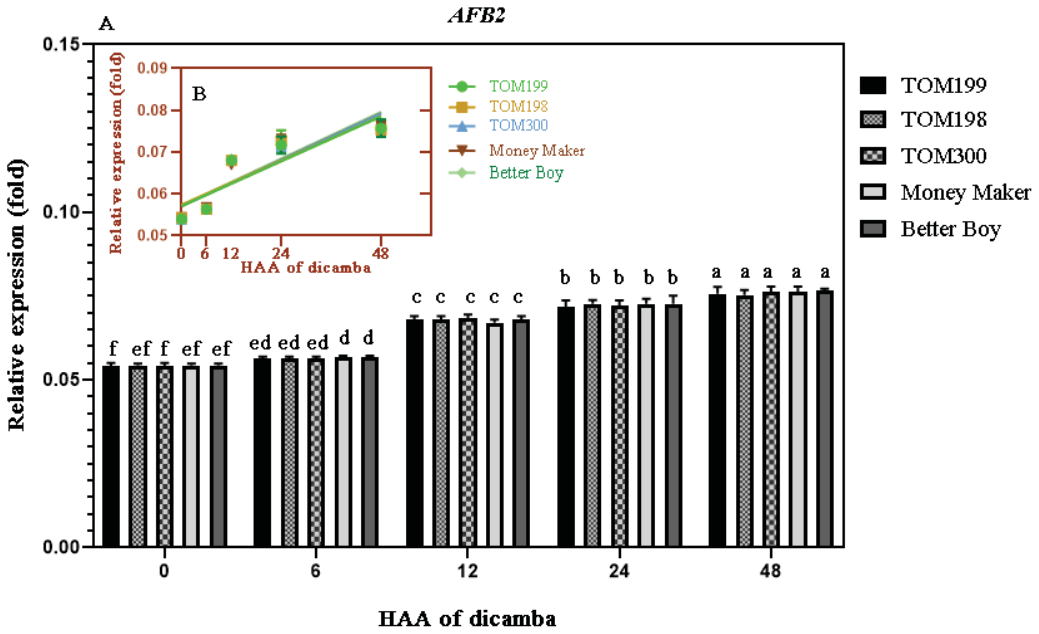

Figure 7. A. Comparison of relative expression of AFB2 in tomato accessions and cultivars leaf tissues among all time points (0, 6, 12, 24, and 48 HAA of dicamba at rate 2.8 g ae ha^{-1}). The analysis was performed with three biological repeats, each in duplicate with similar results. The S.E. of the mean is represented by vertical bars (n=4). Different letters indicate significant differences within each column at P≤0.05 based on the LSD test. B. Comparison of the relationship between the expression level of AFB2 against time points using linear regression equations among tomato accessions and cultivars. The S.E. of the mean is represented by vertical bars (n=4).

DISCUSSION

All three wild accessions showed lower visual injury and dry weight reduction compared to the commercial cultivars after the application of dicamba (Figure 1). Thus, suggesting that wild tomato accessions are tolerant to the application of dicamba at the drift rate (0.01X; 2.8 g ae ha^{-1}). It is important to note that TOM199, TOM198, and TOM300 belong to *Solanum lycopersicum* var. cerasiforme, which have been reported to be tolerant of powdery mildew caused by *Oidium lycopersici* due to a single recessive gene (Ciccarese et al., 1998). , Besides, *S. lycopersicum* var. cerasiformeis is tolerant of cucumber mosaic virus stain Fny (Cillo et al., 2007). Although seeking relationships between disease tolerance and tolerance to dicamba was not one of the goals of this current study, there seems to be an overlap in the signaling and response pathways among different abiotic and biotic stresses in plants (Atkinson and Urwin, 2012). This overlap in signaling pathways may be associated with cross-tolerance phenomena in which plants may develop resistance to other biotic or abiotic stresses (Pastori and Foyer, 2002).

According to the results of the NCBI nucleotide blast, the *1e16* gene was found to be associated with one of the microsatellite markers (U81996) unique to the dicamba-tolerant wild tomato accessions. The *le16* gene is regulated by ABA in aerial vegetative tissues (Lim et al., 2015; Cillo et al., 2007). The *1e16* gene was previously isolated from a drought-induced tomato leaf cDNA library, where it was expressed in high levels in drought-stressed stems and petioles (Lim et al., 2015). The *1e16* gene is also expressed in response to other abiotic stresses such as PEG-mediated water deficit, salinity, cold stress, heat shock, and exogenous applications of ABA (Lim et al., 2015). On the other hand, in the mechanism of action of auxinic compounds (phytohormone and synthetic auxins), the TIR1/AFB [a small family of F-box proteins, including the transport inhibitor

response 1 (TIR1), and homolog auxin-binding F-box (AFB) proteins] plays a vital role as auxin receptors (Grossmann, 2010). Once TIR1/AFB auxin receptors recognize the auxin herbicides, the auxin binding targets Aux/IAA transcriptional repressor proteins to SCFTIR1/AFBs E3 ligase for degradation by the ubiquitin-proteasome pathway (Grossmann, 2010; Chapman and Estelle, 2009; Calderon-Villalobos et al., 2010; Guilfoyle, 2007). The TIR1/AFB auxin receptors act as an F-box recognition component for protein substrate of an Skp1-cullin-F-box protein (SCF) E3 ubiquitin ligase (Grossmann, 2010; Calderon-Villalobos et al., 2010; Guilfoyle, 2007). Consequently, losing Aux/IAA repressors results in the suppression of transcriptional activator proteins or auxin response factors (ARFs) that activate the transcription of auxin-responsive genes (Grossmann, 2010; Chapman and Estelle, 2009; Calderon-Villalobos et al., 2010; Guilfoyle, 2007). This suppression leads to the overexpression of the ACC synthase gene in ethylene production and the 9-cis-epoxycarotenoid dioxygenase (NCED) gene in ABA biosynthesis (Grossmann, 2010; Chapman and Estelle, 2009; Calderon-Villalobos et al., 2010; Guilfoyle, 2007). Overproduction of ethylene results in the downward curvature of leaves (leaf epinasty) and tissue swelling, and regulates auxin levels locally through inhibition of auxin transport (Grossmann, 2010). Additionally, ethylene stimulates NCED activity post-transcriptionally, leading to lasting ABA biosynthesis. The NCED catalyzes xanthophyll cleavage, leading to increased production of xanthoxin and ABA (Grossmann, 2010; Chapman and Estelle, 2009; Calderon-Villalobos et al., 2010; Guilfoyle, 2007), while ABA is distributed throughout the plant and mediates stomatal closure, thus limiting transpiration and carbon assimilation, accompanied by an overproduction of reactive oxygen species (Grossmann, 2010). Cyanide is another compound produced in stoichiometrically equivalent amounts to ethylene, in the presence of auxin herbicides (Yip and Yang, 1988). The oxidation of ACC, catalyzed by ACC oxidase, is what leads to the production of HCN, together with ethylene and CO_2 (Grossmann, 2010; Guilfoyle, 2007; Mockaitis and Estelle, 2008). Based on all the events mentioned above, numerous biochemical pathways become active in response to auxin herbicides, which are, in turn, associated with various genes, one of these being the *1e16* (Ko et al., 2006; Li et al., 2011a). Therefore, all the above evidence leads us to the fact that the *1e16* gene may have a potential role in conferring tolerance to dicamba.

Moreover, the amount of H_2O_2 and HCN were increased in cultivars over time so that the maximum levels of these compounds were observed at 48 HAA of dicamba (Figs. 2 and 3); however, both cultivars were similar in their H_2O_2 and HCN levels at all time points (Figs. 2 and 3). Following the application of auxin herbicides, ethylene biosynthesis is generally stimulated through the induction of ACC synthase, particularly in foliage tissues, and is gradually increased, resulting in abnormal growth of the plant (Grossmann, 2010; Abeles et al., 1992; Abel and Theologis, 1996). Reactive oxygen species may then be overproduced, about 24 h after the application of auxin herbicide (Romero-Puertas et al., 2004a; Grossmann, 2010; Romero-Puertas et al., 2004b). Contrary to the mentioned studies, we observed H_2O_2 overproduction as early as 12 HAA of dicamba (Figure 2). Light microscopy revealed that the primary difference between pea (*Pisum sativum* L., CV. Lincoln) plants treated with 2,4-D, and their untreated controls, were observed in their mesophyll cells (Romero-Puertas et al., 2004a). The authors suggested that 2,4-D induces severe oxidative stress in pea plants, which leads to the increased production of H_2O_2 and O_2.-, leading to the inhibition of photosynthesis and ultimately cell death (Romero-Puertas et al., 2004b). As discussed earlier, the presence of HCN indicates the occurrence of ACC oxidation in the plant, which also results in the production of ethylene and CO_2 (Grossmann, 2010; Guilfoyle, 2007; Mockaitis and Estelle, 2008).

The expression of *TIR1*, *AFB1* and *AFB2* genes and the concentration of H_2O_2 and HCN were simultaneously increased in both susceptible cultivars (Money Maker and Better Boy) over time (Figs. 2, 3, 5, 6, and 7). This was not true for all three dicamba-tolerant accessions (TOM199, TOM198, and TOM300) in terms of *TIR1* expression and concentration of H_2O_2 and HCN (Figs. 2, 3 and 5). The three tolerant accessions and susceptible

cultivars were similar in terms of *AFB1* and *AFB2* expression at each time point after dicamba treatment (Figs. 6 and 7). Similarly, Gleason et al. (2011) indicated that the expression level related to relative dicamba-induced auxin-responsive gene IAA1 in *tir1-1*, *afb5*, and *tir1-1*/*afb5* mutants was significantly lower than in control plants (a wild type of *Arabidopsis*). Although they showed that the expression pattern of IAA5 was different, its relative expression in dicamba-induced transcription in *afb5* and *tir1-1*/*afb5* was lesser than control plants (Gleason et al., 2011). Binding of TIR1 with auxin herbicides ultimately promotes the degradation of Aux/IAA (Mockaitis and Estelle, 2008). Although AFB1 and AFB2 are homologs (with 61-72% amino acid identity) of TIR1, and *TIR1* confers tolerance/resistance to dicamba, these proteins are not associated with dicamba tolerance (Walsh et al., 2006). Therefore, it can be concluded that increased levels of relative expression of the *TIR1* gene in susceptible cultivars over time confirms the presence of dicamba in effective concentration as early as 48 HAA of dicamba (Figure 5). The reason for the decrease in the expression level of *TIR1* in tolerant/resistant plants may be due to the absence of binding between Aux/IAA repressors and TIR1 (Tan et al., 2007). Moreover, the presence of a mutation in the *TIR1* gene develop a change in the binding site of TIR1 protein (Tan et al., 2007), thus preventing the binding of dicamba with this protein (Gleason et al., 2011). To gain insight into understanding the differences in the relative expression level of *TIR1* between tolerant accessions and cultivars, it is foremost essential to know that Aux/IAA repressor proteins (Aux/IAAs) on binding to the promoters of auxin-responsive genes can suppress the expression of auxin-responsive genes at a low concentration of auxin (natural or synthetic) (Chapman and Estelle, 2009; Mockaitis and Estelle, 2008; Tan et al., 2007; Song, 2014). Conversely, by increasing the auxin (natural or synthetic) concentrations, the expression of the *ARF* gene is stimulated via the ubiquitin-mediated degradation of transcriptional repressors (Aux/IAAs) (Grossmann, 2010; Chapman and Estelle, 2009; Guilfoyle, 2007; Mockaitis and Estelle, 2008). There is a binding site on TIR1 where auxinic compounds can bind, thus playing the role of a molecular glue in stabilizing the interaction between receptor protein (including TIR1 and its homologs AFBs), and Aux/IAA repressors (as its substrates) (Tan et al., 2007).

Based on our findings, it is concluded that there are significant differences in the concentration of H_2O_2 and HCN plus expression level of *TIR1* in dicamba-tolerant wild tomato accessions (TOM199, TOM198, and TOM300) compared with the commercial tomato cultivars (Money Maker and Better Boy). As indicated earlier, a mutation in the binding pocket of the *TIR1* gene may confer dicamba-tolerance to plants (Jugulam et al., 2005; Tan et al., 2007). Additional molecular aspects associated with dicamba tolerance at higher rates will need to be investigated. Understanding the dicamba tolerance mechanisms will guide the plant breeders in developing auxin resistant tomato. The availability of herbicide-resistant tomato lines will allow growers to have more options for herbicide applications with reduced residual activity, which in turn will create broader choices for potential rotational crops in intervening seasons. Ultimately, growers will be able to easily control weeds, especially yellow nutsedge and purple nutsedge, the entire growing season without injury to the tomato plants and fruit. The use of herbicide-tolerant tomato can also encourage reduced or no-till practices, which is more sustainable.

CONFLICT OF INTEREST

There is no conflict of interest to declare.

ACKNOWLEDGMENTS

This research was partially funded by the Specialty Crop Block Grant sponsored by the Mississippi Department of Agriculture and Commerce/U.S. Department of Agriculture – Agriculture Marketing Service and is based upon work that is supported by the National Institute of Food and Agriculture, U.S. Department of Agriculture, Hatch project under accession number 230060. The authors would like to thank Swati Shrestha, Shandrea Stallworth, Gourav Sharma, Edicarlos Castro, and Ziming Yue for their assistance throughout the study.

LITERATURE CITED

Abel S, Theologis A. Early genes and auxin action. Plant Physiol. 1996; 111: 9-17.

Abeles FB, Morgan PW, Saltveit Jr ME. 1992. Ethylene in plant biology. Academic press, Inc. 33-42 pp.

Atkinson NJ, Urwin PE. The interaction of plant biotic and abiotic stresses: from genes to the field. J. Exp. Bot. 2012; 63: 3523-3543.

Benor S, Zhang M, Wang Z, Zhang H. Assessment of genetic variation in tomato (*Solanum lycopersicum* L.) inbred lines using SSR molecular markers. J. Genet. Genom. 2008; 35: 373-379.

Calderon-Villalobos LI, Tan X, Zheng N, Estelle M. Auxin perception—structural insights. Cold Spring Harb. Perspect. Biol. 2010; a005546.

Chapman EJ, Estelle M. Mechanism of auxin-regulated gene expression in plants. Annu. Rev. Genet. 2009; 43: 265-285.

Cillo F, Pasciuto MM, De Giovanni C, Finetti-Sialer MM, Ricciardi L, Gallitelli D. Response of tomato and its wild relatives in the genus Solanum to cucumber mosaic virus and satellite RNA combinations. J. Gen. Virol. 2007; 88: 3166-3176.

Cobb A. 1992. Auxin-type herbicides, in: Herbicides and Plant Physiology, Chapman and Hall, Inc. 82–106 pp.

Dharmasiri N, Dharmasiri S, Estelle M. The F-box protein TIR1 is an auxin receptor. Nature. 2005; 435: 441.

Fagliari JR, Oliveira Jr. RSD, Constantin J. Impact of sublethal doses of 2, 4-D, simulating drift, on tomato yield. J. Environ. Sci. Health B. 2005; 40: 201-206.

Gleason C, Foley RC, Singh KB. Mutant analysis in Arabidopsis provides insight into the molecular mode of action of the auxinic herbicide dicamba. PloS One. 2011; 6: e17245.

Gressel J, Segel LA, LeBaron HM. 1982. Interrelating factors controlling the rate of appearance of resistance: the outlook for the future, in: Herbicide Resistance in Plants, Wiley, Inc. 325-347 pp.

Grossmann K. Mode of action of auxin herbicides: a new ending to a long, drawn out story. Trends Plant Sci. 2000; 5: 506-508.

Grossmann K. Auxin herbicides: current status of mechanism and mode of action. Pest Manage. Sci. 2010; 66: 113-120.

Grossmann K, Kwiatkowski J. Selective induction of ethylene and cyanide biosynthesis appears to be involved in the selectivity of the herbicide quinclorac between rice and barnyard grass. J. Plant Physiol. 1993; 142:457-66.

Grossmann K, Kwiatkowski J. Evidence for a causative role of cyanide, derived from ethylene biosynthesis, in the herbicidal mode of action of quinclorac in barnyard grass. Pestic Biochem. Physiol. 1995; 51:150-60.

Guilbault GG, Kramer DN, Hackley E. A new substrate for fluorometric determination of oxidative enzymes. Anal. Chem. 1967; 39: 271.

Guilfoyle, T. Sticking with auxin. Nature. 2007; 446(7136): 621-622.

Hemphill DD, Montgomery ML. Response of vegetable crops to sublethal application of 2, 4-D. Weed Sci. 1981; 29: 632-635.

Ivanchenko MG, Den Os D, Monshausen GB, Dubrovsky JG, Bednářová A, Krishnan N. Auxin increases the hydrogen peroxide (H_2O_2) concentration in tomato (*Solanum lycopersicum*) root tips while inhibiting root growth. Ann. Bot. 2013; 112: 1107-1116.

Jordan TN, Romanowski RR. Comparison of dicamba and 2, 4-D injury to field grown tomatoes. HortScience 1974; 9:74–75.

Jugulam M, McLean MD, Hall JC. Inheritance of picloram and 2, 4-D resistance in wild mustard (*Brassica kaber*). Weed Sci. 2005; 53: 417-423.

Kepinski S, Leyser O. The Arabidopsis F-box protein TIR1 is an auxin receptor. Nature. 2005; 435: 446.

Kern AJ, Chaverra ME, Cranston HJ, Dyer WE. Dicamba-responsive genes in herbicide-resistant and susceptible biotypes of kochia (*Kochia scoparia*). Weed Sci. 2005; 53: 139-145.

Ko JH, Yang SH, Han KH. Upregulation of an Arabidopsis RING-H2 gene, XERICO, confers drought tolerance through increased abscisic acid biosynthesis. The Plant J. 2006; 47(3): 343-355.

Korir NK, Diao W, Tao R, Li X, Kayesh E, Li A, Zhen W, Wang S. Genetic diversity and relationships among different tomato varieties revealed by EST-SSR markers. Genet. Mol. Res. 2014; 13: 43-53.

Kruger GR, Johnson WG, Doohan DJ, Weller SC. Dose response of glyphosate and dicamba on tomato (*Lycopersicon esculentum*) injury. Weed Technol. 2012; 26: 256-260.

Lambert JL, Ramasamy J, Paukstelis JV. Stable reagents for the colorimetric determination of cyanide by modified König reactions. Anal. Chem. 1975; 47: 916-918.

Lee H, Xiong L, Gong Z, Ishitani M, Stevenson B, Zhu JK. The Arabidopsis HOS1 gene negatively regulates cold signal transduction and encodes a RING finger protein that displays cold-regulated nucleo–cytoplasmic partitioning. Genes Develop. 2001; 15: 912-924.

Li CW, Su RC, Cheng CP, You SJ, Hsieh TH, Chao TC, Chan MT. Tomato RAV transcription factor is a pivotal modulator involved in the AP2/EREBP-mediated defense pathway. Plant Physiol. 2011; 156: 213-27.

Lim SD, Jung CG, Park YC, Lee SC, Lee C, Lim CW, Kim DS, Jang CS. Molecular dissection of a rice microtubule-associated RING finger protein and its potential role in salt tolerance in Arabidopsis. Plant

Mol. Biol. 2015; 89: 365-384.
Livak KJ, Schmittgen TD. Analysis of relative gene expression data using real-time quantitative PCR and the 2ΔΔC(T) Method. Methods 2001; 25: 402–408.
Lovelace ML, Talbert RE, Scherder EF, Hoagland RE. Effects of multiple applications of simulated quinclorac drift rates on tomato. Weed Sci. 2007a; 55: 169-77.
Lovelace ML, Talbert RE, Hoagland RE, Scherder EF. Quinclorac absorption and translocation characteristics in quinclorac-and propanil-resistant and-susceptible barnyardgrass (Echinochloa crus-galli) biotypes. Weed Technol. 2007b; 21: 683-7.
Ludwig-Müller J. Auxin conjugates: their role for plant development and in the evolution of land plants. J. Exp. Bot. 201; 62:1757-73.
Mithila J, Hall JC, Johnson WG, Kelley KB, Riechers DE. Evolution of resistance to auxinic herbicides: historical perspectives, mechanisms of resistance, and implications for broadleaf weed management in agronomic crops. Weed Sci. 2011; 59: 445-57.
Mockaitis K, Estelle M. Auxin receptors and plant development: a new signaling paradigm. Annu. Rev. Cell Dev. Biol. 2008; 24: 55-80.
Parry G, Calderon-Villalobos LI, Prigge M, Peret B, Dharmasiri S, Itoh H, Lechner E, Gray WM, Bennett M, Estelle M. Complex regulation of the TIR1/AFB family of auxin receptors. Proc. Natl. Aca. Sci. 2009; 106: 22540-22545.
Pastori GM, Foyer CH. Common components, networks, and pathways of cross-tolerance to stress. The central role of "redox" and abscisic acid-mediated controls. Plant Physiol. 2002;129: 460-468.
Pearson WR. An introduction to sequence similarity ("homology") searching. Curr. Pro. Bioinfor. 2013; 42: 3-1.
Pearson WR, Lipman DJ. Improved tools for biological sequence comparison. Proc. Natl. Aca. Sci. 1988; 85: 2444-2448.
Plant ÁL, Cohen A, Moses MS, Bray EA. Nucleotide sequence and spatial expression pattern of a drought- and abscisic acid-induced gene of tomato. Plant Physiol. 1991; 97: 900-906.
Portillo M, Fenoll C, Escobar C. Evaluation of different RNA extraction methods for small quantities of plant tissue: Combined effects of reagent type and homogenization procedure on RNA quality-integrity and yield. Physiol. Plant. 2006; 128: 1-7.
Qin F, Sakuma Y, Tran LS, Maruyama K, Kidokoro S, Fujita Y, Fujita M, Umezawa T, Sawano Y, Miyazono KI, Tanokura M. Arabidopsis DREB2A-interacting proteins function as RING E3 ligases and negatively regulate plant drought stress–responsive gene expression. Plant Cell 2008; 20: 1693-707.
Raghavan C, Ong EK, Dalling MJ, Stevenson TW. Regulation of genes associated with auxin, ethylene and ABA pathways by 2, 4-dichlorophenoxyacetic acid in *Arabidopsis*. Funct. Integr. Geno. 2006; 6: 60-70.
Romero-Puertas MC, McCarthy I, Gómez M, Sandalio LM, Corpas FJ, Del Rio LA, Palma JM. Reactive oxygen species-mediated enzymatic systems involved in the oxidative action of 2, 4-dichlorophenoxyacetic acid. Plant Cell Environ. 2004a; 27: 1135-48.
Romero-Puertas MC, Rodríguez-Serrano M, Corpas FJ, Gomez MD, Del Rio LA, Sandalio LM. Cadmium-induced subcellular accumulation of $O_2 \cdot -$ and H_2O_2 in pea leaves. Plant Cell Environ. 2004b; 27: 1122-1134.
Sabba RP, Ray IM, Lownds N, Sterling TM. Inheritance of resistance to clopyralid and picloram in yellow starthistle (*Centaurea solstitialis* L.) is controlled by a single nuclear recessive gene. J. Hered. 2003; 94: 523-527.
Song Y. Insight into the mode of action of 2, 4-dichlorophenoxyacetic acid (2,4-D) as an herbicide. J. Integr. Plant Biol. 2014; 56: 106-13.
Sterling TM, Hal JC. Mechanism of action of natural auxins and the auxinic herbicides. Crit. Rev. Toxicol. 1997; 1: 111-142.
Tan X, Calderon-Villalobos LI, Sharon M, Zheng C, Robinson CV, Estelle M, Zheng N. Mechanism of auxin perception by the TIR1 ubiquitin ligase. Nature. 2007; 446: 640.
Tromas A, Paque S, Stierlé V, Quettier AL, Muller P, Lechner E, Genschik P, Perrot-Rechenmann C. Auxin-Binding Protein 1 is a negative regulator of the SCF TIR1/AFB pathway. Nature Comm. 2013; 4: 2496.
Valenzuela-Valenzuela JM, Lownds NK, Sterling TM. Clopyralid uptake, translocation, metabolism, and ethylene induction in picloram-resistant yellow starthistle (*Centaurea solstitialis* L.). Pestic. Biochem. Physiol. 2001; 71: 11-19.
Walsh TA, Neal R, Merlo AO, Honma M, Hicks GR, Wolff K, Matsumura W, Davies JP. Mutations in an auxin receptor homolog AFB5 and in SGT1b confer resistance to synthetic picolinate auxins and not to 2, 4-dichlorophenoxyacetic acid or indole-3-acetic acid in Arabidopsis. Plant Physiol. 2006; 142: 542-552.
Weinberg T, Stephenson GR, McLean MD, Hall JC. MCPA (4-chloro-2-ethylphenoxyacetate) resistance in hemp-nettle (*Galeopsis tetrahit* L.). J. Agric. Food Chem. 2006; 54: 9126-9134.
Yip WK, Yang SF. Cyanide metabolism in relation to ethylene production in plant tissues. Plant Physiol. 1988; 88: 473-476.
Zangoueinejad R, Alebrahim MT, Tseng TM. Evaluation of auxin tolerance in selected tomato germplasm under greenhouse and field conditions. Weed Technol. 2019; 33: 815-822.

In Vitro Seed Germination Response of Corn, Cotton, and Soybean to Temperature

Charles Hunt Walne, Firas A. Alsajri, Bandara Gajanayake, Suresh Lokhande, Ramdeo Seepaul, Chathurika Wijewardana, and K. Raja Reddy

Department of Plant and Soil Sciences, Mississippi State University, Mississippi State, MS 39762, USA

Corresponding Author: K. Raja Reddy, E-mail: krreddy@pss.msstate.edu

ABSTRACT

Seed germination is the first developmental phase in a plant's life cycle that is followed by emergence from the soil, successful seedling and establishment, and fruitful yield. Seed germination is influenced by multiple environmental factors such as temperature, moisture, and aeration. An *in vitro* experiment was conducted to quantify the effects of temperatures ranging from 10°C to 42.5°C on germination properties of corn, cotton, and soybean seeds. Cumulative seed germination was recorded over time, was fitted with a three-parameter sigmoidal function to calculate maximum seed germination and seed germination rate. Maximum seed germination was significantly influenced by the interaction of temperature and species. The seed germination rate was further analyzed as a function of temperature by fitting bilinear and quadratic functions to the data. Cardinal temperatures (minimum, optimum, and maximum) were estimated from that regression analysis. Corn displayed the highest optimal temperature of 34.6°C. Cotton showed higher minimum and maximum cardinal temperatures than both corn and soybean. The cardinal temperatures and functional relationships between seed germination rate and temperature determined in this experiment will be useful to update crop simulation models and assess the best planting dates for rapid, successful germination based on environmental conditions.

Keywords: Cardinal temperatures, corn, cotton, soybean, maximum seed germination, optimum temperature, seed germination models, seed germination rate

Abbreviations: MSG, maximum seed germination; SGR, seed germination rate

INTRODUCTION

In Mississippi, soybean [*Glycine max* (L.) Merr.], cotton (*Gossypium hirsutum* L.), and corn (*Zea mays* L.) are three of the most widely grown agronomically important crop species. In 2018, these crops accounted for 0.9, 0.251, and 0.19 million ha of production in Mississippi, respectively. Also, these three crops are widely grown across the United States. In 2018, there were 361 million ha of soybean, 5.6 million ha of cotton, and 361 million ha of corn planted in the United States (USDA-NASS, 2019). Moreover, these crops are often rotated amongst each other from year to year, shifting total acreage amongst these three species. Crops are usually sown in field conditions when soil temperatures are above the minimum temperatures for the individual crop species and with adequate soil moisture levels. Temperature conditions vary temporally and spatially across these crop belts and fluctuate due to variations in weather conditions immediately after sowing.

Corn planting in Mississippi usually begins in early March when environmental conditions are still cold and wet. Most soybeans grown in Mississippi are planted by the end of May, but some producers continue planting through June if double-cropping after wheat (*Triticum aestivum* L.). For cotton, the optimal planting window is from mid-April to mid-May (Anapalli et al., 2016).

For crops grown in the field, a uniform plant stand is necessary to achieve maximum grain yield (Rutto et al., 2014). Uniform stand establishment has been documented, holding a positive correlation with in-season crop growth, development, and final grain yield (Egli, 1993; Kolchinski et al., 2005; Mondo et

al., 2015; Alsajri et al., 2019). Seeds must quickly germinate and emerge in the same relatively short window of time to achieve a uniform stand. Rutto et al. (2014) demonstrated that plants with delayed emergence surrounded by new emerging plants display a delay in leaf stage and plant height. Such a delay can cause shadowing from neighboring plants, reduced light penetration through the canopy leading to lowered radiation capture, and increased competition for moisture and nutrients as earlier emerged plants often have more developed and extensive root systems (Weiner, 1990). Corn yields have been found to decrease due to uneven emergence even if in-row plant spacing is relatively uniform (Nafziger et al., 1991), especially at high plant populations. For each day an individual corn plant's emergence is delayed, a decline in the plant's final yield is paralleled (Ford and Hicks, 1992). This situation leaves the farmer with no practical solutions to combat loss in yield potential attributed to uneven emergence. In soybean, Egli (1993) found that seedlings with early emergence always exhibited a competitive advantage over later emerging plants. This rapid emergence led to higher growth rates, more seeds per plant, and higher yields per plant. Wheeler et al. (1997) also found similar results where earlier emerging cotton plants correlated to higher yields per plant.

The rate of emergence, and thus the uniformity of a stand, is a direct function of the interaction of a seed and its environment. Important environmental factors that influence emergence include temperature, moisture, compaction, soil aeration, pests, and microbes (Hatfield and Egli, 1974). Schneider and Gupta (1985) concluded that corn emergence was influenced by temperature more than the soil matric potential and soil aggregate size distribution. Emergence is directly influenced by temperature as it drives both seed germination and coleoptile elongation (Blacklow, 1973). Sub- and supra-optimal temperatures have been shown to affect both seed germination capacity and rate (Hsu et al., 1984; Roberts, 1988; Seepaul et al., 2011), ultimately influencing total emergence and rate of emergence.

Germination is the first step in a plant's life cycle and initiates growth from a dormant embryo to ultimately begin the process of seedling emergence. This critical growth stage begins with imbibition, a period of water uptake from the seed's surroundings, and culminates with the emergence of the radicle. Biologically, germination is simply defined as the "emergence of the embryonic root (radicle) through the seed covering (Heatherly and Hodges, 1999)." The maximum seed germination percentage is commonly used to describe a seed lot's ability to germinate. This percentage is calculated from a test conducted under near-optimal laboratory conditions and only measures a seed lot's maximum potential to produce healthy seedlings; the germination rate is not considered. Research indicates that factors such as seed quality and the maternal environment may significantly impact maximum seed germination (Wijewardana et al., 2019b). Seed vigor, however, may be more appropriate to describe a seed's true potential under field conditions. The AOSA has defined seed vigor as "those seed properties which determine the potential for rapid, uniform emergence, and development of normal seedlings under a wide range of field conditions (Egli, 1993; Heatherly and Hodges, 1999)". Most importantly, this concept addresses the importance of uniform emergence and establishment under variable environmental conditions. Unfortunately, information on seed vigor is often not readily available for commercial varieties of major crop species.

Besides, germination and emergence are both influenced by temperature and other environmental factors such as moisture and aeration. When soil moisture and aeration are not limiting, the soil temperature is the most influential factor for seed germination rate (Garcia-huidobro et al., 1982; Gummerson, 1986; Gajanayake et al., 2011). Temperature affects germination capacity and rate by influencing three key physiological processes: the rate of seed deterioration, the rate of dormancy loss, and the actual rate of germination (Roberts, 1988). Research indicates that there is a wide range of temperatures in which germination can occur, and, within this range, germination rate increases following an increase from the base temperature required for germination and the optimal temperature, and then the germination rate decreases as temperatures rise above the optimal temperature until

reaching the maximum temperature at which germination can occur (Roberts, 1988). Roberts (1988) also reports that the optimum temperature to achieve the fastest rate of germination is typically higher than the optimal temperature for maximum seed germination.

When studying seed germination, experiments conducted in the field often run into issues with uncontrollable factors such as temperature, light, and moisture. These factors all play critical roles in influencing germination (Wuebker et al., 2001). In vitro experiments can be conducted to reduce the effects of these confounding factors and isolate the dependent variable of interest. Previous studies investigating temperature effects on seed germination have been undertaken on crops where germination data is fitted to empirically derived growth models such as those presented by Shafii and Price (2001). These growth models allow calculation of a theoretical maximum of germination percent and the germination rate, both of which can be useful indicators of seed vigor when measured under stress (Seepaul et al., 2011). These germination characteristics have been further analyzed by calculating three cardinal temperatures (minimum, T_{min}; optimum, T_{opt}; and maximum, T_{max}). These critical temperatures represent the range of temperatures in which germination can occur. Shafii and Price (2001) suggested that determining cardinal temperatures is an essential and critical component of biological studies involving plant processes and temperature.

Much of the previous research conducted for corn, cotton, and soybean at sowing focuses on relationships between temperature and emergence. Alsajri et al. (2019) reported that soybean emergence increased with temperature quadratically with an estimated minimum temperature of 10.6°C required for germination and optimal temperature of 36.7°C. However, temperatures were not measured above 35.4°C. Hatfield and Egli (1974) reported that as the mean soil temperature increased, the germination rate increased up to an optimal temperature of 30.0°C and then declined as the temperature continued to rise. Other research indicates varying results with optimal temperatures ranging from 25 to 36°C (Edwards, 1934; Ellis et al., 1987a). In corn, early research suggests a wide range of optimal temperatures as well, ranging from as low as 28.0°C to as high as 37.5°C (Lehenbauer, 1914). In a review article, Sánchez et al. (2014) suggested the optimal temperature for corn emergence may fall between 26 and 33°C, with emergence occurring between a minimum of 10°C and maximum temperature 40°C. For cotton, research has shown that emergence rates increase as soil temperatures rise from 20°C to 35°C (Reddy et al., 2017). Ashraf et al. (1994) concluded that MSG for cotton is significantly higher at 25°C than at 40°C, and optimal temperature for cotton germination was suggested to fall between 28-30°C. However, few studies quantified the effects of temperature on seed germination by calculating cardinal temperatures for agronomically important row crop species. To our knowledge, this is the first comparative study of corn, cotton, and soybean germination responses to temperature. Cardinal temperatures for germination have been reported for numerous other species including pearl millet (*Pennistem typhoides* S. & H.) (Garcia-huidobro et al., 1982), sugar beet (*Beta vulgaris*) (Gummerson, 1986), Johnson grass (*Sorghum halepense* L.) (Arnold et al., 1990), switchgrass (*Panicum virgatum* L.) (Seepaul et al., 2011), ornamental pepper (*Capsicum annuum* L.) (Gajanayake et al., 2011), grass species (Jordan and Haferkamp, 1989), and a wide range of cover crop species (Tribouillois et al., 2016).

The objectives of this study were to (1) quantify seed germination capacity and seed germination rate at multiple temperatures using *in vitro* germination assay for corn, cotton, and soybean, (2) calculate cardinal temperatures (T_{min}, T_{opt}, and T_{max}) for seed germination rate, and (3) test for differences among the tested species for each calculated trait.

MATERIALS AND METHODS

Facilities and Experimental Protocol

An *in vitro* seed germination experiment was conducted at the Environmental Plant Physiology Laboratory located on the campus of Mississippi State University (33 28’15.4” N, 88 46’55.4” W), Mississippi State, Mississippi, USA. The experiment was designed and set up following the guidelines

described by the Association of Official Seed Analysts (AOSA, 2011). A Fisher Scientific Incubator 810 was used to provide necessary temperature control described later in this section (Fisher Scientific, Inc., Suwanee, GA, USA). Germination tests conducted inside the incubator included no artificial or natural light.

Our experimental design was completely randomized, with replications completed overtime at each target temperature. Each temperature and species combination was replicated four times. Each replicate consisted of 100 seeds randomly selected from the seed lot placed on disinfected trays between two layers of paper towels moistened with 250 mL of distilled water. Paper towels were disinfected by running each towel in the microwave oven for 30 seconds. A second tray was placed on top and secured using clips to ensure water did not evaporate during experimentation. Trays were stacked vertically in the incubator in a completely randomized order. Seeds were germinated at eight temperature setpoints: 10, 15, 20, 25, 30, 35, 40, and 42.5°C. Temperature treatments were imposed one hour before beginning germination to ensure the incubator reached desired set points before experimentation began. Three Watchdog Model 100 data loggers (Spectrum Technologies Inc., Aurora, IL, USA) were placed in the incubator to ensure temperature remained consistent within the incubator. All temperatures were maintained within ± 1.0°C of the desired setpoints throughout experimentation.

Data Collection

Seeds were counted, recorded, and discarded every two hours until germination was complete, germination ceased for three consecutive days, or 15 total days had passed. Germination was considered complete when the radicle emerged from the seed embryo and reached a length greater than or equal to half the length of the seed itself.

Curve Fitting for Cumulative Seed Germination Time Course Data

Using Sigmaplot 13 (Systat Software Inc., San Jose, CA, USA), cumulative seed germination data for each replicate was fitted to a three-parameter sigmoidal function (Eq. 1). Details on fitting germination data to this type of curve were described in detail by Shafii and Price (2001). This function provides a mathematical estimation of the asymptote (theoretical maximum seed germination capacity, MSG.), the shape and steepness of the curve (proportional to the rate of germination), and the time to reach 50% of the asymptote (t_{50}).

$$Y_t = MSG\ [1 + \exp(-t - t_{50})/G_{rate} \qquad \text{[Eq. 1]}$$

where: Y_t is the cumulative % germination achieved at time t

MSG is the asymptote, or theoretical maximum seed germination achievable

G_{rate} is a coefficient proportional to the rate of germination

T_{50} is the time required to reach 50% of MSG.

Maximum Seed Germination and Seed Germination Rate Calculation

The MSG was derived directly from equation 1. The seed germination rate (SGR) was then calculated as the reciprocal of t_{50} ($1/t_{50}$) (Eq. 2). Seed germination rate has been calculated using a similar method by Seepaul et al. (2011) and Gajanayake et al. (2011).

$$SGR = 1/t_{50} \qquad \text{[Eq. 2]}$$

The SGR was further analyzed by regressing SGR against average temperature followed by fitting the data to either a quadratic or bilinear model, using the highest R^2 and lowest RMSE values as the criterion. Accordingly, a bilinear equation best described the relationship between corn and cotton SGR and temperature (Eq. 3 and 4), and a quadratic response best described the relations of SGR and temperature (Eq. 5).

For bilinear: if $t <= T_{opt}$ use Eq. 3, otherwise use Eq. 4

$$Y = [a(T_{opt} - t) + b(t - t_1)] / (T_{opt} - t_1) \qquad \text{[Eq. 3]}$$

$$Y = [b(t2 - t) + c(t - T_{opt})] / (t_2 - T_{opt}) \qquad \text{[Eq. 4]}$$

where the regression coefficients for corn were, a = 0.0796, Topt =34.6, t_1 = 10, and t_2 = 40 and the regression coefficients for cotton were, a = 0.1275, Topt =26.715, t_1 =15, and t_2 = 40.

For soybean, a quadratic function best described the SGR response to temperature.

SGR for cotton = -1.0561 + 0.143*t – 0.0025*t^2;

R^2 = 0.98 [Eq. 5]

where t is the average temperature

Cardinal Temperature Estimation

The bilinear functions provide the Topt for corn and cotton SGR (Eq. 3 and 4), while T_{min} and T_{max} were derived by extrapolation and were calculated as the lower and upper x-intercept, respectively, estimated using regression coefficients (Eq. 6 and 7).

$T_{min} = [T_{opt}(a) + t_1(-b)] / (a-b)$ [Eq. 6]

$T_{max} = [T_{opt}(-c) + t_2(b)] / (b-c)$ [Eq. 7]

Similarly, the T_{min}, T_{opt}, and T_{max} for soybean seed germination rate were calculated using the coefficients generated from the regressions between SGR, and temperature. T_{opt} was calculated as the temperature at which SGR was at its highest (Eq. 8). T_{min} and T_{max} were derived by extrapolation and were calculated as the lower and upper x-intercept, respectively (Eq. 5 and 10) for soybean.

$T_{opt} = -b/(2c)$ [Eq. 8]

$T_{min} = \{-b + [sqrt(b^2 – 4ac)]\}/2c$ [Eq. 9]

$T_{max} = \{-b - [sqrt(b^2 – 4ac)]\}/2c$ [Eq. 10]

Also, the maximum achievable seed germination rate (SGR_{max}) was then calculated for each species by estimating SGR at T_{opt} using either the bilinear or quadratic function equations (Eq. 3 and 5).

Data Analysis

A two-way ANOVA was conducted using the general linear model procedure in SAS 9.4 (SAS Institute, Inc, Cary, NC, USA) to determine the significant effects of temperature, species, and their interaction. Means were separated using Fisher's least significant difference (LSD.) at an alpha level of 0.05. For the cardinal temperatures, a 95% confidence interval was constructed to exemplify differences among species. All graphing and regression constant generation were completed in SigmaPlot 13 (Systat Software Inc., San Jose, CA, USA).

RESULTS AND DISCUSSION

Knowledge and prediction of crop seed germination, and thus, seedling emergence useful for crop management. The results demonstrate strong effects of incubation temperature on MSG and SGR of corn, cotton, and soybean crop species; the functional relationships and the cardinal temperatures

Cumulative Germination Time-course Data

Following the sigmoidal curve pattern seen in Figure 1, germination began slowly, incurred a period of rapid germination, and then slowed again as the maximum germination percentage is approached in all the three crops studied. Similar functions have been observed by Seepaul et al. (2011), Gajanayake et al. (2011), and Wijewardana et al. (2019) to model seed germination, emergence, and other plant growth characteristics switchgrass, ornamental peppers, and soybean, respectively. The average r^2 of the sigmoidal function for all repetitions was 0.95 minimum and a maximum of 1.0

Table 1. Maximum seed germination percentage (MSG) and seed, and soybean, for various germination traits.

Variable	Seed germination parameters	
	Maximum seed germination (MSG, %)	Seed germination rate (SGR, d^{-1})
Temperature	***†	***
Species	***	***
Temperature*Species	***	***

†*** = *P*-value <0.001.

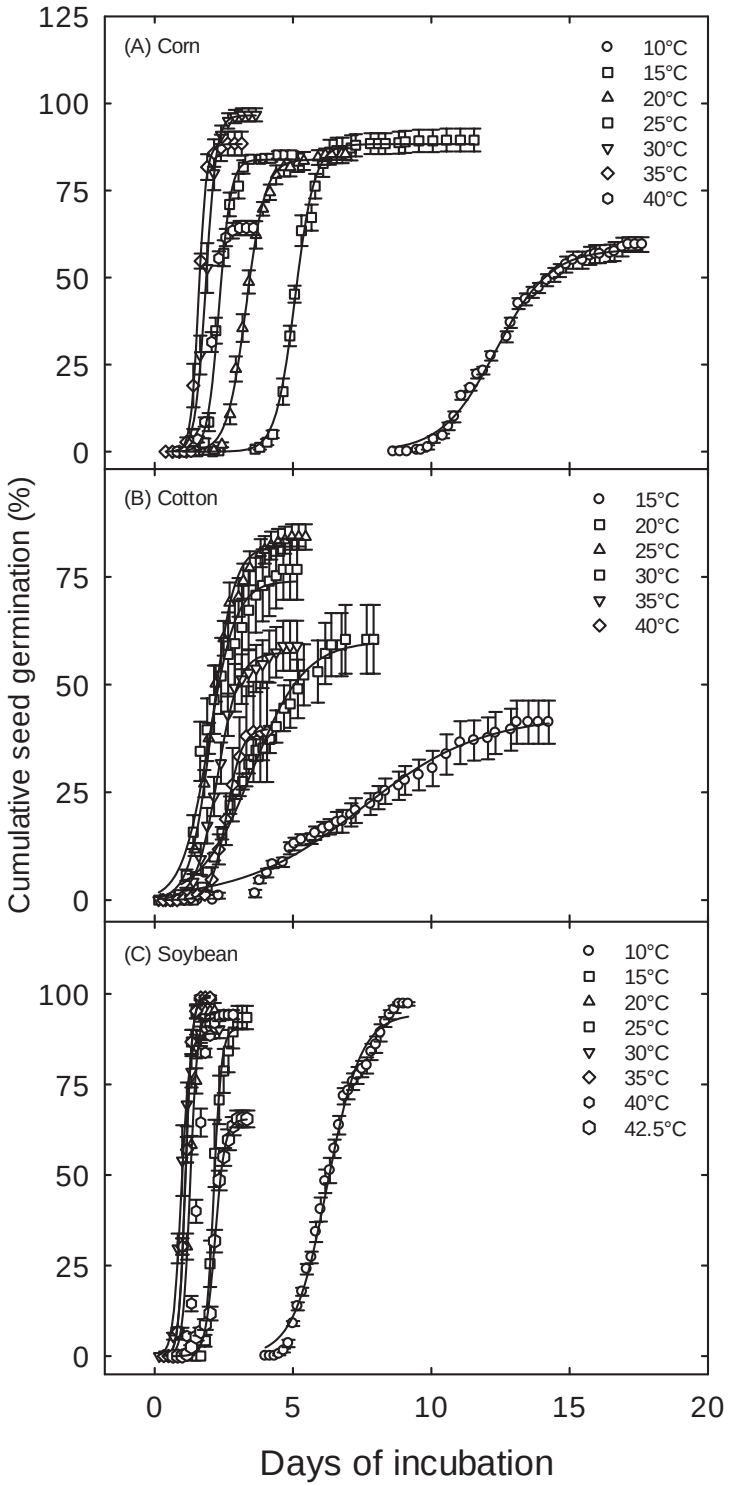

Figure 1. Seed germination time course (mean ± SE, n = 4) of (A) corn, (B) cotton, and (C) soybean species at a range of temperatures. Symbols represent observed cumulative germination data, and lines indicate a germination time course fitted using a 3-parameter sigmoidal function.

Maximum Seed Germination

Crop species and temperature significantly affected (P<0.05) MSG (Table 1, Figure 2). The MSG exemplifies the maximum number of seeds with the potential to germinate under its environment (Wijewardana et al., 2019a). The relationship between MSG and temperature differed between each species, and no consistent trend was discovered. Corn MSG was significantly (P<0.05) higher at 30 ^{o}C than any of the other tested temperatures, whereas MSG was significantly lower at 10^{o}C and 40°C (Table 1). No significant differences (P<0.05) were observed between the 15, 20, 25, and 35 °C treatments. Cotton achieved the greatest MSG at 25 ^{o}C, although this value was not significantly different (P<0.05) than germination at 30°C; MSG for cotton was, however, lower (P<0.05) at the most extreme temperatures of 15 and 40 ^{o}C. For soybean, MSG did not differ (P<0.05) between 10 and 40^{o}C. However, at 42.5 °C, MSG for soybean was significantly lower than at all other temperatures. Thus, temperatures between 10 and 40 °C did not appear to influence soybean MSG, whereas corn and cotton were affected at both high and low extremes. Although temperature effects were evident with MSG, we did not use this trait for any further analysis, such as cardinal temperature calculation. Temperature effects were not consistent among the three tested species, and no clear functional trend was detected. Also, previous research indicates that MSG is heavily influenced by non-genetic seed traits such as seed quality (Ellis et al., 1987b), parental plant environment (Fenner, 1991; Wijewardana et al., 2019b), and the time between seed harvest and germination.

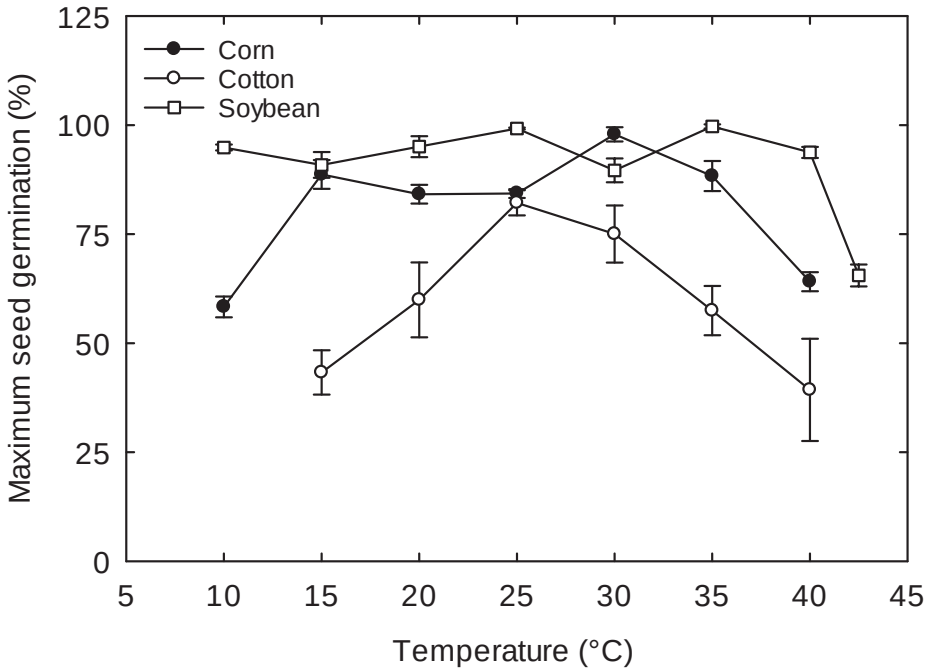

Figure 2. The average maximum seed germination for corn, cotton, and soybean plant species across a wide range of temperatures. The values are mean ± SE four replications.

Seed Germination Rate

Like MSG, the seed germination rate (SGR) differed (P<0.05) among the three species and temperature (Table 1, Figure 3). However, a similar trend was observed for all three species, and a precise functional fit existed. As temperatures were elevated from sub-optimal towards T_{opt}, SGR steadily increased. When temperatures continued to rise above T_{opt} into supra-optimal levels, SGR began to decline. The relationship between SGR and temperature for each

species was adequately fitted to either a bi-linear or quadratic function (Figure 3). The functions were selected based on the higher r^2 value and lower RMSE among several fitted equations. Corn and cotton were best described by a bilinear function, whereas soybean was best fit to a quadratic function. These functions provide the necessary equation parameters to calculate the cardinal temperatures for each species.

The SGR_{max} exemplified the highest estimated SGR attainable for each species at T_{opt} and differed between all three species. Soybean achieved the highest SGR_{max} (0.98 d^{-1}) followed by cotton (0.528), and then corn (0.0124). Species with a higher SGR_{max} would be more likely to emerge uniformly, even under environmental conditions where SGR may be hindered.

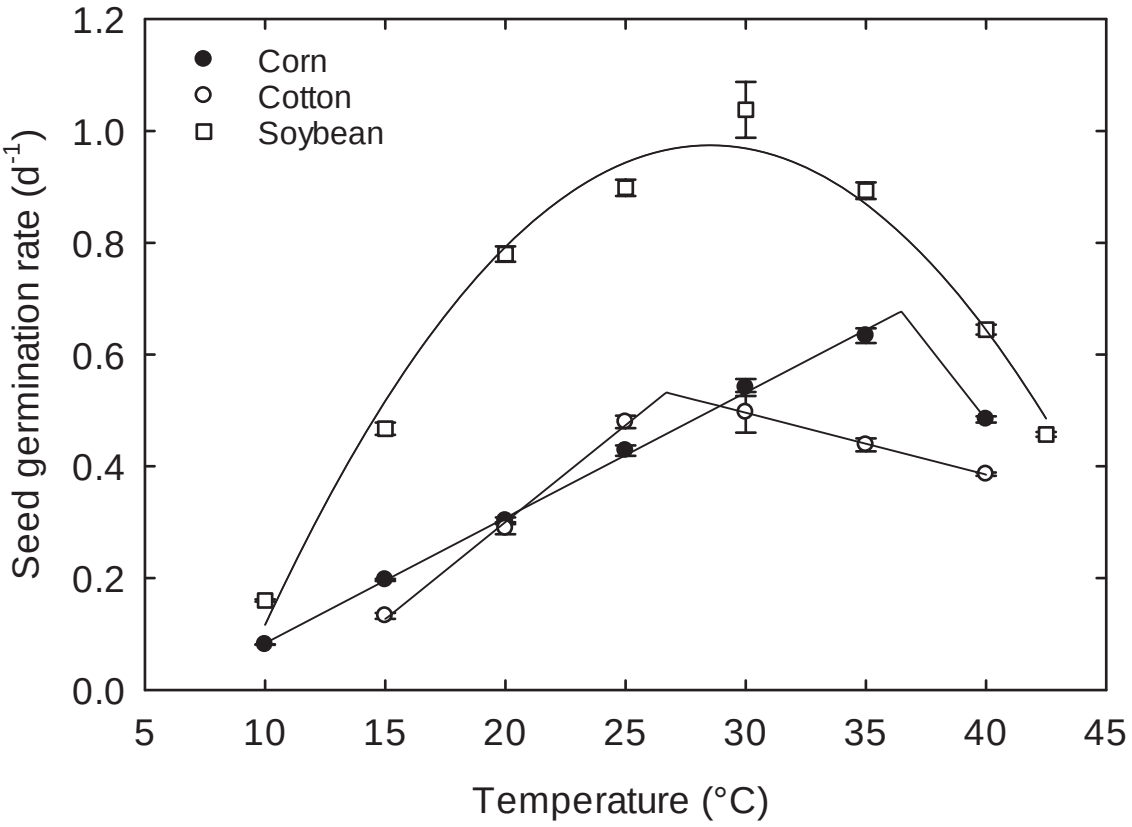

Figure 3. The average seed germination rate for corn, cotton, and soybean plant species is presented at all tested temperatures. These values were fitted to either a bilinear or quadratic function to calculate cardinal temperatures.

Cardinal Temperature Calculation

Corn had the highest T_{opt} at 34.6 °C, while the T_{opt} for cotton and soybean was not significantly different (P<0.05), with respective values of 26.715 and 28.6 °C. T_{min} and T_{max} were estimated by calculating the temperatures at which the seed germination rate reaches zero above and below T_{opt}. Corn and soybean displayed the lowest T_{min}, 6.5 °C, and 8.9 °C, respectively, but were not significantly different. The T_{min} for cotton was 11.3 °C. The T_{max} values of corn and soybean, 57.0 and 48.1°C, respectively, did not differ either. Cotton displayed a very high T_{max} of 82.9 °C. These cardinal temperatures are estimates produced through extrapolation; they do not suggest that successful seed germination will occur at every temperature within the cardinal temperatures; however, they do provide valuable insight to the sensitivity of each species to sub and supra optimal temperatures at germination. Also, determining the

T_{opt} for each species can help to update best management practices for selecting optimal planting dates. The cardinal temperatures and functional relationships between seed germination and temperature could also be useful for updating and validating various crop simulation models.

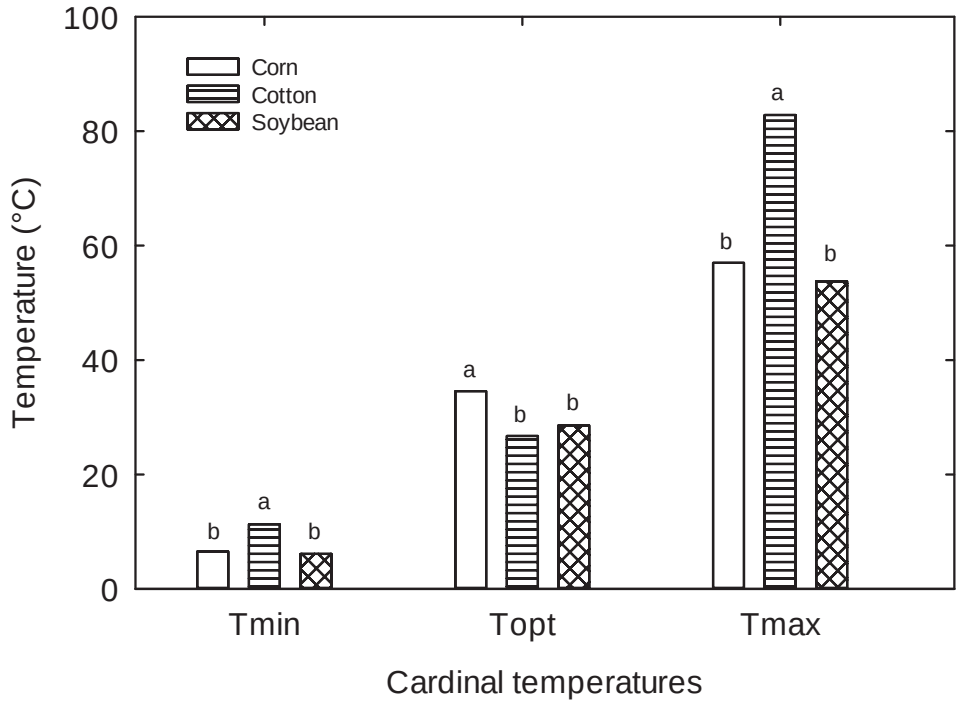

Figure 4. The cardinal temperatures (Minimum -T_{min}, Optimum -T_{opt}, and maximum - T_{max}) of corn, cotton, and soybean crop species. Differing letters indicate a difference among the species within the respective cardinal temperature category at $P = 0.05$ probability level.

CONCLUSION

Cumulative seed germination was successfully described using a three-parameter sigmoidal function in all three crop species, corn, cotton, and soybean, which provided critical estimates of both maximum seed germination and seed germination rate. The average temperature and species both had a significant influence on maximum seed germination and seed germination rate in all the crops. Maximum seed germination was lower at the lowest and highest temperatures for corn and cotton but was only lower at the highest temperature for soybean. Seed germination rate for temperature was accurately described by a bilinear function for corn and cotton, whereas a quadratic function best fitted the relationship for soybean. Cardinal temperatures calculated by extrapolating the functions to determine x-intercepts and optimal temperatures determined by calculating the vertex of the functions varied among the three crops studied. Corn had a higher optimal temperature than soybean and cotton, whereas cotton had a higher minimum and maximum temperatures compared with corn and soybean. The functional relationships between temperature and corn (Morell et al., 2016), cotton (Reddy et al., 2002; Thorp et al., 2014), and soybean (Jones et al., 2003) seed germination rate and optimal temperatures could be used to improve the functionality of respective crop models for field applications.

CONFLICT OF INTEREST

There is no conflict of interest to declare.

ACKNOWLEDGMENTS

We thank David Brand for technical assistance and graduate students of the Environmental Plant Physiology Laboratory at Mississippi State University for their support during data collection. We also thank the Mississippi Corn Promotion Board and the National Institute of Food and Agriculture, NIFA 2016-34263-25763, and MIS 043040 for partial funding for this research.

LITERATURE CITED

Association of Official Seed Analysts. Rules for testing seeds. Assoc. Official Seed Analysys, 2011; Las Cruces, NM, USA.

Alsajri FA, Wijewardana C, Krutz LJ, Irby JT, Golden B, Reddy KR. Quantifying and validating soybean seed emergence model as a function of temperature. Am. J. Plant Sci. 2019; 10, 111-124. doi: 10.4236/ajps.2019.101010

Arnold RLB, Ghersa CM, Sanchez RA, Insausti P. Temperature effects on dormancy release and germination rate in *Sorghum halepense* (L.) Pers. seeds: a quantitative analysis. Weed Res. 1990; 30: 81-89. doi: 10.1111/j.1365-3180.1990.tb01690.x.

Ashraf M, Saeed MM, Qureshi. MJ. Tolerance to high temperature in cotton (*Gossypium hirsutum* L.) at initial growth stages. Environ. Exp. Bot. 1994; 34: 275-283. doi: 10.1016/0098-8472(94)90048-5.

Blacklow WM. Simulation model to predict germination and emergence of corn (*Zea mays* L.) in an environment of changing temperature. Crop Sci. 1973; 13: 604-608. https://doi.org/10.2135/cropsci1973.0011183X001300060006x

Edwards TI. Relations of germinating soybeans to temperature and length of incubation time. Plant Physiol. 1934; 9: 1-30. doi: 10.1104/pp.9.1.1.

Egli DB. Relationship of uniformity of soybean seedling emergence to yield. J. Seed Technol. 1993; 17: 22-28.

Ellis RH, Simon G, Covell S. The influence of temperature on seed germination rate in grain legumes: III. A comparison of five faba bean genotypes at constant temperatures using a new screening method. J. Exp. Bot. 1987a; 38; 1033-1043. doi: 10.1093/jxb/38.6.1033

Ellis RH, Simon G, Covell S. The influence of temperature on seed germination rate in grain legumes: III. A comparison of five faba bean genotypes at constant temperatures using a new screening method. J. Exp. Bot. 1987b; 38: 1033-1043. doi: 10.1093/jxb/38.6.1033

Fenner, M. The effects of the parent environment on seed germinability. Seed Sci. Res. 1991; 1: 75-84. doi: 10.1017/S0960258500000696

Ford JH, Hicks DR. Corn growth and yield in uneven emerging stands. J. Prod. Agric. 1992; 5: 185-188. doi: 10.2134/jpa1992.0185

Gajanayake B, Trader BW, Reddy KR, Harkess RL. Thermotolerance classification of ornamental pepper cultivars using seed germination traits. Seed Technol. 2011; 33: 134-146. http://www.jstor.org/stable/23433423

Garcia-huidobro J, Monteith JL, Squire GR. Time, temperature and germination of pearl millet (*Pennisetum typhoides* S. & H.): I. Constant temperature. J. Exp. Bot. 1982; 33: 297-302. doi: 10.1093/jxb/33.2.288

Gummerson RJ. The effect of constant temperatures and osmotic potentials on the germination of sugar beet. J. Exp. Bot. 1986; 37: 729-741. doi: 10.1093/jxb/37.6.729

Hatfield JL, Egli DB. Effect of temperature on the rate of soybean hypocotyl elongation and field emergence 1. Crop Sci. 1974; 14: 423-426. doi: 10.2135/cropsci1974.0011183x001400030025x

Heatherly LG, Hodges HF, editors. Soybean Production in the Midsouth. 1999; CRC Press LLC, Boca Raton, FL, USA.

Hsu FH, Nelson CJ, Chow WS. A mathematical model to utilize the logistic function in germination and seedling growth. J. Exp. Bot. 1984; 35: 1629-1640. doi: 10.1093/jxb/35.11.1629.

Delouche JC. Influence of moisture and temperature levels on the germination of corn, soybeans and watermelons. Proc. Assoc. Off. Seed Anal. 1953; 43, 117-126. https://www.jstor.org/stable/23433082?seq=1#metadata_info_tab_contents (accessed 30 June 2020).

Jordan, G.L., and M.R. Haferkamp. Temperature responses and calculated heat units for germination of several range grasses and shrubs. J. Range Manag. 1989; 42: 41-45. doi: 10.2307/3899656 42, No. 1

Kolchinski EM, Schuch LOB, Peske ST. Vigor de sementes e competição intra-específica em soja. Ciência Rural 2005; 35: 1248-1256. doi:

10.1590/s0103-84782005000600004

Lehenbauer P. Growth of maize seedlings in relation to temperature. Physiol. Res. 1914; 1: 247-288.

Morell FJ, Yang HS, Cassman KG, Wart JV, Elmore RW, Licht M, Coulter JA, Ciampitti IA, Pittelkow CM, Brouder SM, Thomison P, Lauer J, Graham G, Massey R, Grassini P. Can crop simulation models be used to predict local to regional maize yields and total production in the U.S. Corn Belt?, Field Crops Res. 2016; 192: 1-12. https://doi.org/10.1016/j.fcr.2016.04.004.

Mondo VHV, Dias MAN, Cicero SM. Maize seed vigor and its effects on crop cultivation cycle. Brazilian J. Agric. - Rev. de. Agric. 2015; 90: 168-178. doi: 10.37856/bja.v90i2.178

Nafziger ED, Carter PR, Graham EE. Response of corn to uneven emergence. Crop Sci. 1991; 31: 811-815. doi: 10.2135/cropsci1991.0011183x003100030053x

Reddy KR, Kakani VG, McKinion JM, Baker DN. Applications of a cotton simulation model, GOSSYM, for crop management, economic and policy decisions. In: Ahuja LR, Ma L, Howell TA (Eds.) Agricultural System Models in Field Research and Technology Transfer, 2002, Pp. 33-73, CRC Press, LLC, Boca Raton, FL, USA.

Reddy KR, Brand D, Wijewardana C, Gao W. Temperature effects on cotton seedling emergence, growth, and development. Agron. J. 2017; 109, 1379-1387. doi: 10.2134/agronj2016.07.0439

Roberts EH. 1988. Temperature and seed germination. Symp. Soc. Exp. Biol. 42: 109-132.

Rutto E, Daft C, Kelly J, Chim BK, Mullock J, Torres G, Raun B. Effect of delayed emergence on corn (*Zea mays* L.) grain yield. J. Plant Nutr. 2014; 37: 198-208. doi: 10.1080/01904167.2013.859691

Sánchez B, Rasmussen A, Porter JR. Temperatures and the growth and development of maize and rice: A review. Glob. Chang. Biol. 2014; 20, 408-417. doi: 10.1111/gcb.12389

Schneider EC, Gupta SC. Corn emergence as influenced by soil temperature, matric potential, and aggregate size distribution. Soil Sci. Soc. Am. J. 1985; 49: 415-422. doi: 10.2136/sssaj1985.03615995004900020029x

Seepaul R, Macoon B, Reddy KR, Baldwin B. Switchgrass (*Panicum virgatum* L.) intraspecific variation and thermotolerance classification using *in vitro* seed germination assay. Am. J. Plant Sci. 2011; 2: 134-147. doi: 10.4236/ajps.2011.22015

Shafii B, Price WJ. Estimation of cardinal temperatures in germination data analysis. J. Agric. Biol. Environ. Stat. 2001; 6, 356-366. doi: 10.1198/108571101317096569

Thorp KR, Ale S, Bange MP, Barnes EM, Hoogenboom G, Lascano R.J, McCarthy AC, Nair S, Paz JO, Rajan N, Reddy KR, Wall GW, White JW. Development and application of process-based simulation models for cotton production: A review of past, present, and future. Cotton Sci. 2014; 18: 10-47. http://www.cotton.org/journal/2014-18/1/upload/JCS18-10.pdf

Tribouillois H, Dürr C, Demilly D, Wagner MH, Justes E. Determination of germination response to temperature and water potential for a wide range of cover crop species and related functional groups. PLoS ONE 11(8): e0161185. https://doi.org/10.1371/journal.pone.0161185

USDA-NASS. 2019. Agricultural Statistics, 2019. https://www.nass.usda.gov/

Weiner J. 1990. Asymmetric competition in plant populations. Trends Ecol. Evol. 1990; 5: 360-364. doi: 10.1016/0169-5347(90)90095-U

Wheeler TA, Gannaway JR, Kaufman HW, Dever JK, Mertley JC, Keeling JW. Influence of tillage, seed quality, and fungicide seed treatments on cotton emergence and yield. J. Prod. Agric. 1997; 10: 394-400. doi: 10.2134/jpa1997.0394

Wijewardana C, Alsajri FA, Reddy KR. Soybean seed germination response to *in vitro* osmotic stress. Seed Technol. 2019a; 39: 143-154

Wijewardana C, Reddy KR, Krutz LJ, Gao W, Bellaloui N. Drought stress has transgenerational effects on soybean seed germination and seedling vigor. PLoS One 2019b; 14. doi: 10.1371/journal.pone.0214977

Wuebker EF, Mullen RE, Koehler K. Flooding and temperature effects on soybean germination. Crop Sci. 2001; doi: 10.2135/cropsci2001.1857

85th ANNUAL MEETING

MISSISSIPPI GULF COAST CONVENTION CENTER

BILOXI, MS

FEBRUARY 11-12, 2021

SUBMIT ABSTRACTS BY NOV. 1, 2020

Make sure to Register to receive Complimentary Membership

Can also be done on-line at : https://msacad.org/join-mas

Membership/Registration opens July 1, 2020

Renew and join early to avoid late fees

MISSISSIPPI ACADEMY OF SCIENCES ABSTRACT FORM/MEMBERSHIP FORM

ABSTRACT INFORMATION

Abstract Title:_____
Name of Presenting Author(s): _____
If you are a student please fill-out the next line
Name of Mentor and e-mail of Mentor _____
(Telephone_____Email_____

Check the division in which you are presenting

__ Agriculture and Plant Science
__ Biomaterials
___Cellular, Molecular, and Dev. Biol
__ Chemistry and Chem. Engineering
__ Ecology and Evolutionary Biology
__ Geology and Geography
__ Health Sciences/Population Health
__ History and Philosphy of Sciences
__ Math., Computer Sci and Statistics
__ Marine and Atmospheric Sciences
__ Physics and Engineering
__ Psychology and Social Sciences
__ Science Education
__ Zoology and Entomology

Complete either the Membership/Pre-Registration form if you plan to attend and present at the meeting if you do not plan to attend the meeting please complete the membership form

MEMBERSHIP/ PRE-REGISTRATION INFORMATION
New ___ Renewal___
Mr. Ms. Dr._____
Address _____
City, State, Zip _____
School or Firm _____
Telephone_____ **Email**_____

PLEASE INDICATE DIVISION YOU WISH TO BE AFFILIATED _____
Before January 8, 2021…….Regular Member/Pre-Registraion $150 Student Member/ Pre-registration $50
After January 8, 2021……. Regular Member/Registraion $200 Student Member/ Pre-registration $60

MEMBERSHIP INFORMATION
New ___ Renewal___
Mr. Ms. Dr._____
Address _____
City, State, Zip _____
School or Firm _____
Telephone_____ **Email**_____

PLEASE INDICATE DIVISION YOU WISH TO BE AFFILIATED _____
Regular Member $30 **Student Member $10** **Life Member $600**
Educational Member $550 **Corporate Patron $1500** **Corporate Donor $1,000**

CHECKLIST
Please complete the following:
__ Enclose title of abstract (even if abstract has been submitted electronically)
__ Complete membership/registration form (this form)
__ Enclose the following payments (Make checks payable to Mississippi Academy of Sciences)
__ $25 per abstract
__ $150 regular membership/pre-registration fee OR $50 student membership/pre-registration fee
__ You must supply a check #_____ or P.O. #_____ (or indicate Pay Pal confirmation) _____

MISSISSIPPI ACADEMY OF SCIENCES—ABSTRACT INSTRUCTIONS
PLEASE READ ALL INSTRUCTIONS BEFORE YOU SUBMIT YOUR ABSTRACT ON-LINE

- Your paper may be presented orally or as a poster. Oral presentations are generally 15 minutes. The speaker should limit the presentation to 10-12 minutes to allow time for discussion; longer presentations should be limited accordingly. Instructions for poster presentations are linked here.
- Enclose a personal check, money order, institutional check, or purchase order for $25 publication charge for each abstract to be published, payable to the Mississippi Academy of Sciences. The publication charge will be refunded if the abstract is not accepted.
- The presenting author must be a member of the Academy at the time the paper/poster is presented. Payment for membership of one author must be sent for the abstract to be accepted.
- Attendance and participation at all sessions requires payment of registration.
- Note that three separate fees are associated with submitting and presenting a paper at the annual meeting of the Mississippi Academy of Sciences.
    1. An abstract fee is assessed to defray the cost of publishing abstracts and
    2. A membership fee is assessed to defray the costs of running the Academy.
    3. Membership/Preregistration payment ($130 regular; $50 student) may accompany the abstract, or you may elect to pay this fee before January 8th, or pay full late membership/registration fees at the meeting ($180 regular, $60 student).
- Abstracts may **only** be submitted on line via a link through the MAS website.The appropriate abstract fees can be paid via Paypal or sent via mail to Barbara Holmes at the Academy address.
- **Late abstracts will be accepted with a $10 late fee during November increased to $25 after that. Late abstracts will be accepted only if there is room in the appropriate division. They will be published in the April issue of the MAS JOURNAL.**
- Submit your appropriate fees NO LATER THAN January 8h, 2019.

Ms. Lisa McCammon
Mississippi Academy of Sciences
Post Office Box 55907
Jackson, MS 39296-5907

GUIDELINES FOR POSTER PRESENTATIONS

- The Academy provides poster backboards. Each backboard is 36" high by 48"' wide. Mount the poster on the board assigned to you by your Division Chairperson. Please do not draw, write, or use adhesive material on the boards. You must provide your own thumb tacks.
- Lettering for your poster title should be at least 1" high and follow the format for your abstract. Lettering for your poster text should be at least 3/8" high.
- Posters should be on display during the entire day during which their divisional poster session is scheduled. They must be removed at the end of that day.
- Authors must be present with their poster to discuss their work at the time indicated in the program.

Author Guidelines

Editorial Policy. The Editorial Board publishes articles on all aspects of science that are of general interest to the scientific community. General articles include short reviews of general interest, reports of recent advances in a particular area of science, current events of interest to researchers and science educators, etc. Research papers of sufficiently broad scope to be of interest to most Academy members are also considered. Articles of particular interest in Mississippi are especially encouraged.

Research papers are reports of original research. Submission of a manuscript implies that the paper has not been published and is currently at the time of submission being considered for publication elsewhere. At least one of the authors must be a member of the Academy, and all authors are encouraged to join.

Manuscripts. Submit the manuscript electronically to the Mississippi Academy of Sciences under your profile in the member location of the website. Please also provide a cover letter to the Editor of the Journal. The cover letter should authorize publication: give the full names, contact information, for all authors; and indicate to whom the proofs and correspondence should be sent. Please notify the Editor on any changes prior to publication.

Manuscripts must adhere to the following format:

- One inch margins on 8.5 x 11 inch paper;
- Text should be left-justified using twelve point type;
- Double spaced throughout, including the title and abstract;
- Arabic numerals should be used in preference to words when the number designates anything that can be counted or measured (7 samples, 43 species) with 2 exceptions:
- To begin a sentence (Twenty-one species were found in…)
- When 2 numeric expressions are adjacent in a sentence. The number easiest to express in words should be spelled out and the other left in numeric form (The sections were divided into eight 4-acre plots.).
- Measurements and physical symbols or units shall follow the International System of Units (SI *Le Système international d'unités*) with metric units stated first, optionally followed by United States units in parentheses. *E.g.*: xx grams (xx ounces); and
- Avoid personal pronouns.

Format

Abstract. In 250 or fewer words summarize any new methods or procedures critical to the results of the study and state the results and conclusions.

Introduction. Describe the knowledge and literature that gave rise to the question examined by, or the hypothesis posed for the research.

Materials and methods. This section should describe the research design, the methods and materials used in the research (subjects, their selection, equipment, laboratory or field procedures), and how the findings were analyzed. **For all human and animal studies please indicate Institutional Approval** in this section**.**

Results. The text of the results should be a descriptive narrative of the main findings, of the reported study. This section should not list tabulated data in text form. Reference to tables and figures included in this section should be made parenthetically in the text.

Discussion. In this section compare and contrast the data collected in the study with that previously reported in the literature. Unless there are specific reasons to combine the two, as explained by the author in the letter of transmittal, Results and Discussion should be two separate sections.

Acknowledgments. Colleagues and/or sources of financial support to whom thanks are due for assistance rendered in completion of the research or preparation of the manuscript should be recognized in this section rather than in the body of the text.

Author Disclosures. Pleae identify all conflicts of interest. In not applicable please indicate

---

Literature cited. List references alphabetically. Cite references in the text by author and year of publication (e.g., Smith, 1975; Black and Benghuzzi, 2011; Smith et al., 2010; Smith, 2011a, 2011b). The following examples illustrate the style to be used in the literature list.

Black DA, Lindley S, Tucci M, Lawyer T, Benghuzzi H. A new model for the repair of the Achilles tendon in the rat. J Invest Surg. 2011; 24(5): 217-221.

Pearson HA, Sahukhal GS, **Elasri** MO, Urban MW. Phage-bacterium war on polymeric surfaces: can surface-anchored bacteriophages eliminate microbial infections? Biomacromolecules. 2013 May 13;14(5):1257-61.

Bold, H.C., C.J. Alexopoulos, and T. Delevoryas. 1980. Morpholgy of plants and fungi, 4th ed. Harper and Row, New York. 819 pp

Web-page

- name of author(s) -if known
- title of the work - in quotes, if known
- title of the Web page - in italics, if applicable
- date of last revision
- URL
- Date accessed

Example:

Ackermann, Ernest. "Writing Your Own Web Pages." *Creating Web Pages.* 23 Oct. 1996. http://people.umw.edu/~ernie/writeweb/writeweb.html 10 Feb. 1997.

File available by anonymous FTP

- name of author(s) -if known
- title of the work - in quotes, if known
- date of last revision
- URL
- Date accessed

Example:
American Civil Liberties Union. "Briefing paper Number 5, Drug Testing in the Work Place." 19 Nov. 1992. ftp://ftp.eff.org/pub/Privacy/Medical/aclu_drug_testing_workplace.faq 13 Feb. 1997.

Please Tables and Figures at the end of the manuscript submitted.

Tables. Tables must be typed double spaced, one table to a page, numbered consecutively, and placed at the end of the manuscript. Since tables must be individually typeset, consolidation of data into the smallest number of tables is encouraged. A horizontal double underline should be made beneath the title of the table, and single underlines should be made the width of the table below the column headings and at the bottom of the table. Do not use vertical lines, and do not place horizontal lines in the interior of the table. Use footnotes, to clarify possible questions within the table, should be noted by asterisks, daggers, or other symbols to avoid confusion with numerical data. Tables should be referred to parenthetically in the text, for example (Table 1).

Figures and illustrations. Figures may be photographs, computer -generated drawings, or graphs and should be placed at the end of the manuscript and referenced in the appropriate place.. All illustrations are referred to as “Figures” and must be numbered consecutively. Illustrations other than those generated by the author(s) must include permission for use and credit to the originator. Each figure must have a complete legend that is typed, double-spaced, on a separate sheet which precedes the figures in the manuscript. Figures should be referred to parenthetically in the text, for example (Fig. 1).

Footnotes. Text footnotes **should not be used**

Submission Preparation Checklist

As part of the submission process, authors are required to check off their submission's compliance with all of the following items, and submissions may be returned to authors that do not adhere to these guidelines.

1. The submission has not been previously published, nor is it before another journal for consideration (or an explanation has been provided in Comments to the Editor).
2. The text adheres to the stylistic and bibliographic requirements outlined in the Author Guidelines.
3. I acknowledge that if my manuscript is peer-reviewed and accepted for publication, there will be a paper charge fee of $50/page for **non-Academy members**.
4. The manuscript file is in Microsoft Word format.

Copyright Notice

Authors who publish with this journal agree to the following terms:

1. Authors retain copyright and grant the journal right of first publication
2. Authors are able to enter into separate, additional contractual arrangements for the non-exclusive distribution of the journal's published version of the work (e.g., post it to an institutional repository or publish it in a book), with an acknowledgement of its initial publication in this journal.
3. Authors are permitted and encouraged to post their work online (e.g., in institutional repositories or on their website) prior to and during the submission process, as it can lead to productive exchanges, as well as earlier and greater citation of published

Science Matters

Exemplary education taught by renowned faculty in cutting-edge classrooms and laboratories.

Department of Agricultural & Environmental Sciences

Bachelor of Science in Agricultural Sciences

Concentrations

- *Agribusiness*
- *Agricultural Leadership, Education & Communication*
- *Biotechnology*
- *Environmental Sciences*
- *Food and Animal Sciences*

Master of Science in Agricultural Sciences

Concentrations

- *Agribusiness Management & Analysis*
- *Agricultural Education*
- *Biotechnology*
- *Food Supply Chain Management*

Master of Science in Environmental Science

Concentrations

- *Plant Sciences*
- *Natural Resources*
- *Geospatial Information Sciences*

Master of Science in Food & Animal Sciences

Ph.D. in Biological Sciences

Department of Human Sciences

Bachelor of Science in Family & Consumer Sciences

Concentrations

- *Child Development & Family Studies*
- *Fashion Merchandising*
- *Food and Nutritional Sciences (Dietetics)*
- *Food Service Management*

Enroll Now

www.tnstate.edu/agriculture/

TENNESSEE STATE UNIVERSITY

College of Agriculture

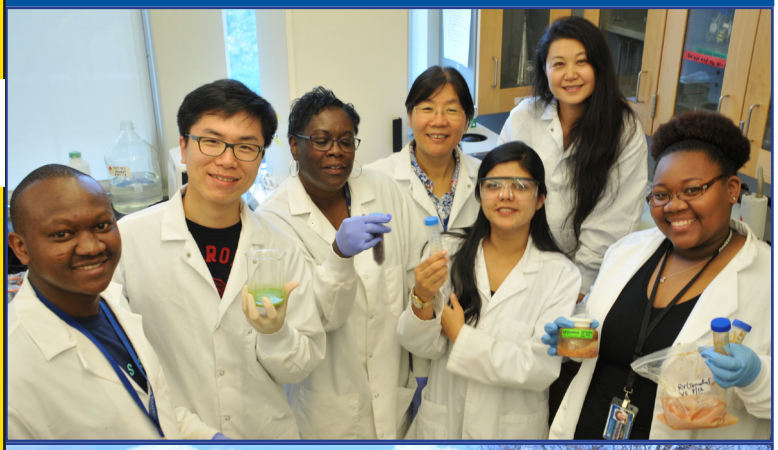

Admissions Info Undergraduates
Everett Jolley
(615) 963-2594
evjolley@tnstate.edu

Undergraduate Scholarships
Dr. De'Etra Young
(615) 963-5123
dyoung23@tnstate.edu

Graduate Admissions & Research Assistantships
Dr. Bharat Pokharel
(615) 963-6054 • bpokhare@tnstate.edu

Mississippi Academy of Sciences
Post Office Box 55907
Jackson, MS 39296-5907

Coden: JMSS-A **ISSN 0076-9436** **Volume 65, Number 3 July 2020**